MAGMATIC EVOLUTION OF MAURITIUS, WESTERN INDIAN OCEAN.

by

ALISTAIR NAPIER BAXTER, B.Sc.

Thesis presented for the Degree of Doctor of Philosophy of the University of Edinburgh in the Faculty of Science.

1972.

ABSTRACT

The island of Mauritius lies in the western Indian Ocean at 57°30'E. and 20°20'S., approximately 1000 Km. E. of Madagascar and 1100 Km. W. of the Central Indian Ocean Ridge, and forming with the adjacent islands of Reunion and Rodriguez, the Mascarene Islands. Several lines of evidence suggest that each island has developed independently, away from the Central Indian Ocean Ridge.

Mauritius is entirely volcanic, and three distinct series are recognised:

(1) OLDER SERIES

Relatively explosive "central type" activity constructed a shield volcano with an alternating lava/agglomerate sequence. The lavas form a differentiated series of oceanites, ankaramites, olivine basalts, basalts, hawaiites, mugearites and feldsparphyric basalts, with associated ultramafic and anorthositic inclusions, and a related radial dyke swarm. A slight erosional unconformity is recognised within the series, separating the shield phase from a later group of feldsparphyric basalts, hawaiites, mugearites and high level trachytic bodies. Following cessation of activity the shield was reduced by erosion to a group of peripheral massifs.

(2) INTERMEDIATE SERIES

Activity recommenced with the eruption of a suite of alkali olivine basalts and basanitoids, now seen only in the S.W. of the island. Volumetrically this group is much smaller than either the Older or Younger Series.

(3) YOUNGER SERIES

Following a further pause in activity, volcanism recommenced with the eruption of a voluminous series of alkali olivine basalts. Eruption was initially probably of "fissure type", but terminated in localised eruption from a median N.N.E.-S.S.W. line of 21 very low angled shield volcanoes.

The Older Series basic lavas show a marked transitional character. The differentiated nature of the series is reflected in well defined chemical trends which can be satisfactorily explained in terms of low pressure crystal fractionation of observed phenocryst phases from a transitional basalt parental magma. A model for the origin of the parental magma is proposed, involving approximately 7% partial melting of a garnet lherzolite mantle, with subsequent polybaric, polyphase fractionation.

The Intermediate Series lavas are a relatively uniform group of alkali olivine basalts, showing a trend to basanitoidal compositions. Major element trends and those of some trace elements are poorly defined, but the incompatible elements K, P, Ti, Ba, Rb, Sr, Zr show an extremely well developed trend clearly unrelated to any likely low pressure fractionation scheme. Several models for the formation of these lavas are discussed, and a scheme involving approximately 16% partial melting of a garnet lherzolite, with variable degrees of eclogite fractionation, and subsequent polybaric polyphase fractionation is proposed.

The Younger Series forms a relatively undifferentiated

suite of alkali olivine basalts. Major and trace element data generally show trends compatible with the fractionation of olivine, the dominant phenocryst phase in these lavas, however slight cross trends are seen in the incompatible elements, similar to those observed in the Intermediate Series. A model for the formation of the lavas is proposed, involving approximately 11% partial melting of a garnet lherzolite and subsequent polybaric, polyphase fractionation. The slight cross trends apparent in the incompatible element group are attributed to small, variable amounts of eclogite fractionation in the primitive magma, or slight variations in the degree of partial melting.

CONTENTS

INDEX TO CHAPTERS

APPENDICES

INDEX TO FIGURES

INDEX TO TABLES

INDEX TO PLATES

1. INTRODUCTION

1.1. REGIONAL SETTING

The island of Mauritius lies in the western Indian Ocean at 57°30' E. and 20°20' S., 1000 Km. east of Madagascar and 1100 Km. west of the Central Indian Ocean Ridge. With the islands of Reunion, 170 Km. W.S.W. and Rodriguez, 650 Km. E.N.E. it forms the geographic group known as the Mascarene Islands, Fig. 1.1. Elliptical in outline, with major axis running N.N.E.-S.S.W., Mauritius has an area of approximately 1850 Km^2.

Considerable work has been done over the last decade on the physiography and tectonic evolution of the central and western Indian Ocean and the reader is referred to the papers of Heezen and Tharp (1965(a),(b), 1966), Fisher, Johnson and Heezen (1967), Fisher, Sclater and McKenzie (1971) and McKenzie and Sclater (1971) for a full discussion, which is beyond the scope of this thesis. A summary of the information relevant to Mauritius, extracted from these papers, is given below.

The three Mascarene islands form separate topographic entities. Reunion rises as a vast independent shield volcano, slightly elliptical, with long axis running N.W.-S.E. Rodriguez is the exposed portion of a narrow E.-W. trending ridge which intersects the Mascarene Plateau north of Mauritius. While both these structures rise off the abyssal plain, Mauritius forms part of a much larger structure and is the southern extension of the Mascarene Plateau, a major structural unit of the Indian Ocean. The plateau extends

FIG. 1.1.

Regional setting of Mauritius and simplified bathymmetry of the western Indian Ocean.
from, McDougall and Chamalaun (1969).

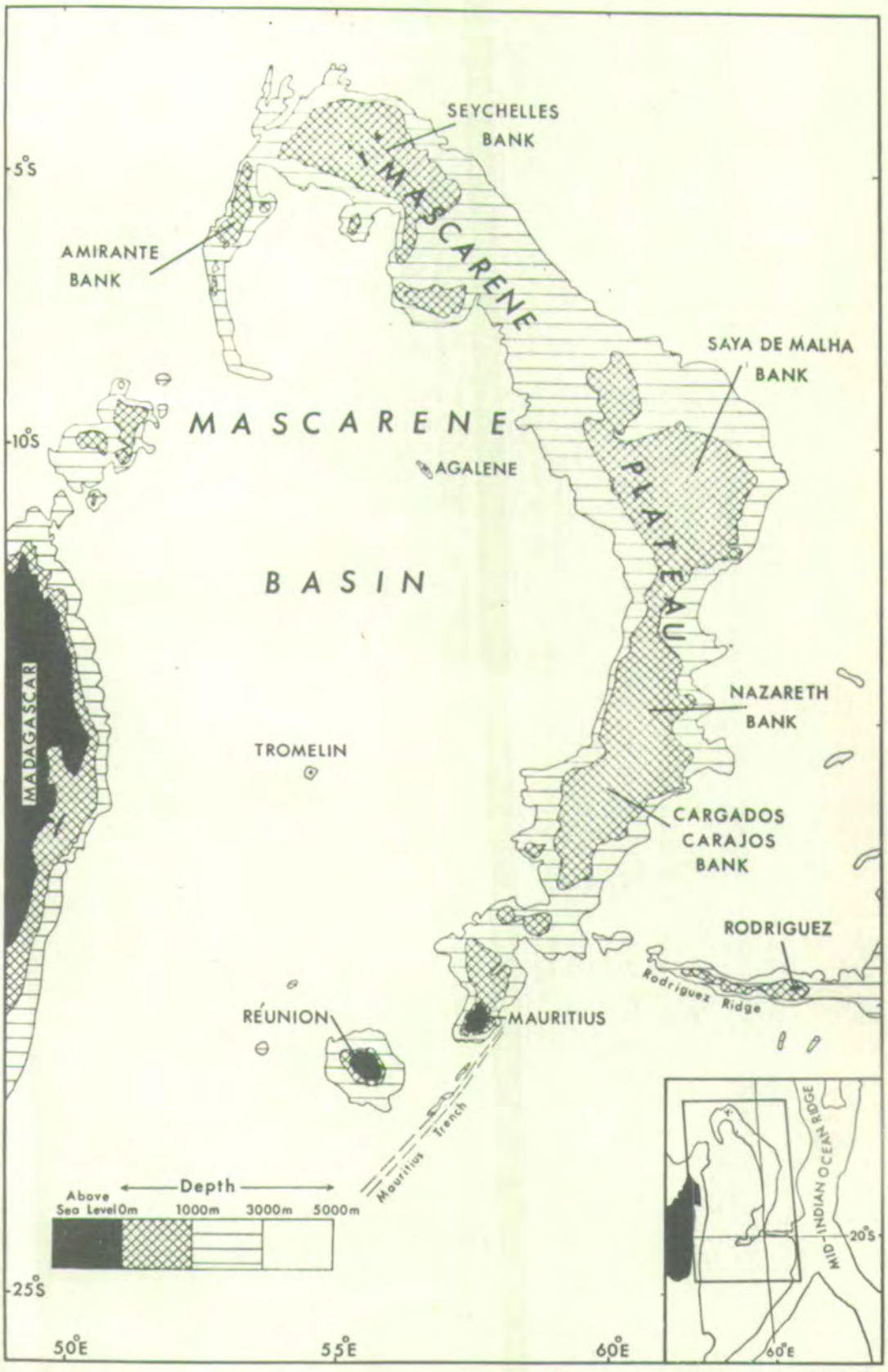
SEYCHELLES BANK
MASCARENE PLATEAU
AMIRANTE BANK
SAYA DE MALHA BANK
MASCARENE BASIN
AGALENE
NAZARETH BANK
TROMELIN
CARGADOS CARAJOS BANK
RODRIGUEZ
Rodriguez Ridge
MADAGASCAR
RÉUNION
MAURITIUS
Mauritius Trench
Above Sea Level
Depth
0m
1000m
3000m
5000m
5°S
10°S
25°S
50°E
55°E
60°E
MID-INDIAN OCEAN RIDGE
20°S
60°E

southwards in a slight arc from the Seychelles over a distance of 2300 Km. and is expressed as a series of shallow submarine banks. It is a faulted, aseismic, composite structure rising steeply from the sea floor, underlain in the north around the Seychelles Bank by continental crust, Shor and Pollard (1963), Davies and Francis (1964), Matthews and Davies (1966) and composed of volcanic rocks underlain by oceanic crust south of the Saya de Malha Bank, Shor and Pollard (1963), Bunce et al. (1966).

The topographic independence of the three Mascarene islands reflects their separate origins and although they show a crude E.N.E. alignment away from the ridge, potassium-argon dating by McDougal and Chamalaun (1969) shows no progressive increase in age with distance from the ridge, contrary to the hypothesis of Wilson (1963) for the formation of oceanic islands.

Although the overall trend of the Central Indian Ocean Ridge is N.-S., Fisher, Sclater and McKenzie (1971) and McKenzie and Sclater (1971) have demonstrated that the active ridge segments lie N.W.-S.E. with spreading rates of approximately 2.3 cm./year N.E.-S.W. These authors further show that the Mascarene Plateau and its apparent analogue on the eastern side of the ridge, the Chagos-Laccadive Ridge, bound the magnetic anomalies and fracture zones of the present spreading episode (0 - 20 m.y. ago), separating them from an earlier sequence with markedly different E.-W. anomalies (> 20 m.y. ago). Reconstructions based on the rotation of present epicentres and the structural units about calculated spreading poles suggest that the Mascarene Plateau and the

Chagos-Laccadive Ridge initially lay along an early plate margin on the site of the present Central Indian Ocean Ridge, and that this plate boundary was a N.-S. transform fault separating an ancient E.W. lying Carlsberg Ridge and South East Indian Ridge, (See Fig. 9, Fisher, Sclater and McKenzie (1971)). Volcanism along this transform fault prior to the development of the present spreading episode is believed to have constructed the Chagos-Laccadive Ridge and the Mascarene Plateau south of the Saya de Malha Bank, which linked up with the Seychelles continental fragment.

An age of at least 20 m.y. is inferred for the Mascarene Plateau by this hypothesis, and as the initiation of the Mauritian volcanic pile from the sea floor is dated at approximately 12 m.y., McDougall and Chamalaun (1969) it appears that Mauritius cannot be simply related to the volcanism which may have constructed the Mascarene Plateau. It is possible therefore, that the island may have developed independently, away from the plate margin, located by coincidence at the end of the Mascarene Plateau.

1.2. LOCAL SETTING

Locally the submarine topography of Mauritius is irregular, Fig. 1.2. The island is bounded to the west by a steep linear scarp interpreted mainly on topographic evidence as a right lateral fault displacing Mauritius southwest, Fisher, Johnson and Heezen (1967). A shallow bank extends northwards for 26 Km. and encompasses several small islands relating to the Mauritian structure. To the east

FIG. 1.2.

Submarine topography near Mauritius.

Contours in metres.

From, Fisher, Johnson and Heezen (1967).

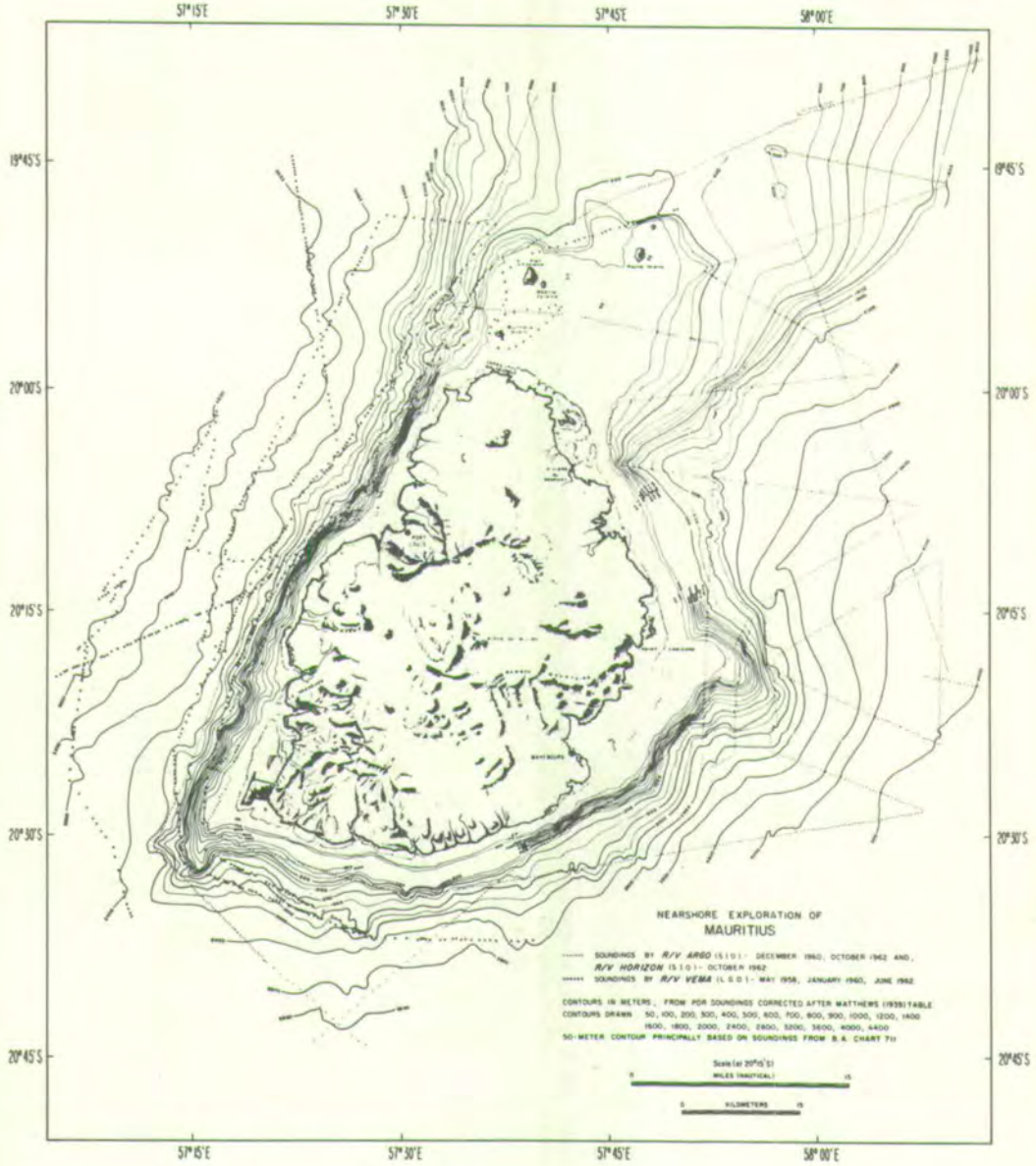
57°15'E
57°30'E
57°45'E
58°00'E
19°45'S
20°00'S
20°15'S
20°30'S
20°45'S
NEARSHORE EXPLORATION OF
MAURITIUS
SOUNDINGS BY R/V ARGO (S10) - DECEMBER 1960, OCTOBER 1962 AND,
R/V HORIZON (S10) - OCTOBER 1962
SOUNDINGS BY R/V VEMA (L60) - MAY 1958, JANUARY 1960, JUNE 1962
CONTOURS IN METERS, FROM FOR SOUNDINGS CORRECTED AFTER MATTHEWS (1939) TABLE
CONTOURS DRAWN 50, 100, 200, 300, 400, 500, 600, 700, 800, 900, 1000, 1200, 1400
1600, 1800, 2000, 2400, 2800, 3200, 3600, 4000, 4400
50-METER CONTOUR PRINCIPALLY BASED ON SOUNDINGS FROM U.S. CHART 711
Scale (at 20°15'S)
MILES (NAUTICAL)
KILOMETERS

and south the island slopes down towards the abyssal plains, but is sharply terminated in the south-east by the Mauritius Trench, a major tectonic structure running south-west for some 1400 Km.

Unlike many oceanic volcanic islands e.g. Hawaii, Menard (1964), Mauritius and the neighbouring Reunion are not surrounded by a moat. These structures are generally recognised as an isostatic response to local loading of the crust by the volcanic pile and their absence has been used to imply non-equilibrium. However gravity surveys in the Mauritius region, Takin (1966) indicate a pronounced local compensation interpreted as a depression of the crust by the volcanic pile. Fisher, Johnson and Heezen (1967) suggest that slumping and turbidity current deposits may have buried any incipient moat structures.

1.3. PHYSIOGRAPHY

The island has a sub-tropical to tropical maritime climate and lies within the south-east trade belt. As rainfall on small isolated landmasses like Mauritius is largely orographic, the south and central parts of the island receive the bulk of the rainfall, producing a dense vegetation while the north and west lie in the rain shadow and develop a semi-arid scrub cover. Consequently the pattern of outcrop on the island is highly variable, from limited fresh exposure in the south to excellent fresh outcrop in the open ground in the north and west.

Mauritius can be divided into three main physical units, Map 1. (back pocket):

(a) Central Plateau.

(b) Peripheral Massifs.

(c) Northern Plain.

(a) Central Plateau

This has the form of an undulating plain which rises gently towards a N.N.E.-S.S.W. trending ridge of small shield volcanoes which form the main watershed on the island. It has a mean elevation of around 500 m. rising to a maximum of 684 m. at Curepipe Point - the largest of the shields. The surface of the plateau is structural in origin, being only slightly dissected by erosion and is composed of a recent series of slightly dipping olivine-basalts.

(b) Peripheral Massifs

In contrast these form a discontinuous ring of rugged peaks surrounding the Central Plateau. They have a mean elevation of around 600 m. rising abruptly to rocky peaks such as Piton de la Riviere Noire (827 m.) in the S.W., Le Pouce (812 m.) and Pieter Both (822 m.) in the N.W. and Pic Bambou (641 m.) in the east. They have steep inland slopes and shallow seaward dipping ridges separated by deeply incised valleys. This group stands out sharply from the otherwise subdued terrain and represents the erosional relics of a major shield structure now partially buried by the flows which constructed the Central Plateau and Northern Plain, Plate 1.1.

(c) Northern Plain

Beyond the peripheral massifs in the north, lies a broad plain which represents the extension of the Central Plateau structure, but at a lower level. It has a mean

PLATE 1.1.

Contrasting topography of the Central Plateau and the Peripheral Massifs.

View west from Slim's trachyte over structural slopes of Younger Series shields, towards the Older Series Port Louis Massif.

elevation of about 100 m., rising gently towards the median line of shields. The low elevation and absence of any earlier units suggests that this area has been constructed directly from sea level - probably over a marine bevelled platform of the earlier shield structure.

The island has a radial drainage pattern. Overall control on the river systems is exercised by the median N.N.E. - S.S.W. trending watershed of the recent shield volcanoes, and the relative youth of this structure is seen by the absence of rivers cutting the watershed and capturing the headwaters and catchement area of other systems. Many of the rivers run through the highly incised valleys of the peripheral massifs and their courses may in part be inherited from systems active during the denudation of this massive volcano, prior to the eruption of the later lavas and formation of a new watershed and drainage pattern. The formation of complex valley fill structures due to the localization of river activity through successive volcanic events, is discussed in Chapter 2.

1.4. PREVIOUS RESEARCH

The first modern account of the geology of Mauritius was given by Darwin (1844) who recognised the volcanic structure of the island and distinguished two lava series, one constructing the Central Plateau and Northern Plains, and the other the Peripheral Massifs. Following an account by De Haga Haig (1895) of the occurrence of "crystalline chlorite schist" on the island, which had later been cited in support of Wegener's (1929) hypothesis that oceanic islands were lithospheric fragments left behind by the drifting continents, Shand (1933) visited Mauritius and correctly redescribed the "schist" as a foliated trachyte intrusion.

Two local geologists, De Chazal and Baissac (1949) provided the first comprehensive account of the geology of the island, correctly recognising three lava series and a system of dykes related to the early lavas of the Peripheral Massifs. Their mapping however, differs considerably from that of a party of geologists from Cape Town University who spent 3 months on the island and in two companion papers, Simpson (1950) and Walker and Nicolaysen (1954) described the geology and petrology. Simpson's (1950) mapping has provided the basis for all subsequent work and has required only minor alterations. As the geology will be fully described in Chapter 2, only an outline of Simpson's conclusions are given here:

Apart from marginal reef deposits the island is entirely volcanic and composed of two major geological units separated by a large unconformity viz:

1. Older Series

(a) Early Phase

2. Younger Series

(b) Late Phase

The Older Series occupies the mountainous areas of the island, comprising a radially dipping series of olivine basalts and subordinate more evolved lavas with the form of a large shield volcano and cut by a system of basaltic dykes and trachyte intrusives. A prolonged quiescent period following the construction of the shield resulted in extensive erosion of the structure to a series of peripheral massifs. Activity recommenced with eruption of the Younger Series olivine basalts over the stumps of the Older Series. An erosional unconformity recognised within this series separates an Early Phase seen only in the south-west, from a Late Phase erupted through a median line of vents running N.N.E.-S.S.W. through the island.

Considerable confusion has resulted from the terminology of the Younger Series, and hereafter it is proposed to call the Early Phase lavas the Intermediate Series, and the Late Phase lavas the Younger Series.

More recently McDougall and Chamalaun (1969) provided an absolute time scale for the Mauritian rocks, using potassium-argon dating. Simpson's (1950) evolutionary scheme for the island was confirmed by McDougall and Chamalaun (1969), who showed the Older Series shield to have been constructed sub-aerially over a period from 7.8 - 6.8 m.y. ago with more evolved flows and trachytes formed around

5.5 m.y. ago. The Intermediate Series lavas were dated at 3.5 - 2.0 m.y. and the Younger Series at 0.7 - 0.17 m.y. old.

1.5. PRESENT RESEARCH

The present work forms part of a continuing systematic investigation of the Western Indian Ocean islands under the leadership of Dr. B.G.J. Upton at Edinburgh University and Dr. W.J. Wadsworth of Manchester University.

Since the original papers of Simpson (1950) and Walker and Nicolaysen (1954), concepts of the origin and significance of oceanic volcanic islands and the origin of basaltic rocks have changed considerably and it had become apparent that Mauritius required reinvestigation. Consequently, the writer spent 10 weeks on the island in the summer of 1969 with the first aims of redescribing the geology and making a detailed sample collection.

The relative lack of recent information on Mauritius meant that a major objective was the systematic description of the petrography, mineralogy and chemistry of the lavas. Following on this essentially descriptive phase the major aim of the research was the construction of a petrogenetic scheme for the formation and differentiation of the lavas both at high crustal levels, and in terms of their probable origin in the upper mantle, by extrapolation of the data into experimentally defined natural and synthetic rock systems.

2. GEOLOGY

2.1. INTRODUCTION

Apart from a fringing reef and some minor peripheral carbonate deposits, Mauritius is entirely constructed of volcanic rocks. Three distinct geological units termed the Older, Intermediate and Younger Series are recognised on the island, the former separated from the latter two series by a major unconformity while the Intermediate and Younger Series are separated by a relatively minor unconformity. The Older Series can be subdivided into an early, shield building phase marked by eruption of alternating beds of agglomerate and picrite-basalt, olivine-basalt and hawaiite flows, cut by a related radial dyke swarm; and a later more evolved suite of feldsparphyric basalts, hawaiites and mugearites unconformably capping the shield and associated with endogenous trachyte domes.

A long pause in activity followed, with profound erosion of the pile. Activity recommenced, apparently restricted to the south-west of the island, with the eruption of the Intermediate Series olivine-basalts over the eroded Older Series and following a further limited break in activity during which these lavas were mildly incised, the Younger Series lavas were erupted from a line of small shield volcanoes running N.N.E.-S.S.W. through the centre of the island.

There has been no historic activity on Mauritius and it would appear that volcanism is now extinct.

The geology of Mauritius together with sample localities, is summarised in Map 1 (back pocket) and to which reference

should be made for the following discussion. The major structural units, extracted from this map, are presented in Fig. 2.1.

Where absolute ages are quoted through the text, these are taken from the potassium-argon dating of McDougall and Chamalaun (1969).

2.2. OLDER SERIES

A. Introduction

The Older Series typically form the peripheral massifs of the island. Fig. 2.1. shows their distribution and though masked by the Intermediate and Younger Series lavas, their general absence towards the centre of the island is striking. The massifs themselves show long seaward dipping extensions separated by deep valleys only partially filled by the Intermediate and Younger Series lavas and it is evident that the Older Series had been highly eroded prior to the eruption of these later series which now largely bury the old erosion surface. This pattern of outcrop, with a highly reduced central area and peripheral massifs separated and incised by deep valleys is very similar to that seen to be produced by extreme amphitheatre-headed valley erosion, e.g. Hawaii, Stearns (1966), Reunion, Upton and Wadsworth (1966) and Anjouan, Flower (1970) and to which it is logically attributed.

Two distinct units are recognised within the Older Series, separated by an angular unconformity. The first, a shield building phase, consists of agglomerates, ankaramites, oceanites and olivine-basalts, with subsidiary hawaiites and

FIG. 2.1.

Simplified geological map of Mauritius,

showing major structural units.

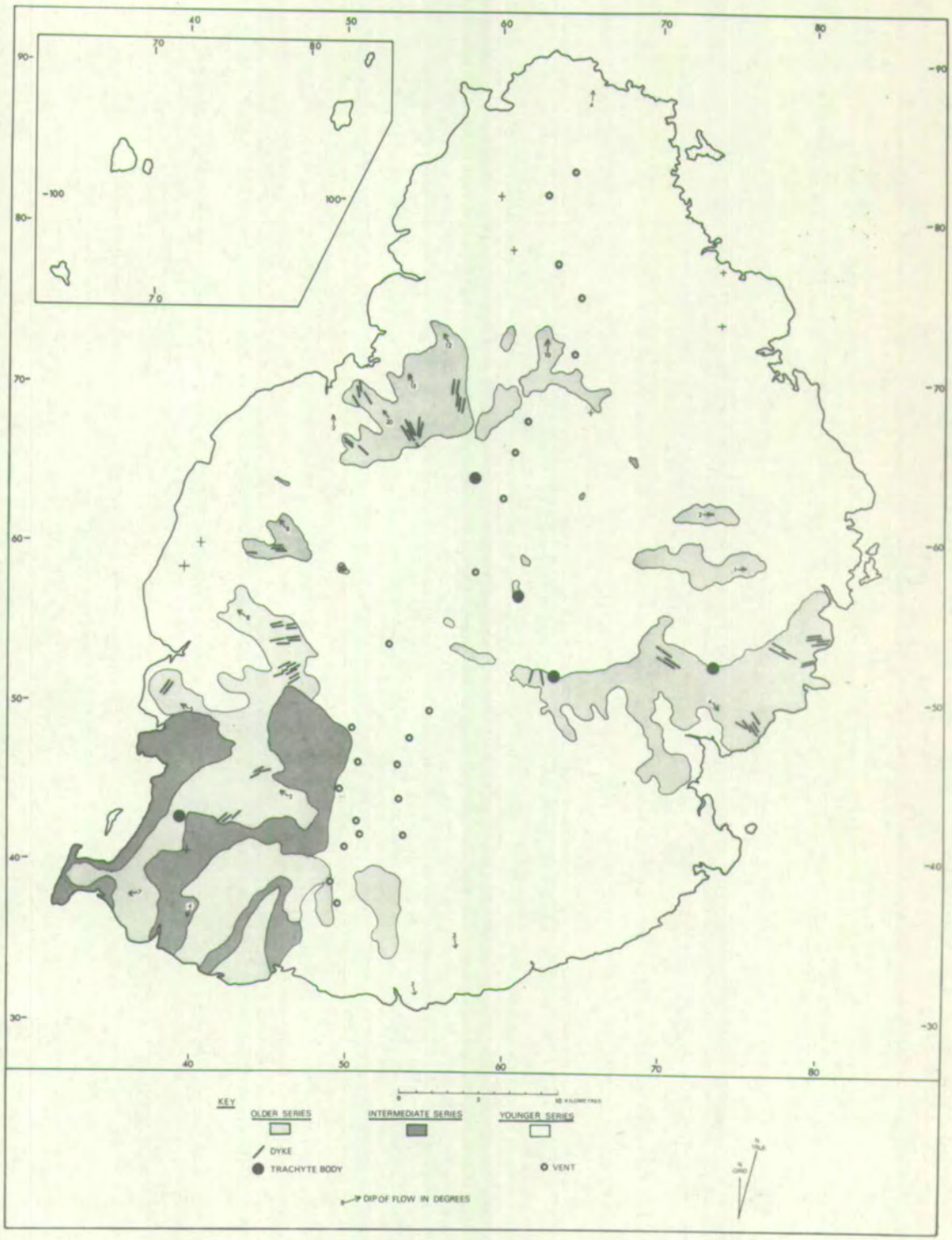
KEY
OLDER SERIES
INTERMEDIATE SERIES
YOUNGER SERIES
DYKE
TRACHYTE BODY
VENT
DIP OF FLOW IN DEGREES

much rarer feldsparphyric basalts and mugearites towards the top of the succession. Associated with this phase is a radial dyke swarm. The subaerial portion of the shield reaches a maximum thickness of around 800 m. and is dated as being erupted over a period from 7.8 - 6.8 m.y. ago. The second phase consists of a sequence of feldsparphyric basalts, hawaiites and mugearites which unconformably overlie the shield structure on Fayence and Blanche mountains and in the Black River gorge, and are associated with endogenous domes of trachyte. Volumetrically this unit is much less significant than the shield, but more may be concealed beneath the Intermediate and Younger Series lavas or has been removed by erosion. The unit reaches a maximum thickness of 300 m. on Blanche mountain and is dated at around 5.5 m.y.

For the purposes of description the Older Series can be conveniently divided into two groups viz:

Extrusives - Lavas, Agglomerates.

Intrusives - Dykes, Endogenous Domes and associated minor structures.

These are described separately in the following sections.

B. Extrusives

Agglomerates

The abundance of agglomerates in the Older Series would suggest that the shield building phase was accompanied by more explosive eruption than is typical of many oceanic islands, e.g. Hawaii, Stearns (1966), Grand Comore, Strong (1972), Reunion, Upton and Wadsworth (1966) and Tahiti,

McBirney and Aoki (1968), where construction was achieved by the quiet emission of floods of olivine-basalt. The agglomerates are apparently restricted to the shield phase, indicating less violent eruption of the more evolved lavas.

Typically the agglomerates form beds < 10 m. thick, dominantly composed of angular blocks of lava (< 30 cm. diameter) set in a finer fragmentary matrix. Occasional agglomerate blocks are found, indicating some reworking of earlier deposits. Bombs and other structures indicative of fluid ejection are never seen. Beds are often highly indurated and may weather out as positive features. The thickness of any one bed is highly variable and surfaces are often very irregular, probably a result of the random nature of airfall deposits and the ease with which they can be eroded before consolidation. Lavas erupted over these surfaces have locally a highly variable dip and makes measurement of the general dip difficult. Boles are commonly found in the agglomerates but much less frequently in the lavas; and this may indicate pauses in activity sufficiently long for laterization of the already partially degraded agglomerates to occur, but not generally sufficient to reduce a fresh lava. Commonly alternations of thin lava flows and agglomerates underlie massive flow units, suggesting spasmodic explosive and eruptive activity prior to major lava eruptions. Zeolitisation of the agglomerates is often seen, and a bed may be zeolitised while surrounding lavas are untouched, possibly reflecting the differing degrees of permeability of the two rock types.

Lavas

Generally the lavas of the shield phase dip radially away from a focus towards the centre of the island, varying from 6-12°. Locally in the Port Louis massif, however, dips of up to 20° N.W. are encountered; these may be the result of slumping or related to the linear fault paralleling the island's western margin, but the surrounding Younger Series lavas have obscured the field relations.

In contrast to these moderate to high shield angles, the evolved lavas on Fayence and Blanche mountains and in the Black River gorge dip seawards at low angles (1-2°). Their near horizontal attitude, differentiated nature and younger age than the shield phase led McDougall (1969) to suggest they formed part of a caldera fill. However there is no obvious lateral correlation of flows between the adjacent Fayence and Blanche mountains as might be expected for horizontal ponded caldera fills while their definite seaward dip and pronounced elongate form suggests a possible origin as valley fills in the eroded shield phase, which have now weathered out as positive features.

Flow thickness is highly variable; in the Port Louis massif the upper 200 m. of the succession is recognisable as five major flows or flow units each up to 30 m. thick, separated by alternations of relatively thin (< 10 m.) lava flows and agglomerates. Similarly the upper portion of the Corps de Garde/Mt. St. Pierre massif is composed of four major flows up to 30 m. thick, separated by thin (< 10 m.) lava/agglomerate alternations. More generally however, flows

vary from 5-10 m.

Jointing is common in the flows and vertical columnar jointing is increasingly well developed in thicker flows, probably in response to their slower cooling rates. Thinner flows, and almost inevitably the bases of thicker flows show a tendency to develop jointing parallel to the flow surfaces. Macdonald (1967) ascribes this style of jointing to movement after the lava is too viscous to flow, with resultant shearing along flow planes. The distinct association, at least in Mauritius, of this horizontal jointing with the base of a flow, makes the structure a useful marker in more poorly exposed areas.

In the more evolved flows, particularly on Fayence and Blanche, a platy lamination often develops parallel to the flow surfaces due to alignment of groundmass feldspar. Flow alignment of feldspar phenocrysts is seen in some feldspar-phyric basalts, hawaiites and mugearites.

On Tamarin and Lion mountains, peridotitic (dunite and rarer wehrlite) inclusions are found. These inclusions are generally small (< 5 cm.), angular and occasionally show obvious signs of disintegration into the lava. In both cases the inclusions are associated with phyric olivine basalts and on Tamarin mountain there is a distinct sequence approximately 100 m. thick, of basalts increasing upwards in phyric olivine and culminating in an oceanitic flow carrying predominantly dunite inclusions. Allied to this trend is a tendency for these flows to become increasingly scoriaceous upwards, and this unit may offer clear evidence of elutriation of cumulus material.

C. Intrusives

Dykes

Simpson (1949) recorded a system of basaltic dykes, related to the Older Series and with an "ill defined trend N.E.-S.W." Mapping by the present writer shows these to form part of a well developed radial dyke swarm focussed on the centre of the island, see Fig. 2.1. Dykes cutting the later evolved flows on Fayence and Blanche mountains are absent, which suggests that the swarm is restricted to the shield building phase of the Older Series.

Megascopically the dykes cover the same compositional range as the shield lavas and it is likely that some may have acted as feeders to flows, e.g. Lion mountain where inclusion-bearing dykes are associated with compositionally indistinguishable inclusion-bearing flows.

The dykes are typically vertical, generally from 1-3 m. but occasionally up to 15 m. thick. Commonly they weather out as positive features. Horizontal columnar jointing is common even in the thinnest dykes, in contrast to the flows where good jointing is developed only in the thicker units. This may reflect their differing environments; thin flows chill relatively fast against the atmosphere while dykes cool more slowly, insulated by a relatively warm lava pile.

Radial dyke systems are relatively common, e.g. Rhum, Richey (1961), Gough Island, Le Maitre, (1962), Aden, Cox et al. (1968) and they are generally believed to result from filling of radial tension fractures caused by stress due to upwelling magma beneath a volcanic centre. Such a mode of

formation fits well with the restriction of the Older Series swarm to the early shield building phase.

Linear dyke swarms comparable to those associated with the rift zones of Hawaii, Stearns (1966) are absent, while the dyke pattern and radial dips suggests that the Older Series volcanism was of "central type" rather than "fissure type".

Endogenous domes and associated minor structures

Trachytes, the most evolved rocks of the Older Series are typically found as jointed and foliated bodies, probably with the form of endogenous domes. As no flows emanate from these domes, they are classed here, for convenience, as intrusives although it is realised that they are essentially extremely high level bodies which may have had some surface expression e.g. Atkins et al. (1964), Stearns (1966). Five intrusions have been found, viz:

1. Chamarel
2. La Selle
3. Camizard
4. Slims Trachyte
5. Piton de Milieu

1. Chamarel

This crops out in the south-west of the island as a roughly circular body 75 m. in diameter. The trachyte has a well developed foliation produced by flow alignment of alkali feldspar crystals; the foliation defines a domical

structure with a vertical central zone inclining outwards to margins dipping outwards at 25°. A breccia zone of indeterminate thickness is found on the western margin of the body, containing angular trachyte fragments (< 10 cm. diameter) with rarer basaltic clasts, set in a fine fragmentary matrix. This is interpreted as an autobreccia and may reflect the probably high viscosity of the trachyte magma and its emplacement in a rapidly cooling near-surface environment. Locally the shield series dips away from the intrusion at high angles and probably reflect upwarping of the beds during emplacement of the trachyte.

2. La Selle

This is a roughly circular trachyte body with a diameter of around 150 m., eroded as the name suggests, into a broad saddle-like structure. Foliation is developed, though less spectacularly than at Chamarel and dips away and downward from the centre, again indicating a dome-like structure. Columnar jointing is developed, with vertically inclined columns at the centre of the body, surrounded by units dipping inwards at around 80°.

3. Camizard

The Camizard trachyte is an oval shaped intrusion with major axis of approximately 200 m. running E-W and minor N-S axis of around 100 m. No foliation is seen in this fine-grained trachyte, but columnar jointing is well developed with central vertical columns splaying out to highly inclined columns dipping inwards at around 20°, on the eastern and

western margins. The ease of access by weathering agents down the vertical joints has produced the present shape of the body, which has a reduced central zone with eastern and western peaks formed of the less vulnerable inclined columns.

4. Slim's Trachyte

A small conical trachyte hill crops out in the north of the central plateau, and is the exposed portion of a presumably much larger body, now buried by the Younger Series lavas. It is generally highly weathered and shows no jointing or foliation structures.

5. Piton de Milieu

This is a broad linear intrusive running east-west for 200 m. in the centre of the island. No megascopic foliation is seen but columnar jointing is exceptionally well developed. Like Camizard two peaks are separated by a central depression containing near vertical columns. Generally the columnar arrangement is simple, with outward dipping highly inclined columns curving inwards to a horizontal log-like stack, which form the east and west peaks. However an extremely anomalous area occurs below the western peak, where near vertical columns curve back horizontally out of the body, in the opposite manner to the main arrangement, Plate 2.1. These horizontal columns appear to merge into those of the main system with no discordance, suggesting that both are part of the same intrusion.

PLATE 2.1.

Anomalous jointing zone in the Piton De Milieu trachyte.

Explanation in text.

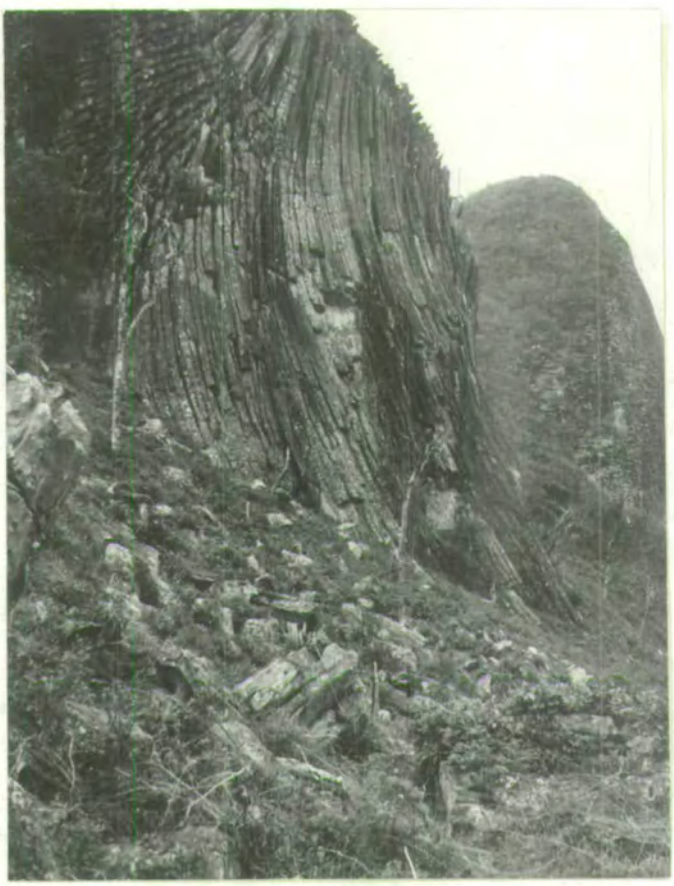

Structure of Trachytes

A pronounced domical structure is indicated in the coarse foliated trachytes of Chamarel and La Selle. In the intrusions of Camizard and Piton de Milieu no foliation is seen, but a strong jointing system is developed. Assuming as a first approximation that columnar jointing develops at right angles to the cooling surfaces, a domical structure is indicated for Camizard and a funnel-shaped structure for Piton de Milieu.

Columnar jointing is generally accepted as resulting from tensile failure perpendicular to surfaces of maximum stress within a cooling body, Jaeger (1961), Spry (1962). In simple regular structures these surfaces will lie parallel to the isotherms, but in more irregular bodies complex stress systems may develop and stress and isotherm surfaces may not be parallel. Consequently caution must be exercised in inferring the shape of bodies from jointing orientations. This may explain the anomalous zone on Piton de Milieu but more generally the symmetry of the jointing pattern through the intrusives suggest a regular stress system and hence the validity of using joint orientations to work out the shapes of the bodies.

As they are described here, the Older Series trachytes are very similar to the endogenous domes described from Hawaii, Stearns (1966) and Ascension, Atkins et al. (1964). These are extremely high level bodies which commonly merge into trachyte flows, originating from a funnel or dyke-like body and warping up the surrounding strata, with the formation

of marginal autobreccias. The Piton de Milieu body may represent the lower part of such a structure, while Camizard, Chamanel and La Selle are the upper, truly domical bodies.

Trachytic dykes and sills are occasionally found adjacent to the main intrusives. On Mount Lagrave a thin sill dips at 20° east towards the main La Selle body only 1 Km. away, and at Chamarel a thin trachyte dyke runs east-west away from the intrusion. These structures most probably represent offshoots from the main bodies.

2.3. INTERMEDIATE SERIES

A break in activity of approximately 1.5 m.y. followed the eruption of the final evolved phase of the Older Series during which extreme erosion of the volcanic pile took place. Activity recommenced around 3.5 m.y. ago with the eruption of the Intermediate Series olivine basalts over the old land surface, and was apparently restricted to the south-west of the island, although more flows may be hidden beneath the Younger Series lavas.

Extensive explosive activity marked the recommencement of volcanism, as the base of the Intermediate Series is marked by an agglomerate bed at least 40 m. thick, over which the olivine-basalts were erupted. The lavas built up the high plateau west of Mare aux Vacoas and partially filled the valleys cut in the Older Series at Black River, Baie du Cap and the R. Jacotet valley, reaching a maximum thickness of about 300 m. in these areas. Generally the series is poorly exposed due to the high rainfall and dense vegetation in the

south-west of the island.

The lavas are a uniform series of compact to vesicular olivine-basalts. Flows are horizontal in the high plateau and dip seawards in the valley fills, to a maximum of 4^{o} at Baie du Cap. Individual flows vary in thickness from 1-10 m., with columnar jointing developed in the less vesicular lavas. Elongation of vesicles in the direction of flow is common, while rubbly flow surfaces indicate the lavas to be of aa type. Interbasaltic boles are common, particularly at Baie du Cap and suggests frequent pauses in activity.

Back projection of flow dips indicates a source for the lavas in the area around Mare aux Vacoas, however any eruptive centre has been concealed beneath the Younger Series lavas.

2.4. YOUNGER SERIES

A. Introduction

Eruption of the Intermediate Series lavas ceased around 1.9 m.y. ago and a quiescent period of 1.2 m.y. followed during which these flows were incised, and the Older Series further reduced. Activity recommenced about 0.7 m.y. ago and lasted for approximately 0.5 m.y. during which the Younger Series olivine basalts were erupted, from a line of relatively small, coalescing shield volcanoes running N.N.E.-S.S.W. through the centre of the island, Fig. 2.1. The trend of the shields closely parallels the fault bounding the western margin of the island and the Younger Series volcanism may be closely related to its development.

In contrast to the distinctly "central type" volcanism of the Older Series, the alignment of the Younger Series shields is striking and it seems likely that this period of activity initiated as a "fissure-type" eruption which terminated in localised eruption of olivine basalts from vents.

B. Lavas

The lavas vary from compact to highly vesicular olivine basalts and characteristically have a much coarser texture than either the Older or Intermediate Series lavas. Flows are relatively very thin, varying from 0.2 - 2 m. with rare 5 m. units, and commonly have well developed lateritic soils between them, indicating frequent pauses in activity. The lavas are generally horizontal or dip slightly away from the shields at up to 4°. At their contact with the Older Series, flows are often banked up, dipping back towards their point of origin - a feature which is tentatively ascribed to sagging of the lava flow as it cools and degasses. Individual flows often appear very young and on Plaine des Roches flow surfaces are exceptionally well preserved with only minimum vegetation growth. These display excellent pahoehoe structures and ropy areas are common with curved ridges indicating flow direction. Lava tunnels are very common and frequently form extensive underground drainage systems, while pressure ridges and tumuli are common, particularly on Plaine des Roches.

Eruption of the flows was accompanied by little explosive activity, and only one thin 1 m. agglomerate bed is found,

at Grande Riviere North-West, containing sub-rounded lava fragments (< 10 cm. diameter) in a finer matrix with occasional fusiform bombs (< 20 cm. long), indicative of ejection in a partly molten state.

C. Shield Structures

Twenty-one main shield volcanoes are found in the Younger Series, with numerous minor and parasitic cones lying along the trend. The shields vary from 10-20 Km. in diameter and are characterised by very low angle profiles (generally 1-3°) compared with the Older Series (6-12°) or many other shields, e.g. La Grille (7°), Strong (1970) and Hawaii (3-10°), Stearns (1966), Fig. 2.2. Shield angles are probably controlled by the viscosity of the magma and the style of eruption, and these low angle structures probably reflect rapid quiet emission of highly mobile lava. Similar low angle shields associated with highly mobile flows are found in the post-glacial volcanics of Iceland, Noe-Nygaard (1968).

The shields are well preserved in profile, particularly in the drier northern areas, and show broad shallow craters up to 100 m. in diameter and 30 m. deep. Small pit craters and nested cones aligned with the main trend are found on the crater floors of the larger shields, e.g. Curepipe Point, Bar Le Duc and L'Escalier. These minor cones are highly weathered but their high slope angles (10-20°) suggests they may be cinder cones.

Drowning of the craters of Bassin Blanc, Grand Bassin and seasonally that of Trou aux Cerfs has produced crater lakes.

FIG. 2.2.

Profiles of some Younger Series shield structures, with slope angles shown in degrees.

A - B. E.-W. section across Bar Le Duc

C - D. E.-W. section across Curepipe Pt.

Vertical exaggeration x 4.

Lines of section indicated on Map 1, (back pocket).

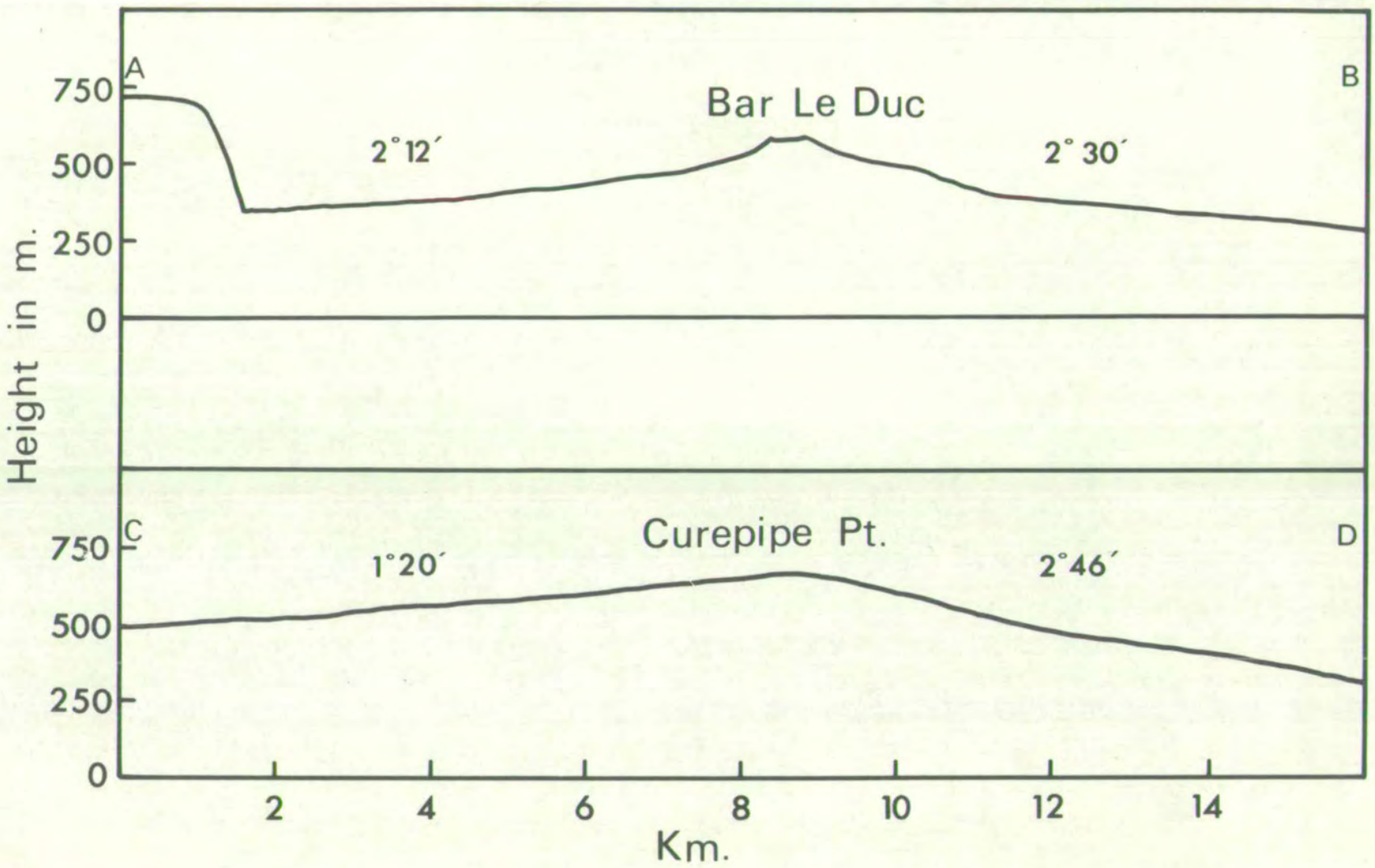
A
B
750
500
250
0
Bar Le Duc
2°12′
2° 30′
Height in m.
C
D
750
500
250
0
Curepipe Pt.
1°20′
2°46′
2
4
6
8
10
12
14
Km.

The Younger Series activity extended on to the shallow bank north of the island, where submarine activity constructed Flat Island, Gunners Coign, Serpent and Round Island. A landing was not possible during the period spent on Mauritius, but Simpson (1949) describes them as eroded basaltic tuff cones now exposed by eustatic changes in sea-level.

D. Valley-Fill Structures

In the S.W. of the island, persistent localization of river activity over the entire volcanic history of Mauritius, has resulted in successive superimposed valley fills. Thus a valley cut in the Older Series during the quiescent period and later filled by Intermediate Series lavas, was partially reexcavated in the pause before eruption of the Younger Series lavas, which in turn partially filled the new valley, Fig. 2.3. Similar structures are described by Stearns (1966), from Keenae Valley, Maui.

2.5. REEFS AND ASSOCIATED CARBONATE DEPOSITS

The island is surrounded by an offshore fringing reef, broken opposite major river mouths where brackish, turbid water prevents coral growth.

Raised reefs are found locally overlying the Younger Series lavas near Baie du Cap, and are related by Simpson (1949) to eustatic sea-level changes during the Pleistocene, who used them to relatively date the cessation of Younger Series activity.

FIG. 2.3.

Section E.-W. from Fantasie (G.R.414369) - Luchon (G.R. 466373) across R. Jacotet valley, showing probable nature of valley-fill structures.

Vertical exaggeration x 11.


= Older Series


= Intermediate Series


= Younger Series

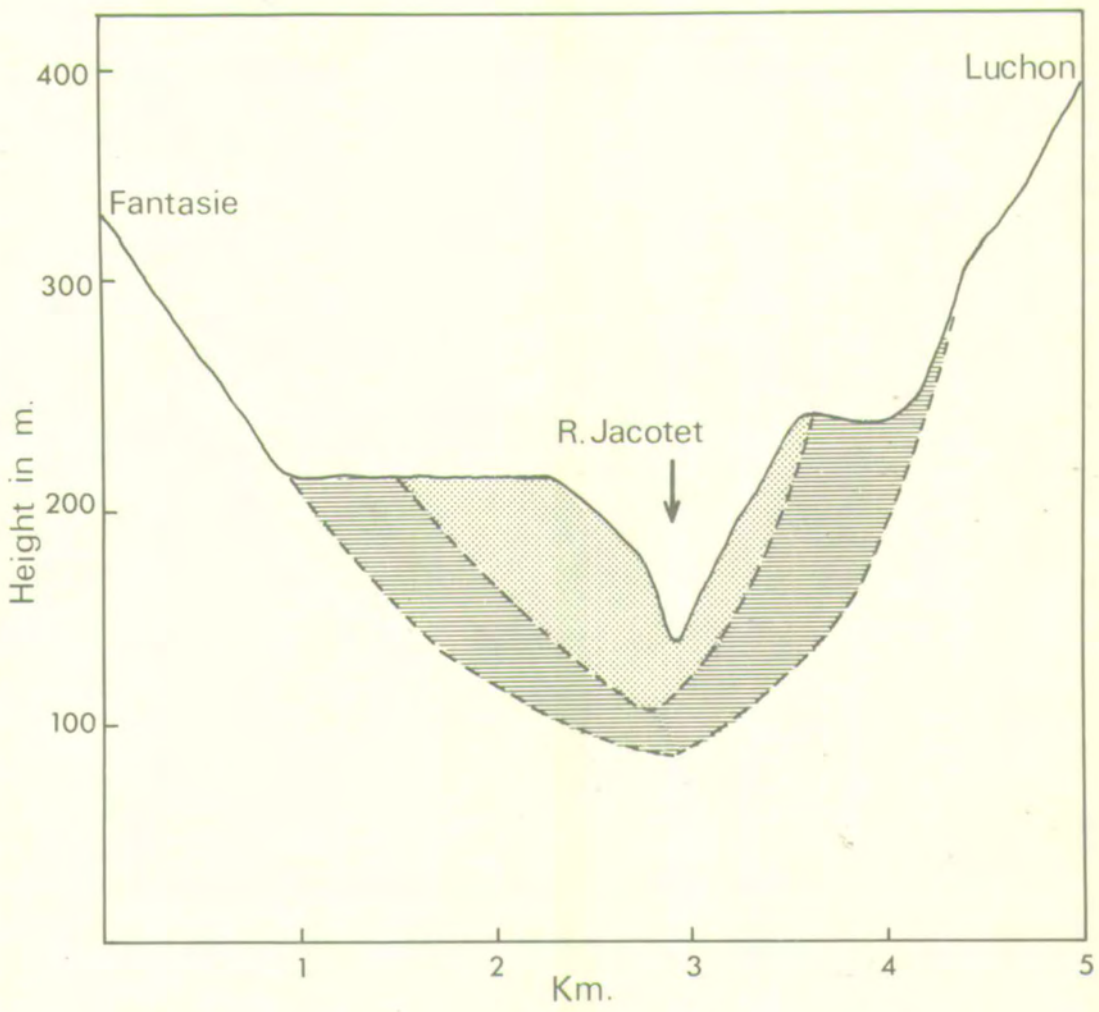
400
300
200
100
Height in m.
Fantasie
Luchon
R. Jacotet
1
2
3
4
5
Km.

Beach rock deposits are occasionally found near the high water mark, indiscriminately cementing reef debris, basalt blocks etc. Evaporation of interstitial water during low tide causes precipitation of calcite between the fragments, eventually cementing them together.

2.6. VOLCANIC EVOLUTION

A sequence of events, first recognised on Hawaii, Stearns (1966) often marks the development of oceanic volcanic islands, and is summarised below:

1. Shield forming phase
2. Caldera or collapse stage
3. Evolved stage - eruption of minor volumes of evolved magma
4. Erosion stage - reduction of shield
5. Rejuvenation stage - eruption of small volumes of strongly undersaturated basalts.

Walker and Nicolaysen (1954) noted the approach of Mauritian volcanism to this scheme, relating the formation of the Older Series to stage 1 and the hawaiites, mugearites and trachytes to stage 3. No indication of a caldera stage was found, but the reduction of the shield was related to stage 4 and the Intermediate Series - some of which are strongly undersaturated - was equated with stage 5.

Although the Mauritian scheme shows some analogy with that on Hawaii, the similarities should not be overstressed, as significant differences occur. In particular the Older Series shield was constructed by "central type" eruptions accompanied by explosive activity and a radial dyke swarm in contrast to the quiet "fissure type" eruption of olivine basalts which constructed Hawaii, while the final phase of activity on Mauritius - the Younger Series - has no direct equivalent on Hawaii.

3. PETROGRAPHY

3.1. INTRODUCTION

Apart from the limited data of Shand (1933), Walker and Nicolaysen (1954) provided the first systematic description of the petrography of the Mauritian volcanics. The Younger and Intermediate Series lavas were classed as alkali olivine basalts, with the latter showing a trend towards more strongly undersaturated basanitoidal compositions. The Older Series was described as a differentiated sequence of oceanites, ankaramites, olivine basalts, feldsparphyric basalts and the more evolved oligoclase basalts, trachyandesites, trachytes and phonolitic trachytes. The normative ol + hy nature of the Older Series was recognised, but as the term tholeiite was then restricted to qz normative compositions, Tilley (1950), an alkaline affinity was implied.

3.2. CLASSIFICATION

A systematic scheme of classification is the basis of any rigorous description of a rock suite. None of the numerous schemes proposed is ideal, but a combination satisfies most requirements. However the disadvantage remains that classification quantifies what is in reality a natural spectrum of compositions. The scheme used for the Mauritian volcanics has two main aims; firstly to separate and define the main magma types, and secondly to provide names for individual rocks within each type. Definition of the main magma types is best achieved by a comparison of their degree of normative saturation and relative alkalinity

and Fig. 3.1., a projection from plagioclase in the normative basalt system Qz - Ne - Di - Ol - Plag and Fig. 3.2., a silica-total alkalis plot, summarise these properties for the Mauritian volcanics. Several points should be noted about Fig. 3.1.:

(1) Only rocks whose normative basalt components > 80% are plotted. This avoids distortion and effectively restricts the projection to basaltic compositions.

(2) The positions of the projected points are sensitive to variations in the oxidation state. Post-magmatic oxidation e.g. by serpentinization or iddingsitisation of olivine, increases normative hypersthene at the expense of olivine. In an attempt to remove this effect, analyses were reduced where necessary to the mean oxidation state of the freshest samples. For the Older Series this corresponds to a ratio ($FeO/FeO + Fe_2O_3$) of 1:3.80 and for the Intermediate and Younger Series 1:6.48. This difference in ratio between the series appears to be real, as reducing the Older Series to 1:6.48 causes it to markedly straddle the basaltic thermal divide (located close to the plane di - ol - plag, and operative to 8 Kb.) producing separate alkalic and tholeiitic groups which is not borne out by the petrography, mineralogy and chemistry, which indicate one coherent series.

(3) Because of their different oxidation states, the <u>absolute</u> position of the Older Series and the other two cannot be compared. This does not apply to comparisons of the Intermediate and Younger Series, both of which have been reduced to the same ratio.

FIG. 3.1.

Normative projection of basaltic compositions from plagioclase onto the planes nepheline-diopside-forsterite and diopside-forsterite-silica. (Mol. %).

1 = Older Series ($FeO/FeO + Fe_2O_3$ = 1:3.80).

2 = Intermediate Series ($FeO/FeO + Fe_2O_3$ = 1:6.48).

3. = Younger Series ($FeO/FeO + Fe_2O_3$ = 1:6.48).

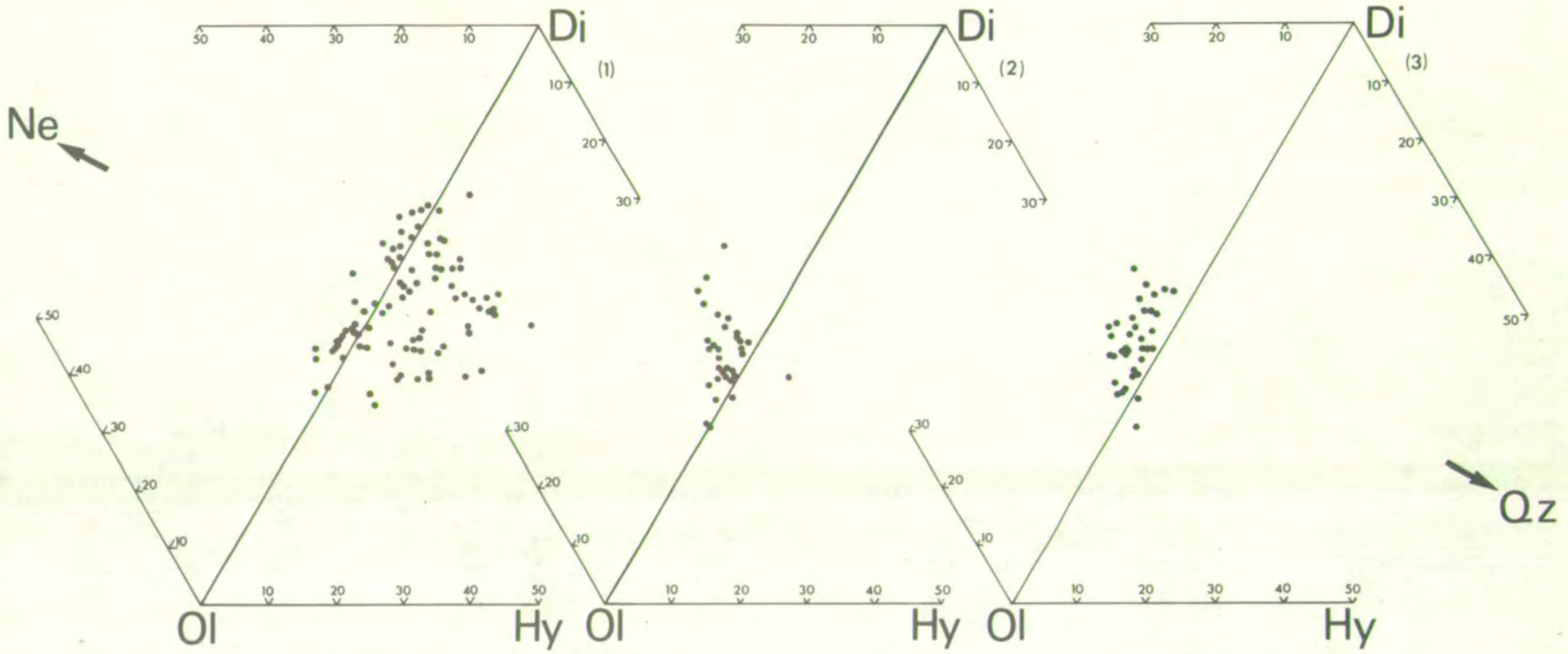
Di
(1)
Ne
Ol
Hy
Di
(2)
Ol
Hy
Di
(3)
Qz
Ol
Hy

(4) The di - ol - plag composition plane and the basaltic thermal divide are not coplanar, the divide extending slightly into the nepheline normative volume, O'Hara (1968). Analyses showing minor normative nepheline may therefore still lie to the tholeiitic side of the divide, this apparent anomaly arising from the use of the plane di - ol - plag as the plane of critical undersaturation in the normative basalt system.

The transitional nature of the Older Series basalts is clear; the bulk of the analyses either show minor normative nepheline and probably lie to the tholeiitic side of the divide or lie in the field of olivine tholeiite as defined by Yoder and Tilley (1962) and termed mildly alkaline and transitional by Coombs (1963). These are characterised by normative olivine + hypersthene and show their alkaline affinities by the absence of an olivine-liquid reaction relationship, the presence of one high calcium clinopyroxene and interstitial groundmass alkali feldspar.

The Intermediate and Younger Series lavas are typical undersaturated alkali olivine basalts with the trend of the Intermediate Series towards basanitoidal compositions apparent.

Fig. 3.2. is a silica total alkalis ($Na_2O + K_2O$) plot with the line subdividing the Hawaiian lavas into tholeiitic and alkaline suites added for comparison. The alkaline nature of the Intermediate and Younger Series is clear, while the alkaline affinities of the Older Series tholeiites are emphasised by comparison with the Hawaiian tholeiites. Oceanic occurrences of transitional tholeiites are not rare,

FIG. 3.2.

Alkali-silica plots for the Mauritian volcanics. Solid line indicates the boundary between Hawaiian tholeiitic and alkaline series, taken from MacDonald and Katsura (1964).

1 = Older Series.

2 = Intermediate Series.

3 = Younger Series.

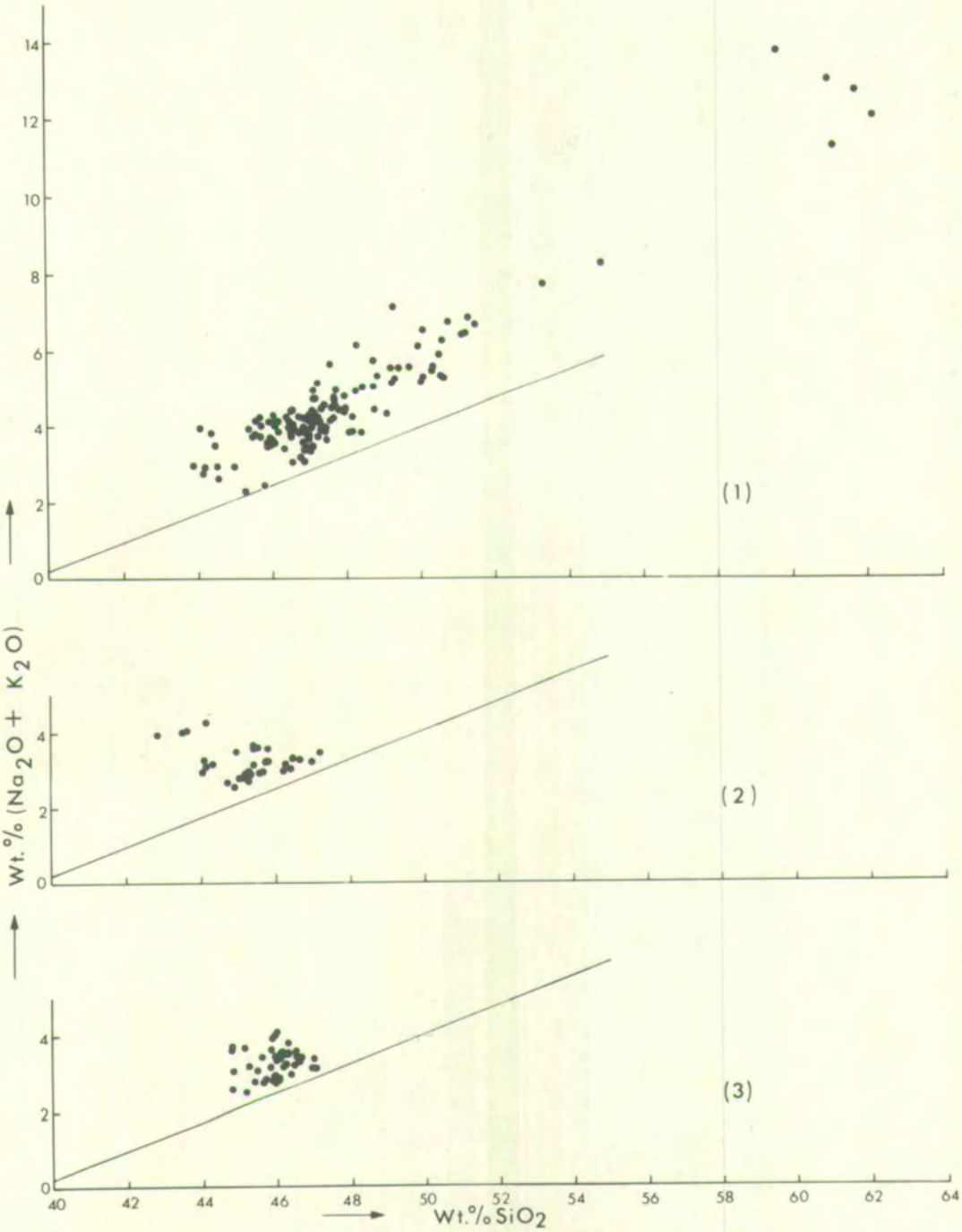
14
12
10
8
6
4
2
0
(1)
Wt.% (Na2O + K2O)
4
2
0
(2)
4
2
0
(3)
40
42
44
46
48
50
52
54
56
58
60
62
64
Wt.% SiO2

e.g. St. Paul, Girod et al. (1971), Anjouan, Flower (1970), Reunion, Upton and Wadsworth (1966), Galapagos, McBirney and Aoki (1966) and Easter Island, Bandy (1937).

Table 3.1. summarises the classification scheme and defines the rock names used. For the basic rocks the definitions follow those of MacDonald and Katsura (1964) but with the marginally nepheline normative basalts and olivine tholeiites grouped under the general term transitional. The classification of the evolved rocks is based on that of Upton (1973, in press) which combines differentiation index and a silica-total alkalis plot in a determinative grid. The precise boundaries between the evolved groups are somewhat arbitrary, c.f. Tilley and Muir (1964), Thompson et al. (1972) and reflects the inherent difficulty in classifying a continuum of compositions.

3.3. GENERAL PETROGRAPHY

Individual petrographic data for all analysed specimens is tabulated in Appendix 4. The scope of this section is to describe and compare the general petrography of the rock types within the three series. Table 3.2. summarises the distribution of rock types through the series and Table 3.3. is a comparison of their phenocryst assemblages.

TABLE 3.1.

CLASSIFICATION OF MAURITIAN VOLCANICS

SERIES	OLDER SERIES		INTERMEDIATE & YOUNGER SERIES	
CHARACTER	TRANSITIONAL		UNDERSATURATED	
NORM	OL + HY OR MINOR NE	ESSENTIAL PHENOCRYSTS	Ne < 5%	Ne > 5%
D.I. < 35 T.A. < 5.0	PICRITE BASALT / OCEANITE / ANKARAMITE	O > C O ± C > 15% C > O	OCEANITE	
	TRANSITIONAL OLIVINE BASALT	5% < O ± C < 15%	ALKALI OLIVINE BASALT	OLIVINE BASANITOID
	TRANSITIONAL BASALT	O ± C < 5%	ALKALI BASALT	BASANITOID
	FELDSPARPHYRIC BASALT	$P > 15\% \ (\pm \frac{O}{C} \ T < 5\%)$		
35 < D.I. < 50 3.0< T.A. <7.0	HAWAIITE			
50 < D.I. < 65 7.0< T.A. <10.0	MUGEARITE			
65 < D.I. < 80 8.0< T.A.<13.5	BENMOREITE (ABSENT)			
D.I. > 80 T.A. > 8.0	TRACHYTE / 0-10% NORM Ne PHONOLITIC TRACHYTE			

O = OLIVINE

C = CLINOPYROXENE

P = PLAGIOCLASE

T = TITANOMAGNETITE

D.I. = DIFFERENTIATION INDEX

T.A. = TOTAL ALKALIS ($Na_2O + K_2O$)

TABLE 3.2.

RELATIVE DISTRIBUTION OF MAURITIAN ROCK TYPES

ROCK TYPE	OLDER SERIES	INTERMEDIATE SERIES		YOUNGER SERIES	
	TRANSITIONAL	ALKALINE	BASANITOIDAL	ALKALINE	BASANITOIDAL
PICRITE BASALT	9.3%	10.0%	6.0%	-	-
OLIVINE BASALT	26.2%	60.0%	18.0%	60.0%	8.0%
BASALT	26.2%	6.0%	-	30.0%	2.0%
FELDSPARPHYRIC BASALT	3.5%				
HAWAIITE	25.3%				
MUGEARITE	6.0%				
TRACHYTE & PHONOLITIC TRACHYTE	3.5%				

TABLE 3.3.

PHENOCRYST ASSEMBLAGES IN MAURITIAN VOLCANICS

OLDER SERIES

1. OLIVINE.
2. OLIVINE + CLINOPYROXENE.
3. OLIVINE + CLINOPYROXENE + PLAGIOCLASE.
4. OLIVINE + PLAGIOCLASE + TITANOMAGNETITE.
5. OLIVINE + CLINOPYROXENE + PLAGIOCLASE + TITANOMAGNETITE.
6. OLIVINE + CLINOPYROXENE + PLAGIOCLASE + TITANOMAGNETITE + KAERSUTITE.
7. OLIVINE + CLINOPYROXENE + PLAGIOCLASE + TITANOMAGNETITE + KAERSUTITE + APATITE.
8. OLIVINE + CLINOPYROXENE + PLAGIOCLASE + ANORTHOCLASE.
9. ANORTHOCLASE.
10. ANORTHOCLASE + NEPHELINE
11. ANORTHOCLASE + NEPHELINE + CLINOPYROXENE

INTERMEDIATE SERIES

1. OLIVINE.
2. OLIVINE + CLINOPYROXENE.

YOUNGER SERIES

1. OLIVINE.
2. OLIVINE + PLAGIOCLASE.

A. OLDER SERIES.

Picrite Basalts (Plates 3.1., 3.2.)

Oceanites and ankaramites are brought together under the heading of picrite basalts to emphasise the gradation from one to the other. Oceanites make up 85% of the picrite basalts sampled, but carry up to 13.5% by volume of clinopyroxene phenocrysts. Olivine phenocrysts show compositional variation from Fo_{81-70} and typically occur as euhedral and more rarely anhedral crystals up to 5 mm. long. Iddingsitisation is common, particularly at crystal margins, with occasional fresh olivine overgrowths indicating at least some of the alteration to be high temperature and pre-consolidation. Two generations of olivine phenocrysts are present in some oceanites (e.g. A163), an euhedral group, crystallized from the lava, and an anhedral group showing strain lamellae and almost certainly derived from actively disintegrating dunite inclusions found in these lavas. Opaque spinels are commonly included in the olivine phenocrysts, which show no obvious compositional zoning. Clinopyroxene phenocrysts are generally fresh, euhedral and up to 8 mm. long. Zoning is common, and typically colourless - green diopside or pale brown diopsidic - augite cores are zoned to purple titanaugite rims, compositionally indistinguishable from the groundmass pyroxene. Plagioclase phenocrysts are rare, occurring in only one sample (A10, An_{68}) where it reaches 3.5% by volume. The groundmass texture varies from granular to intersertal with occasional sub-alignment of plagioclase lathes. Typically the groundmass consists of olivine, pale brown to

PLATE 3.1. (x 7) Plane Polarised Light.

Oceanite (A118) from the Older Series.
Euhedral-subhedral olivine phenocrysts in
a slightly vesicular fine grained groundmass.

PLATE 3.2. (x 6) Plane Polarised Light.

Ankaramite (A228) from the Older Series.
Euhedral-subhedral olivine (white) and
clinopyroxene (grey) phenocrysts.

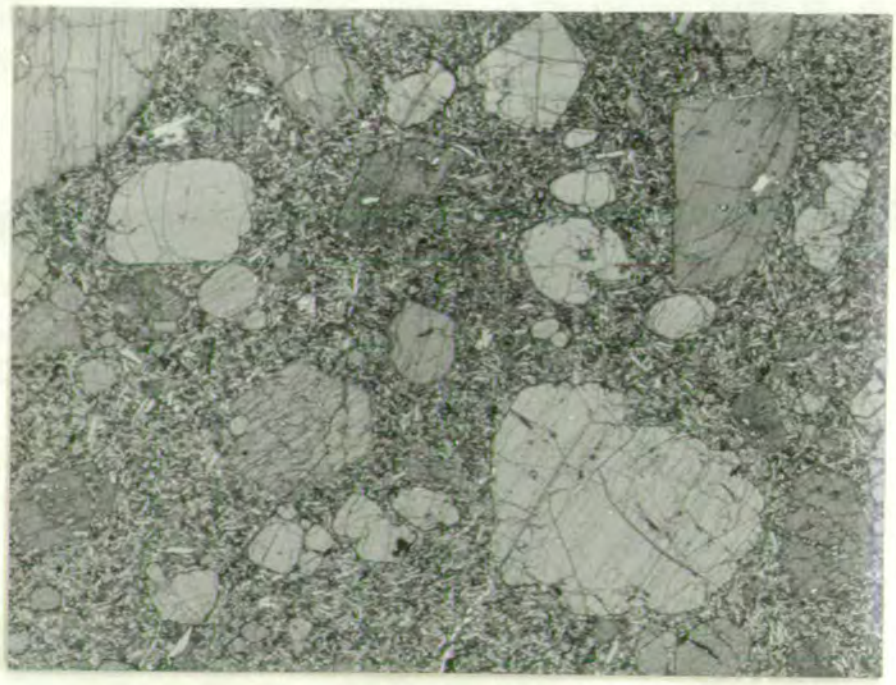

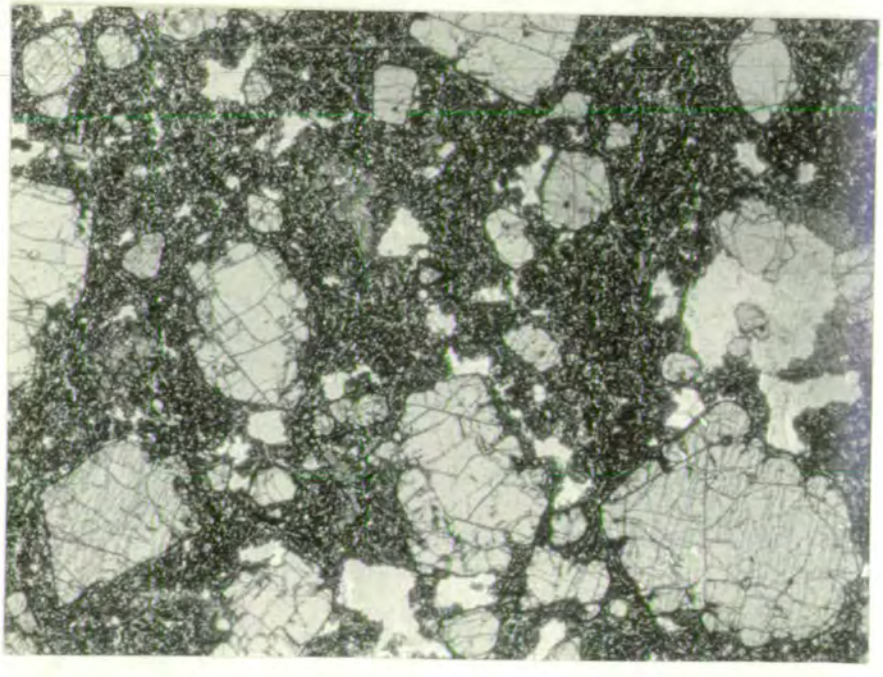

purple titanaugite, plagioclase (An_{65-55}), titanomagnetite octahedra and more rarely, ilmenite lathes, and interstitial alkali feldspar. Accessory apatite needles are present.

Transitional Olivine Basalts (Plate 3.3.)

With decreasing ferromagnesian phenocryst content, picrite basalts pass into olivine basalts. Plagioclase phenocrysts (An_{73-54}) are found in 50% of these lavas and generally form between 1-3% by volume. Other than the increased occurrence of plagioclase, these lavas show the same mineralogical and textural features as the picrite basalts.

Transitional Basalts (Plate 3.4.)

The term is restricted here to rocks of basaltic composition with less than 5% phenocrysts, typically olivine, (Fo_{81-70}) and a pale brown zoned augite rather than the diopsidic augites of the picrite and olivine basalts. Phenocryst plagioclase is uncommon and occurs in only 15% of the samples where it may reach 3% by volume. Typically euhedral, the phenocrysts are zoned from An_{68-52}, with occasional andesine rims.

The more basic samples have essentially the same groundmass mineralogy as the picrite and olivine basalts, but types transitional to hawaiite show increased groundmass titanomagnetite octahedra, reduced olivine and increased plagioclase, generally more sodic (An_{52-48}). Groundmass textures are similar, but with increasing plagioclase content, flow alignment becomes prominent.

PLATE 3.3. (x 30) Plane Polarised Light.

Transitional olivine basalt (A123) from the Older Series.

Large subhedral marginally iddingsitised olivine phenocryst and rounded clinopyroxene in a fine grained groundmass.

PLATE 3.4. (x 10) Plane Polarised Light.

Transitional basalt (A160) from the Older Series.

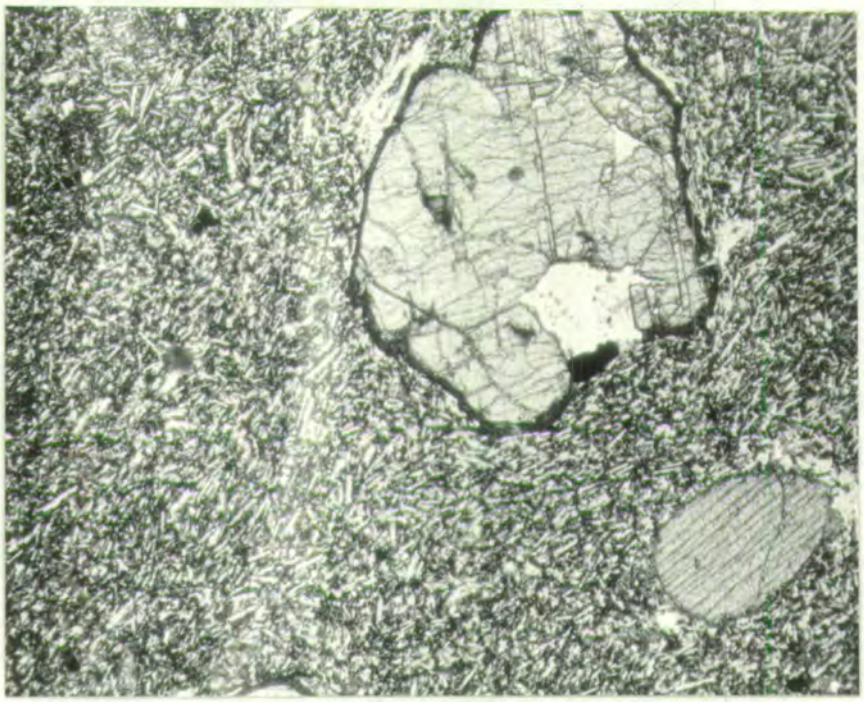

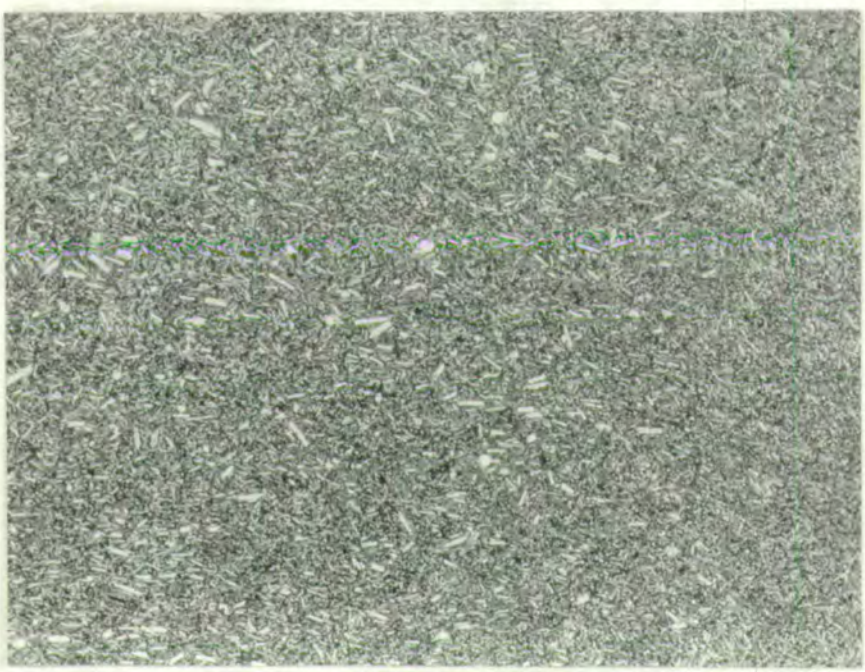

Feldsparphyric Basalts (Plate 3.5.)

These are a rare but petrographically distinct group of rocks on Mauritius, forming only 3% of samples collected from the Older Series. They occur predominantly in the post shield phase of the Older Series, with hawaiites and mugearites, to which they may be genetically related.

Typically they are basic rocks (D.I. < 35), highly porphyritic (> 20%), with plagioclase as the dominant phenocryst phase (< 30%) and minor olivine (Fo_{76}, < 3.5%) and titanomagnetite (< 3%). The plagioclase is distinctly more calcic (An_{88-76}) than is found in the rest of the Older Series and occurs both as euhedral phenocrysts and angular polycrystalline inclusions. There is no pronounced embayment or marginal zonation of the phenocrysts or inclusions, which are apparently in equilibrium with the groundmass of olivine, pale brown augite, titanomagnetite, plagioclase (An_{68-60}) and interstitial alkali feldspar.

Hawaiites (Plate 3.6.)

Basalts grade naturally into more evolved Hawaiites and the transition is marked in the groundmass by decreasing olivine, increasing titanomagnetite and plagioclase - generally a zoned andesine. The Mauritian hawaiites fall into two broad, petrographically distinct but chemically overlapping groups, one feldsparphyric, which makes up 70% of the hawaiites, and an aphyric group.

Feldsparphyric hawaiites carry up to 28% of phenocrysts, predominantly plagioclase (< 15%) but with olivine (< 4%), clinopyroxene (< 8%), titanomagnetite (< 3%) and kaersutite

PLATE 3.5. (x 9) Plane Polarised Light.

Feldsparphyric basalt (A190) from the Older Series.

Euhedral-subhedral plagioclase phenocrysts in a fine grained groundmass.

PLATE 3.6. (x 9) Plane Polarised Light.

Hawaiite (A269) from the Older Series.

Sub-aligned plagioclase, ore rimmed kaersutite and clinopyroxene phenocrysts in a fine grained plagioclase rich groundmass.

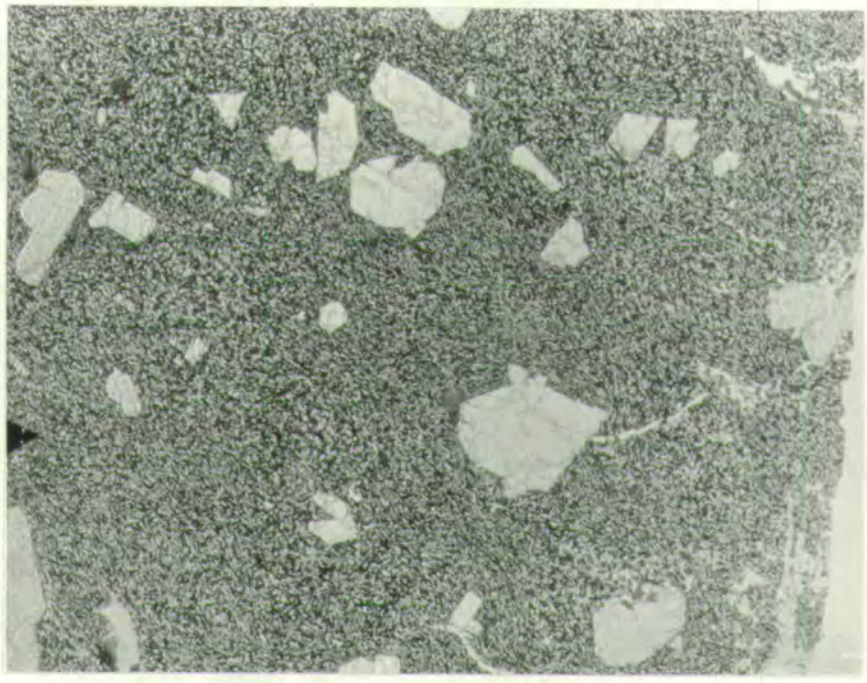

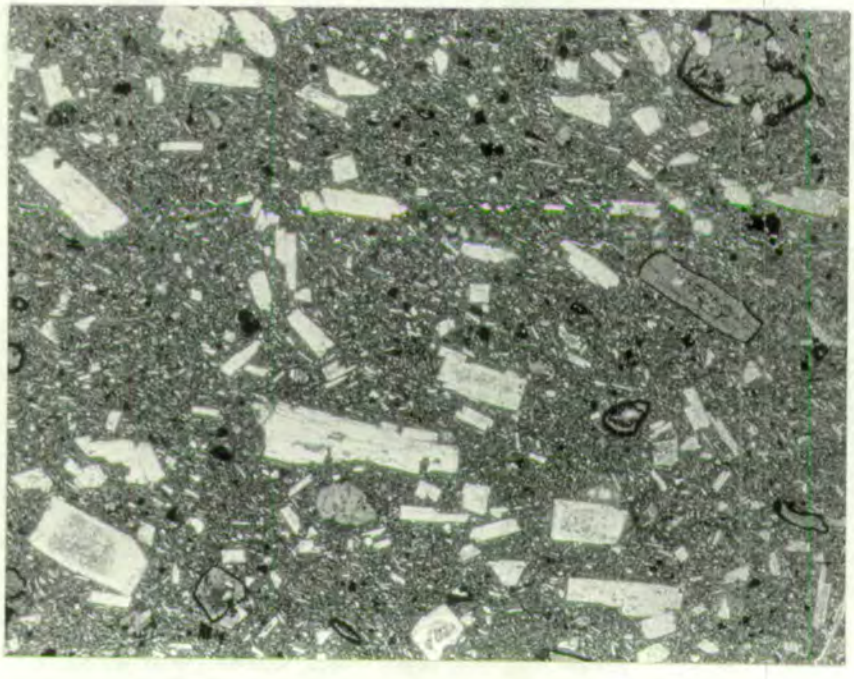

(< 5%). Plagioclase phenocrysts are typically euhedral and zoned from labradorite (An_{66-50}) cores to andesine (An_{48-32}) margins, with occasional alkali feldspar mantles. Clinopyroxene phenocrysts are generally zoned, euhedral brown-purple titanaugites often with deeply coloured rims, while euhedral iddingsitised olivine phenocrysts are more common in types transitional to basalt. The relative iron enrichment of the hawaiites is reflected in the occurrence of phenocrystal titanomagnetite, typically as large euhedral octahedra. Strongly pleochroic kaersutite phenocrysts are found in the more evolved hawaiites and their strong disequilibrium with the liquid, at the time of quenching, is indicated by the development of broad opacite rims, culminating in opacite pseudomorphs.

The aphyric hawaiites and the groundmass of the feldsparphyric group is dominantly composed of zoned andesine (An_{41-28}), purple-brown titanaugite, titanomagnetite and olivine, with interstitial alkali feldspar. The aphyric group and the groundmass of feldsparphyric hawaiites transitional to basalt, are generally richer in mafic minerals. Textures vary from intersertal to trachytoid in the more evolved plagioclase rich hawaiites.

Mugearites (Plate 3.7.)

Like the more basic hawaiites, Mauritian mugearites can be broadly separated into a feldsparphyric group, forming approximately 70% of the samples, and an aphyric group.

The feldsparphyric mugearites contain up to 15% by

PLATE 3.7. (x 7) Plane Polarised Light.

Mugearite (A267) from the Older Series.

Plagioclase (white), clinopyroxene (grey) and titanomagnetite phenocrysts (black) in a fine grained groundmass.

PLATE 3.8. (x 30) Plane Polarised Light.

Phonolitic trachyte (A264) from the Older Series.

Anorthoclase (white) and aegirine-augite (dark grey) phenocrysts set in a highly fluidal groundmass.

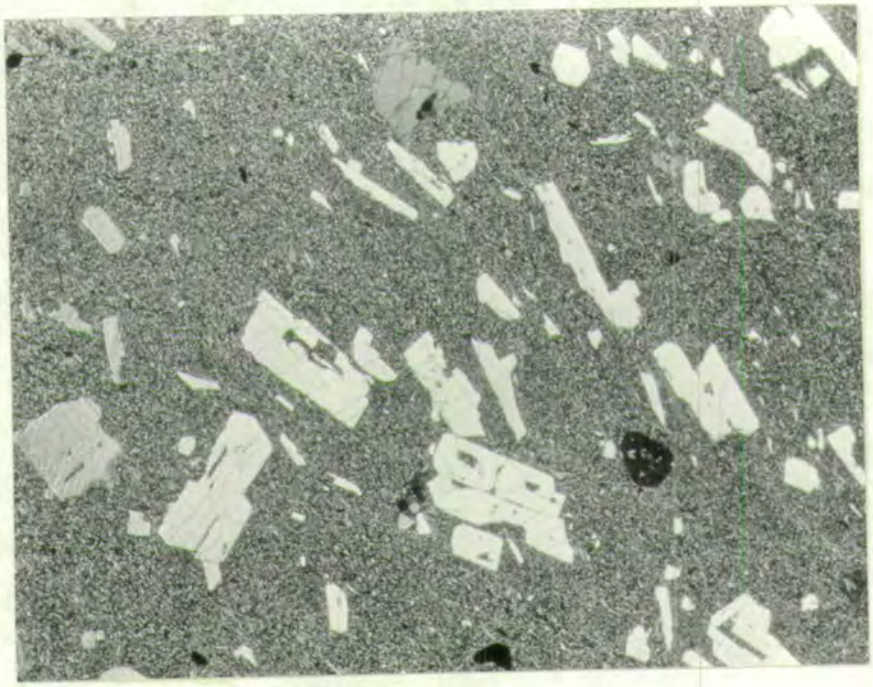

volume of phenocrysts, mainly plagioclase (< 16%) showing andesine (An_{45-30}) cores zoned to oligoclase (An_{15}) margins, but with minor olivine (< 1.8%), clinopyroxene (< 1.3%), titanomagnetite (< 1.0%), apatite (< 0.8%), kaersutite (trace) and alkali feldspar (trace). Anorthoclase phenocrysts appear in the most evolved mugearite, A78 (D.I. = 62), apparently in equilibrium with oligoclase (An_{15}), indicating that the liquid encountered a two feldspar field. Euhedral iddingsitised olivines are relatively rare as is clinopyroxene, which occurs as a brown ferroaugite, or greenish slightly pleochroic aegerine-augite, the high alkali content of the group being reflected in the uptake of Na^+ into the pyroxene structure. Apatite phenocrysts appear for the first time, and are unique to the mugearites. They typically occur as euhedral crystals crowded with minute, acicular, brown, high birefringence inclusions - probably rutile. Similar inclusions in apatites are described by Le Maitre (1962), from Gough Island. The apatites show a distinct association with titanomagnetite phenocrysts, and the rutile inclusions increase noticeably towards them, suggesting an origin in apatite growth adjacent to areas of high titanium concentration.

Aphyric mugearites have essentially the same mineralogy as the groundmass of the feldsparphyric group, with zoned oligoclase (An_{30-14}), titanomagnetite, brown-mauve clinopyroxene, apatite, minor olivine and interstitial alkali feldspar. The more evolved mugearites are distinctly poor in olivine and rich in oligoclase, with reduced titanomagnetite. Textures are typically sub-trachytoid to trachytoid.

Trachytes and Phonolitic-Trachytes (Plate 3.8.)

These represent the most evolved compositions of the Older Series and at the present erosion level are volumetrically scarce, forming only 3.5% of samples collected.

Trachytes ..... (Norm. Qz or Hy) A249, A261

Phonolitic Trachytes .... (Norm. Ne < 10%) A185, A260, A264.

The subdivision of the group is based on the degree of normative saturation. Three of the samples are significantly undersaturated and are termed phonolitic trachytes. The other two samples are just saturated but show some discordance between modal and normative mineralogy, e.g. A249, with 2% normative hypersthene carries approximately 5% modal phenocryst nepheline. It seems likely that the 1:3.80 oxidation ratio is insufficiently reducing for these iron depleted compositions and that in reality, A249, and probably A261 are mildly undersaturated.

All the trachytes are porphyritic, carrying up to 25% phenocrysts. Anorthoclase phenocrysts occur in all samples, reaching 25% by volume in A264, typically euhedral, fresh, marginally zoned, simply twinned and showing fine cross-hatch twinning. Phenocryst nepheline is found in three samples (A185, A249, A260) reaching 10% by volume. Microphenocryst aegirine-augite occurs in two samples (A185, A264).

The groundmass is invariably flow aligned, composed mainly of anorthoclase, with flakes of aegirine-augite and minor aenigmatite; nepheline is rarely seen in the groundmass. Rare marginally oxidised fayalitic olivines are found in the groundmass of A261.

Inclusions

Three groups of inclusions are found in the Older Series volcanics, and each shows a specific association with a particular rock type, viz:

Inclusion	Association
Ultrabasic: dunite and wehrlite	Picrite basalts and phyric olivine basalts, Lion Mtn, Tamarin Mtn, Pt. Louis.
Bytownitic anorthosite	Feldsparphyric basalts, Mt. Laporte and Black River gorge.
Mafic syenite (1 occurrence only).....	Phonolitic trachyte, Piton de Milieu.

(i) Ultrabasic inclusions: dunite and wehrlite (Plates 3.9., 3.10.)

These are restricted to the more olivine rich basalts and typically occur as small (< 10 cm. diameter) angular fragments. A subdivision can be recognised within this group separating inclusions carrying deformed olivine from those with undeformed olivine crystals. Strain lamellae in olivines are generally accepted as resulting from solid state deformation and implies that these inclusions were once part of a consolidated body which was subsequently stressed. Inclusions of this type are found on Tamarin and Lion mountains and vary from dunites with interstitial patches of a greenish diopsidic-augite, to rarer wehrlites with diopsidic augite poikilitically enclosing olivine crystals. Comparison of olivine from the host lava and the inclusions indicates them to be compositionally indistinguishable (Fo_{81}), and the inclusions can often be seen in a degraded form, feeding deformed

PLATE 3.9. (x 5) Plane Polarised Light.

Dunite inclusion in the Older Series transitional olivine basalt (A224).

PLATE 3.10. (x 6) Plane Polarised Light.

(Central portion of plate). Wehrlite inclusion in the Older Series oceanite (A24).

Centre of inclusion shows rounded olivines poikilitically enclosed in clinopyroxene.

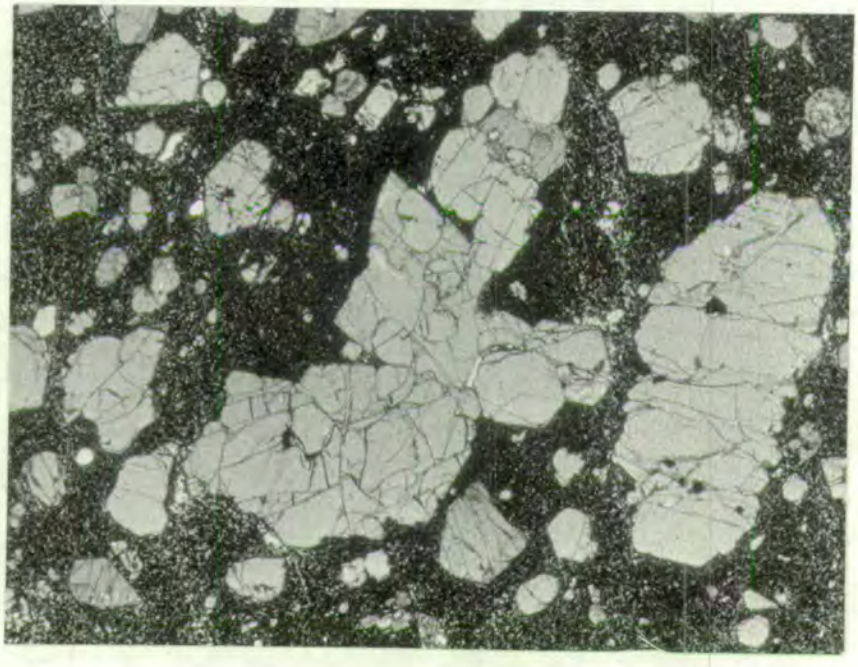

olivine crystals to the lavas.

Inclusions carrying undeformed olivines are found in the pyroxene rich picrite basalts of the Port Louis mountains. Typically they occur as sub-rounded fragments (< 1 cm. diameter) of wehrlite with green unzoned diopsidic augite poikilitically enclosing large olivine phenocrysts, and are compositionally indistinguishable from the phenocryst phases in the lavas.

(ii) Bytownitic anorthosites (Plate 3.11.)

These occur as small (< 1 cm. diameter) inclusions within the feldsparphyric basalts and are composed of large interlocking, unzoned plagioclase crystals (An_{88-76}) identical to the phenocrysts, with rare interstitial titanomagnetite. General equilibrium between the inclusion and host lava is indicated by the absence of strong marginal zonation, and the linear unresorbed margins of the inclusions.

(iii) Mafic Syenite (Plate 3.12.)

One small angular inclusion of a mafic syenite was found in the Piton de Milieu trachyte showing reaction margins indicative of strong disequilibrium with the host magma. It is composed of large subhedral antiperthite feldspars with interstitial kaersutite, biotite, aegirine-augite and occasional titanomagnetite and accessory apatite.

Both the ultrabasic and anorthositic inclusions display textures similar to those of cumulates from layered mafic plutons, Wager (1968). In particular the wehrlites, with

PLATE 3.11. (x 7) Plane Polarised Light.

Bytownitic anorthosite inclusions in the Older Series feldsparphyric basalt (A193).

PLATE 3.12. (x 9) Plane Polarised Light.

Mafic syenite inclusion in the phonolitic trachyte (A264).

Description in text. Host trachyte is shown in lower left hand margin of plate.

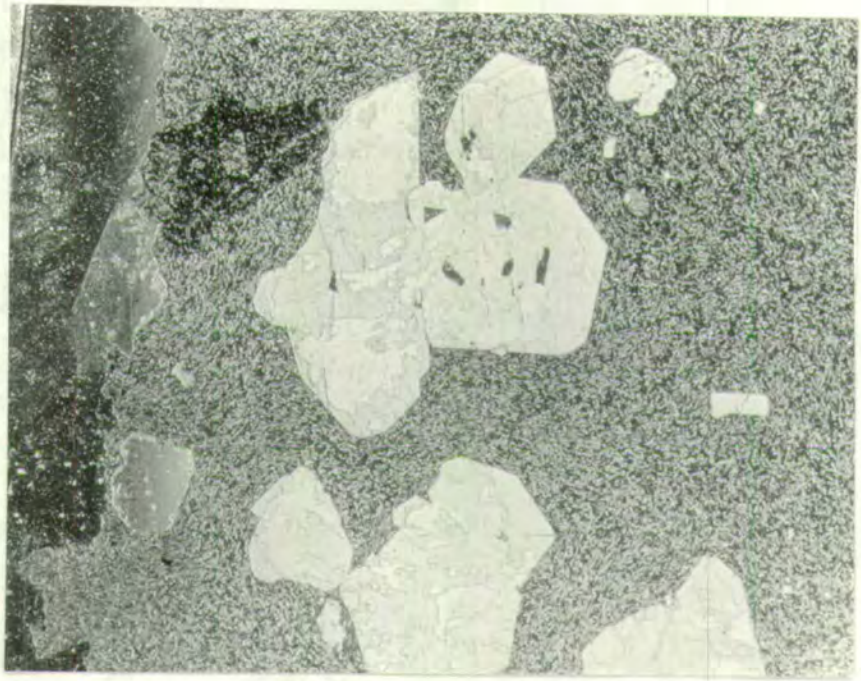

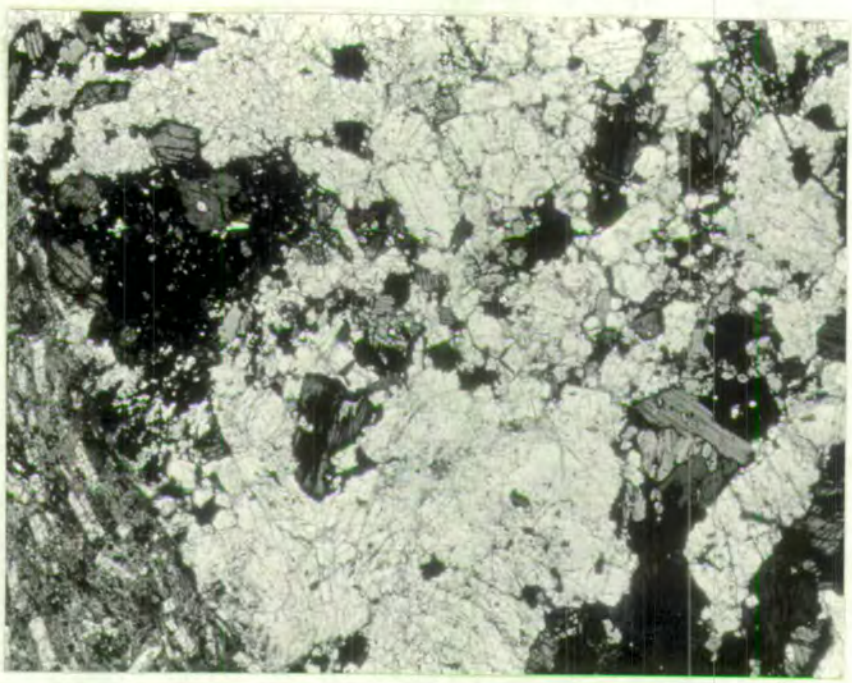

clinopyroxene poikilitically enclosing olivine, could be described as olivine heteradcumulates and the unzoned virtually monominerallic anorthosites, as adcumulates. It seems possible that the inclusions could be derived from layered cumulates in some sub-volcanic magma chamber. The association of inclusions with porphyritic magmas is striking and it is apparent that in some cases, cumulus enrichment of the lavas is being effected by the addition of degraded inclusion material. More importantly in carrying the inclusions, the lavas must have been adjacent to the source material and it seems reasonable that they themselves represent cumulus enriched magmas from near the floor of the magma chamber.

B. INTERMEDIATE SERIES (Plates 3.13., 3.14)

The renewal of volcanic activity on Mauritius, with the eruption of the Intermediate Series lavas, marks a change of magma type from the transitional tholeiites of the Older Series to a suite of alkali olivine basalts with basanitic affinities. The transition from alkali basalt to basanite is set arbitrarily at 5% normative nepheline, MacDonald and Katsura (1964). As none of the Intermediate Series basanites carry modal nepheline, they are more correctly termed basanitoids.

Alkali olivine basalt is the dominant rock type of the series (60%), with subordinate alkali basalts (6%) and oceanites (10%). Basanitoids form 24% of the series, mainly alkali olivine basanitoids (18%) and minor oceanitic basanitoids (6%).

PLATE 3.13. (x 28) Plane Polarised Light.

Alkali olivine basanitoid (B6) from the Intermediate Series.

Subhedral olivine and euhedral prismatic clinopyroxene phenocrysts.

PLATE 3.14. (x 30) Plane Polarised Light.

Oceanite (B29) from the Intermediate Series.

Marginally iddingsitised olivine phenocrysts in a fine grained groundmass. Note elongate olivine phenocryst with pronounced axial cavity.

PLATE 3.15. (x 100) Plane Polarised Light.

Skeletal olivine microphenocryst in the Intermediate Series oceanite (B33).

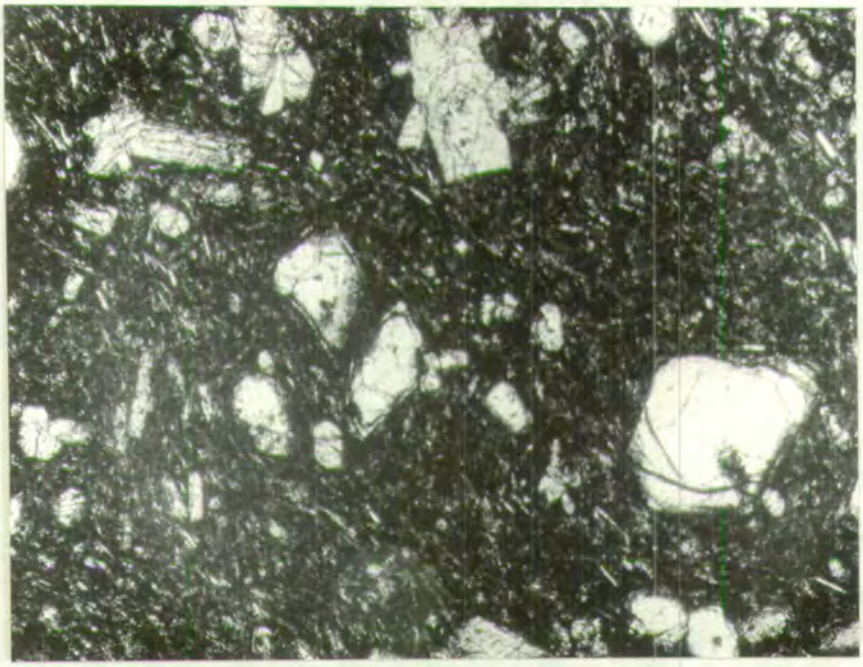

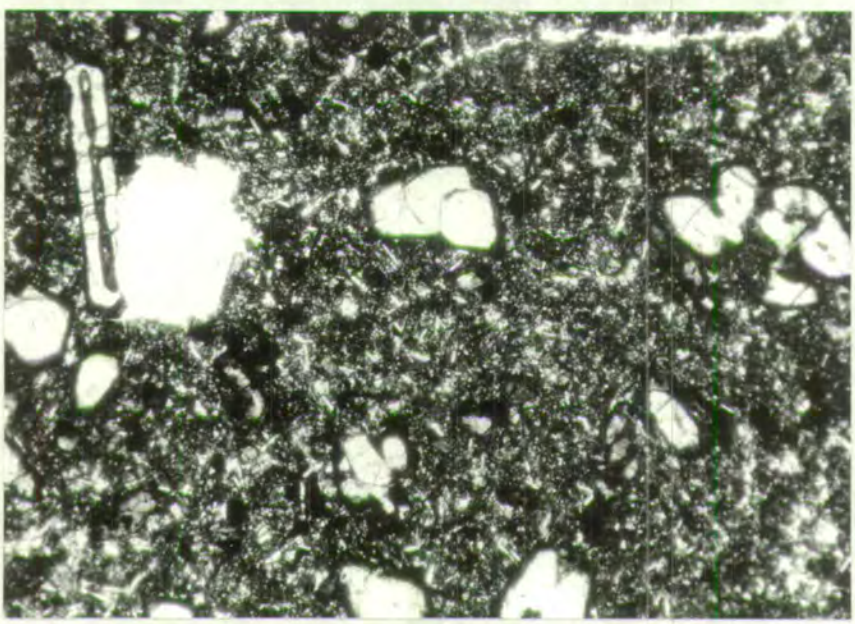

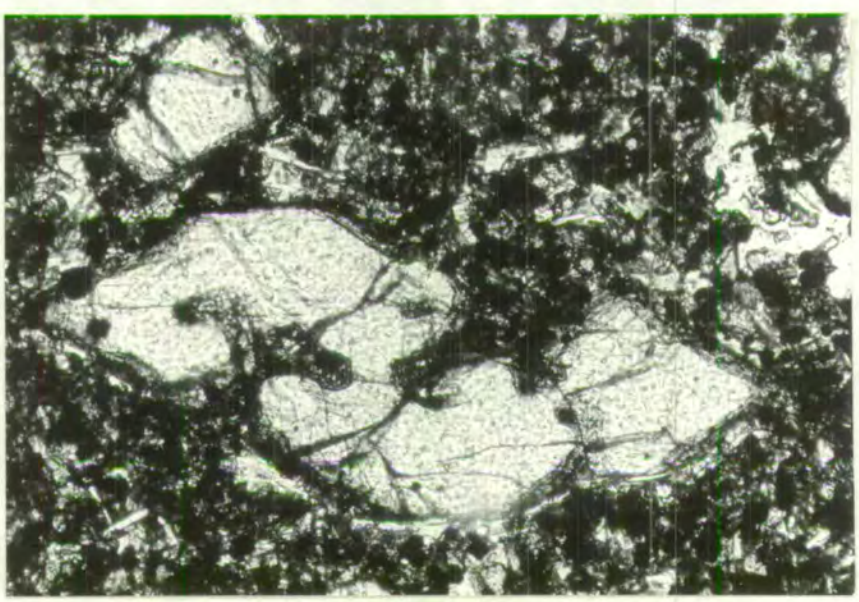

The lavas are mildly vesicular (Average 5%, range 0-20%) and are typically microphyric, with olivine as the dominant microphenocryst phase. Olivine microphenocryst compositions vary from Fo_{90-71} and crystals are generally euhedral, marginally iddingsitised and often display skeletal form, showing axial cavities, deep embayments and arrowhead terminations (Plate 3.15.), and probably resulting from rapid extrusion and quenching of these lavas. Two generations of olivine are recognised in some samples, with the appearance of anhedral crystals showing strain lamellae - and possibly derived from degraded dunite inclusions.

Clinopyroxene appears as a minor microphenocryst phase in the more undersaturated basanitoids, reaching a maximum of 2.2% by volume. Typically it occurs as subhedral crystals of colourless-green diopsidic augite with zoned rims of mauve titanaugite indistinguishable from the groundmass pyroxene.

With varying microphenocryst content, the alkali olivine basalts pass into oceanites and alkali basalts. The groundmass varies from medium to fine grained and texturally from intersertal to sub-ophitic in the coarser samples. Typically it is composed of olivine, mauve-purple titanaugite, zoned plagioclase (An_{64-50}) and scattered titanomagnetite octahedra, with interstitial alkali feldspar. Minor interstitial brown glass occurs in the finer grained groundmasses. The most undersaturated basanitoids appear to be relatively reduced in plagioclase and enriched in titanaugite.

C. YOUNGER SERIES (Plates 3.16., 3.17)

The Younger Series lavas are the product of the final magmatic event on Mauritius, and are volumetrically much more extensive than the Intermediate Series lavas. They form a group of alkali olivine basalts (70%) and alkali basalts (30%), 10% of which fall just in the basanitoid field, with a maximum of 7.8% normative nepheline. The rocks are relatively highly vesicular (Average 12%, Range 0-37%) and are generally fresh. Complete gradation is seen between two end member textural types. The first, a phyric olivine basalt has a fine granular-intersertal groundmass and generally occurs around the vents. The second type is an extremely coarse grained ophitic olivine basalt, in which it is virtually impossible to discriminate between phenocryst and matrix, with any degree of accuracy.

Olivine is the dominant phenocryst in the Younger Series, varying from Fo_{86-72} and found as euhedral, often skeletal crystals in the vent type and as large rounded crystals in the coarser variants. Marginal iddingsitisation is common, with fresh olivine overgrowths frequently seen in the coarser lavas.

Plagioclase appears as a minor phenocryst phase in some more evolved, less magnesian rocks of the vent type and apparently also in some evolved coarse grained lavas - although again the grain size makes accurate assessment difficult. Typically euhedral and often strongly zoned, the plagioclase ranges from An_{68-52}.

The groundmass of the venttype is typically granular

PLATE 3.16. (x 30) Plane Polarised Light.

"Vent type" alkali olivine basalt (C54) from the Younger Series.

Subhedral marginally iddingsitised olivine phenocrysts set in a sub ophitic groundmass.

PLATE 3.17. (x 16) Plane Polarised Light.

Coarse ophitic alkali olivine basalt (C76), from the Younger Series.

Plagioclase (white), olivine (light grey), clinopyroxene (dark grey).

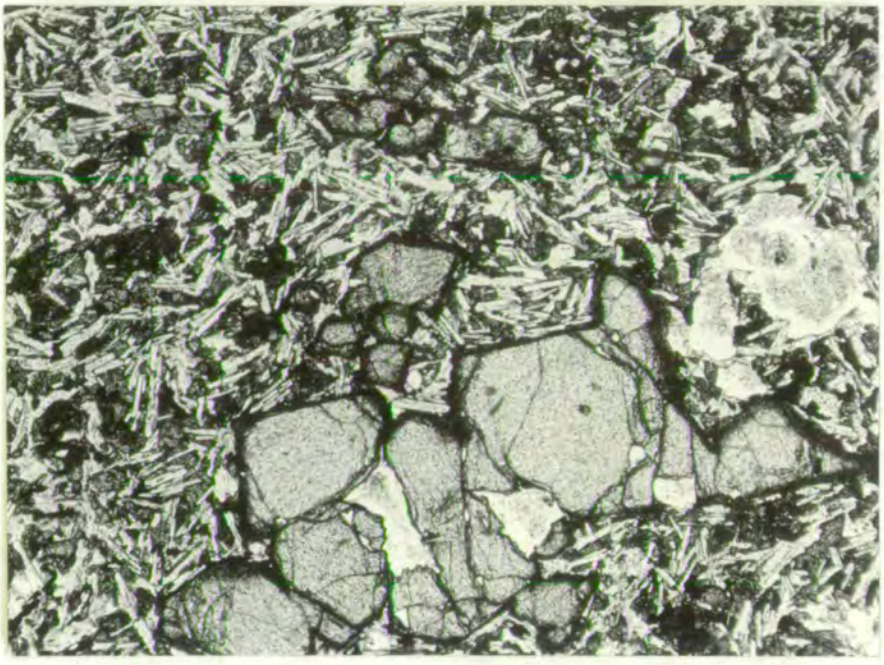

to intersertal and consists of brown-mauve titanaugite, plagioclase, olivine, titanomagnetite octahedra and interstitial alkali feldspar. In the coarse type the groundmass texture is ophitic, with large mauve-brown titanaugites, zoned strongly to deep purple margins which may be rimmed by a pleochroic deep green aegirine-augite, zoned plagioclase (An_{60-52}) of highly variable size, rounded olivines, titanomagnetite octahedra and large interstitial pockets of alkali feldspar. The extreme zonation seen in the pyroxenes and the coarseness of the group may have an origin in rapid crystal growth in a fast cooling flow, producing extreme <u>in situ</u> fractionation of the liquid.

4. MINERALOGY

4.1. INTRODUCTION

The effectiveness of crystal fractionation as a major process producing differentiation of parental basalt magmas under near surface conditions has been repeatedly demonstrated by workers over the last fifty years. More recently it has been shown that most erupted basalts are highly evolved relative to the partial melts of likely mantle material and that they represent, in part at least, the products of polybaric crystal fractionation of these primitive magmas, O'Hara (1968). It is clear that in order to evaluate the role of crystal fractionation in the Mauritian lavas, a knowledge of their mineral chemistry - particularly phenocryst phases - is required.

Forty-five partial or complete chemical analyses of minerals from the three Mauritian series are presented, along with relevant optical determinations. A variety of analytical techniques was used, including XRD, XRF and Electron Microprobe, the method for any one analysis being a function of the relative abundance of the mineral, its ease of separation and the particular analytical requirements. Sample preparation, analytical techniques and estimates of their precision are described in appendices (1) and (2).

4.2. OLIVINE

Analyses of twenty-three olivines from the three Mauritian lava series are presented in table 4.1.

TABLE 4.1.

ANALYSED OLIVINES FROM MAURITIAN VOLCANICS

Oxides in wt.%

Trace elements in p.p.m.

O = Oceanite

A = Ankaramite

FB = Feldsparphyric basalt

H = Hawaiite

D = Dunite

AOB = Alkali olivine basalt

AOBtd = Alkali olivine basanitoid

* = Probe analysed sample without separate FeO, Fe_2O_3 determinations.

n.d. = not done.

OLDER SERIES

Rock No.	A24	A28	A246	A228 Core	A228 Rim	A69	A20	A268	A170	A170
Rock Name	O	O	A	A	A	FB	H	H	D Nodule	O Host
Analytical Method	XRF	XRF	XRF	PROBE	PROBE	XRD	XRD	XRD	XRD	XRD
Occurrence	Pheno	Pheno	Pheno	Pheno	Pheno	Pheno	Pheno	Pheno	Nodule	Pheno
Mol.% Fo	81.10	77.80	79.40	81.60	79.96	70.90	74.70	71.00	81.00	81.00
SiO_2	39.55	39.10	39.10	38.46	38.37					
Al_2O_3	0.63	0.62	0.59	0.00	0.00					
TiO_2	0.12	0.13	0.10	0.00	0.00					
Fe_2O_3	0.10	0.16	0.25	*	*					
FeO	17.40	20.00	18.63	17.52	18.89					
MnO	0.22	0.24	0.24	n.d.	n.d.					
MgO	42.22	39.61	40.77	43.62	42.30					
CaO	0.50	0.40	0.39	0.43	0.41					
Na_2O	0.00	0.00	0.00	0.00	0.00					
K_2O	0.06	0.06	0.06	0.00	0.00					
P_2O_5	0.01	0.00	0.01	n.d.	n.d.					
Total	100.81	100.32	100.14	100.03	99.97					
Ni	2125	1860	2150							
Cr	850	250	600							
V	5	5	5							
Sr	7	7	15							
Rb	5	7	2							
Ba	20	20	15							
Zr	0	0	0							
Y	5	5	6							

INTERMEDIATE SERIES

Rock No.	B4	B7	B31	B34	B40	B41	B42	B43
Rock Name	AOB	AOBtd	O	AOBtd	AOBtd	AOB	O	O
Analytical Method	XRD	XRD	XRD	XRD	XRD	XRD	XRD	XRD
Occurrence	Pheno	Pheno	Pheno	Pheno	Pheno	Pheno	Pheno	Pheno
Mol.% Fo	74.70	86.08	86.08	89.90	70.90	75.90	88.60	89.90

YOUNGER SERIES

Rock No.	C18	C20	C29	C38	C79	C92
Rock Name	AOB	AOB	AOB	AOBtd	AOB	AOB
Analytical Method	XRD	XRD	XRD	XRD	XRD	XRD
Occurrence	Pheno	Pheno	Pheno	Pheno	Pheno	Pheno
Mol. % Fo	72.20	75.90	72.15	86.10	84.80	73.40

A. Older Series

Olivine crystallized through the entire compositional range of the Older Series lavas. Typically it forms a major phenocryst and groundmass component in the basic lavas, diminishing and becoming restricted to the groundmass with increasing evolution, occurring only in trace amounts in the trachytes, reflecting the progressive reduction in Fe + Mg. The absence of an olivine-liquid reaction typical of tholeiitic magmas demonstrates the alkaline affinities of the series.

Olivine compositions show some relation to bulk lava chemistry, varying from Fo_{82-78} in the picrite-basalts to Fo_{70} in the fieldsparphyric hawaiite A269. Measurement in more evolved lavas was precluded by the virtual restriction of olivine to small groundmass crystals, but if the relation to bulk lava chemistry is maintained they must be increasingly fayalitic.

B. Intermediate and Younger Series

Olivine is the dominant phenocryst phase in both the Intermediate and Younger Series lavas, and is a major component of the groundmass. Though compositionally much more restricted than the Older Series, these lavas show a wide range of olivine compositions from Fo_{90-71} in the Intermediate Series and Fo_{86-72} in the Younger Series. Neither group shows any clear relation between bulk lava chemistry and olivine composition, which may indicate a lack of equilibrium between the phenocrysts and the host lava.

4.3 CLINOPYROXENE

Thirteen analyses of clinopyroxenes from the Older Series lavas are listed in table 4.2, with one published analysis of an ophitic titanaugite from the Younger Series, taken from Walker and Nicolaysen (1954).

A. Older Series

Clinopyroxene is a major phenocryst phase in the Older Series, and is ubiquitous in the groundmass. Analysed phenocrysts are calcium-rich and lie close to the diopside-salite-ferrosalite boundary at 45% Ca, as defined by Deer et al. (1963). The evolutionary trend from picrite-basalt to trachyte is accompanied by solid solution changes within the clinopyroxene structure, Mg^{2+} being increasingly replaced by Fe^{2+} in pyroxenes from more evolved lavas, and ultimately in groundmass clinopyroxene from the trachyte A185, Na^{+} replaces Ca^{2+} to form aegirine-augite.

Zoning is common in phenocrysts, and typically the outer rim is compositionally indistinguishable from the groundmass pyroxene. Slight reverse zoning is apparent in a phenocryst from A269 with a core $Ca_{43}Mg_{40}Fe_{17}$ surrounded by a more magnesian and less iron rich rim with a composition $Ca_{46}Mg_{41}Fe_{13}$.

Clinopyroxene from the picrite-basalts is typically diopsidic, with an average composition of $Ca_{46}Mg_{44}Fe_{10}$ while that from the more evolved hawaiites is richer in iron, less magnesian and slightly less calcic, averaging $Ca_{45}Mg_{40}Fe_{15}$. Pale-green ferroaugite $Ca_{45}Mg_{24}Fe_{31}$ phenocrysts are found in the Piton de Milieu trachyte A264. Groundmass pyroxene from

TABLE 4.2. (Two Pages)

ANALYSED CLINOPYROXENES FROM MAURITIAN VOLCANICS

Oxides in wt. %

Trace elements in p.p.m.

O = Oceanite

A = Ankaramite

H = Hawaiite

PT = Phonolitic trachyte

AOB = Alkali olivine basalt

A269(a),(b) = different phenocrysts from A269.

Analysis 48a from Walker & Nicolaysen (1954)

* = Probe analysed samples without separate FeO, Fe_2O_3 determinations.

n.d. = not done

Fe = FeO + Fe_2O_3 + MnO

Series	OLDER												YOUNGER
Rock No.	A24	A28	A246	A228 Core	A228 Rim	A20	A269(a) Core	A269(a) Rim	A269(b)	A268	A72	A264	A185	48a
Rock Name	O	O	A	A	A	H	H	H	H	H	H	PT	PT	AOB
Analytical Method	XRF	XRF	XRF	PROBE	PROBE	XRF	PROBE	PROBE	PROBE	PROBE	XRF	PROBE	XRF	"WET"
Occurrence	Pheno	Pheno	Pheno	Pheno	Pheno	Pheno	Pheno	Pheno	Pheno	Pheno	Pheno	Pheno	G/Mass	G/Mass
SiO_2	51.51	49.66	51.13	51.46	51.33	49.47	48.44	49.41	49.49	47.78	49.69	48.75	52.45	48.01
Al_2O_3	4.40	6.20	4.73	2.91	3.27	6.02	3.97	3.93	5.11	7.64	5.65	2.20	3.43	5.30
TiO_2	1.14	1.89	1.33	1.03	1.10	1.76	1.18	1.61	1.27	2.16	1.89	1.18	0.39	2.49
Fe_2O_3	0.10	1.45	0.70	*	*	0.75	*	*	*	*	0.75	*	26.00	1.29
FeO	5.41	5.76	5.19	5.34	5.25	7.04	10.01	8.08	8.87	9.72	7.39	18.87	*	7.55
MgO	15.29	13.67	14.99	15.90	15.91	13.26	13.65	13.87	14.86	12.15	14.16	8.06	1.12	12.57
CaO	21.30	21.60	21.60	22.80	22.97	20.90	20.55	21.25	20.89	20.90	20.00	20.89	9.31	21.89
Na_2O	0.32	0.52	0.39	0.00	0.00	0.52	1.28	0.64	0.65	0.65	0.50	1.07	6.79	0.44
K_2O	0.08	0.10	0.08	0.00	0.00	0.10	0.04	0.06	0.01	0.00	0.10	0.01	0.52	n.d.
P_2O_5	0.12	0.14	0.14	n.d.	n.d.	0.12	n.d.	n.d.	n.d.	n.d.	0.14	n.d.	0.00	n.d.
MnO	0.09	0.10	0.10	n.d.	n.d.	n.d.	n.d.	n.d.	n.d.	n.d.	n.d.	n.d.	n.d.	0.14
Total	99.76	101.09	100.38	99.44	99.83	99.94	99.12	98.85	101.15	101.00	100.27	101.03	100.01	99.68
Ni	255	242	300											
Cr	3550	1650	3100											
V	200	290	230											
Sr	46	60	70											
Rb	0	5	7											
Ba	5	15	15											
Zr	25	70	40											
Y	12	17	24											

FORMULA TO 6 O

SERIES	OLDER													YOUNGER
ROCK No.	A24	A28	A246	A228 Core	A228 Rim	A20	A269(a) Core	A269(a) Rim	A269(b)	A268	A72	A264	A185	48a
Si)	1.89	1.82	1.87	1.90	1.89	1.84	1.84	1.86	1.83	1.77	1.84	1.89	1.97	1.81
Al^{iv})Z	0.11	0.18	0.13	0.10	0.11	0.16	0.16	0.14	0.17	0.23	0.16	0.10	0.03	0.19
Al^{vi})	0.08	0.09	0.07	0.03	0.03	0.10	0.02	0.04	0.05	0.10	0.09	0.00	0.12	0.04
Ti)	0.03	0.05	0.04	0.03	0.03	0.05	0.03	0.05	0.04	0.06	0.05	0.04	0.01	0.07
Fe)X	0.17	0.22	0.18	0.17	0.16	0.24	0.32	0.25	0.27	0.30	0.25	0.61	0.73	0.28
Mg)Y	0.84	0.75	0.82	0.88	0.87	0.73	0.78	0.78	0.82	0.67	0.78	0.47	0.06	0.71
Ca)	0.84	0.85	0.85	0.90	0.91	0.83	0.84	0.86	0.83	0.83	0.79	0.87	0.38	0.88
Na)	0.02	0.04	0.03	0.00	0.00	0.04	0.10	0.05	0.04	0.04	0.04	0.08	0.50	0.03
K)	0.00	0.00	0.00	0.00	0.00	0.00	0.00	0.00	0.00	0.00	0.00	0.00	0.03	0.00
Mol. %														
Wo(Ca)	45.41	46.70	45.95	46.15	46.91	46.11	43.30	45.50	43.23	46.11	43.41	44.62	32.50	46.81
En(Mg)	45.41	41.21	44.32	45.13	44.85	40.56	40.21	41.27	42.71	37.22	42.86	24.10	5.12	37.77
Fs(Fe)	9.19	12.09	9.73	8.72	8.25	13.33	16.50	13.23	14.06	16.67	13.74	31.28	62.38	15.42

CIPW Norms for samples with FeO and Fe_2O_3 determinations.

Series	OLDER				YOUNGER
Rock No.	A24	A28	A20	A72	48a
Qz	0.00	0.00	0.00	0.00	0.00
Ne	0.00	1.55	0.93	0.00	2.02
Hy	3.63	0.00	0.00	1.30	0.00
Di	75.32	72.08	71.20	68.00	74.12
Ol	4.89	4.13	6.08	8.05	3.56
Or	0.47	0.58	0.59	0.59	0.00
Ab	2.72	1.49	2.69	4.22	0.00
An	10.37	14.20	13.80	12.84	12.52
Mt	0.15	2.08	1.09	1.08	1.88
Ilm	2.17	3.55	3.34	3.58	4.74
Ap	0.29	0.33	0.28	0.33	0.00

the Chamanel trachyte was separated and analysed, and proved to be an aegirine-augite. Insufficient sample was available for a separate Fe_2O_3 determination on this pyroxene but comparable aegirine-augites, Deer et al. (1963) have high Fe^{3+} contents and it seems likely that this balances the charge deficiency caused by Na^+ replacing Ca^{2+}.

Fig. 4.1. plots the analysed sodium-poor clinopyroxenes in the pyroxene quadrilateral, Poldervaart and Hess (1951), (i.e. molecular proportions of Ca-Mg-Fe), summarises the trend and for comparison shows analysed trends from tholeiitic and alkaline suites. It is clear that the trend of the Older Series clinopyroxenes is more typical of that from alkaline magmas and that it lacks the marked inflexion towards calcium-poor compositions and has no coexisting calcium-poor pyroxene, features typical of tholeiitic suites.

Fig. 4.2. shows tie lines between coexisting olivine-clinopyroxene compositions (in the same quadrilateral). The systematic distribution and parallelism of the tie lines suggest that the two phases crystallized in equilibrium with each other and shows that the clinopyroxene has a consistently higher Mg/Fe ratio than the coexisting olivine.

Coombs (1963) demonstrated a relationship between magma type and the normative composition of the clinopyroxene, where alkali basalts carry a ne-normative pyroxene and tholeiites a clinopyroxene with considerable hy + ol or minor qz. The transitional nature of the Older Series is clear, with analysed pyroxenes containing either minor ne or hy + ol.

The Al_2O_3 content of the clinopyroxenes lies within

FIG. 4.1.

Ca:Mg:Fe(Tot.) ratios of analysed sodium poor clinopyroxenes from the Older Series lavas.

(Mol. propns.)

$Fe(Tot.) = Fe^{2+} + Fe^{3+} + Mn$

Δ = Data

1 = Trend of clinopyroxenes from the Black Jack sill, Wilkinson (1956).

2 = Trend of Skaergaard clinopyroxenes, Brown (1957).

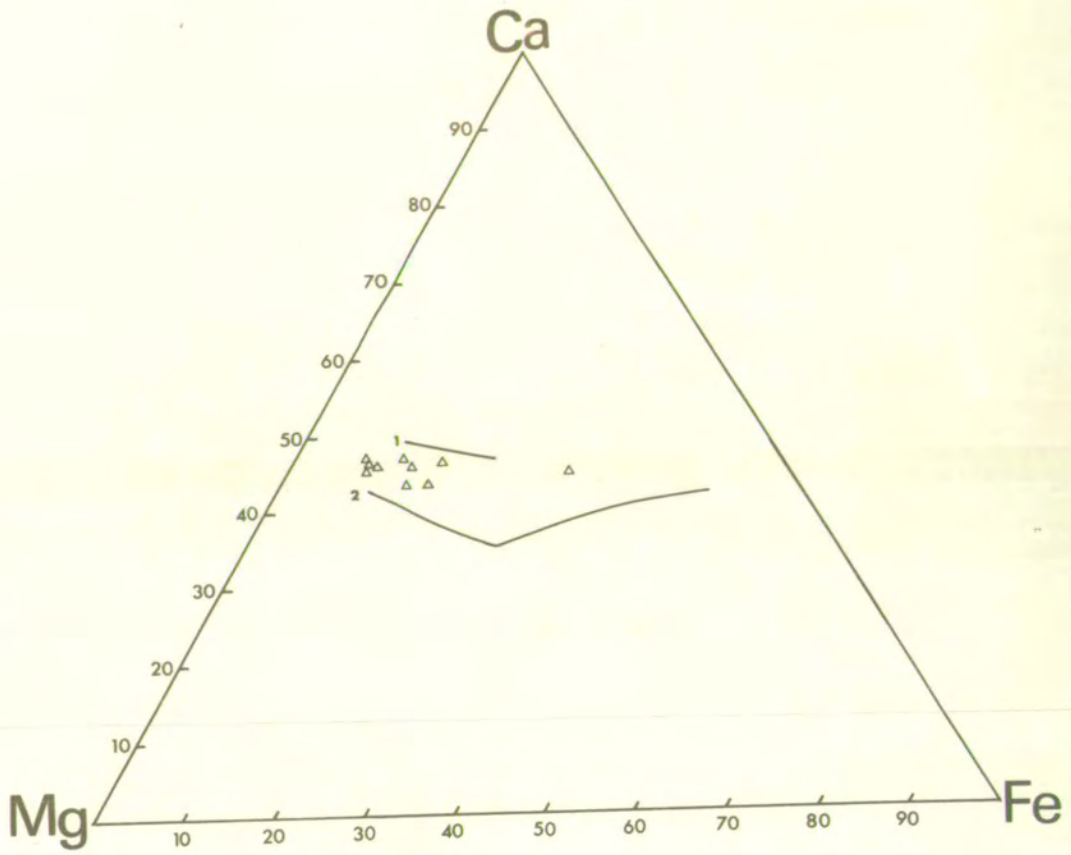
Ca
Mg
Fe
90
80
70
60
50
40
30
20
10
10
20
30
40
50
60
70
80
90
1
2

FIG. 4.2.

Tie-lines for coexisting olivines and clinopyroxenes from the Older Series lavas, in the Ca:Mg:Fe(Tot) diagram. (Mol. propns).

□ = Olivines

△ = Clinopyroxenes.

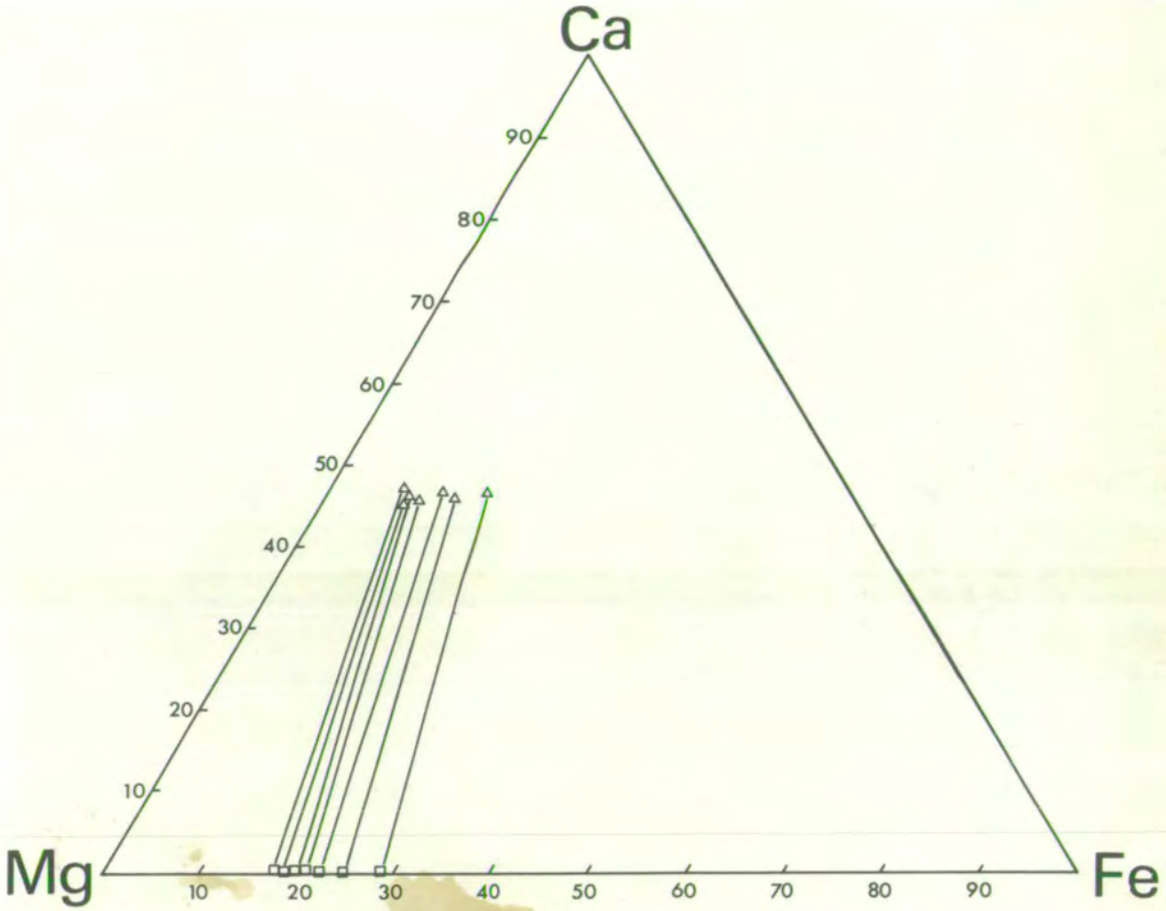
Ca
Mg
Fe
90
80
70
60
50
40
30
20
10
10
20
30
40
50
60
70
80
90

the normal range of the diopside-ferroaugite group, Brown (1967) and varies from 2.2-7.64 wt. %. Approximately 70% of the available aluminium goes into tetrahedral sites in the clinopyroxene, replacing silica and a pronounced negative correlation exists between the silica content of the clinopyroxene and total and tetrahedral aluminium, fig. 4.3,a. Increase in aluminium in the clinopyroxene, particularly in tetrahedral sites is associated with an increasing FeO/MgO ratio, fig. 4.3,b. and rising TiO_2 content in the mineral, fig. 4.3,c. The factors controlling aluminium content are not clearly understood and have been the subject of considerable research. Clark et al. (1962) have shown that increased pressure favours the entry of Ca-Tschermacks molecule and hence Al_2O_3 into the diopside structure. However as increasing Al_2O_3 is linked to rising TiO_2 and FeO/MgO ratio, generally an indicator of increasing fractionation and decreasing temperature, it would seem unlikely that pressure is a major control in the Older Series. Hytönen and Schairer (1961), working at 1 atmosphere in the synthetic system enstatite-diopside-anorthite demonstrated an increase in Ca-Tschermacks molecule in diopside with decreasing temperature, to a maximum of 15% Al_2O_3 and Kushiro (1960) has suggested that titanium enters octahedral sites to maintain charge balance with the tetrahedral aluminium. The positive correlation between aluminium and titanium has been investigated by Yagi and Onuma (1967), who show from 1 atmosphere experiments in the pseudobinary system $CaMgSi_2O_6 - CaTiAl_2O_6$, increasing solid solution of $CaTiAl_2O_6$ in diopside with decreasing temperature, to a maximum of 11%. Fig. 4.4. relates

FIG. 4.3.

Total Al_2O_3 and % Al_Z variation in clinopyroxenes from the Older Series.

(a) Against Wt.% SiO_2 in clinopyroxenes.

(b) Against FeO(Tot)/MgO ratio in clinopyroxenes.

(c) Against Wt.% TiO_2 in clinopyroxenes.

Al_Z = proportion of clinopyroxene Z group occupied by tetrahedral Al, = Al_{IV} x 100/Z where Z = 2.

● = Total Al_2O_3 in clinopyroxene, Wt. %.

△ = % Al_Z in clinopyroxene.

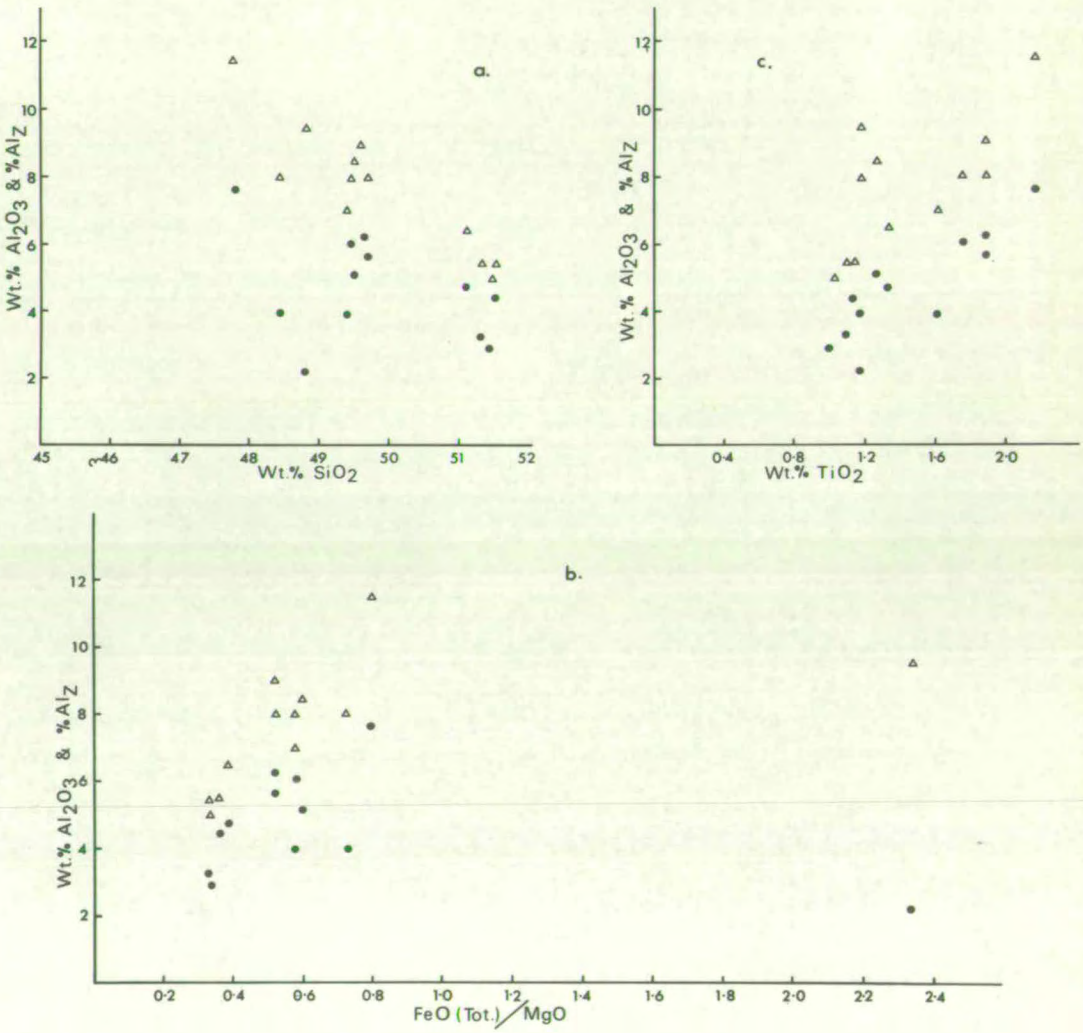
a.
Wt.% Al2O3 & %Alz
Wt.% SiO2
45
46
47
48
49
50
51
52
2
4
6
8
10
12
c.
Wt.% Al2O3 & %Alz
Wt.% TiO2
0·4
0·8
1·2
1·6
2·0
b.
Wt.% Al2O3 & %Alz
FeO (Tot.) / MgO
0·2
0·4
0·6
0·8
1·0
1·2
1·4
1·6
1·8
2·0
2·2
2·4

FIG. 4.4.

Bulk TiO_2 content of lava versus TiO_2 in coexisting clinopyroxene. (Wt.%).

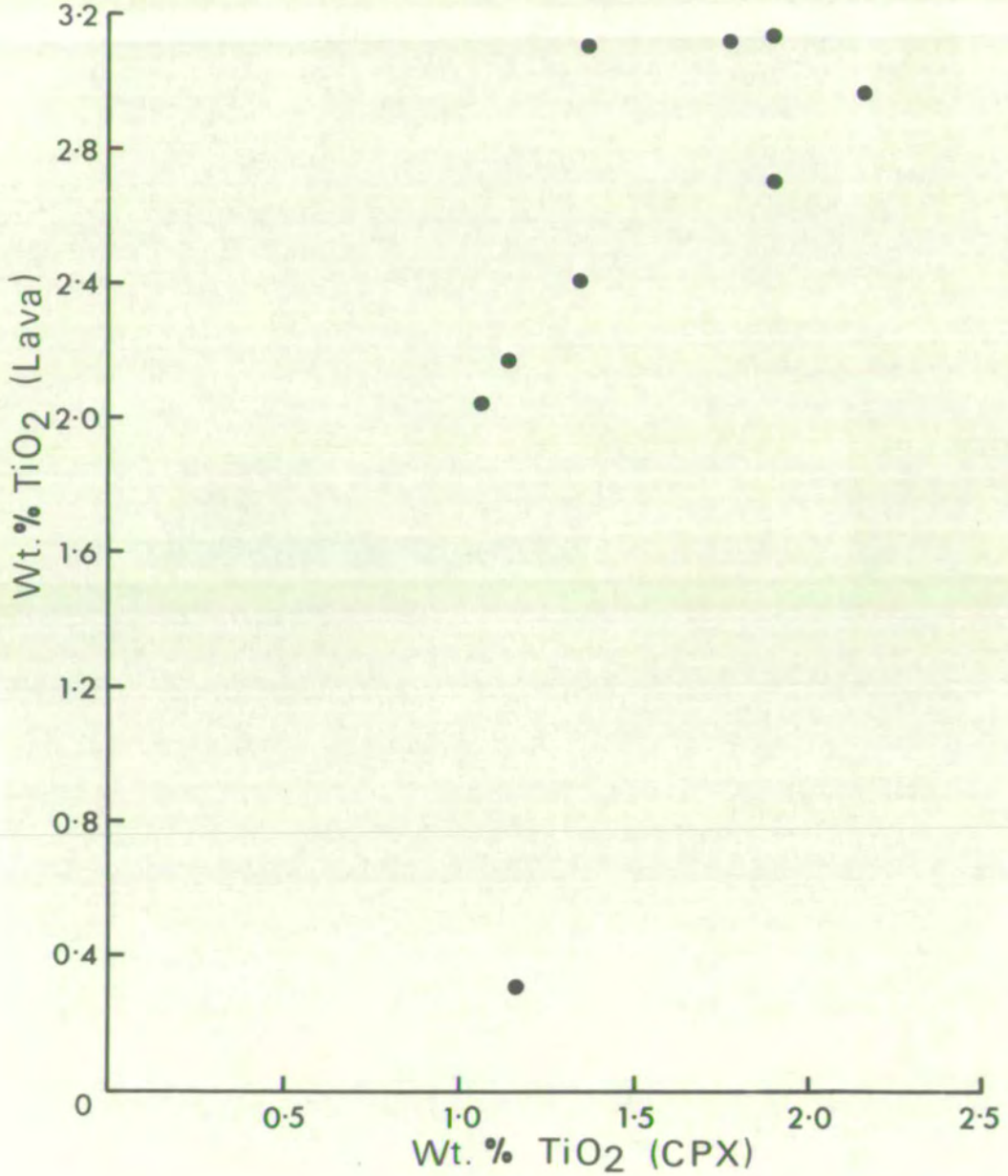
3·2
2·8
2·4
2·0
1·6
1·2
0·8
0·4
0
Wt.% TiO2 (Lava)
0·5
1·0
1·5
2·0
2·5
Wt. % TiO2 (CPX)

the absolute concentration of TiO_2 in the lava to that in the coexisting pyroxene, and apart from the slightly sodic ferroaugite A264, shows a good positive correlation, which might imply that the TiO_2 content of the clinopyroxene is a function of the amount of TiO_2 in the lava.

B. Intermediate and Younger Series

Clinopyroxene is a major groundmass component of both the Intermediate and Younger Series lavas, but appears as a phenocryst phase only in the Intermediate Series, where it occurs in minor amounts. Typically the phenocrysts have green diopsidic cores zoned to mauve titaniferous rims similar to the groundmass clinopyroxene.

Groundmass clinopyroxene from the Younger Series is typically a brown-mauve zoned titanaugite, occasionally with sharp green sodic rims indicating extreme fractionation. Walker and Nicolaysen (1954) present one analysis of an ophitic titanaugite from this series, showing it to be considerably more titanium-rich than the pyroxenes from the Older Series, see table 4.2. With a composition $Ca_{47}Mg_{38}Fe_{15}$, the pyroxene is mildly ne-normative.

4.4. KAERSUTITE

Strongly pleochroic (X = pale yellow, Y = red-brown, Z = deep brown) amphibole phenocrysts appear in the felds-parphyric hawaiites of the Older Series. Typically they occur as euhedral to subhedral prisms surrounded by a thick rim of magnetite or magnetite + clinopyroxene. Complete pseudomorphing occurs, with amphibole replaced by crystalline

aggregates of magnetite + clinopyroxene + plagioclase + occasional secondary deep brown hornblende.

Three analyses of phenocrysts are given in table 4.3. It is clear that the amphibole is titanium rich, with an average of 0.63 atoms of Ti per formula unit. Extensive substitution of Si by Al occurs in the tetrahedral sites, averaging 2.2 atoms per formula unit. By the classifications of both Deer et al. (1963) and Wilkinson (1961), the phenocrysts are typical kaersutites. The thick magnetite rims surrounding the phenocrysts restricted analysis to electron microprobe techniques, which does not discriminate between FeO and Fe_2O_3. As kaersutites show extremely variable FeO/Fe_2O_3 ratios, Kesson and Price (1972) the normative composition limits are shown by calculating the analyses fully reduced and fully oxidised. The iron-magnesium ratios of the kaersutites averages 0.93, considerably higher than the 0.68 of the coexisting clinopyroxene.

Kaersutite is a relatively common phase in evolved basalt-trachyte magmas, particularly from undersaturated suites, Aoki (1963), Ridley (1970), Best (1970). Alteration similar to that described above is ubiquitous, and it would appear that generally kaersutite is unstable in the eruptive environment. The euhedral form of the Older Series kaersutites suggests that they are phenocrysts rather than derived fragments. With the exception of some relatively uncommon F- saturated fluor-kaersutites; Deer et al. (1963), kaersutite is a hydrous mineral and implies the presence, at some time, of relatively high water concentrations in the magma. Yoder

TABLE 4.3. (Two Pages)

KAERSUTITE ANALYSES FROM OLDER SERIES LAVAS

Oxides in wt.%.

Fe(Tot) = Total iron as FeO

(a),(b) = different phenocrysts in A269.

Rock No.	A268	A269(a)	A269(b)
Rock Name	Hawaiite	Hawaiite	Hawaiite
SiO_2	39.03	40.29	40.17
Al_2O_3	14.97	12.60	13.27
TiO_2	5.91	5.23	5.67
FeO(Tot)	10.91	13.01	11.62
MgO	12.90	12.07	13.01
CaO	11.50	11.41	11.87
Na_2O	3.18	2.78	2.65
K_2O	0.84	0.86	0.84
Total	99.23	98.26	99.09
FeO(Tot) MgO	0.84	1.08	0.89

Norm	Totally Reduced	Totally Oxidised	Totally Reduced	Totally Oxidised	Totally Reduced	Totally Oxidised
Qz	0.00	0.00	0.00	0.00	0.00	0.00
Ne	14.69	7.91	12.97	3.20	12.26	3.76
Hy	0.00	0.00	0.00	0.00	0.00	0.00
Di	17.94	9.61	29.97	14.88	26.40	13.44
Ol	24.52	19.32	22.91	16.33	23.12	18.28
Or	0.00	4.95	0.00	5.10	0.00	4.95
Ab	0.00	12.22	0.00	17.72	0.00	15.42
An	24.28	24.01	19.71	19.45	22.03	21.78
Mt	0.00	0.00	0.00	0.00	0.00	0.00
Ilm	11.31	0.00	10.11	0.00	10.87	0.00
Larnite	3.34	0.00	0.28	0.00	1.40	0.00
Perovskite	0.00	10.02	0.00	8.94	0.00	9.62
Leucite	3.92	0.00	4.06	0.00	3.93	0.00
Haematite	0.00	11.96	0.00	14.37	0.00	12.75

Formula to 23 O

Total iron as FeO

Rock No.	A268		A269(a)		A269(b)	
Si	5.69	8.00 Z	5.98	8.00 Z	5.81	8.00 Z
Al^{iv}	2.31		2.02		2.19	
Al^{vi}	0.26	5.04 Y	0.19	5.05 Y	0.07	5.15 Y
Fe	1.33		1.61		1.65	
Mg	2.80		2.67		2.81	
Ti	0.65		0.58		0.62	
Ca	1.80	2.75 X	1.81	2.77 X	1.84	2.75 X
Na	0.89		0.80		0.75	
K	0.06		0.16		0.16	

and Tilley (1962) demonstrated that in the system, basalt (olivine tholeiite)-H_2O where pH_2O = pTotal, amphibole appears as a liquidus phase in the range 1 - 10 Kb. More recently Holloway and Burnham (1972) showed that in the geologically more likely situation where pH_2O < pTotal, kaersutite is a liquidus phase from 975 - 1060°C in the range 2 - 8 Kb. i.e. within the normal temperature range of basaltic magmas. Eruption of the magma to pressures < 2 Kb. at these temperatures moves the amphibole out of its stability field (see fig. 3. Holloway and Burnham, (1972)) and could explain the pseudomorphing and alteration of the phenocrysts. The restriction of kaersutite to the post shield-forming evolved lavas of the Older Series implies that sufficiently hydrous conditions did not develop until the later stages of activity, when the vapour pressure in a sub-volcanic magma chamber might reasonably be expected to be higher, through extensive fractionation of anhydrous minerals (e.g. olivine and clino-pyroxene).

4.5. FELDSPARS

Seven chemical analyses of feldspars from the Older and Younger Series are listed in table 4.4. Optical determinations for all three series are summarised in table 4.5. which also shows the compositional variation of feldspars within the series.

A. Older Series

Feldspar is always a major groundmass phase in the lavas, predominantly plagioclase with minor interstitial

TABLE 4.4. (Two Pages)

FELDSPAR ANALYSES FROM MAURITIAN VOLCANICS

Oxides in wt. %.

trace elements in p.p.m.

FB = Feldsparphyric basalt

H = Hawaiite

PT = Phonolitic trachyte

AOB = Alkali olivine basalt

FeO(Tot) = Total iron as FeO

Series	OLDER SERIES						YOUNGER SERIES
Rock No.	A69	A138	A193	A70	A264	A264	C25
Rock Name	FB	FB	FB	H	PT	PT	AOB
Analytical Method	XRF	XRF	XRF	XRF	PROBE	PROBE	XRF
Occurrence	Pheno	Pheno	Pheno	Pheno	Pheno	G/Mass	Pheno
SiO_2	47.48	47.00	47.29	51.03	65.05	64.63	54.10
Al_2O_3	31.68	31.28	33.23	29.39	19.39	20.46	27.91
TiO_2	0.13	0.11	0.11	0.15	0.00	0.00	0.18
FeO(Tot)	1.67	0.98	1.04	1.81	0.11	0.64	0.90
MgO	0.87	0.59	0.14	0.99	0.00	0.00	0.19
CaO	15.20	16.40	16.70	12.60	0.32	0.38	10.90
Na_2O	1.98	1.99	1.77	3.38	6.74	7.26	4.81
K_2O	0.16	0.17	0.14	0.29	7.41	5.53	0.88
P_2O_5	0.05	0.09	0.12	0.10	n.d.	n.d.	0.29
MnO	n.d.	0.02	0.02	n.d.	n.d.	n.d.	0.02
Total	99.22	98.63	100.56	99.74	99.02	98.90	100.18
Mol %							
An	80.20	81.20	83.20	66.10	1.57	1.95	52.80
Ab	18.80	17.80	16.00	32.10	57.07	65.18	42.20
Or	1.00	1.00	0.80	1.80	41.36	32.87	5.00

Trace element data:

Rock No.	A138	A193	C25
Analytical Method	XRF	XRF	XRF
Ni	25	26	35
Cr	0	0	0
V	0	0	0
Sr	980	720	740
Rb	32	0	25
Ba	60	50	460
Zr	0	0	22
Y	0	3	17

TABLE 4.5.

SUMMARY OF OPTICAL DETERMINATIONS ON MAURITIAN FELDSPARS

	Phenocrysts	Groundmass
OLDER SERIES		
Picrite basalts T. Olivine basalts	An_{73-54}	An_{65-55}
Transitional basalts	An_{68-52}	An_{52-48}
Feldsparphyric basalts	An_{88-76}	An_{68-60}
Hawaiites	(a) Cores An_{66-50} (b) Rims An_{48-32}	An_{41-28}
Mugearites	(a) Cores An_{45-30} (b) Rims An_{30-14} Anorthoclase	An_{30-14}
Trachytes, phonolitic trachytes	Anorthoclase	Anorthoclase
INTERMEDIATE SERIES		
Oceanites, alkali olivine basalts and basanitoids	Absent	An_{64-50}
YOUNGER SERIES		
Alkali basalts, olivine basalts and basanitoids	An_{68-52}	An_{60-52}

alkali feldspar, but only alkali-feldspar in the trachytes and phonolitic trachytes. Plagioclase is a minor phenocryst phase in the basic lavas and only becomes significant in the feldsparphyric basalts, hawaiites and mugearites. Phenocrysts are commonly zoned to more sodic rims generally approximating to the groundmass plagioclase composition, though reverse zoning can occur, e.g. A269 with An_{53} cores rimmed by An_{62}. Both phenocryst and groundmass plagioclase become increasingly sodic with differentiation and in the most evolved mugearites oligoclase An_{15} and anorthoclase phenocrysts are both present. In the trachytic magmas only alkali feldspar crystallizes, typically phenocrysts of zoned anorthoclase set in an anorthoclase groundmass, however electron microprobe analysis of a phenocryst core from the phonolitic trachyte A264 lies just in the sanidine field at $Ab_{57}Or_{41}An_2$ zoned to margins optically indistinguishable from the analysed groundmass anorthoclase $Ab_{65}Or_{33}An_2$.

Lavas become increasingly feldspathic with differentiation, normative feldspar exceeding 65% of the bulk norm by the time hawaiitic compositions are reached. These relatively evolved lavas approach calcium rich compositions within the system $NaAlSi_3O_8 - KAlSi_3O_8 - CaAl_2Si_2O_8$ and the observed feldspar sequence in the Older Series of plagioclase → plagioclase + alkali feldspar → alkali feldspar is comparable to fractional crystallization paths for liquids lying initially in the plagioclase-only field, Tuttle and Bowen (1958). The trend to more sodic alkali feldspar (c.f. phenocryst and groundmass feldspar in A264, table 4.4.) indicates

fractionation towards the low temperature minimum in this system.

Plagioclase phenocrysts (An_{73-54}) from the most basic lavas - the picrite basalts, should approximate to the composition of the first and hence most calcic plagioclase to crystallize from the Older Series lavas. However significantly more calcic phenocrysts are found in the feldsparphyric basalts. Typically unzoned, phenocrysts are calcic bytownites (Average An_{82}) compositionally indistinguishable from bytownitic anorthosite inclusions associated with these lavas. Relatively iron-rich olivine (Fo_{71}) and titanomagnetite occur as minor coexisting phenocrysts in these lavas. The significantly different mineralogy and close association of these lavas with hawaiites and mugearites suggests fundamentally different conditions for their formation.

Yoder (1969(a),(b)) suggests that the presence of water may be significant in controlling the crystallization and composition of plagioclase and has demonstrated that with increasing pressure in water-saturated systems (e.g. Ab-An-H_2O, Di-An-H_2O), eutectics are depressed to lower temperatures and shifted towards markedly more anorthite-rich compositions. In this light the association of the feldsparphyric basalts with the post shield forming lavas, some of which carry hydrous minerals (i.e. kaersutite) may be significant in indicating an origin for the calcic plagioclase under elevated water pressures.

SiO_2, CaO, Na_2O and K_2O make up approximately 97% of the feldspar analyses in table 4.4. The levels of TiO_2,

FeO and MgO are marginally high, c.f. Deer et al. (1963) in some of the separated XRF analysed samples and probably reflect contamination by titanomagnetite and other phases which commonly occur as inclusions within the phenocrysts. Trace-element analyses on feldspars are relatively uncommon, but the two bytownites analysed fall within the normal range, Brown (1967).

B. Intermediate and Younger Series

Plagioclase is a major constituent of the groundmass of both the Intermediate and Younger Series lavas, but appears rarely and only in the Younger Series as a phenocryst, typically as zoned sodic labradorite. The chemical analysis of labradorite from the Younger Series lava C25 (table 4.4.) is significantly higher in the orthoclase molecule than the Older Series analyses, and may reflect contamination by alkali feldspar, which occurs as large interstitial patches. Alkali feldspar is a common interstitial mineral in both series. Relative to the Older Series, plagioclase from the Intermediate and Younger Series is compositionally restricted, and reflects the rather uniform nature of the latter two groups.

4.6. OTHER MINERALS

Titanomagnetite is an ubiquitous groundmass phase in the lavas of all three series, typically occurring as euhedral octahedra. Phenocrysts of titanomagnetite appear in the feldsparphyric basalts, hawaiites and mugearites of the Older Series. Ilmenite plates appear sporadically in the groundmass of some basalts and hawaiites in all three

series. Apatite is a common accessory phase, and appears as phenocrysts crowded with rutile inclusions in the Older Series mugearites. Nepheline is found only in the trachytes and phonolitic trachytes, where it occurs both as a phenocryst and groundmass phase. A careful search was made for nepheline in the basanitoidal Intermediate Series lavas, but was not detected.

5. GEOCHEMISTRY

5.1. INTRODUCTION

223 major and trace element analyses of Mauritian volcanics are presented in Appendix 3, along with their CIPW norms. The location of each specimen is shown in Map 1 (back pocket) and modal petrographic data is tabulated in Appendix 4. The analytical techniques employed together with estimates of precision and accuracy, are described in Appendix 2.

The distribution of analyses between the three series is as follows:

Older Series

Flows	129
Dykes	18
Trachyte Domes	5

Intermediate Series

Flows	33

Younger Series

Flows	38

Systematic vertical and lateral sampling of the three series was undertaken during field work on the island, to provide a representative collection for any analytical scheme. Specimens were selected for analysis on the basis of their petrography and freshness to cover the chemical variation of each series, and the high proportion of Older Series analyses reflects the far greater variation of this group.

5.2. MAJOR ELEMENT CHEMISTRY

A. Frequency Distribution of Major Element Data

The distribution and range of major element concentrations in the three series is displayed in the form of histograms in Fig. 5.1. Several points emerge from these diagrams.

(1) The highly differentiated character of the Older Series, reflected in its wide, skewed compositional range compared with the restricted and more normal distribution of the Intermediate and Younger Series lavas.

(2) The more basic nature of the Intermediate and Younger Series lavas, indicated by lower modes for SiO_2, TiO_2, K_2O, P_2O_5 and higher MgO, relative to the Older Series. CaO, FeO(Tot.), Na_2O and MnO modes are generally similar.

(3) The distinctly higher Al_2O_3 mode of the Younger Series lavas relative to the Intermediate Series, reflected in the crystallization sequence olivine → plagioclase in the former series compared with olivine → clinopyroxene in the latter.

(4) A trend to increased H_2O contents from the Younger Series through the Intermediate, to the Older Series and hence with increasing age, suggesting that secondary, post magmatic hydration processes are operating; also indicated by increased iddingsitization and zeolitization in the Older Series.

B. CIPW Norms

CIPW norms for all analysed specimens are presented in Appendix 3. Analyses have been corrected, where necessary,

FIG. 5.1.

Histograms showing frequency distribution of major elements in the Mauritian volcanics.

1. = Younger Series

2. = Intermediate Series

3. = Older Series

* N.B. Frequency in units of 10 for the Older Series, units of 5 for the Intermediate and Younger Series.

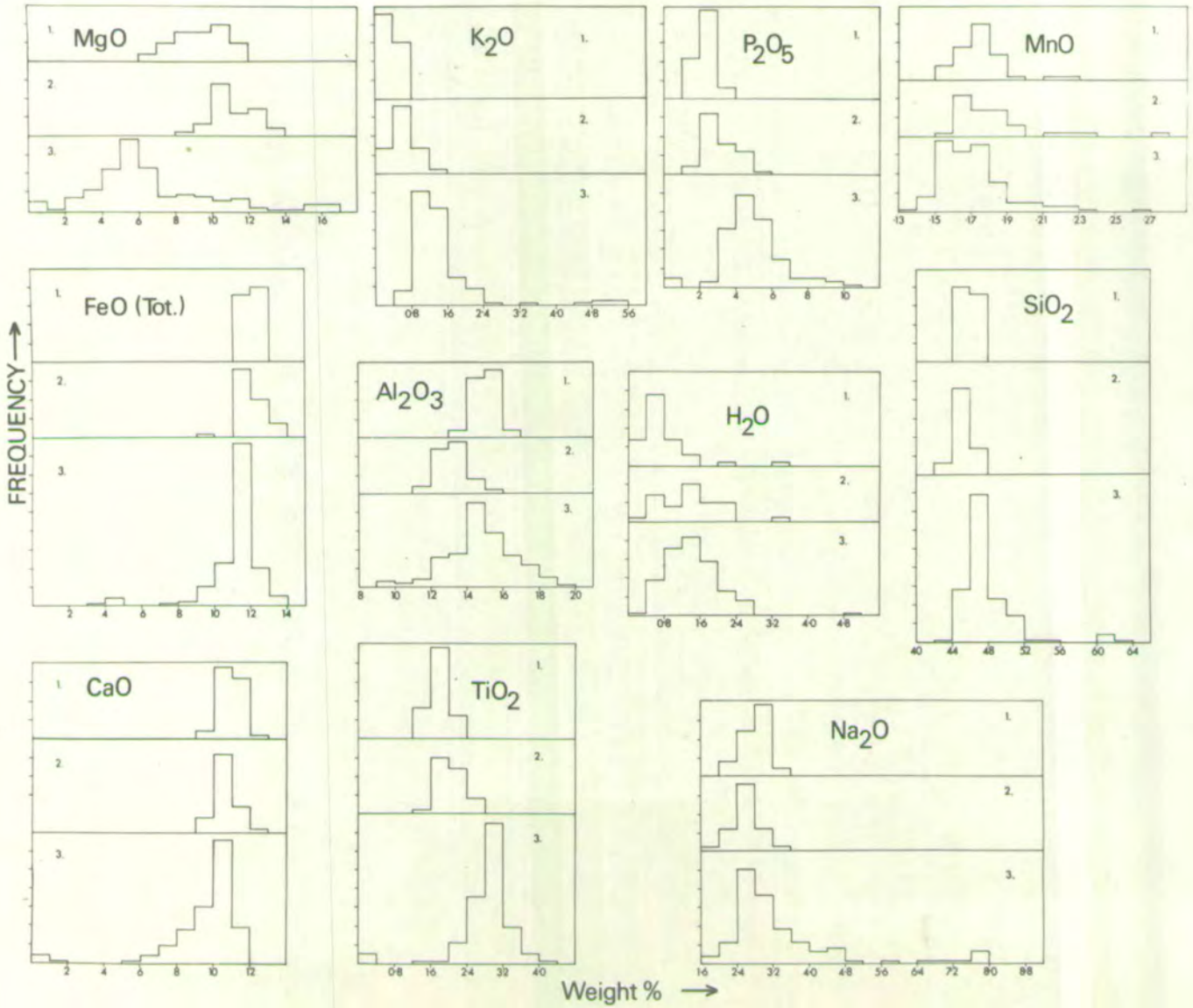
MgO
K2O
P2O5
MnO
FeO (Tot.)
Al2O3
H2O
SiO2
CaO
TiO2
Na2O
FREQUENCY
Weight %

for secondary oxidation effects, according to the scheme outlined in Chapter 3. Several points should be noted from the normative data.

(1) Older Series lavas are either hy + ol normative or carry minor normative ne, emphasising their transitional nature. Picrite basalts rich in clinopyroxene may have become undersaturated through the accumulation of ne-normative clinopyroxene (c.f. bulk analyses A20, A28 and clinopyroxene analyses A20, A28). Both the Intermediate and Younger Series lavas are predominantly ne-normative, with the Intermediate Series extending into basanitoidal compositions to a maximum of 12.2% ne, (B33). Fig. 5.2. summarises the relative silica-saturation distribution of the three series.

(2) Normative olivine, diopside and anorthite decrease while albite and orthoclase increase with differentiation in the Older Series. Low normative orthoclase content in the Younger Series lavas relative to the Older Series, reflects their low K_2O concentrations while the widely varying orthoclase values in the Intermediate Series reflects highly varying K_2O levels in these lavas.

C. Variation Diagrams

Simple oxide variation diagrams of Harker type but with MgO as abcissa, Powers (1955), are presented in Figs. 5.3., 5.4., 5.5. Choosing an oxide (MgO) as an index of differentiation rather than Solidification Index, Kuno et al. (1957) or Differentiation Index, Thornton and Tuttle (1960) has the following advantages:

FIG. 5.2.

Silica-saturation distribution of the Mauritian volcanics.

1. = Younger Series

2. = Intermediate Series

3. = Older Series

* N.B. Frequency in units of 10 for the Older Series, units of 5 for the Intermediate and Younger Series.

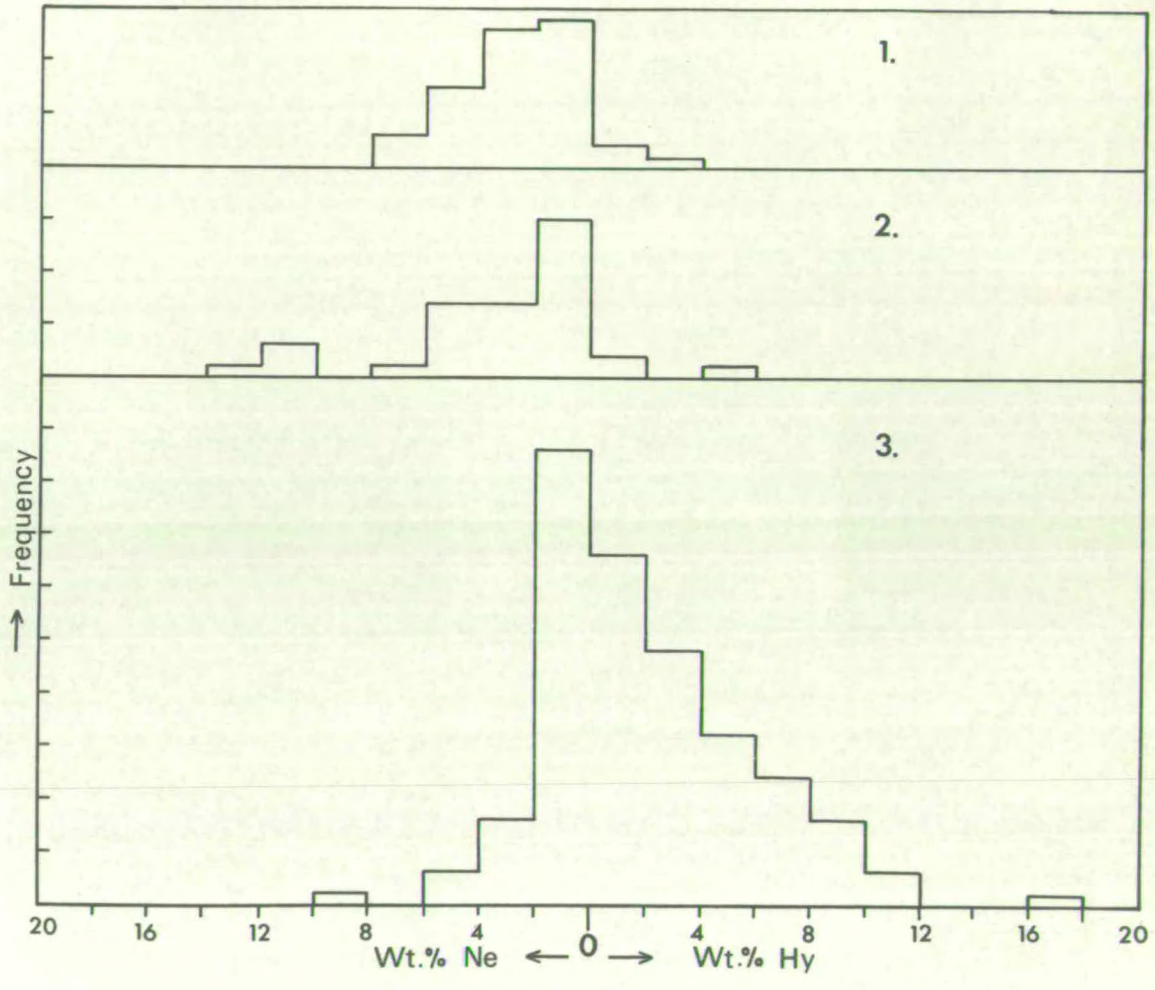
1.
2.
3.
Frequency
20
16
12
8
4
0
4
8
12
16
20
Wt.% Ne
Wt.% Hy

(1) Variation can be simply assessed, unlike that plotted against the more complex artificial indices.

(2) Mineral compositions and control lines can be plotted.

(3) Extract calculations can be performed.

The following criteria were used in selecting MgO as the major index of differentiation:

(1) It shows the largest degree of variance in the analyses of all three series, Table 5.1.

(2) Ferromagnesian minerals, particularly olivine, are major phenocryst phases in the three series, consequently MgO should be highly sensitive to their addition or removal.

D. Older Series

Major oxide plots of the Older Series lavas against MgO summarise the chemical variation, and show well defined trends, Fig. 5.3. A marked change in slope is apparent at 5-6% MgO. Lavas with more than 5-6% MgO include transitional basalts, olivine and picrite basalts and these lie along a well defined trend towards the olivine-clinopyroxene tie line, compatible with their petrography which shows these minerals to be major phenocryst phases. Analyses with less than 5-6% MgO are feldsparphyric basalts, hawaiites, mugearites, trachytes and phonolitic trachytes and show increasing SiO_2, Na_2O, K_2O, Al_2O_3 and decreasing CaO, TiO_2 and FeO(Tot.) The abrupt change in slope coincides with the appearance of plagioclase and titanomagnetite as major phenocryst phases and their fractionation along with olivine and clinopyroxene can explain the changed trend.

TABLE 5.1.

MAJOR ELEMENT VARIANCE OF MAURITIAN VOLCANICS

	Older Series		Intermediate Series		Younger Series	
	a.	b.	a.	b.	a.	b.
SiO_2	9.90	24.60	0.96	20.4	0.38	10.45
Al_2O_3	4.90	12.20	0.74	15.8	0.45	12.40
TiO_2	0.38	1.00	0.08	1.7	0.04	1.10
FeO(Tot.)	2.50	6.20	0.70	14.9	0.18	5.00
MgO	16.60	41.20	1.29	27.5	1.84	50.80
CaO	3.60	8.90	0.35	7.4	0.30	8.30
Na_2O	1.44	3.60	0.09	1.9	0.08	2.20
K_2O	0.60	1.50	0.07	1.5	0.01	0.30
P_2O_5	0.03	0.10	0.01	0.2	*	*
MnO	*	*	*	*	*	*
H_2O	0.28	0.70	0.41	8.7	0.34	9.40

a. = Variance (σ^2)

b. = % Variance

* = Not significant.

FIG. 5.3.

Major element variation diagrams for the Older Series volcanics. (Wt.%).

Dashed lines represent best fit ol + cpx control lines through analyses with > 5% MgO.

Solid lines represent ol - cpx tie lines.

FeO(Tot) = Total iron as FeO

● = Older Series volcanics.

□ = Olivine A24 (Table 4.1)

△ = Clinopyroxene A24 (Table 4.2).

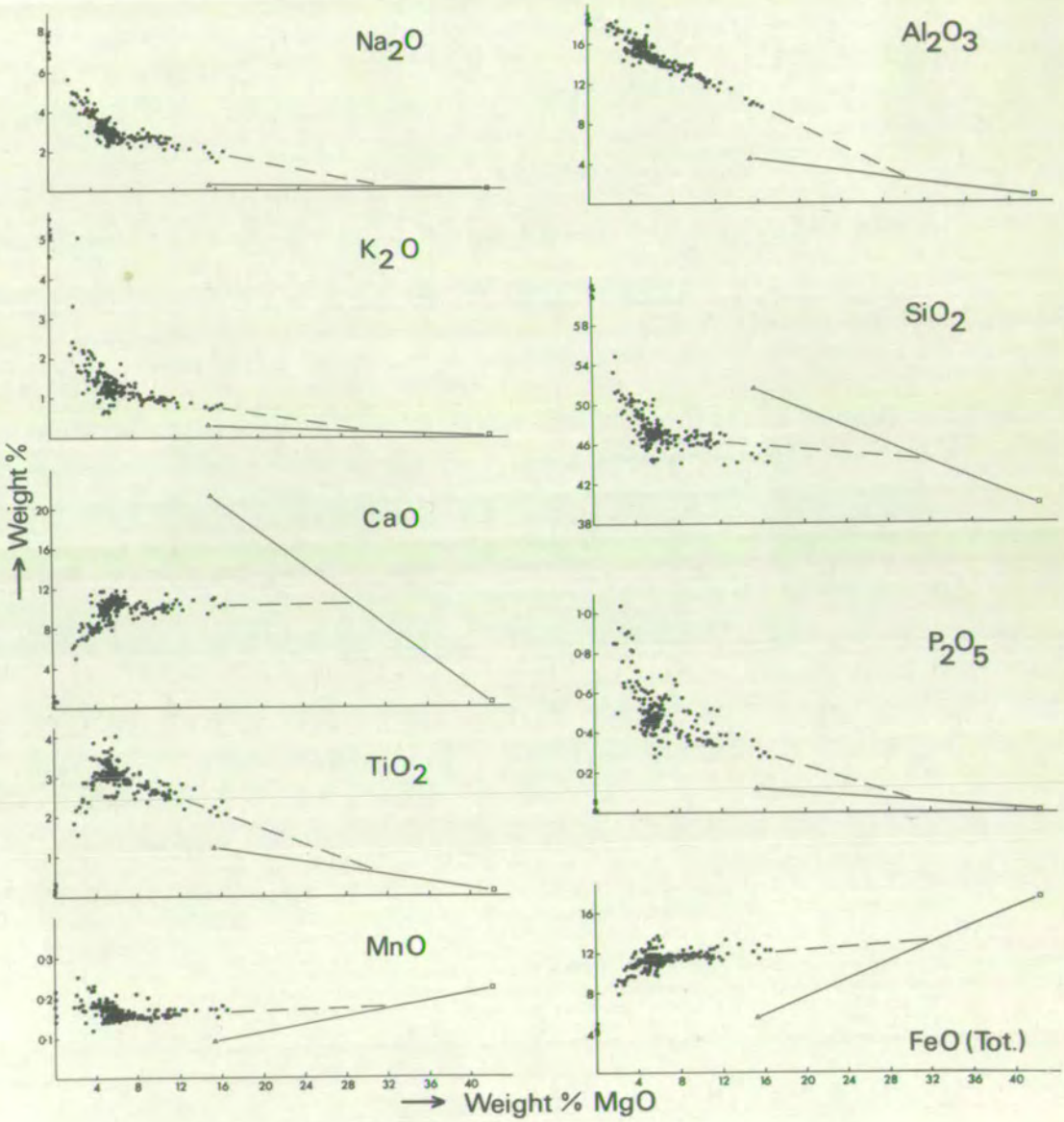
Na2O
Al2O3
K2O
SiO2
CaO
P2O5
TiO2
MnO
FeO (Tot.)
→ Weight %
→ Weight % MgO

Accumulation of plagioclase phenocrysts in the feldsparphyric basalts and hawaiites displaces some of these compositions towards Al_2O_3 rich points away from the main trend of the Al_2O_3 plot. A slight 'tail' backprojecting from the trend is apparent at its junction with the olivine + clinopyroxene trend, particularly in the FeO(Tot.), TiO_2 and CaO plots, and is composed of the feldsparphyric basalts and hawaiites which carry the greatest proportions of phenocryst plagioclase and titanomagnetite within the series. The effects of apatite fractionation can be clearly seen in the P_2O_5 plot, P_2O_5 rising to a maximum of 1.04% (A267) at 2.50% MgO in the mugearites, declining sharply with the appearance of apatite phenocrysts, to virtually zero in the trachytes.

E. Intermediate Series.

Inspection of the major oxide plots for the Intermediate Series lavas shows the restricted compositional range of this group, relative to the Older Series, and the absence of any consistent trend relating all major oxides, Fig. 5.4. Control lines from olivine have been constructed, as this is the predominant phenocryst phase in the lavas, but it is clear that the chemical variation is not simply related to any olivine control line. K_2O shows considerable variation from 0.28 - 1.33% at roughly constant MgO levels, in a pronounced trend away from a point at around 8% MgO. To a lesser extent, both TiO_2 and P_2O_5 show a similar trend to that of K_2O.

FIG. 5.4.

Major element variation diagrams for the Intermediate Series lavas. (Wt.%).

Solid lines represent control lines from the totally analysed olivine A24 (Fo_{81}), compositionally similar to the Intermediate Series olivines (Fo_{90-71}).

● = Intermediate Series lavas

□ = Olivine (A24, Table 4.1).

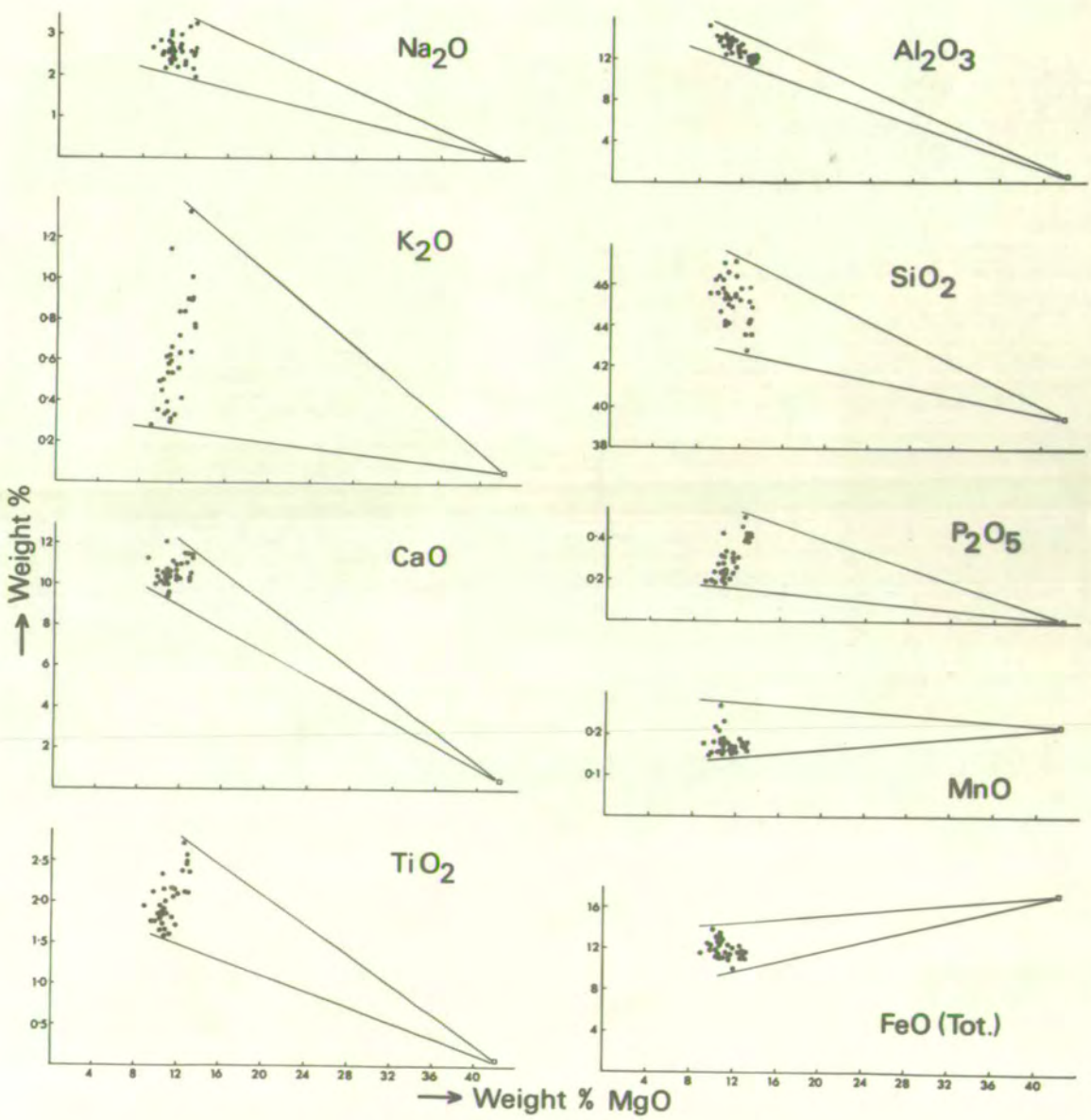
Na2O
Al2O3
K2O
SiO2
CaO
P2O5
MnO
TiO2
FeO (Tot.)
Weight %
Weight % MgO

A correlation matrix for analyses of the Intermediate Series lavas is presented in Table 5.2., and several points emerge from it. A positive correlation exists between K_2O, P_2O_5 and TiO_2, emphasising their similar trends, but more generally the coefficients reflect the absence of any consistent chemical variation in the major elements. The extremely close positive correlation between K_2O, P_2O_5, TiO_2 and Ba, Rb, Sr and Zr is discussed in the trace element chemistry section and the petrogenetic implications of the chemical coherence of this group of elements is fully discussed in Chapters 6 and 7.

F. Younger Series

Since olivine is the major phenocryst phase in the Younger Series lavas, control lines have been constructed from this mineral for all major oxide plots, Fig. 5.5. Unlike the Intermediate Series lavas, the chemical variation shows a consistent pattern and with the exception of K_2O and TiO_2, compositions lie along well defined olivine control lines. K_2O and TiO_2 show trends oblique to the olivine control lines, similar to those seen in the Intermediate Series. Plagioclase phenocrysts appear in the less magnesian lavas of the series, but the extremely close adhesion of composition points to an olivine control line in the Al_2O_3 plot suggests that plagioclase has not been a significant fractionating phase. A correlation matrix for the Younger Series lavas presented in Table 5.3. emphasises the trend and degree of olivine control, with

TABLE 5.2.

CORRELATION MATRIX FOR INTERMEDIATE SERIES ANALYSES

	SiO_2	Al_2O_3	TiO_2	FeO(Tot)	MnO	MgO	CaO	Na_2O	K_2O	P_2O_5	H_2O	Ni	Cr	V	Zr	Y	Ba	Sr	Rb
SiO_2	1.00																		
Al_2O_3	.23	1.00																	
TiO_2	-.39	-.75	1.00																
FeO(Tot)	-.14	.45	-.48	1.00															
MnO	-.33	.14	-.23	.56	1.00														
MgO	-.40	-.84	.64	-.40	-.16	1.00													
CaO	-.42	-.26	.53	-.63	-.25	.31	1.00												
Na_2O	-.11	.18	.16	-.37	-.87	.27	.28	1.00											
K_2O	-.36	-.76	.86	-.53	-.21	.64	.58	.14	1.00										
P_2O_5	-.49	-.82	.90	-.44	.14	.75	.58	.22	.88	1.00									
H_2O	-.17	.11	-.24	.19	.21	-.97	-.28	-.59	-.23	-.20	1.00								
Ni	.15	-.63	.26	-.15	-.20	.59	-.20	-.58	.25	.36	-.14	1.00							
Cr	.24	-.71	.35	-.54	-.28	.61	.21	-.56	.42	.46	-.22	.67	1.00						
V	-.47	-.50	.80	-.18	-.12	.55	.33	.20	.54	.68	-.20	.26	.11	1.00					
Zr	-.50	-.48	.61	-.27	-.70	.41	.61	.51	.68	.72	-.22	.73	.16	.39	1.00				
Y	-.73	.10	-.26	.20	-.95	-.14	-.15	.52	-.15	-.21	-.60	.94	-.78	-.35	.83	1.00			
Ba	-.47	-.86	.91	-.49	-.18	.79	.56	.17	.89	.96	-.19	.42	.53	.67	.65	.11	1.00		
Sr	-.56	-.66	.79	-.55	-.24	.66	.66	.16	.83	.84	.40	.15	.29	.50	.74	-1.00	.82	1.00	
Rb	-.30	-.62	.78	-.49	-.27	.52	.42	.58	.87	.73	-.16	.19	.28	.48	.45	-.21	.75	.78	1.00

FIG. 5.5.

Major element variation diagrams for the Younger Series lavas. (Wt. %).

Solid lines represent control lines from the totally analysed olivine A24 (Fo_{81}), compositionally similar to the Younger Series olivines (Fo_{86-72}).

● = Younger Series lavas.

□ = Olivine (A24, Table 4.1)

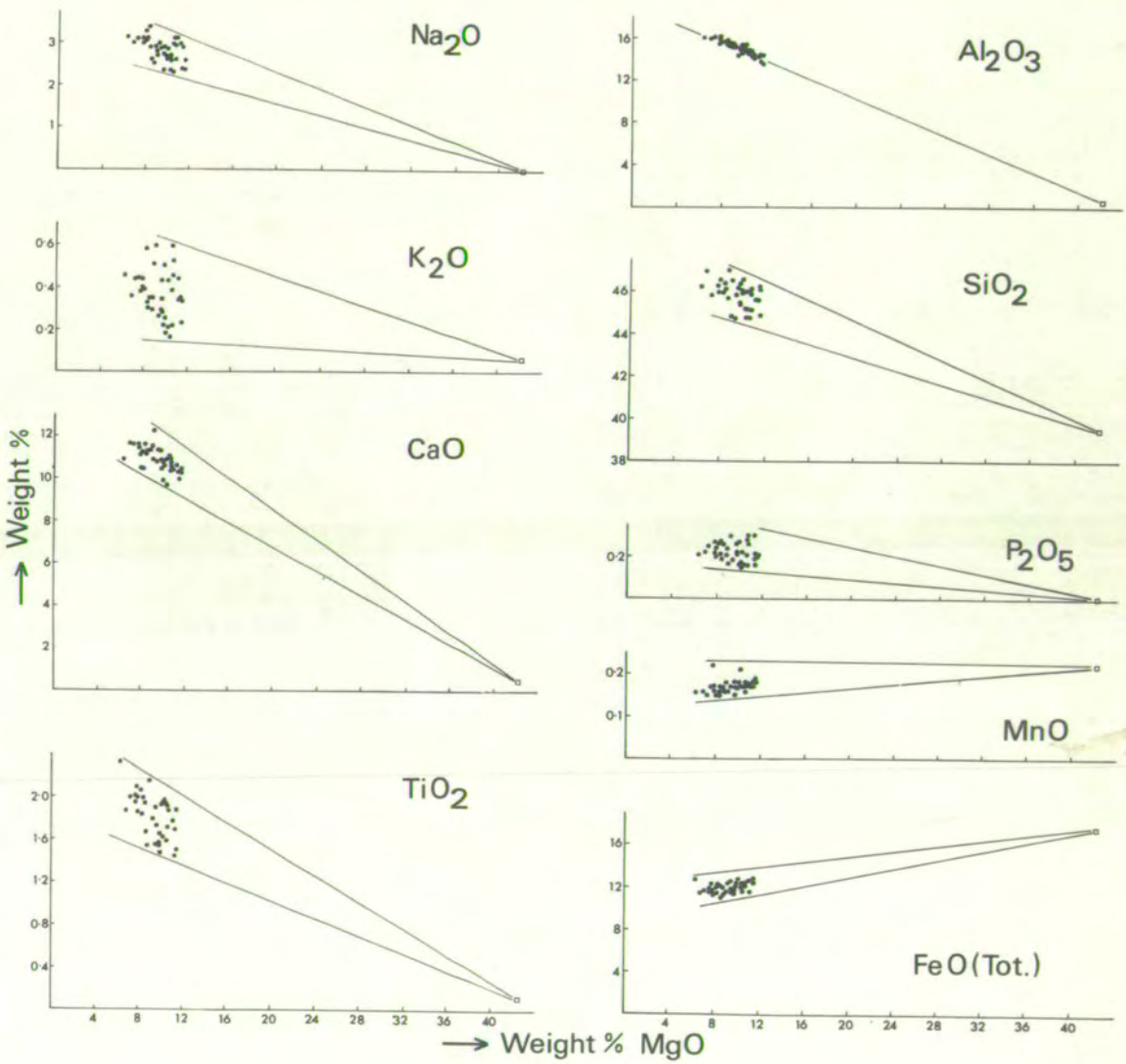
Na2O
Al2O3
K2O
SiO2
CaO
P2O5
MnO
TiO2
FeO(Tot.)
→ Weight %
→ Weight % MgO

TABLE 5.3.

CORRELATION MATRIX FOR YOUNGER SERIES ANALYSES

	SiO_2	Al_2O_3	TiO_2	FeO(Tot)	MnO	MgO	CaO	Na_2O	K_2O	P_2O_5	H_2O	Ni	Cr	V	Zr	Y	Ba	Sr	Rb
SiO_2	1.00																		
Al_2O_3	.48	1.00																	
TiO_2	-.89	.39	1.00																
FeO(Tot)	-.49	-.42	.19	1.00															
MnO	-.57	-.27	-.28	.25	1.00														
MgO	-.46	-.91	-.59	.30	-.33	1.00													
CaO	.19	.51	.39	-.63	-.36	-.55	1.00												
Na_2O	.36	.40	.52	-.20	-.27	-.51	.29	1.00											
K_2O	-.83	.14	.51	-.12	-.29	-.25	.22	.66	1.00										
P_2O_5	-.28	.23	.39	-.13	.28	-.12	.26	.51	.83	1.00									
H_2O	-.45	-.42	.31	.46	.23	.81	-.38	-.62	-.33	-.28	1.00								
Ni	-.35	-.88	-.65	.29	.28	.92	-.60	-.56	-.27	-.16	.90	1.00							
Cr	-.28	-.65	-.52	.18	.30	.70	-.43	-.58	-.28	-.19	.28	.74	1.00						
V	-.15	.32	.55	.22	.90	-.17	.36	.19	.10	.15	-.42	-.25	-.14	1.00					
Zr	.29	.19	.61	-.62	-.26	-.32	.11	.56	.81	.63	-.19	-.32	-.18	.99	1.00				
Y	.38	.38	.35	.13	-.31	-.45	.16	.41	.13	.99	-.22	-.41	-.25	-.71	.28	1.00			
Ba	-.23	-.87	.21	-.18	-.16	.31	.14	.18	.72	.60	-.55	.37	.14	-.66	.73	-.13	1.00		
Sr	-.20	.13	.49	-.23	-.42	-.20	.42	.39	.77	.62	-.21	-.24	-.17	.14	.69	.59	.75	1.00	
Rb	-.23	-.66	.32	-.92	-.10	.21	.51	.50	.79	.71	-.20	-.67	-.12	-.81	.55	-.73	.53	.61	1.00

emphasises the trend and degree of olivine control, with positive coefficients for MgO with FeO(Tot), MnO and negative coefficients with SiO_2, Al_2O_3, CaO and Na_2O.

G. AFM Diagrams

Fig. 5.6. shows the variation of the three series within AFM plots. The extreme differentiation of the Older Series is clear, as is the degree of olivine + clinopyroxene control in the more basic lavas, which lie on a trend away from the olivine and clinopyroxene composition points. The moderate iron-enrichment trend, intermediate to the Hawaiian alkalic and tholeiitic trends and similar to that of the transitional tholeiites of Reunion, may reflect the transitional nature of the Older Series. The Younger Series lavas show a relatively well defined but limited trend to iron enrichment, away from the olivine composition point, while the Intermediate Series lavas show a more scattered pattern, consistent with the absence of any clear major element variation.

5.3. TRACE ELEMENT CHEMISTRY

A. Frequency Distribution of Trace Element Data

Histograms showing the distribution and range of concentrations of trace elements within and between the three lava series are presented in Fig. 5.7. Inspection of the histograms reveals the following features:

(1) The extremely wide range and generally skewed distribution of the Older Series consistent with the pattern observed for the major oxides.

(2) A considerably greater range of Ba, Rb, Sr, Zr values in

FIG. 5.6.

A F M plots for the Mauritian volcanics.

(1) = Older Series

(2) = Intermediate Series

(3) = Younger Series

Solid lines A and T represent the Hawaiian alkalic and tholeiitic trends respectively, MacDonald and Katsura (1964).

Dashed lines represent the limits of the Reunion lavas, Upton and Wadsworth (1966).

● = Data

□ = Olivine A24 (Table 4.1)

△ = Clinopyroxene A24 (Table 4.2)

A = Wt.% $Na_2O + K_2O$.

F = Wt.% iron as FeO.

M = Wt.% MgO.

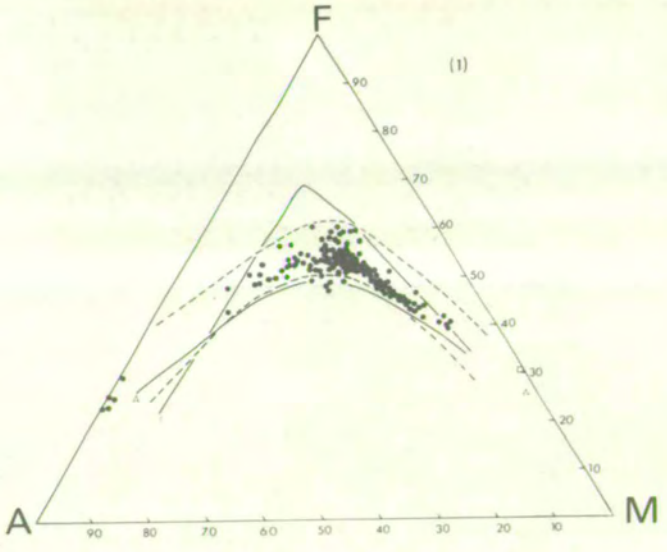
F
(1)
A
M

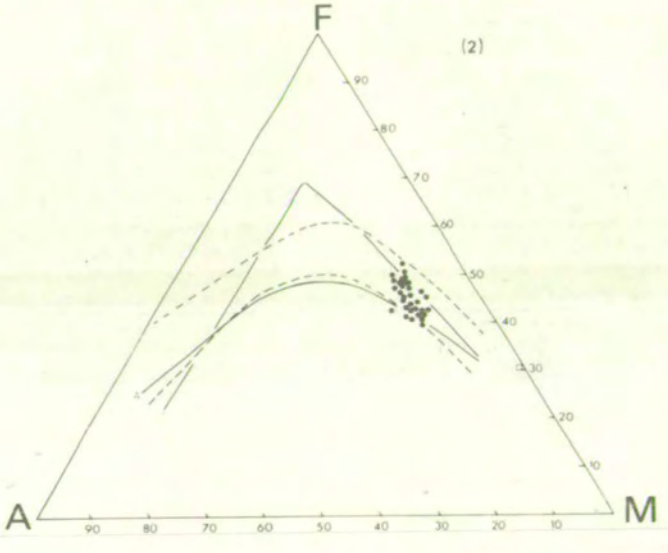
F
(2)
A
M

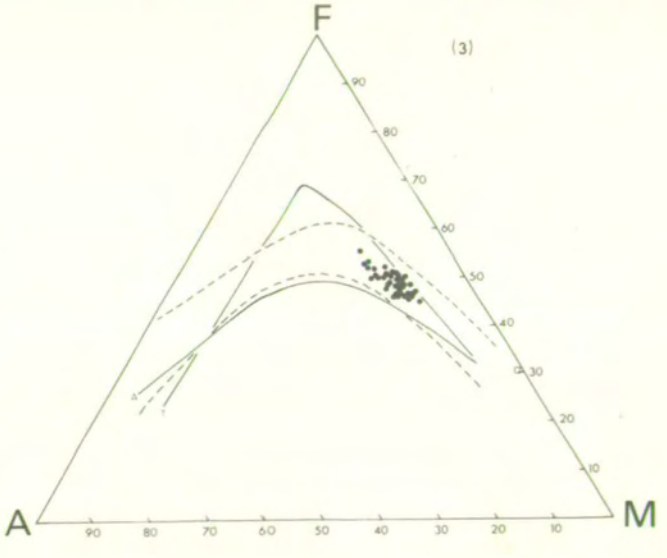
F
(3)
A
M

FIG. 5.7.

Histograms showing frequency distribution of trace elements in the Mauritian volcanics.

1. = Younger Series
2. = Intermediate Series
3. = Older Series.

* N.B. Frequency in units of 10 for the Older Series, units of 5 for the Intermediate and Younger Series.

Interrupted p.p.m. scales for Zr, Y, Ba in Older Series histograms.

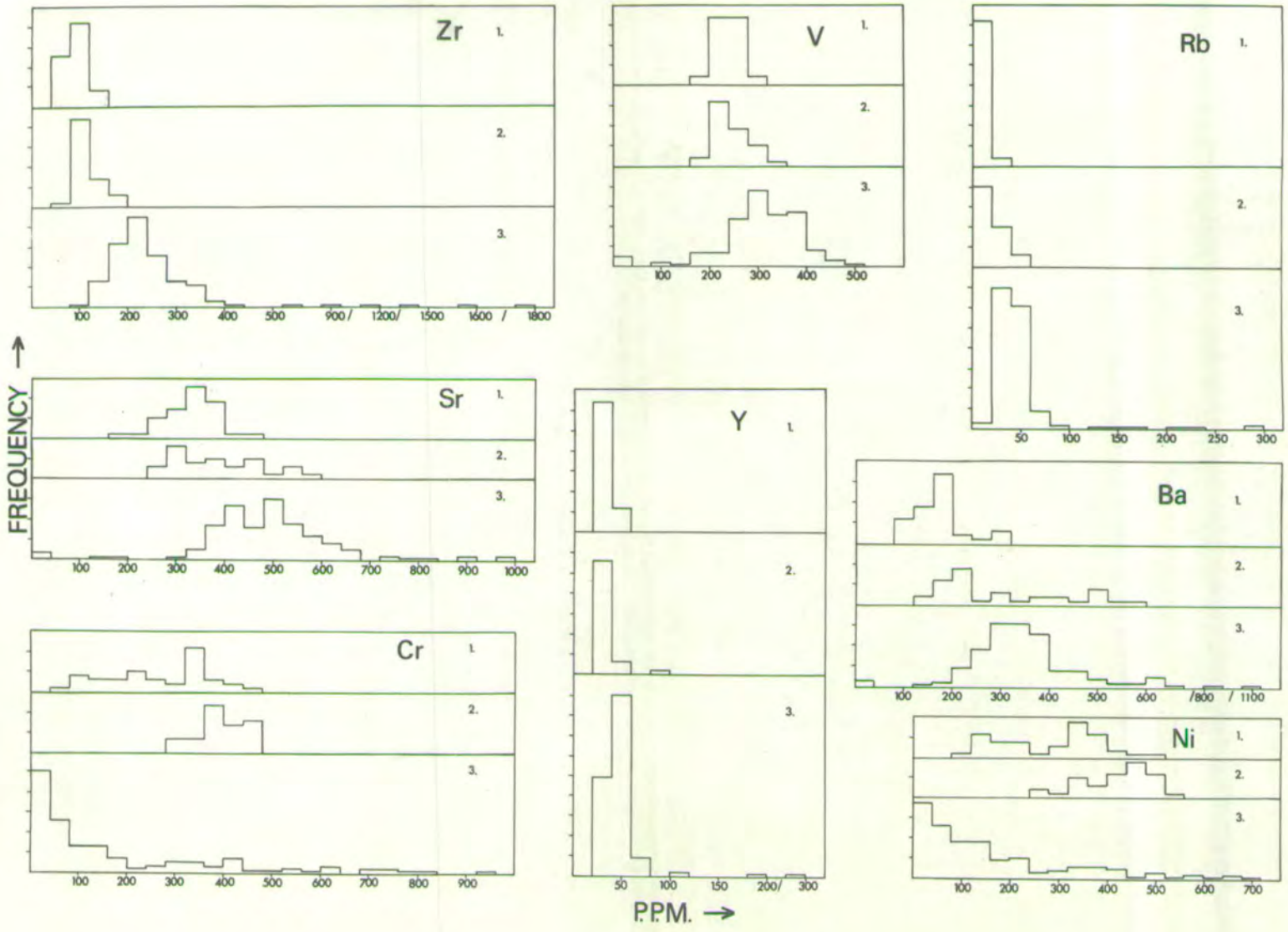
Zr
1.
2.
3.
100 200 300 400 500 900/ 1200/ 1500 1600 / 1800
V
1.
2.
3.
100 200 300 400 500
Rb
1.
2.
3.
50 100 150 200 250 300
FREQUENCY
Sr
1.
2.
3.
100 200 300 400 500 600 700 800 900 1000
Y
1.
2.
3.
50 100 150 200/ 300
Ba
1.
2.
3.
100 200 300 400 500 600 /800 / 1100
Cr
1.
2.
3.
100 200 300 400 500 600 700 800 900
Ni
1.
2.
3.
100 200 300 400 500 600 700
P.P.M.

the Intermediate Series lavas compared with the Younger Series. (3) The wide range of Ni and Cr values in the Younger Series relative to the Intermediate Series lavas.

B. Older Series

Variation diagrams for the Older Series trace elements plotted against MgO are presented in Fig. 5.8. These reinforce the pattern observed in the major oxide plots with lavas containing more than 5-6% MgO lying along an olivine + clinopyroxene control line and the more evolved compositions generally along a line from olivine + clinopyroxene + plagioclase + titanomagnetite, though additional trends specific to a particular element occur. The chemical variation and behaviour of individual trace elements is summarised below.

(i) Barium

Barium proxies for potassium and consequently concentrates in potassic phases, being largely excluded by the mafic minerals, Prinz (1967). Ba rises in the basic lavas from 250 p.p.m. at 16% MgO to 350 p.p.m. at 5-6% MgO where as olivine and clinopyroxene are joined by plagioclase and titanomagnetite, it rises to > 600 p.p.m. in the mugearites. In the most evolved compositions i.e. trachytes and phonolitic trachytes Ba shows highly variable concentrations, from 15-1095 p.p.m. and as the K-rich phase anorthoclase is a major phenocryst in these lavas, it seems likely that fractionation of this mineral has controlled these levels. High Ba levels are restricted to the nepheline free trachytes (A261, A264) while low values only occur in the nepheline bearing trachytes and phonolitic trachytes (A185, A249, A260). Although

FIG. 5.8.

Trace element variation diagrams for the Older Series volcanics, plotted against MgO.

Trace elements in p.p.m.; MgO in Wt.%

Symbols, control lines and tie lines as in Fig. 5.3.

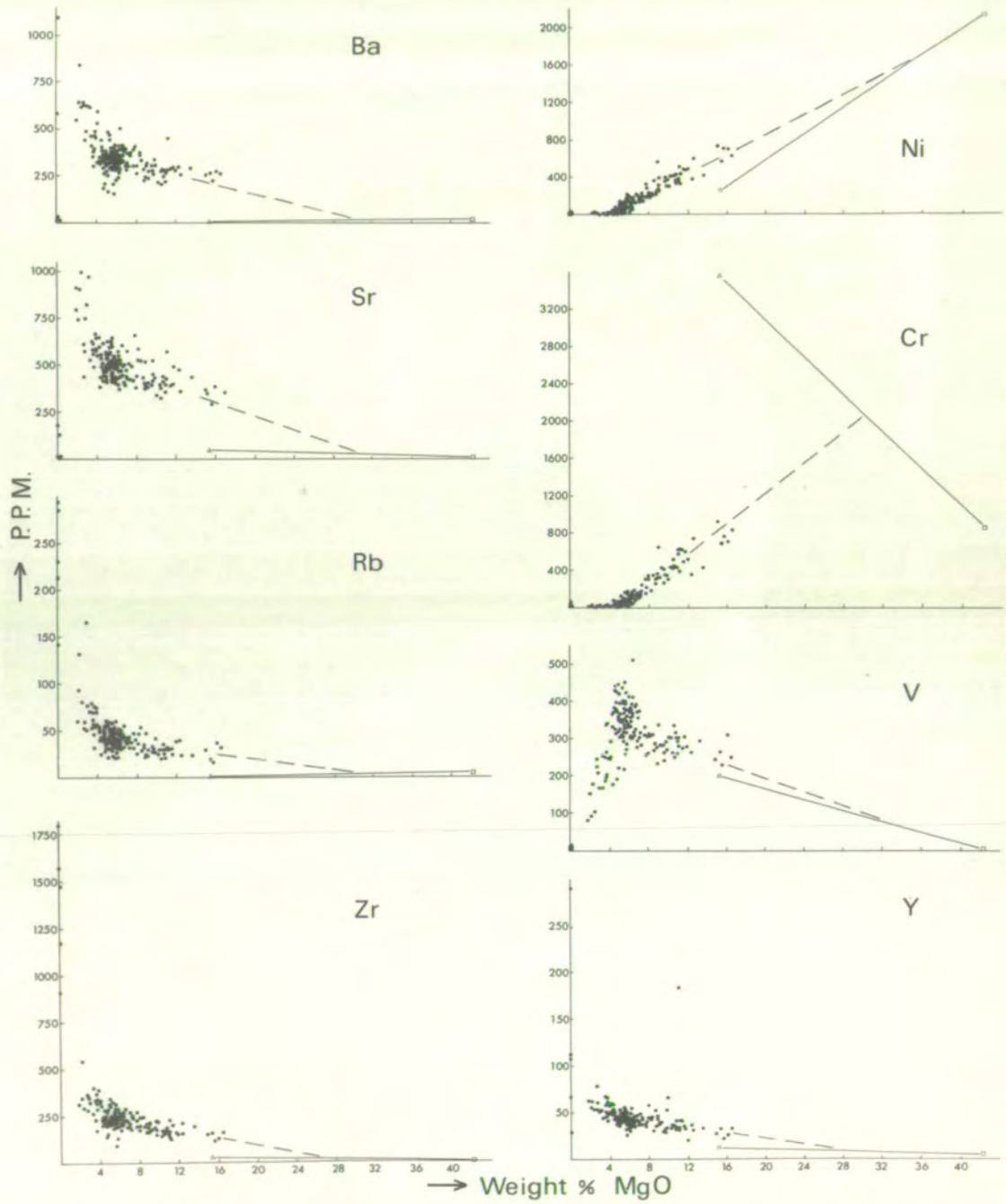
Ba
Ni
Sr
Cr
Rb
V
Zr
Y
P.P.M.
Weight % MgO

nepheline may concentrate Ba, Heier (1964) it is unlikely that fractionation of this phase has produced the observed variation as the major oxide levels of all the trachytes are very similar; a more reasonable explanation is that the low-Ba, nepheline-bearing trachytes represent the most extreme differentiates of the series and that the bulk of the Ba has been removed by earlier fractionation of anorthoclase.

(ii) Strontium

Strontium rises from 350 p.p.m. at 16% MgO along an olivine + clinopyroxene control line to 450 p.p.m. at 5-6% MgO, where as more complex crystallization begins it rises sharply to >900 p.p.m. in the mugearites, declining steeply to 0-180 p.p.m. in the trachytes and phonolitic trachytes. Strontium is known to substitute for Ca in plagioclase, clino-pyroxene and apatite and for K in alkali feldspar, Prinz (1967), Ridley (1970). The sharp rise in Sr levels through the range 6-2.5% MgO, where plagioclase is a major phenocryst phase suggests that crystallization of titanomagnetite + clino-pyroxene + plagioclase enriches the liquid in Sr at a greater rate than depletion due to the degree of plagioclase fraction-ation. The sudden decline in Sr levels coincides with the appearance of anorthoclase and apatite as phenocrysts and is probably related to their fractionation. In particular, apatite carries very high levels of Sr, Deer et al. (1963) and though present in only small amounts, may play a signifi-cant role in depletion. A similar close relationship between Sr levels and apatite fractionation is seen in many alkaline rock series e.g. Hawaii, MacDonald (1968).

(iii) Rubidium

Rubidium rises from 10 p.p.m. at 16% MgO to 40 p.p.m. at 5-6% MgO, increasing sharply along the evolved trend to a maximum of 295 p.p.m. in the trachytes. Rb typically substitutes for Potassium, particularly in K-feldspar and feldsparthoids, Prinz (1967) and the overall variation of Rb is closely comparable to that of potassium.

(iv) Zirconium

Zirconium rises from 125-200 p.p.m. along an olivine + clinopyroxene control line and then sharply below 5-6% MgO as more complex crystallization takes place, to a maximum of 1800 p.p.m. in the trachytes. The persistent rise in Zr is largely attributable to its exclusion by most fractionating phases, Prinz (1967), Jamieson and Clarke (1970). Variable Zr levels in the trachytes and phonolitic trachytes with relatively low levels in the nepheline free trachytes and high levels in the nepheline bearing samples are consistent with the hypothesis suggested in the Ba section that the nepheline-bearing trachytes and phonolitic trachytes represent the most extreme differentiates of the series.

(v) Yttrium

Yttrium is believed to substitute for calcium and is particularly concentrated in apatite and to a lesser extent in ilmenite and magnetite, Prinz (1967). The general pattern of increasing Y in the Older Series to a maximum of 290 p.p.m. in the trachytes, however, would suggest that fractionation of these phases has not materially depleted Yttrium levels in the liquid. Considerable variation from 29-290 p.p.m. occurs in the trachytes and phonolitic trachytes, but shows no

systematic relationship with any other element or parameter.

(vi) Vanadium

Prinz (1967) shows that vanadium substitutes for iron, and is primarily concentrated in magnetite. The observed variation of vanadium in the Older Series is compatible with this, increasing from 225 p.p.m. at 16% MgO to 350 p.p.m. at 5-6% MgO and then declining sharply to 0-11 p.p.m. in the trachytes. A pronounced 'tail' at the junction of the two trends is apparent, similar to that seen in the FeO(Tot), TiO_2 and CaO plots, and comprises those samples carrying phenocryst titanomagnetite.

(vii) Chromium

Chromium shows a pronounced trend dropping steeply along an olivine + clinopyroxene control from >800 p.p.m. at 16% MgO to only 50 p.p.m. at 5-6% MgO, and declining slowly to <30 p.p.m. in the trachytes. Chromium preferentially enters into the clinopyroxene structure and the rapid increase in the more basic lavas reflects their high contents of phenocryst clinopyroxene.

(viii) Nickel

Nickel substitutes for magnesium and preferentially enters into the olivine structure, Deer et al. (1963), Prinz (1967), and the observed variation in the Older Series reflects this, high nickel levels being associated with olivine-rich basic lavas. Ni declines sharply from >600 p.p.m. at 16% MgO to <50 p.p.m. at 5-6% MgO, falling to zero in the trachytes, along the more complex olivine + clinopyroxene + plagioclase + titanomagnetite control line.

C. Intermediate Series

Trace element variation diagrams for the Intermediate Series lavas are presented in Fig. 5.9. In contrast to the poor distribution in most of the major oxide plots, well defined trends are apparent. Ba, Rb, Sr and Zr all show a pronounced shift away from a point around 8% MgO, showing large increases for a relatively small gain in MgO, e.g. Ba 144-571 p.p.m., Rb 4-46 p.p.m., Sr 253-595 p.p.m., Zr 79 - 198 p.p.m. The trend is similar to that in the K_2O, P_2O_5 and TiO_2 plots for the Intermediate Series, a point emphasised by the correlation matrix in Table 5.2. which shows high positive coefficients between these elements. The trend is highly oblique to the olivine control lines and is clearly unrelated to fractionation of olivine, or to any other low pressure fractionation scheme compatible with the basic nature of these lavas, when the poor trends of the major oxides are considered.

The coherence of this group of elements in basic lavas is well known, Jamieson and Clarke (1970) and they have been termed the "incompatible elements", Green and Ringwood (1967) in reference to their exclusion from the major silicate phases stable under upper mantle conditions. As a consequence of this discrimination these elements will be concentrated in the initial partial melts of likely upper mantle material and initial ratios will be preserved, further crystallization serving only to concentrate the group in a linear fashion, if total incompatibility is maintained. Clearly their abundances may provide a key to the petrogenesis and polybaric fractionation history of the lavas, and the significance of

FIG. 5.9.

Trace element variation diagrams for the Intermediate Series lavas, plotted against MgO.

Trace elements in p.p.m.; MgO in Wt.%

Symbols, control lines and tie lines as in Fig. 5.4.

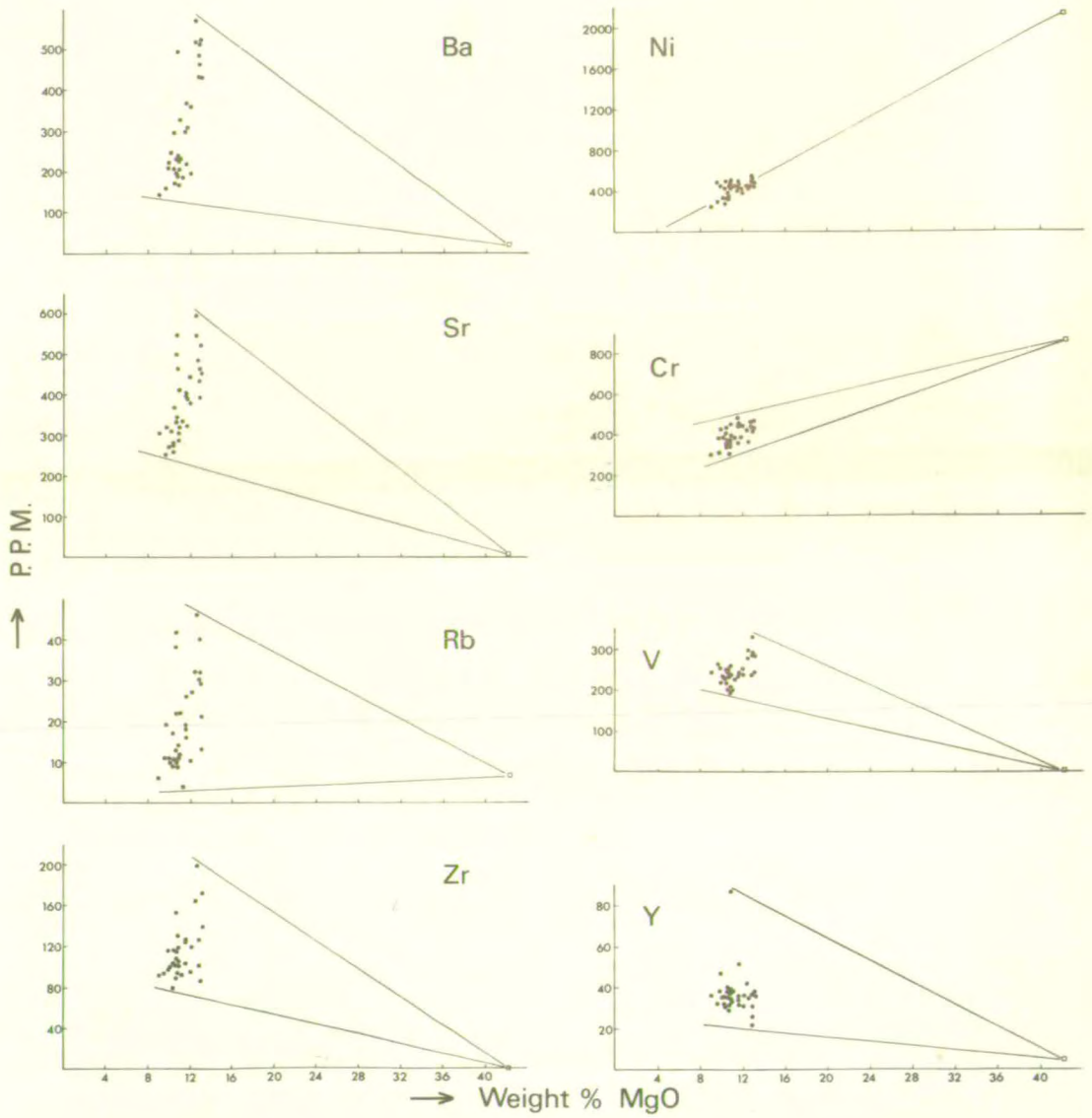
Ba
Ni
Sr
Cr
Rb
V
Zr
Y
P.P.M.
Weight % MgO

their variable levels in the Intermediate Series laves is discussed in chapters 6 and 7.

In contrast to the well defined trends of the incompatible elements, Cr, Ni, V and Y all show scattered trends similar to the major oxide plots.

D. Younger Series

Trace element variation diagrams plotted against MgO, for the Younger Series lavas, are presented in Fig.5.10. The pronounced olivine control seen in the major oxide plots is apparent only in the variation of nickel which rises from 250 p.p.m. at 6% MgO to 400 p.p.m. at 11% MgO. Vanadium and Yttrium show scattered distributions, while chromium analyses lie along a trend rising sharply from 50 p.p.m. at 6% MgO to 470 p.p.m. at 11% MgO, which may be related to the occurrence of small spinels as inclusions within the olivine phenocrysts. Barium follows a trend similar to that in the Intermediate Series lavas, rising from 85-310 p.p.m. away from a point around 8-10% MgO. Similar patterns are observed for Sr, Rb and Zr although the latter two elements show relatively dispersed trends which may be consistent with the effects of olivine fractionation overprinting the earlier cross-trend. A correlation matrix for the Younger Series lavas presented in Table 5.3. shows limited positive correlations within the incompatible group K_2O, Ba, Sr, Rb, Zr, P_2O_5 and TiO_2, compared with the Intermediate Series, consistent with the more dispersed and less extreme variation in this series.

FIG. 5.10.

Trace element variation diagrams for the Younger Series lavas, plotted against MgO.

Trace elements in p.p.m.; MgO in Wt.%.

Symbols, control lines and tie lines as in Fig. 5.5.

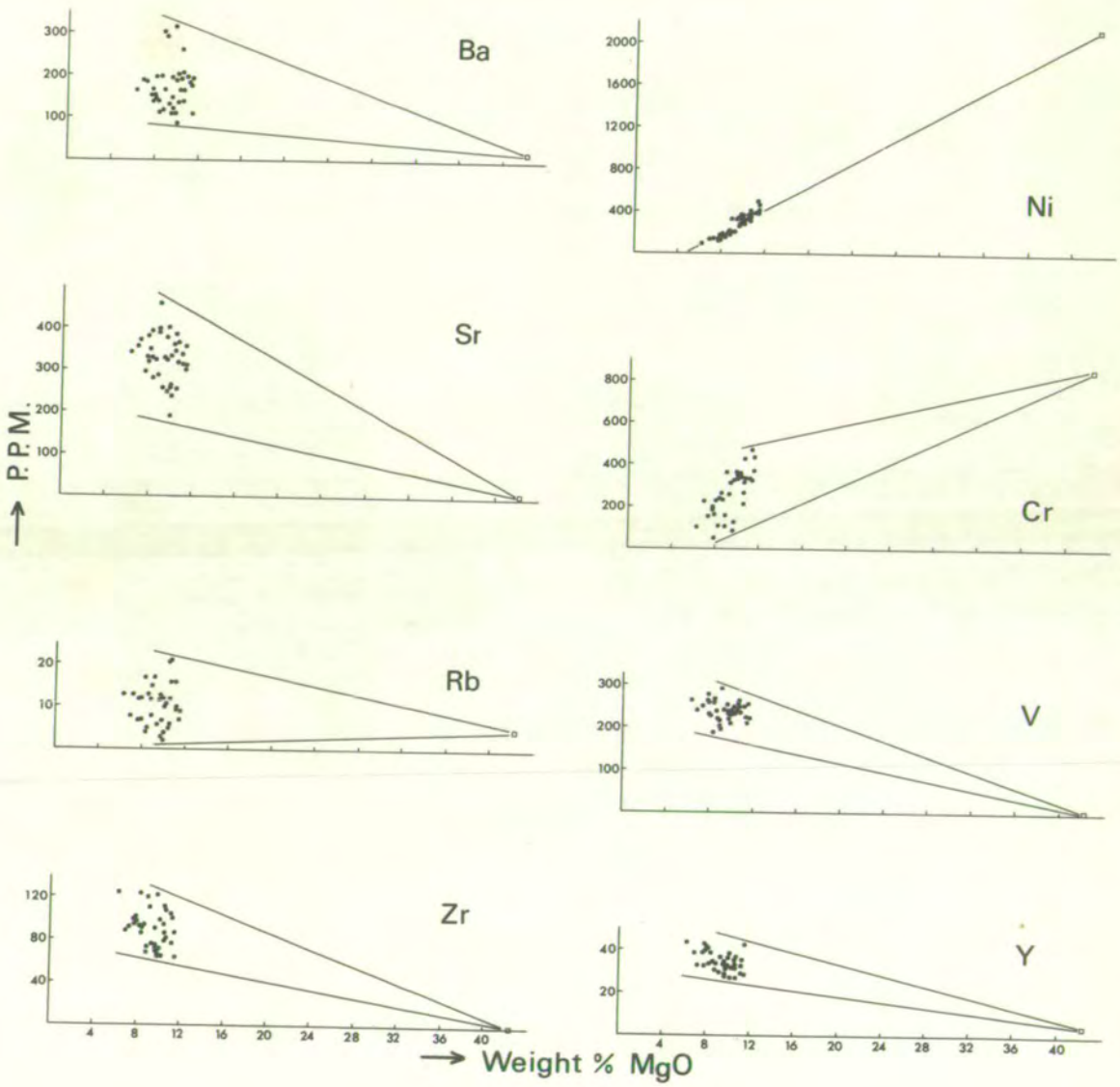
Ba
Ni
Sr
Cr
Rb
V
Zr
Y
P.P.M.
Weight % MgO

E. K/Rb Ratios

Gast (1965, 1968) has demonstrated that K/Rb ratios in basic lavas are of considerable petrogenetic significance, being largely controlled by the nature and initial degree of partial melting in the source material, and the amount and type of subsequent crystal fractionation.

Fig. 5.11 summarises the range of K/Rb values in the three Mauritian series. The bulk of the basic lavas of the Older Series have ratios between 200-350, rather lower than those of the Hawaiian (ca. 500) and Reunion (ca. 400) tholeiitic lavas, McDougall and Compston (1965). A decline in K/Rb values with increasing differentiation is apparent in the Older Series, to a mean of ca. 175 in the trachytes. Decreasing K/Rb ratios with differentiation have been reported from many volcanic provinces, Erlank (1968) and are normally held due to the persistent discrimination against Rb^+ in favour of K^+ in crystallizing lattices - particularly among feldspars. In the Older Series lavas the decline begins in hawaiitic compositions and correlates with the appearance of Kaersutite as a phenocryst phase. Hart and Aldrich (1967) have shown that amphiboles preferentially concentrate K with respect to Rb, and Kesson and Price (1972) show K/Rb ratios from 1000-4400 in some kaersutites. Clearly even limited fractionation of Kaersutite from liquids with basaltic ratios would produce a trend to decreasing K/Rb ratios and it is possible this may have contributed to the decline in the Older Series lavas.

In contrast to the Older Series, the relatively

FIG. 5.11.

K/Rb ratios plotted against Wt.% K, for the Mauritian volcanics.

● = Older Series.

△ = Intermediate Series.

□ = Younger Series.

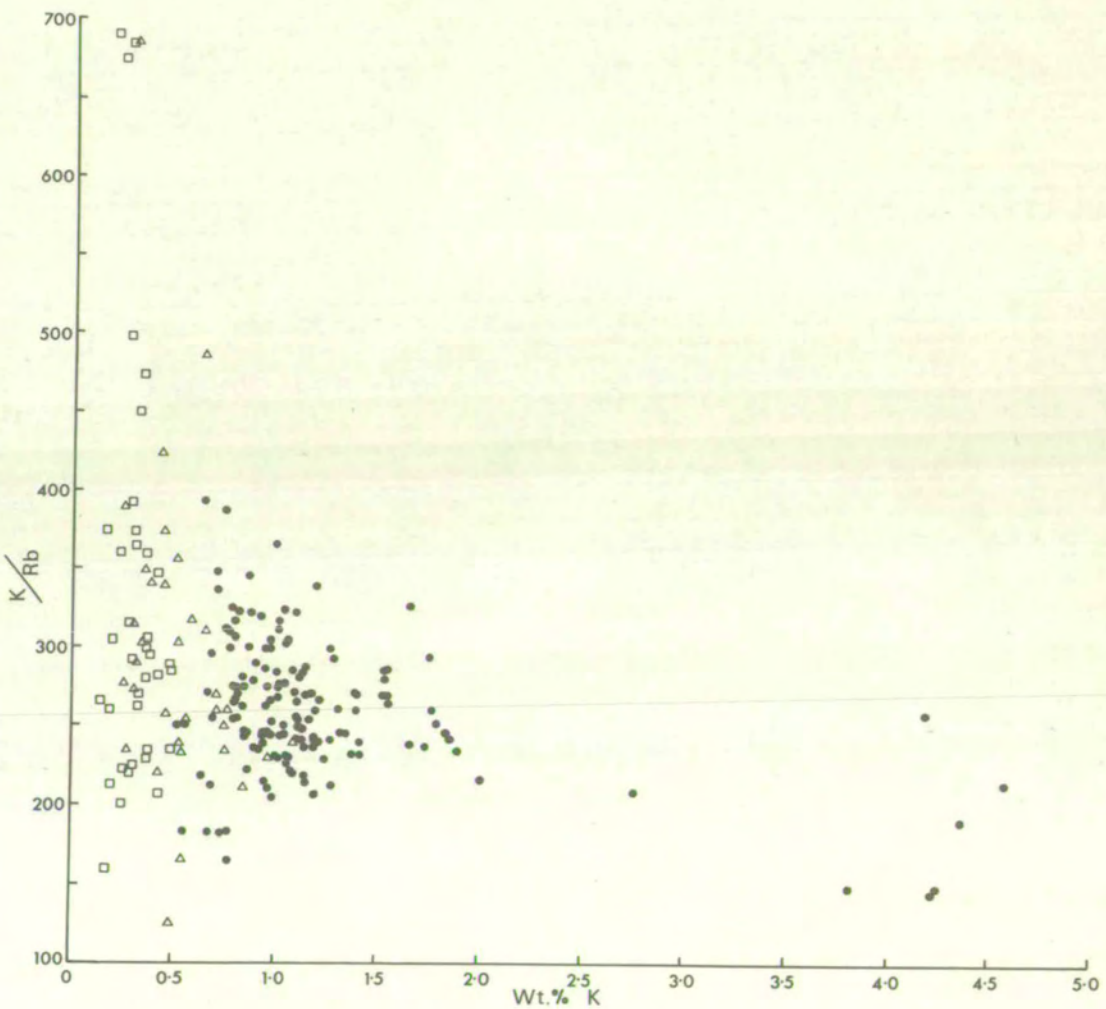
700
600
500
400
300
200
100
K/Rb
0
0·5
1·0
1·5
2·0
2·5
3·0
3·5
4·0
4·5
5·0
Wt.% K

undifferentiated basic lavas of the Intermediate and Younger Series show a much wider range of K/Rb values from 125-686 in the former and 160-691 in the latter, extending into rather lower values than is typical of many oceanic alkali basalt suites, Gast (1968).

6. PETROGENESIS, 1 : LOW PRESSURE DIFFERENTIATION

6.1. INTRODUCTION

The petrography, mineralogy and geochemistry of the Mauritian volcanics have been described in the preceeding chapters. The primary aim of the present chapter is to integrate this data and attempt to show how far the chemical variation of the three series can be explained in terms of the low pressure fractionation of observed phenocryst phases.

If the geochemical consequences of low pressure fractionation can be assessed in each of the three lava series, then clearly any remaining chemical variation should reflect either initial patterns imposed on the primitive magma during its probable formation in the upper mantle, or the effects of any subsequent polybaric fractionation as the magma migrated to high crustal levels. The origin and differentiation of the lavas at elevated pressures is discussed in Chapter 7.

6.2. OLDER SERIES

A. Introduction

It is clear from the preceeding chapters that the Older Series forms a widely differentiated group of lavas, ranging from picrite basalt to phonolitic trachyte. Gradation between the various rock types is apparent in their petrography, mineralogy and in the presence of coherent chemical trends linking different compositions, and implies that they are genetically related, as was appreciated by Walker and

Nicolaysen (1954). Several lines of evidence suggest that crystal fractionation of observed phenocryst phases has controlled the differentiation of this series:

1. A close relationship exists between chemical variation and the nature of phenocrysts present. Fig. 6.1. summarises this relationship and shows that the pronounced change in slope apparent in the major oxide and trace element variation diagrams at 5-6% MgO, coincides with the appearance of titanomagnetite and plagioclase as major phenocryst phases.

2. Compositions with <5-6% MgO show declining FeO(Tot.), TiO_2 and CaO, consistent with the fractionation of titanomagnetite and plagioclase along with clinopyroxene and olivine already crystallizing from the magma.

3. P_2O_5 shows a sudden decline around 2.5% MgO, coinciding with the appearance of apatite as a phenocryst phase.

4. Lavas with >5-6% MgO carry only olivine and clinopyroxene as major phenocryst phases, in agreement with the variation diagrams which show these compositions to lie along well-defined olivine + clinopyroxene control lines. Lavas more magnesian than the most basic aphyric composition - A171 (10.47% MgO) - are strongly enriched in phenocrystal olivine + clinopyroxene, Fig. 6.2., implying an origin by crystal accumulation.

5. The occurrence of inclusions probably derived from cumulates. Dunite and wehrlite heteradcumulates found in the picrite basalts argue strongly for the fractionation of olivine + clinopyroxene, while the presence of bytownitic anorthosite adcumulates are indicative of plagioclase

FIG. 6.1.

The relationship of major element variation to phenocryst occurrence, plotted against MgO, for the Older Series volcanics.

Ne = Nepheline
Tm = Titanomagnetite
Ap = Apatite
Ks = Kaersutite
AF = Alkali Feldspar
Pl = Plagioclase
Ol = Olivine
CPX = Clinopyroxene.

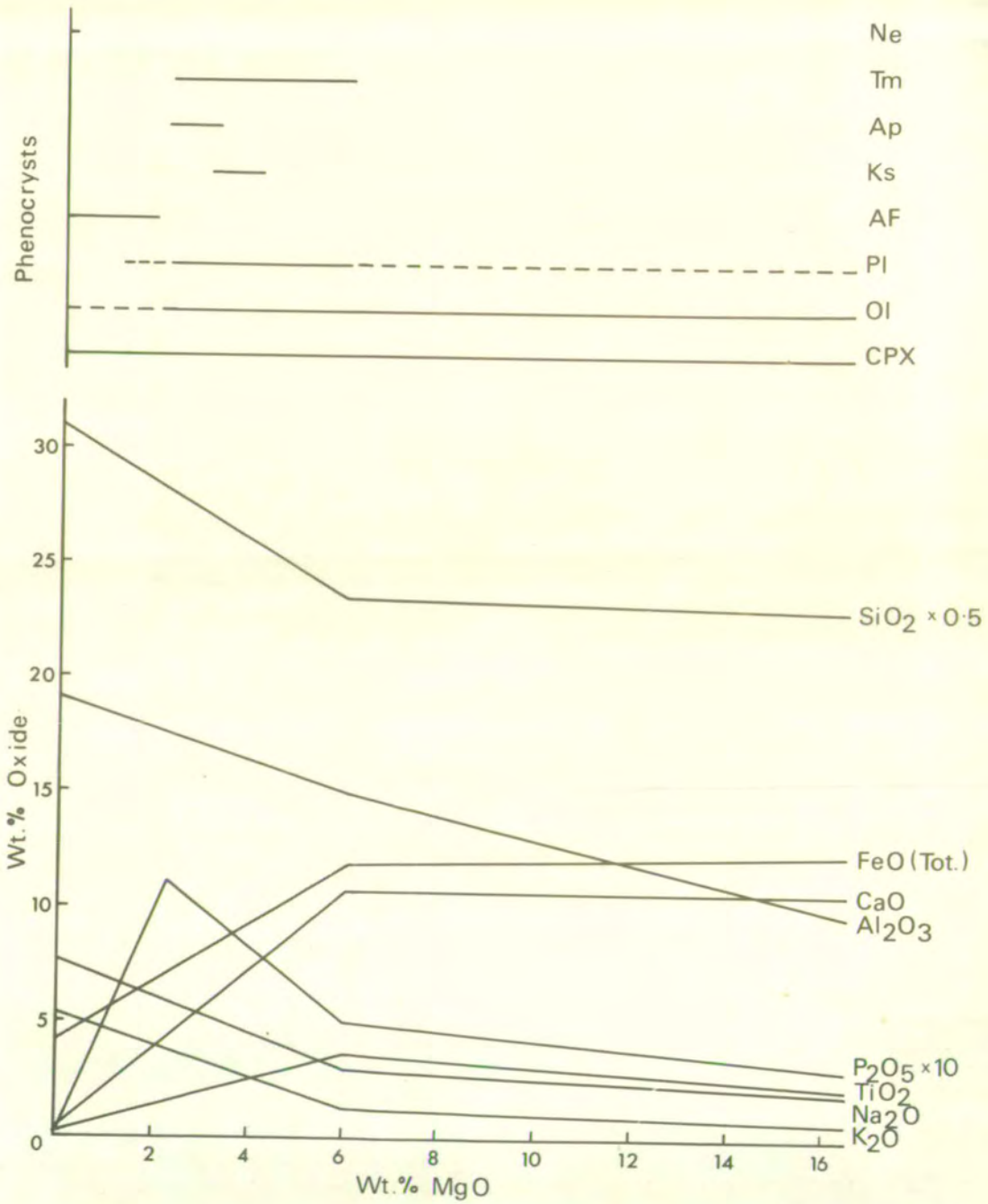
Phenocrysts
Ne
Tm
Ap
Ks
AF
Pl
Ol
CPX
Wt.% Oxide
30
25
20
15
10
5
0
SiO2 ×0·5
FeO (Tot.)
CaO
Al2O3
P2O5 ×10
TiO2
Na2O
K2O
2
4
6
8
10
12
14
16
Wt.% MgO

FIG. 6.2.

MgO content in Older Series basic lavas as a function of olivine + clinopyroxene phenocryst content.

Dashed line indicates upper limit of aphyric lava occurrence.

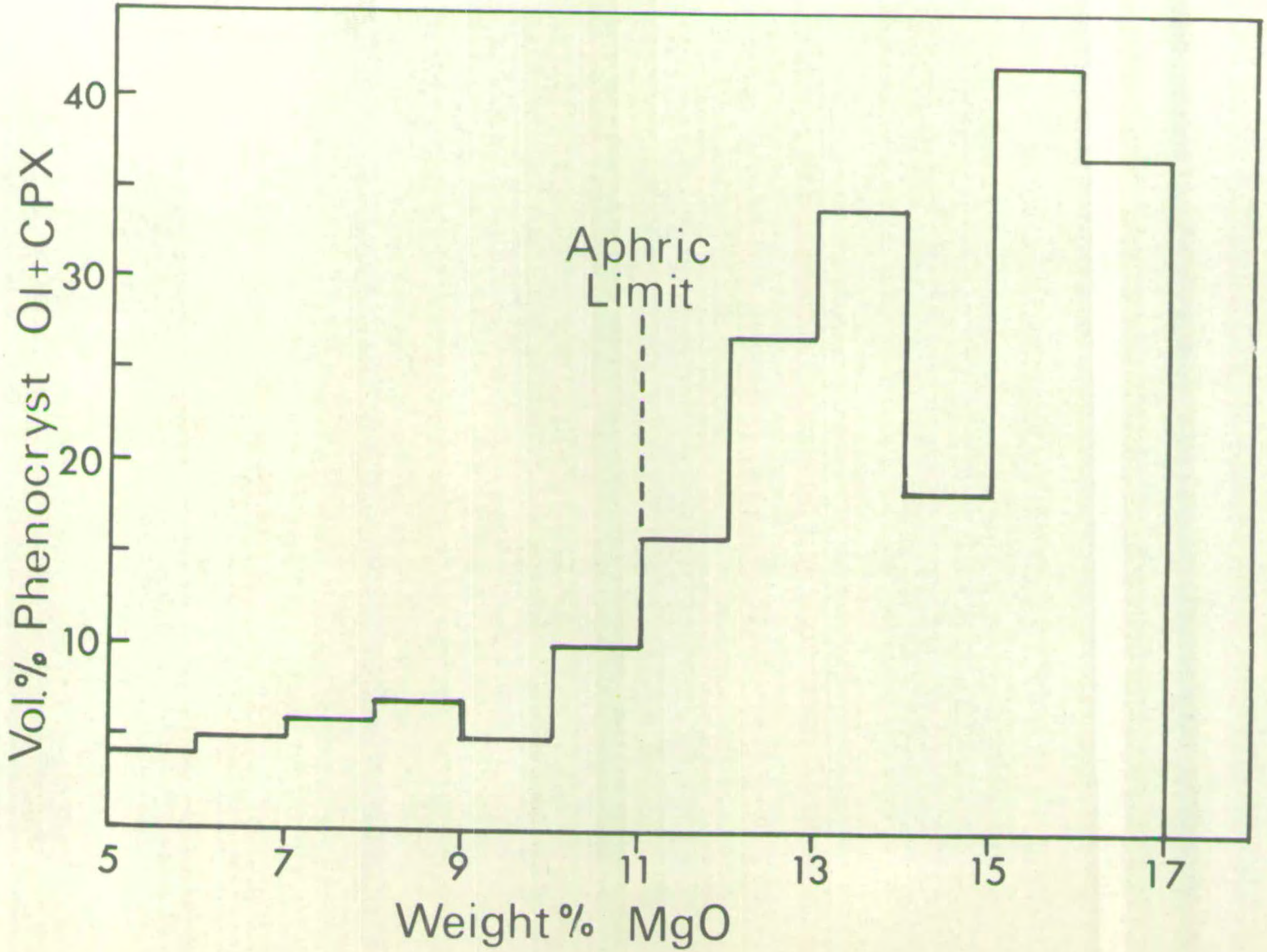
Vol.% Phenocryst Ol+CPX
40
30
20
10
Aphric
Limit
5
7
9
11
13
15
17
Weight % MgO

fractionation.

6. Occurrence of compositional zoning in phenocrysts. Zoning of clinopyroxene and plagioclase phenocrysts in the lavas is extremely common and represents an additional, though probably relatively unimportant, method of fractional crystallization apart from simple physical removal of phenocrysts by sinking out of the magma.

The occurrence of kaersutite phenocrysts, and the evidence of declining K/Rb ratios in the evolved compositions, after the appearance of this phase, might imply some degree of amphibole fractionation; however the absolute extent is difficult to assess as fractionation of the assemblage titanomagnetite + plagioclase + clinopyroxene + olivine effectively covers any major element variation caused by amphibole removal. The major significance of this phase is the indication it gives of the establishment of at least partially hydrous conditions with increasing magmatic evolution, which may explain the origin of the highly calcic bytownite feldspars of the feldsparphyric basalts, as described in Chapter 4.

Aphyric lavas, defined here as those with <5% phenocrysts, have compositions approximating to those of the liquids from which they must have crystallized and are therefore important in evaluating the course of crystallization of the Older Series lavas. Fig. 6.3. shows the distribution of aphyric lava compositions as a function of MgO. It is likely that the more basic liquids approximate to the composition of the parental magma of the Older Series, i.e. the

FIG. 6.3.

Distribution of aphyric lavas in the

Older Series as a function of MgO content.

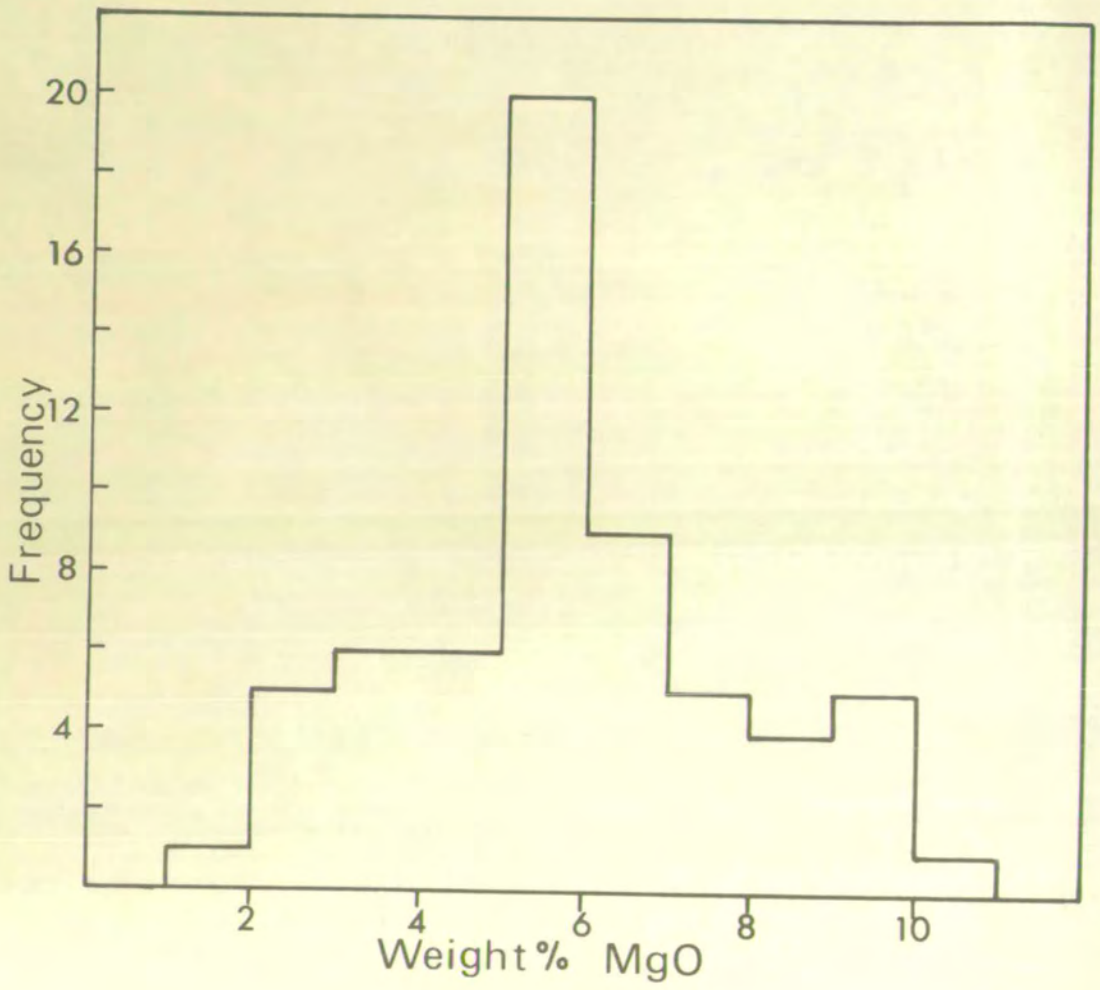
20
16
12
8
4
Frequency
2
4
6
8
10
Weight % MgO

most primitive magma supplied to high crustal levels and from which differentiation of the series took place. The composition of the most basic aphyric rock, A171 (10.4% MgO) given in Table 6.1. is taken for the purposes of calculation as representative of the Older Series parental magma, and from inspection of its norm, its transitional nature is clear.

B. C.M.A.S. Projections

Over the last decade considerable work has been done on melting relations in natural basalts and in synthetic systems approximating to basaltic compositions, and the phase relations at one atmosphere are reasonably well established, Yoder and Tilley (1962), Jamieson (1969, 1970), O'Hara (1968). As the phase diagrams are constructed from the melting relations of basalts from numerous rock suites, Jamieson (1970), their general application is indicated and comparison of the Older Series basalts with the experimentally determined boundaries should provide information both on their crystallization history and the extent of equilibration at one atmosphere.

Considerable geometrical problems arise when attempting to display the phase relations of polycomponent compositions in two or three dimensions; with this in mind, O'Hara (1968) has devised a scheme for reducing the chemical complexity of natural compositions to four end member variables, based on the geochemical coherence of certain elemental groups in basalts. The four end members are termed C, M, A, S where:

TABLE 6.1.

INFERRED OLDER SERIES PARENTAL MAGMA

A171

SiO_2	46.85
TiO_2	2.54
Al_2O_3	12.75
FeO	9.54
Fe_2O_3	2.18
MnO	0.16
MgO	10.47
CaO	10.01
Na_2O	2.59
K_2O	0.95
H_2O	1.47
P_2O_5	0.40
	99.91
Ni	415
Cr	426
V	261
Zr	172
Y	36
Ba	278
Sr	394
Rb	30
K/Rb	264
D.I.	27.96
Qz	0.00
Ne	0.00
Hy	0.79
Di	21.89
Ol	19.62
Or	5.70
Ab	22.26
An	20.68
Mt	3.21
Ilm	4.90
Ap	0.96

Major oxides in wt.%.
Trace elements in p.p.m.

$$C = 56.08\ (CaO - 3\tfrac{1}{3}\ P_2O_5 + 2Na_2O + 2K_2O)$$

$$M = 40.32\ (FeO + MnO + NiO + MgO - TiO_2)$$

$$A = 101.96\ (Al_2O_3 + Cr_2O_3 + Fe_2O_3 + Na_2O + K_2O + TiO_2)$$

$$S = 60.09\ (SiO_2 - 2Na_2O - 2K_2O)$$

expressed in molecular proportions.

Bulk lava compositions, mineral compositions and phase boundaries can all be expressed within the tetrahedron defined by this system, and by projection onto suitable compositional planes from or towards relevant mineral compositions, crystallization paths can be interpreted. Some general points about projections within the C.M.A.S. system should be noted.

1. Jamieson (1970) has demonstrated that to avoid distortion only projections from or towards minerals which are first or second liquidus phases should be used, at one atmosphere.

2. Spurious trends may appear through the obliquity of some mineral composition points to the plane of projection. This is particularly evident in the Olivine (M_2S) projection onto the plane CS - MS - A, where a spurious trend to the Orthopyroxene (MS) composition point develops.

3. With increasing (Na + K)/Ca ratio, the projection scheme breaks down, consequently projection of evolved compositions e.g. hawaiites and mugearites should be avoided.

With the above points in mind, only aphyric basalts (D.I. < 35) and in the case of the Intermediate Series, porphyritic basalts believed to approximate to liquid compositions, were projected into C.M.A.S. As olivine appears to be the first liquidus phase in all three series, phase relations at one atmosphere were examined in the projection

olivine (M_2S) onto the plane CS - MS - A. Clinopyroxene appears as second liquidus phase in the Intermediate and Older Series basalts and the projection, diopside (CMS_2) onto the plane C_3A - M - S has also been used for these two series.

The close approach of the Older Series basalts to the one atmosphere cotectics, Fig. 6.4., particularly evident in the diopside projection suggests that the corresponding magmas underwent considerable low pressure equilibration and fractionation, consistent with the petrographic and chemical evidence.

C. Silica Gap

Compositions intermediate between mugearites and trachytes (e.g. benmoreites, Muir and Tilley (1961)) are absent from analysed samples of the Older Series on Mauritius, and this is expressed in Fig. 6.5. - a silica frequency distribution diagram - by a compositional gap at 56-60% SiO_2. Similar distribution patterns are documented from many oceanic volcanic provinces, Turner and Verhoogen (1960), Chayes (1963) and the compositional break has been termed the "silica gap" or "Daly gap". The interpretation of the gap has been the subject of considerable debate, Chayes (1963), Harris (1963), Macdonald (1963), Le Maitre (1968) and it has been variously ascribed to inadequate field sampling, changes in eruptive mechanisms with increasing evolution, a viscosity maximum in intermediate composition magmas and to fundamentally different origins for the basalt-mugearite and trachyte series.

FIG. 6.4.

Wt.% projections of aphyric Older Series basalts in the system C.M.A.S., after O'Hara (1968).

(a) Projection from diopside onto part of the plane C_3A-M-S.

(b) Projection from olivine onto part of the plane CS-MS-A.

$\triangle$ = Diopside-plagioclase piercing point (a), olivine-plagioclase piercing point (b).

Phase boundaries shown for 1 atmosphere.

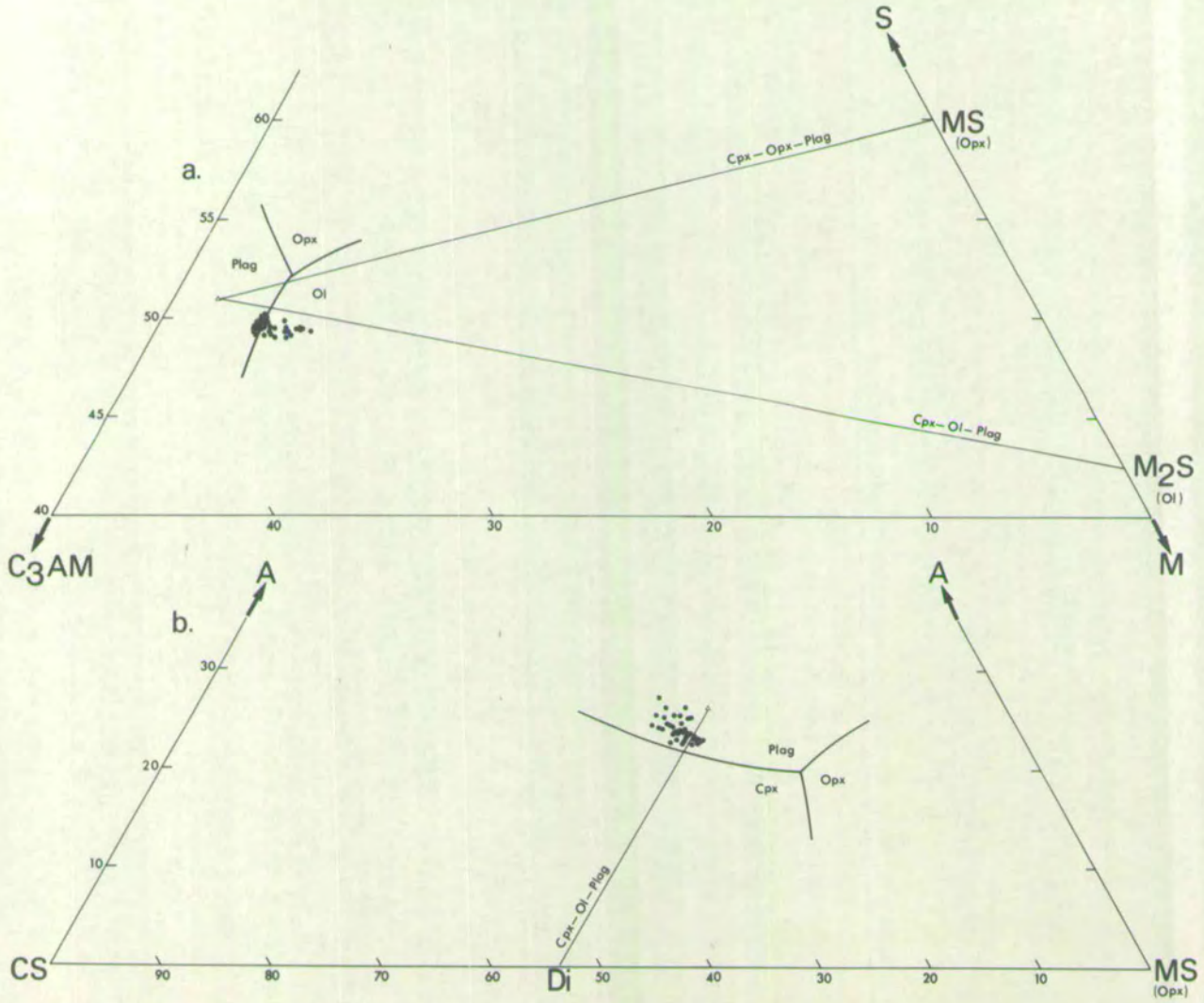
a.
S
MS
(Opx)
Cpx – Opx – Plag
Opx
Plag
Ol
Cpx – Ol – Plag
M2S
(Ol)
C3AM
M
60
55
50
45
40
40
30
20
10
b.
A
A
30
20
10
Plag
Cpx
Opx
Cpx – Ol – Plag
CS
Di
MS
(Opx)
90
80
70
60
50
40
30
20
10

FIG. 6.5.

Frequency distribution of SiO_2 in the

Older Series volcanics.

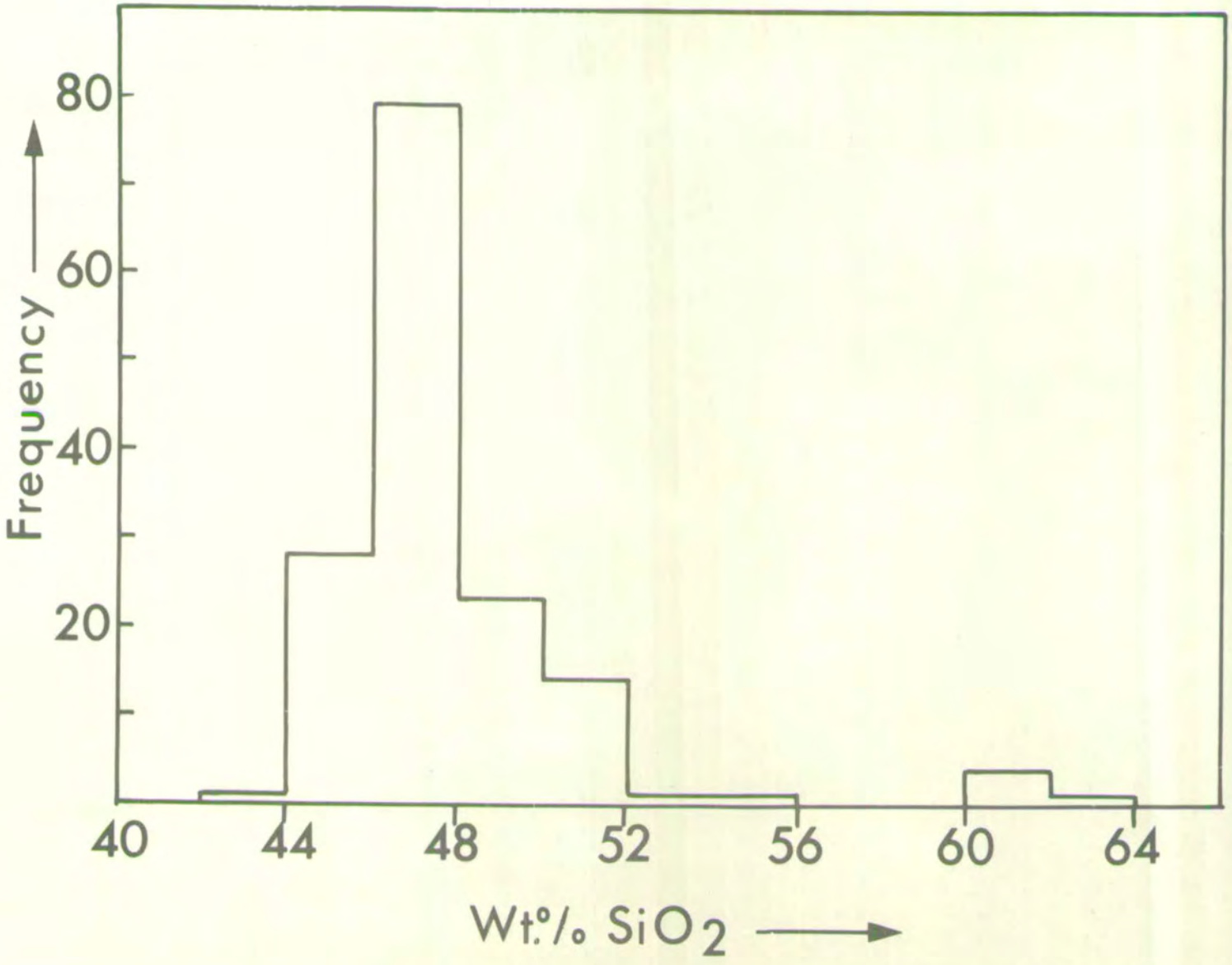
Frequency
80
60
40
20
40
44
48
52
56
60
64
Wt.% SiO2

The representative nature of the Older Series sample can be questioned as it is clear from the preceeding chapters that the upper portions of the shield, which might be expected to carry more evolved lavas, have been largely removed by erosion, while large areas are concealed beneath Intermediate and Younger Series flows. However the presence of all evolved compositions except benmoreite in the analysed sample would seem to require an unreasonable degree of separation for the benmoreites.

The positively skewed distribution of compositions in Fig. 6.5. is compatible with an origin for the differentiation of the lavas by fractional crystallization, the reducing occurrence of evolved lavas corresponding to the successively smaller volumes of available magma, as fractionation proceeds.

The basalt-mugearite series and the trachytes of the Older Series have different modes of occurrence, the former as relatively mobile flows and the latter as viscous high level intrusive domes. It is conceivable that with increasing evolution and viscosity, eruption required the assistance of a vapour phase, but that the vapour pressure in the magma chamber did not exceed the load pressure and boil off until the final stages of fractionation. This would result in only the most extreme differentiates being transported to the upper portions of the shield, less evolved compositions remaining at depth as intrusive bodies. The possibility that processes involving secondary boiling phenomena might control the bimodal distribution of magma compositions was recognised by Le Maître (1968). The relationship of the rare mafic

syenite inclusions in the Piton de Milieu trachyte (A264) is uncertain, particularly as these were too small to be separated and analysed, conceivably however they may represent the less evolved magmas postulated as low level intrusive bodies in this scheme.

D. Trachytes and Phonolitic-trachytes

Small volumes of trachyte and phonolitic-trachyte occur in the Older Series and from inspection of the variation diagrams presented in Figs. 5.3., 5.8. and the chemical variation/phenocryst occurrence plot in Fig. 6.1. it is clear that these compositions represent the end products of protracted fractionation of olivine + clinopyroxene + plagioclase + titanomagnetite. The close approach of normative and modal feldspar compositions, Table 6.2., to the binary minimum $Ab_{65}Or_{35}$, Tuttle and Bowen (1958) and of bulk compositions to the low temperature trough in the "residua system" qz-ne-ks, Fig. 6.6., Tuttle and Bowen (1958), Hamilton and Mackenzie (1965), argue strongly that these rocks are the products of extensive crystal fractionation.

Table 6.2. shows the three phonolitic-trachytes to be significantly undersaturated and the two trachytes marginally saturated, however as one of these (A249) contains modal nepheline it seems likely that the standardised oxidation ratio of $Fe_2O_3/FeO + Fe_2O_3 = 1:3.80$ is not sufficiently reducing and that these samples should in fact be marginally undersaturated.

It is apparent that the transitional Older Series basalts on Mauritius have differentiated towards undersaturated residua and this would appear to require the more evolved

TABLE 6.2.

CHEMICAL AND MINERALOGICAL FEATURES OF OLDER SERIES TRACHYTES AND PHONOLITIC TRACHYTES

SAMPLE		A261	A264	A260	A249	A185
D.I.		87.15	89.99	90.99	91.88	92.20
Ba		908	582	15	18	30
Zr		1095	1175	1475	1582	1798
Wt.% Norm. Saturation		0.58qz	9.81ne	5.62ne	2.2hy	8.9ne
At.% $\frac{Na + K}{Al}$		0.87	1.01	1.01	0.94	0.98
Norm. Fspar	Ab	65.10	61.65	62.98	65.60	60.44
	Or	31.12	38.35	37.02	33.36	39.09
	An	3.77	0.00	0.00	1.05	0.46
Pheno. Fspar	Ab		57.07			
	Or	n.d.	41.36	n.d.	n.d.	n.d.
	An		1.57			
G/mass Fspar	Ab		65,18			
	Or	n.d.	32.87	n.d.	n.d.	n.d.
	An		1.95			
Wt.% Qz+ne+ks		84.61	88.54	89.50	89.23	92.09
Modal Nepheline		No	No	Yes	Yes	Yes

Trace elements in p.p.m.

Feldspar compositions in molecular %.

magmas to cross the low pressure basaltic thermal divide at some point. The nature of the divide in more evolved compositions is uncertain, but the relatively common occurrence of differentiated basalt suites crossing the plane of the divide, e.g. Reunion, Upton and Wadsworth (1972), Skye, Thompson et al. (1972), Hawaii, MacDonald (1968) suggests that it may not be an effective barrier for these compositions.

It was suggested in the previous chapter, that on the basis of barium and zirconium concentrations, the nepheline-bearing trachytes represented the most extreme differentiates of the series; Differentiation Indices presented in Table 6.2. clearly support this view, increasing D.I. correlating with increasing Zr and declining Ba.

As the trachytes approximate closely to compositions within the synthetic system qz-ne-ks, (see Table 6.2.) they can be meaningfully projected into this system and their crystallization history interpreted in the light of experimentally determined phase relations. Fig. 6.6. shows the trachytes and phonolitic-trachytes to plot along the thermal trough (defined by the line joining the alkali feldspar and phonolitic minima, m-M), sub-parallel to the fractionation curves, towards the phonolitic minimum M. Hamilton and Mackenzie (1965), Bailey and Schairer (1966) and Nash et al. have demonstrated both experimentally and in natural lavas, the importance of alkali feldspar fractionation in driving trachytic liquids into the thermal trough and towards the phonolitic minimum in the system qz-ne-ks, indicating that phonolitic magmas may evolve via trachytic members. The

FIG. 6.6.

Wt.% plot of the Older Series trachytes and phonolitic trachytes in the system SiO_2(Qz) - $NaAlSiO_4$(Nepheline) - $KAlSiO_4$(Kalsilite) at pH_2O = 1000 Kg/cm^2.

Thin solid lines represent fractionation paths to the phonolitic temperature minimum M.

m = Alkali feldspar temperature minimum.

M = $NaAlSi_3O_8$-$KAlSi_3O_8$-$KAlSiO_4$-$NaAlSiO_4$ (Phonolitic) temperature minimum.

Phase boundaries and fractionation curves taken from Hamilton and Mackenzie (1965).

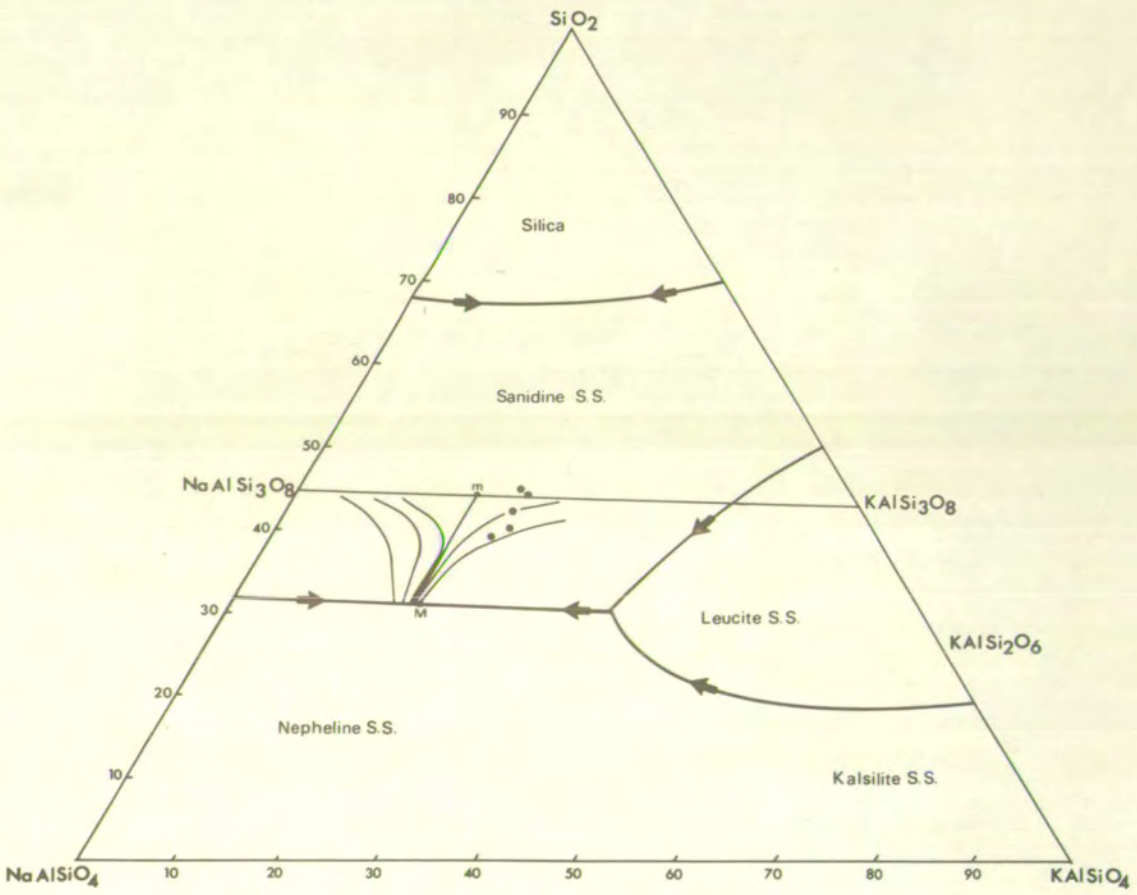
SiO2
90
80
Silica
70
60
Sanidine S.S.
50
NaAlSi3O8
m
KAlSi3O8
40
30
M
Leucite S.S.
KAlSi2O6
20
Nepheline S.S.
10
Kalsilite S.S.
NaAlSiO4
10
20
30
40
50
60
70
80
90
KAlSiO4

ubiquitous presence of anorthoclase phenocrysts in the Older Series trachytes and phonolitic trachytes, combined with the trace element data suggest that the observed trend towards the phonolitic minimum is controlled by alkali feldspar fractionation. It is unlikely however that these lavas are genetically related in the sense that they evolved from one liquid. Comparison of the data from Table 6.2. with the projected positions of the lavas in Fig. 6.6. shows no relationship between the degree of undersaturation and the degree of differentiation shown by the trace element levels and differentiation indices. One possible explanation, compatible with the occurrence of the trachytes as isolated bodies may be that several bodies of trachytic magma but with slightly differing compositions, developed independently within the volcanic pile and that these highly evolved liquids fractionated alkali-feldspar, moving into the thermal trough and towards the phonolitic minimum via the fractionation curves shown in Fig. 6.6. The variable degress of feldspar fractionation required to drive the different compositions into the thermal trough could explain the pattern of trace element levels and differentiation indices, while the initial orientation of the fractionation curves sub-parallel to the Ab - Or join show that this need not be accompanied by a significantly increased degree of undersaturation.

Anorthoclase fractionation is known to play an important role in developing peralkalinity in residual liquids, Abbott (1969), Nicholls and Carmichael (1969), precipitation of early calcic anorthoclase removing aluminium and concentrating total

alkalis in the liquid, analogous to the "plagioclase effect" described by Bowen (1945). Table 6.2. lists peralkaline indices for the lavas, but no consistent trends are apparent.

6.3. INTERMEDIATE SERIES

In contrast to the situation in the Older Series lavas, where chemical variation can be satisfactorily explained in terms of low pressure fractionation of observed phenocryst phases, no consistent patterns are found in the Intermediate Series lavas and several features point to a general lack of low pressure equilibration and fractionation.

1. Compared with the Older Series, the lavas are a relatively uniform suite of alkali olivine basalts, oceanites and basanitoids with no compositions less magnesian than 8.89% MgO.

2. Olivine and more rarely, clinopyroxene, are the only phenocryst phases present in the series. However, no consistent relationship exists between olivine phenocryst content and bulk MgO in the lavas, Fig. 6.7.

3. Major oxide variation diagrams presented in Fig. 5.4. show relatively scattered distributions with no indication of olivine fractionation controlling the chemical variation.

4. The incompatible group of element K, Rb, Ba, Sr, Zr and to a lesser extent Ti and P show well defined trends oblique to and hence unrelated to olivine control, Figs. 5.4., 5.9.

5. CMAS projections, in particular the clinopyroxene projection, show a poor correspondence between lava compositions and 1 atmosphere cotectics, Fig. 6.8.

FIG. 6.7.

MgO content of the Intermediate and Younger Series lavas as a function of olivine phenocryst content.

1. = Intermediate Series.

2. = Younger Series.

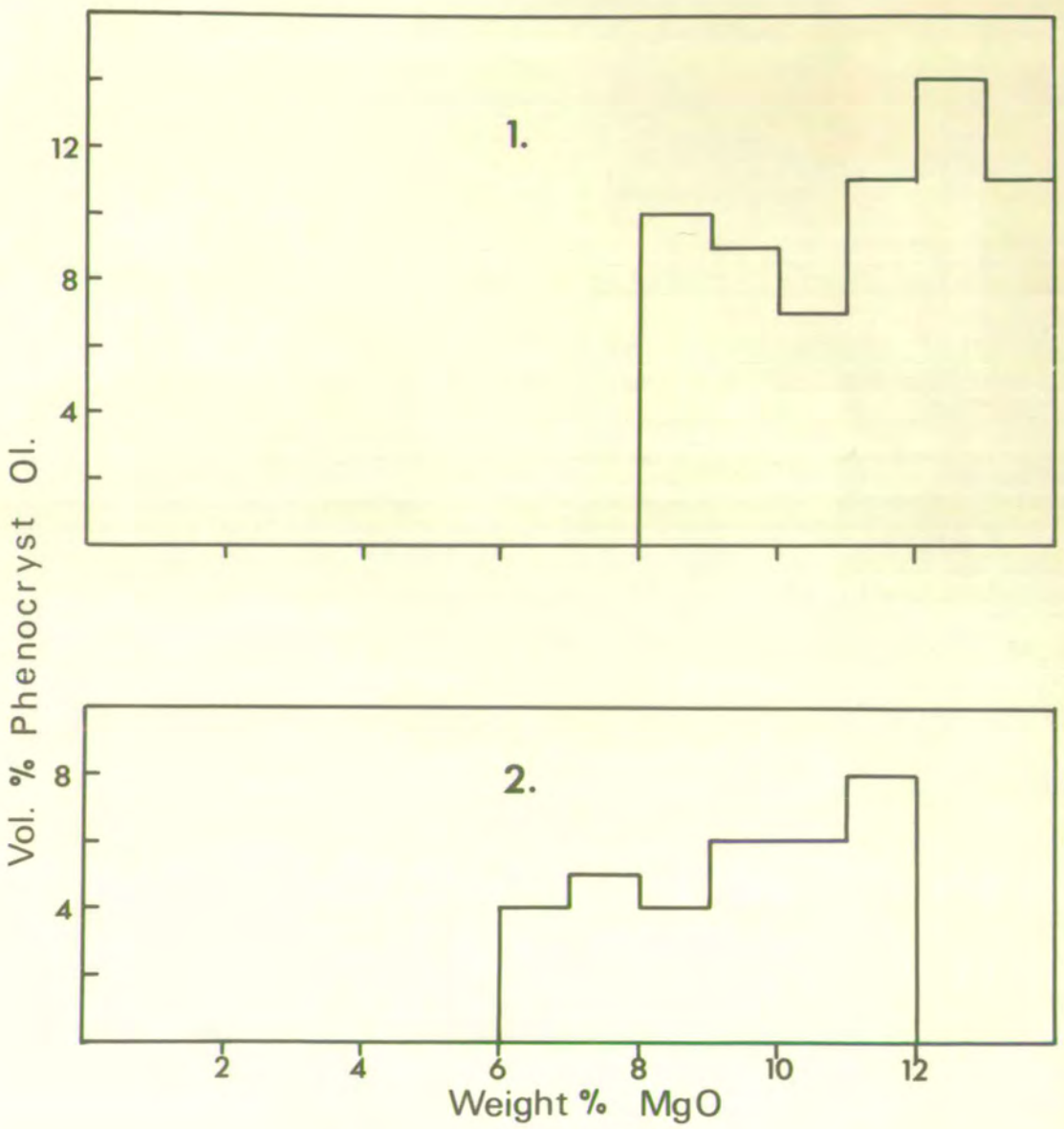
1.
2.
12
8
4
8
4
2
4
6
8
10
12
Vol. % Phenocryst Ol.
Weight % MgO

FIG. 6.8.

Wt. % projections of the Intermediate Series lavas in the system C.M.A.S., after O'Hara (1968).

(a) Projection from diopside onto part of the plane C_3A-M-S.

(b) Projection from olivine onto part of the plane CS-MS-A.

Δ = Diopside-plagioclase piercing point (a), olivine-plagioclase piercing point (b).

Phase boundaries shown for 1 atmosphere.

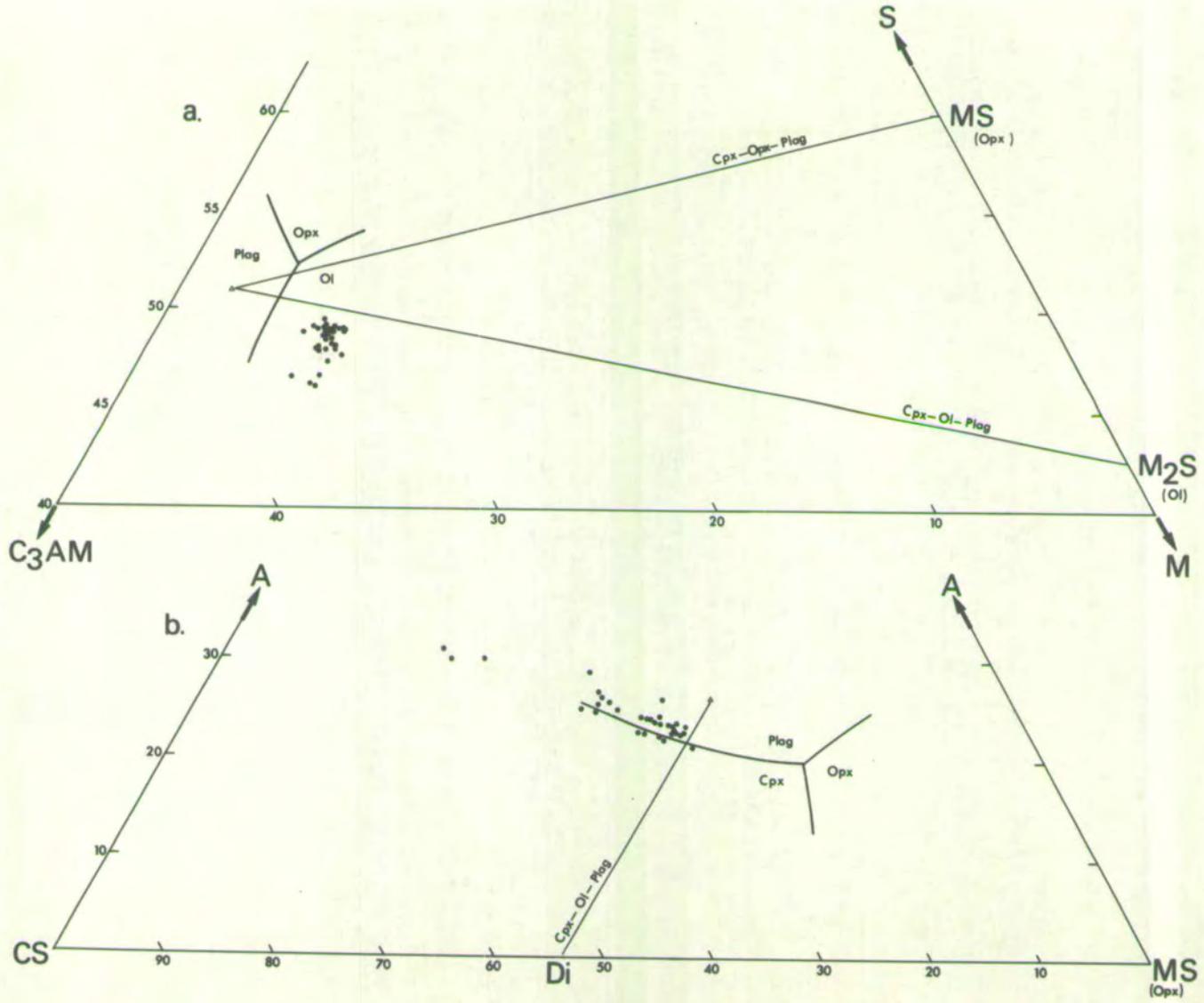
a.
S
MS
(Opx)
Cpx–Opx–Plag
Opx
Plag
Ol
Cpx–Ol–Plag
M2S
(Ol)
C3AM
M
60
55
50
45
40
40
30
20
10
b.
A
A
30
20
10
Plag
Cpx
Opx
Cpx–Ol–Plag
CS
Di
MS
(Opx)
90
80
70
60
50
40
30
20
10

6. Olivine phenocrysts commonly exhibit skeletal form, with embayments and axial cavities, and when related to points 2, 3 and 4 above, may be construed as evidence that olivine did not participate significantly in fractionation in these lavas, which may therefore approximate to liquid compositions.

As each sample may represent an original liquid composition, and the incompatible elements show a relatively large variation for small changes in major element chemistry, no single analysis can adequately represent the Intermediate Series parental liquid composition, which is best displayed by two analyses covering the range of incompatible element variation, shown in Table 6.3. Bearing in mind the absence of consistent major oxide trends and the restricted phenocryst mineralogy of these lavas, it is clear that the pattern of incompatible element variation with trends oblique to olivine control lines cannot be related to any likely low pressure fractionation scheme and must therefore reflect an earlier high pressure event.

6.4. YOUNGER SERIES

Unlike the Intermediate Series lavas, the Younger Series lavas show more consistent geochemical trends, which can be largely related to fractionation of observed phenocryst phases at low pressures. The predominant phenocryst phase is olivine, joined occasionally in less magnesian samples by plagioclase, in contrast to the crystallization sequence olivine → clinopyroxene of both the Older and Intermediate

TABLE 6.3.

COMPOSITIONAL RANGE OF INFERRED INTERMEDIATE SERIES PARENTAL MAGMAS

	B.9.	B.34
SiO_2	45.60	42.80
TiO_2	1.89	2.71
Al_2O_3	15.39	12.12
Fe_2O_3	1.70	3.80
FeO	10.14	8.82
MnO	0.18	0.18
MgO	8.89	12.58
CaO	11.32	11.09
Na_2O	2.68	2.60
K_2O	0.28	1.33
H_2O	0.90	1.61
P_2O_5	0.20	0.51
	99.17	100.15
Ni	250	427
Cr	304	367
V	244	296
Zr	92	198
Y	36	35
Ba	144	571
Sr	307	595
Rb	6	46
K/Rb	388	240
D.I.	22.91	21.69
Qz	0.00	0.00
Ne	2.18	10.23
Hy	0.00	0.00
Di	21.33	28.05
Ol	19.28	23.22
Or	1.68	7.99
Ab	19.05	3.47
An	29.64	17.76
Mt	2.70	2.83
Ilm	3.65	5.23
Ap	0.90	1.23

Major oxides in wt. %
Trace elements in p.p.m.

Series lavas. The often extremely coarse texture of the Younger Series lavas makes assessment of phenocryst abundances difficult. However some correlation between increasing MgO and phenocryst olivine, indicative of composition control by olivine addition/subtraction, is apparent in Fig. 6.7.

Major oxide variation diagrams presented in Fig. 5.5. generally reinforce the indications of olivine fractionation, well defined compositional trends lying along olivine control lines. In particular the strong degree of olivine control evident in the MgO/Al_2O_3 plot, suggests that the plagioclase phenocrysts found in the less magnesian lavas, have not fractionated significantly. Aphyric lava compositions plot close to the 1.atm. cotectics in the olivine projection in CMAS, Fig. 6.9., implying low pressure equilibration. As clinopyroxene is neither first nor second liquidus phase, this projection has been omitted for the Younger Series lavas. The more scattered trends of the incompatible elements K, P, Ti, Ba, Rb, Sr, Zr, seen in Figs. 5.5. and 5.10, partly oblique to the olivine control lines, may indicate the operation of some early high pressure process similar to that seen in the Intermediate Series lavas, which has now been largely overprinted by the effects of low pressure olivine fractionation.

The most basic aphyric sample, C50 (10.18% MgO), is taken here as representative of the Younger Series parental magma, and its analysis and norm is presented in Table 6.4., showing it to be a typical alkali basalt.

FIG. 6.9.

Wt.% projection of aphyric Younger Series lavas into the system C.M.A.S., after O'Hara (1968).

Projection from olivine onto part of the plane CS-MS-A.

△ = Olivine-plagioclase piercing point.

Phase boundaries shown for 1 atmosphere.

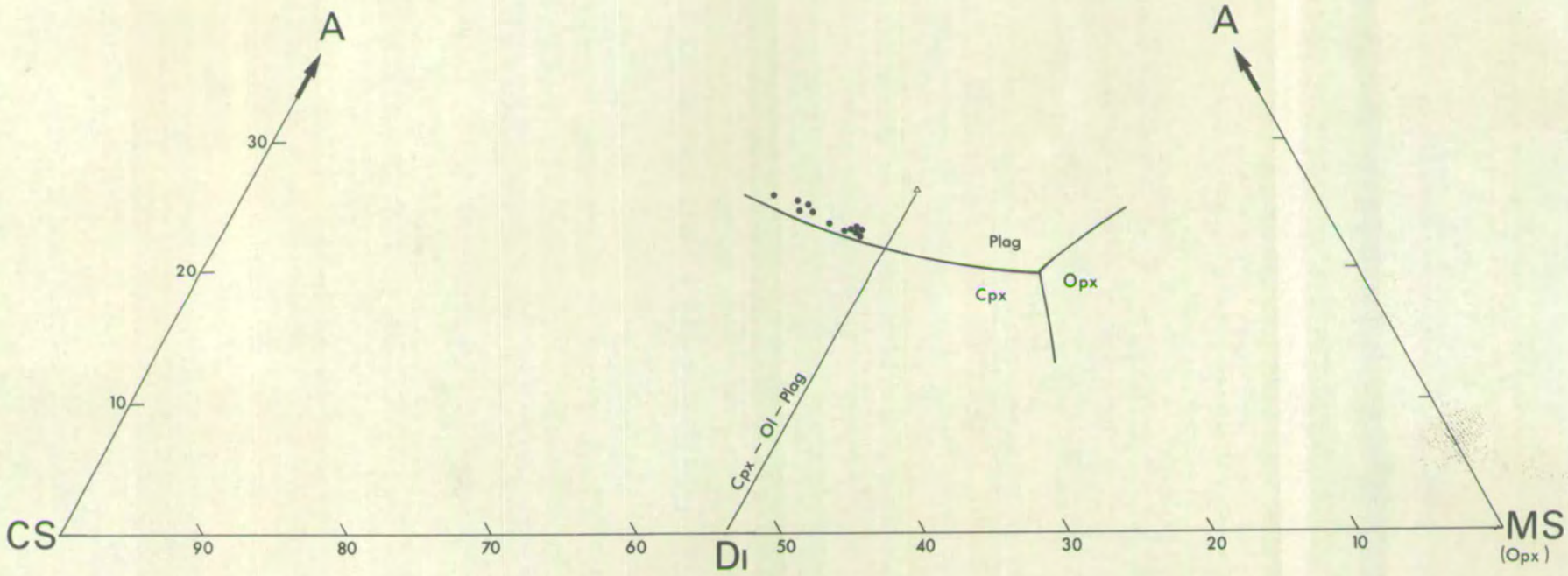
A
30
20
10
CS
90
80
70
60
Di
50
40
30
20
10
MS
(Opx)
A
Plag
Cpx
Opx
Cpx – Ol – Plag

TABLE 6.4.

INFERRED YOUNGER SERIES PARENTAL MAGMA.

C50

SiO_2	45.23	
TiO_2	1.93	
Al_2O_3	14.53	
Fe_2O_3	2.42	
FeO	9.98	Major oxides in wt. %
MnO	0.17	Trace elements in p.p.m.
MgO	10.18	
CaO	10.86	
Na_2O	2.69	
K_2O	0.43	
H_2O	0.55	
P_2O_5	0.22	
	99.19	
Ni	320	
Cr	345	
V	250	
Zr	99	
Y	39	
Ba	200	
Sr	333	
Rb	10	
K/Rb	358	
D.I.	22.78	
Qz	0.00	
Ne	3.40	
Hy	0.00	
Di	21.55	
Ol	21.94	
Or	2.58	
Ab	16.81	
An	26.67	
Mt	2.81	
Ilm	3.72	
Ap	0.53	

7. PETROGENESIS, 2 : ORIGIN OF MAGMA TYPES

7.1. INTRODUCTION

In the preceeding chapter the extent of low pressure crystal fractionation of the three main lava groups on Mauritius was discussed. The aim of this chapter is to investigate the genesis and possible polybaric crystallization histories of these three series from their presumed origin in the upper mantle. The limitations imposed by likely upper mantle compositions, their experimentally determined polybaric melting relations and the observed major and trace element chemistry of the parental basalts are discussed, and a possible petrogenetic scheme for the formation and subsequent differentiation of the lavas is proposed.

7.2. UPPER MANTLE MODELS

Independently derived estimates of upper mantle composition based on geophysical measurements, Ringwood (1969), chondritic Earth models, Ringwood (1966a,b) or ultramafic nodules in volcanic rocks in volcanic rocks, Harris et al. (1967), O'Hara (1968, 1970) all show a general convergence on some form of peridotite as the most likely material. Investigation of the melting relations of various peridotites under likely upper mantle conditions can provide some limitations on bulk compositions which can account for the compositional range of erupted basalts.

Two basic peridotite models have been proposed for the composition of the upper mantle and hence the source of basaltic magmas. Ringwood (1962), Ringwood et al. (1964)

and Green and Ringwood (1967) have suggested various "pyrolite" models - theoretically derived compositions with a general mineralogy olivine + 2 aluminous pyroxenes. These pyrolite models represent an attempt to derive a mantle composition by combining various proportions of material considered by these authors to be residual mantle after partial melting - variously dunite or alpine-type peridotite - with basalt considered by them to represent the primary magma formed in the melting event - generally an Hawaiian olivine tholeiite.

O'Hara (1968), who gives a detailed review of the development of the various pyrolites has questioned the validity of these models, pointing out the non-primary nature of the Hawaiian basalt and that equilibria involving garnet must control the initial partial melting of these peridotite compositions - a view supported by Ito and Kennedy (1967, 1968). Further serious objections to these models lie in the excessive degrees of partial melting required to yield liquids capable of evolving to basalts (up to 40%, Green and Ringwood (1967)) while O'Hara (1968, 1970) has noted that in general the bulk composition of these pyrolites and in particular their high Ca/Al ratio which predicts the formation of lherzolite residua on partial melting, cannot account for the occurrence of harzburgite and garnet-harzburgite nodules in kimberlites.

A model based on the composition of garnet-lherzolite nodules in kimberlites has been proposed by Harris et al. (1967), O'Hara (1968, 1970) while a more general garnet

lherzolite composition has been inferred by Ito and Kennedy (1967). Small degrees of partial melting (<15%) of these compositions under likely upper mantle conditions, i.e. 100 Km., 30 Kb., yields liquids capable of evolving to cover the observed range of erupted basalt compositions, while predicting the formation of peridotite nodules in volcanic rocks either as residua from partial melting (garnet-harzburgite and harzburgite) or as cognate cumulates. Olivine and orthopyroxene-liquid reactions have also been predicted, allowing processes such as eclogite fractionation, O'Hara and Yoder (1967), capable of explaining the differing incompatible element enrichment levels in tholeiitic and alkaline lavas.

Although clearly dependent on the present limited knowledge of melting relations at elevated pressures, the capacity of the garnet-lherzolite model to explain both the observed range of basaltic compositions and the variety of peridotite nodules in volcanic rocks is striking. When related to the occurrence of garnet-lherzolite nodules in an environment suggestive of rapid transport from great depth, in association with nodules predicted as residua from its partial melting it would seem likely that at least to a first approximation garnet-lherzolite may be representative of the upper mantle composition.

An average analysis of 15 garnet-lherzolite nodules from kimberlites, calculated by Carswell and Dawson (1970) is accepted here, with modification, as probably representative of the upper mantle composition, and is presented in Table 7.1.

TABLE 7.1.

POSTULATED UPPER MANTLE COMPOSITION

4.	SiO_2	46.10	
4.	TiO_2	0.26	
4.	Al_2O_3	2.16	
4.	Fe_2O_3	2.42	
4.	FeO	4.40	
4.	MnO	0.11	Wt. %
4.	MgO	41.95	
4.	CaO	1.64	
4.	Na_2O	0.17	
4.	P_2O_5	0.02	
		99.23	

1.	K	150	
3.	Rb	0.5	
3.	Ba	14	
3.	Sr	15	PPM
2.	Zr	30	
4.	Ni	2440	
4.	Cr	1195	

SOURCES

1. Gurney and Berg (1969). Average phlogopite-free lherzolite.
2. Vinogradov (1962)
3. Griffin and Murthy (1969)
4. Carswell and Dawson (1970). Average of 15 garnet-lherzolites in kimberlite.

The petrographic indications of secondary alteration and phlogopitisation by the highly potassic kimberlite groundmass, in several of the samples used in calculating this average, Carswell and Dawson (1970) suggests that the high potassium figure (1300 ppm. K) results from contamination. This value has been accordingly rejected. Gurney and Berg (1969) have investigated the relationship between potassium and phlogopite in peridotites and conclude that a value of 150 ppm. K is likely in phlogopite-free samples, and this figure is used in Table 7.1. Trace element data for garnet-lherzolites is rare; the values for nickel and chromium are taken from Carswell and Dawson (1970) while those for Ba, Sr and Rb are based on estimates given by Griffin and Murthy (1969) calculated from the levels of these elements in the constituent minerals of garnet-lherzolite. The figure for Zr is taken from Vinogradov (1962) and represents an average of several ultrabasic rock types.

7.3. DERIVATION OF MAGMA TYPES

Experimental work by O'Hara (1963a,b, 1965, 1968, 1970), O'Hara and Yoder (1963, 1967) and Ito and Kennedy (1967, 1968) has consistently shown that under likely upper mantle conditions i.e. circa 100 Km., 30 Kb., the partial melting product of garnet-lherzolite is a hypersthene-normative picrite-basalt, and that increased melting only enhances the tholeiitic character as more orthopyroxene and olivine enter the liquid. The experimental evidence for a tholeiitic primary magma is strongly supported by the natural occurrence of picritic tholeiitic magmas which approximate closely to

the composition and phase relations of these initial melts and which show a highly primitive chemistry, Clarke (1970), Jamieson (1966). If, as seems likely, the bulk of basaltic magmas originate from partial melting of garnet-lherzolite in the upper mantle, then clearly processes must exist which allow at some stage the derivation of under-saturated magmas from primary tholeiitic liquids.

Fig. 7.1., a projection from diopside into the plane C_3A-M-S, taken from O'Hara (1968) summarises some of the experimentally determined melting and phase relations of a four-phase lherzolite (ol+cpx+opx+garnet, spinel or plagio-clase depending on pressure) in the pressure range 1 bar - 30 Kb., and which are relevant to the genesis and polybaric crystallization history of the picritic tholeiitic partial melt of a garnet-lherzolite formed at 30 Kb. It can be seen that with decreasing pressure, in the range 10-20 Kb. where spinel replaces garnet as the stable aluminous phase, the in-variant point and phase boundaries are displaced towards more aluminous compositions, crossing the plane plag-di-ol into nepheline normative volumes. Partial melts formed in this pressure range will be nepheline normative, while liquids fractionating towards the invariant point may move from silica-saturated to undersaturated compositions. The most important feature of this movement of the invariant point is that potentially it allows tholeiitic liquids formed at 30 Kb., in equilibrium with garnet-harzburgite or harzburgite to move into nepheline-normative compositions by fractionation of harzburgite followed by lherzolite or of lherzolite alone

FIG. 7.1.

Wt.% projection from diopside onto part of the plane C_3A-M-S, showing the effects of pressure on phase equilibria in the system C.M.A.S., after O'Hara (1968).

Phase boundaries shown for 1 b., 15 Kb., 20 Kb., 30 Kb.

CD = Postulated garnet-lherzolite mantle composition (see Table 7.1).

A, B, C, D = invariant point at 1 b, 15, 20, 30 Kb.

Δ = Diopside-plagioclase piercing point.

Opx = Orthopyroxene

Ol = Olivine

Sp = Spinel

Gt = Garnet

Plag = Plagioclase

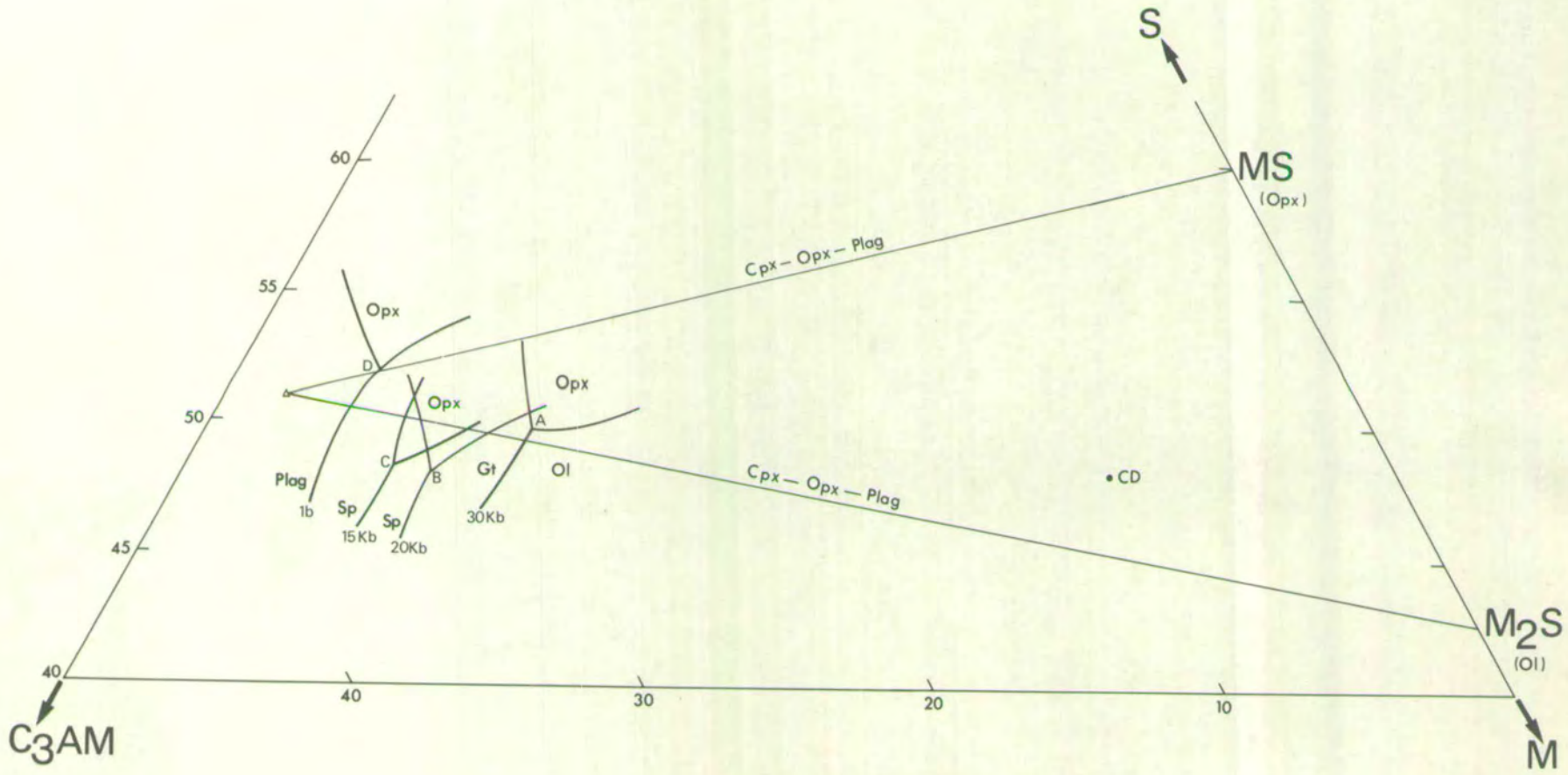
S
MS
(Opx)
Cpx — Opx — Plag
Opx
Opx
Opx
D
A
C
B
Plag
1b
Sp
15 Kb
Sp
20Kb
Gt
30Kb
Ol
Cpx — Opx — Plag
• CD
M2S
(Ol)
C3AM
M
60
55
50
45
40
40
30
20
10

if their rate of ascent is slow enough or rate of cooling sufficiently fast for them to attain this cotectic equilibrium. As noted by O'Hara (1968) the common occurrence of lherzolite nodules in undersaturated lavas may be significant in indicating the operation of such a process in the formation of nepheline normative magmas, however it cannot in itself explain the generally higher levels of K_2O and incompatible elements associated with these compositions, relative to tholeiitic magmas.

An alternative or complimentary scheme for deriving undersaturated liquids from primary tholeiites via bimineralli eclogite fractionation has been suggested O'Hara and Yoder (1967) and O'Hara (1968). By its nature this process must be restricted to pressures greater than 25 Kb. where garnet is the stable aluminous phase in the source lherzolite. Bimineralli eclogite with its high normative hypersthene content (see Table 4, p. 33, O'Hara & Yoder (1967)) can, if fractionated, effectively drive initially tholeiitic liquids towards nepheline normative compositions. An essential requirement for eclogite fractionation is that orthopyroxene and olivine are either lost by reaction or do not crystallize from the initial partial melt. A liquid-orthopyroxene reaction at 30 Kb. has been demonstrated by O'Hara and Yoder (1967) but the case for losing olivine is less clearly established, requiring as it does, a restricted compositional range for the initial melt, see O'Hara and Yoder p. 106 (1967). Nevertheless eclogite fractionation remains a likely possibility, strongly supported by the occurrence of eclogite nodules in undersaturated lavas and kimberlites, and by its

pronounced capacity for enriching liquids in the incompatible elements, described in the next section.

If the Mauritian lavas do originate from partial melting of garnet-lherzolite in the upper mantle, then it should be possible to apply the data shown in Fig. 7.1. to interpreting both the origin and diversification of the main magma types. Fig. 7.2., a diopside projection into the plane C_3A-M-S, shows the relation of the aphyric basaltic lavas of the three series (Older, Intermediate and Younger) to the experimentally determined polybaric melting and phase relations. Possible evolutionary paths for the three series are schematically represented within the diagram but it should be realised that these depict only the general trends, many paths being possible within the limiting conditions for each group. For the following discussion reference should be made to Fig. 7.2., which assumes that all three groups are derived initially at 30 Kb. from the partial melt with composition A, of a garnet-lherzolite CD with the composition shown in Table 7.1.

The essential feature of the Older Series basalts is their transitional nature, close to the basaltic thermal divide which lies roughly parallel to and just to the under-saturated side of the compositional plane plag-di-ol, and which becomes operative at pressures below about 8 Kb., O'Hara (1968). Small degrees of garnet-harzburgite or harzburgite fractionation from the melt A as the magma rises slowly with falling pressure from 30 Kb., sufficient to keep the magma close to the plane plag-di-ol, followed by a more rapid

FIG. 7.2.

Possible polybaric fractionation paths for the derivation of Mauritian magma types from a garnet-lherzolite partial melt at 30 K.b., shown in a wt. % projection from diopside onto part of the plane $C_3A - M - S$.

Symbols and phase equilibria as in Fig. 7.1.

(1) = Field of Older Series aphyric basalts.

(2) = Field of Younger Series aphyric basalts.

(3) = Field of Intermediate Series lavas.

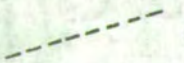
= Fractionation paths for Older Series.

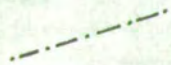
= Fractionation paths for Younger Series.

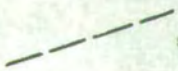
= Fractionation paths for Intermediate Series.

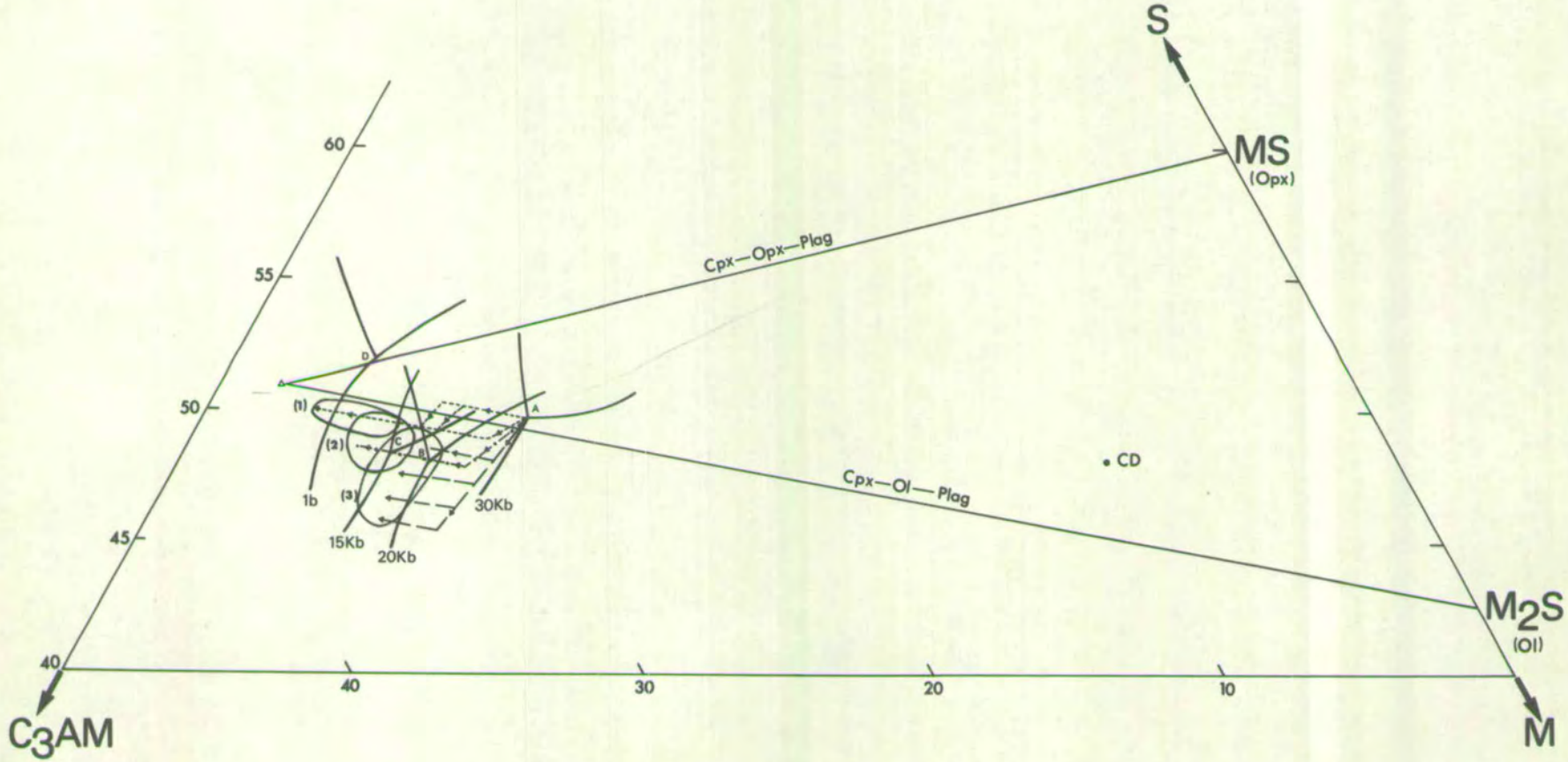
S
MS
(Opx)
Cpx—Opx—Plag
Cpx—Ol—Plag
CD
M2S
(Ol)
C3AM
M
60
55
50
45
40
40
30
20
10
D
A
C
B
(1)
(2)
(3)
1b
15Kb
20Kb
30Kb

ascent within the primary phase volume of olivine could produce the observed features. Alternatively the initial melt could rise within the expanding primary phase volume of olivine slowing sufficiently at some point between 15-30 Kb. to allow small degrees of lherzolite fractionation to move the magma towards the plag-di-ol plane.

The establishment of the thermal divide separating alkaline and tholeiitic basalts at <8 Kb. means that if the undersaturated Intermediate and Younger Series lavas are derived from a tholeiitic parent, then the derivation must occur above this pressure. A variety of evolutionary paths can account for the formation of the Intermediate Series lavas, which range from alkali-olivine basalt to more strongly undersaturated basanitoids. Variable degrees of eclogite fractionation at pressures above 25 Kb., followed by a more rapid ascent within the expanding primary phase volume of olivine; or garnet harzburgite or harzburgite fractionation followed by extensive lherzolite fractionation in the pressure range 15-25 Kb., with subsequent more rapid ascent within the olivine phase volume, or any combination of these, could produce the Intermediate Series lavas. While it is not possible to choose between these processes on the basis of the major element chemistry of the erupted lavas, the incompatible element levels may be a significant discriminator, and the limitations imposed by these are discussed in the next section.

A similar but less extreme process of polyphase fractionation in the range 15-30 Kb. can account for the mildly undersaturated Younger Series alkali-olivine basalts. Small

amounts of eclogite removal at pressures above 25 Kb. followed by ascent within the olivine primary phase volume, or ascent from 30 Kb. fractionating olivine, with some interruption in the intermediate pressure range 15–25 Kb. with lherzolite fractionation; or some combination of these processes, will produce the features of this series.

It is clear from this discussion that the essential difference between tholeiitic and alkaline magmas arises from the degree of polyphase polybaric fractionation which the initially tholeiitic partial melt undergoes. Essentially this means that alkaline lavas either rise more slowly or cool more rapidly from 100 Km., allowing cotectic equilibrium to be reached with subsequent polyphase fractionation, while tholeiitic magmas rise more rapidly so that they maintain equilibrium only with olivine whose phase volume is expanding with decreasing pressure, and consequently fractionate predominantly olivine on the way to the surface. In this scheme, transitional lavas result from small degrees of polyphase fractionation superimposed on an evolutionary path of primarily olivine fractionation. There seems to be no reason why a suite of lavas cannot be formed which will straddle the basaltic thermal divide at low pressures, and the transitional Skye basalts of Eocene age, Thompson et al. (1972) may represent this condition.

7.4. INCOMPATIBLE ELEMENT VARIATION

Considerable variation occurs in the levels of the incompatible group of elements K, P, Ti, Ba, Sr and Zr,

particularly in the basic Intermediate Series lavas where strong trends towards enrichment in this group are clearly unrelated to plausible low pressure fractionation schemes.

Several workers have noted the frequently independent behaviour of the incompatible elements relative to major element variation in basaltic lavas, Green and Ringwood (1967), O'Hara (1968), Jamieson and Clarke (1970). The high enrichment factors in some basalts relative to likely mantle concentrations has prompted recognition that by itself the passive concentration of incompatibles in residual liquids as magmas fractionate towards the surface cannot adequately explain these levels, except for the special case of eclogite fractionation discussed below, as the amounts of crystal fractionation requires would produce liquids with a non-basaltic major element chemistry. Clearly additional processes must be operating at depth to produce the observed variation and several mechanisms have been proposed, which are discussed below:

1. Degree of Partial Melting

The extremely high liquid-crystal distribution coefficients which control the concentration of the incompatible elements in residual liquids equally require that they are concentrated in the initial partial melts of mantle material, Gast (1968), Griffin and Murthy (1969). As the bulk of these elements enter the first few percent of the liquid, increasing degrees of melting have a diluting effect, providing a range of potential magmas with essentially similar major element concentrations but variable levels of incompatible elements.

Estimates of enrichment factors for variable degrees of partial melting of garnet-lherzolite presented in Table 7.2. show that factors of 4-18 may be attainable with 20-5% partial melting, considered by O'Hara (1968) to represent the probable limits of effective partial melting in the mantle, (magma segregation being unlikely with smaller amounts of liquid while higher degrees are precluded by their excessive energy requirements). Magma genesis models involving high, circa 50% partial melting e.g. Jackson and Wright (1970) are not only constrained by their energy requirements but also require excessively high degrees of fractionation to generate observed enrichment factors unless a mantle composition radically richer in potassium and other incompatible elements than is generally accepted, is invoked. Extremely small degrees of melting of a garnet lherzolite containing trace amounts of titaniferous phlogopite have been proposed by Dawson (1972) to explain the high enrichment factors in kimberlites and potassic-mafic lavas. Although melting involving phlogopite would produce a liquid enriched in K, Rb, Ba, Sr and Ti it cannot account for the P enrichment factors, while the existence of primary mica in garnet-lherzolite, even in trace amounts, has not yet been convincingly demonstrated.

Accepting a model of 20-5% melting, giving factors of 4-18, then further fractionation to a maximum of around 40% (primarily olivine) could produce enrichment factors of 7-31 without loss of basaltic major element chemistry, and as these values approach those of the Mauritian parental basalts,

TABLE 7.2.

ENRICHMENT FACTORS IN GARNET-LHERZOLITE PARTIAL MELTS

% MELTING	5	10	20
K	18	10	5
Rb	16	9	4
Ba	18	9	4
Sr	17	9	12
Zr	-	-	2
P_2O_5	-	-	5
TiO_2	-	-	3

SOURCES

5 and 10% melting data taken from Griffin and Murthy (1969)

20% melting data from Clarke (1970).

Mean of 7 Baffin Island basalts relative to garnet-lherzolite, Table 7.1.

see Table 7.3., the possibility must be considered that this process has controlled enrichment factors in these lavas.

Assuming total element incompatibility, enrichment factors, initial element concentrations and final concentrations in the liquid are simply related by the expression:

$E = 100/V$ Where: E = Enrichment factor

V = Vol. % of liquid remaining or produced.

Using this expression, the degrees of partial melting required to produce the observed enrichment factors of the Mauritian parental basalts have been calculated, assuming a maximum of 40% subsequent fractionation, and these are presented in Table 7.4. Although this is only an approximation and numerous combinations of fractionation and melting exist, the broadly similar major element concentrations of the parental basalts implies that they have undergone comparable degrees of crystal fractionation. Although there is no reason to reject partial melting as the major enrichment control in the case of the Older and Younger Series lavas, it is unlikely that the extremes required to produce the range of Intermediate Series enrichment factors could operate simultaneously, as the intimate association of these lavas in the field would require. A more general criticism of the mechanism lies in its inability to produce the much higher enrichment factors found in many alkaline and tholeiitic suites, given the above limits to effective partial melting and clearly some other or additional processes must be operating.

TABLE 7.3.

CALCULATED ENRICHMENT FACTORS FOR MAURITIAN PARENTAL MAGMAS.

SERIES	OLDER	INTERMEDIATE		YOUNGER
Sample	A171	B9	B34	C50
K	53	15	73	24
Rb	63	13	96	21
Ba	20	10	41	14
Sr	26	20	40	22
Zr	6	3	7	3
P_2O_5	20	10	26	11
TiO_2	10	7	10	7
MEAN	26	11	38	15

FACTORS CALCULATED RELATIVE TO GARNET-LHERZOLITE MANTLE, TABLE 7.1. MEAN CALCULATED AFTER EXCLUSION OF MAXIMUM AND MINIMUM VALUE.

TABLE 7.4.

PARTIAL MELTING MODELS FOR MAURITIAN PARENTAL MAGMAS

SERIES	OLDER	INTERMEDIATE		YOUNGER
SAMPLE	A171	B9	B34	C50
ENRICHMENT FACTOR	26	11	38	15
% FRACTIONATION	40	40	40	40
% PARTIAL MELTING	7	16	5	11

2. Eclogite Fractionation

The conditions under which eclogite fractionation can take place have been described in Section 7.3. One of the most striking features of eclogites is their close compositional similarity to the initial partial melt of garnet-lherzolite at 30 Kb, see Fig. 7.3. The result of this near coincidence is that if eclogite fractionation takes place the incompatible elements will be strongly concentrated in the residual liquids for relatively small movements towards nepheline-normative compositions. Although criticially dependent on the bulk composition of the fractionating eclogite, this mechanism can potentially account for the extremely high enrichment factors in some basaltic magmas and if carried to extremes could produce residual liquids similar to the potassic-mafic lavas, carbonatites and kimberlite groundmass, O'Hara and Yoder (1967), O'Hara (1968).

O'Hara and Yoder (1967) have described in considerable detail the geochemical consequences of eclogite fractionation, and it seems likely that the ratio K_2O/Na_2O is the most sensitive indicator of the process, through the preferential entry of sodium into the omphacitic clinopyroxene of the eclogite. Generally then, extensive eclogite fractionation would be expected to result in increasing K_2O/Na_2O, incompatible element levels and increasing degree of undersaturation in magmas.

Table 7.5. shows some estimated degrees of eclogite fractionation which would be required to produce the enrichment levels of the Mauritian parental magmas, for various degrees

FIG. 7.3.

Relation of eclogite compositions to partial melt product, A, of garnet-lherzolite at 30 K.b., shown in a wt.% projection from olivine onto part of the plane CS - MS - A.

Lined area represents field of some natural and synthetic biminerralic eclogites, taken from O'Hara (1968,1969), O'Hara and Yoder (1967).

Subsolidus solid-solution fields shown for garnet, orthopyroxene and clinopyroxene at 30 Kb., after O'Hara (1968).

CD = Postulated garnet-lherzolite mantle composition (see Table 7.1).

Δ = Olivine-plagioclase piercing point.

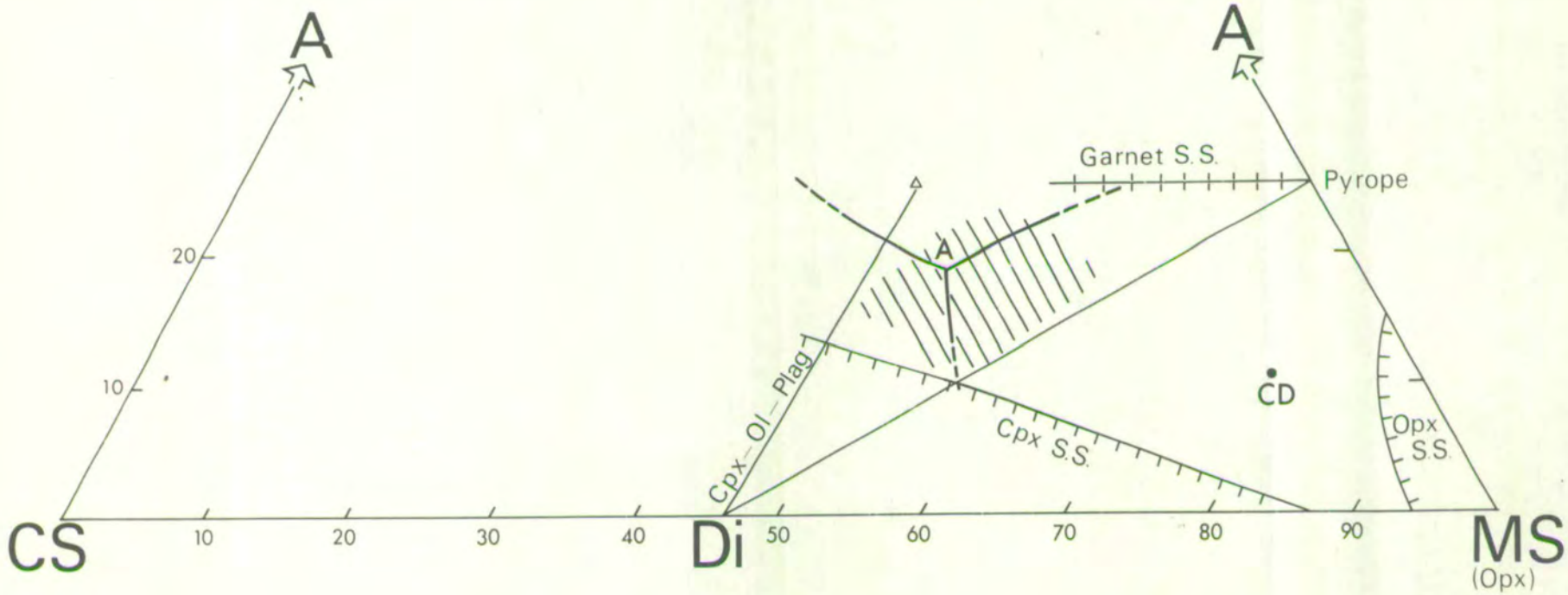
A
20
10
CS
10
20
30
40
Di
50
60
70
80
90
MS
(Opx)
A
Garnet S.S.
Pyrope
A
Cpx–Ol–Plag
Cpx S.S.
CD
Opx
S.S.

TABLE 7.5.

ECLOGITE FRACTIONATION MODELS

Enrichment Factors in Parental Magmas: Older Series (A171) = 26
Intermediate Series (B9, B34) = 11-38
Younger Series (C50) = 15

SERIES	% MELTING	% ECLOGITE FRACT.	% SUBSEQ. FRACT.	RESULT. FACTOR	MODEL
	7	0	40	26	MELTING ONLY
OLDER	10	24	40	26	ECLOGITE A
	20	67	40	26	ECLOGITE B
	16	0	40	11	MELTING ONLY
INTERMEDIATE	5	0	40	38	MELTING ONLY
	16	71	40	38	ECLOGITE C
	11	0	40	15	MELTING ONLY
YOUNGER	20	67	40	15	ECLOGITE D

of partial melting, assuming 40% subsequent fractionation towards the surface. In the case of the Older Series lavas it appears unnecessary to invoke eclogite fractionation, as the partial melting model would seem to be adequate, and the relatively restricted conditions required are unlikely to prevail during an active shield building event where large volumes of magma are continually supplied to the surface. This argument could equally apply to the voluminous highly mobile Younger Series lavas, however the evidence of slight cross-trends in some incompatible element variation diagrams might imply that small degrees of eclogite fractionation have occurred.

A model of extensive eclogite fractionation, however, seems to fit the Intermediate Series. Variable degrees of eclogite fractionation up to a maximum of 71% can produce the range of enrichment factors in the series, from the most depleted lava B9. Inspection of the analyses in Appendix 3 shows a general trend towards increasing undersaturation with rising incompatible element levels, while Fig. 7.4. clearly shows a linearly increasing K_2O/Na_2O ratio with increasing K_2O, precisely the trend expected if eclogite fractionation is the controlling process.

3. Wall-Rock Reaction

Green and Ringwood (1967) have proposed a process of wall rock reaction for enriching magmas in incompatible elements. Essentially the process depends on the attempts of a rising mantle partial melt to equilibrate by further partial melting of, and reaction with, surrounding cooler mantle

FIG. 7.4.

Wt. % K_2O vs K_2O/Na_2O ratio for the Intermediate Series lavas.

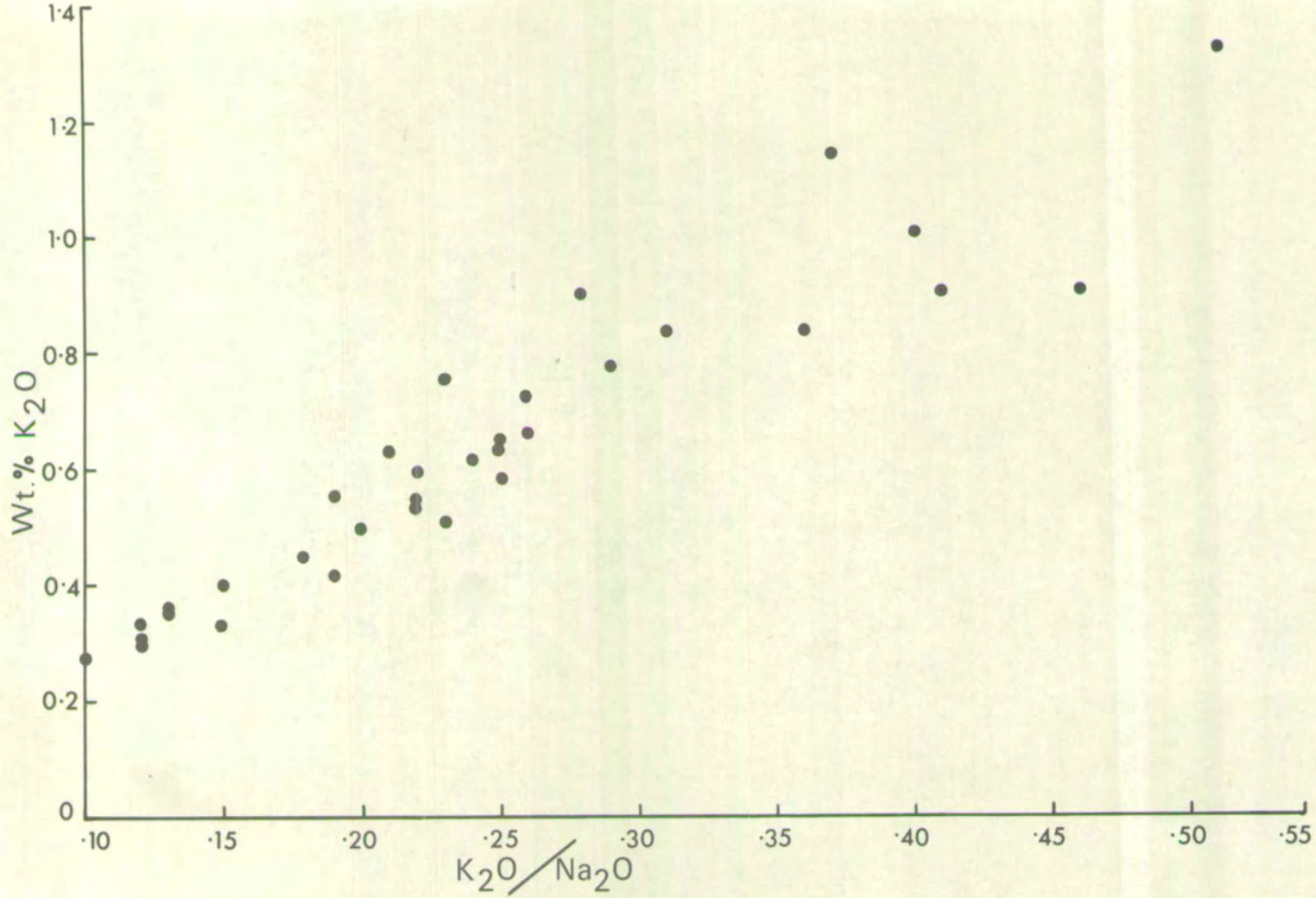
1·4
1·2
1·0
0·8
0·6
0·4
0·2
0
Wt.% K_2O
·10
·15
·20
·25
·30
·35
·40
·45
·50
·55
K_2O / Na_2O

material, leading to a pronounced incompatible element concentration within the liquid. The mechanism is similar to the zone refining process described by Harris (1957) and reiterated by Harris and Middlemost (1970) in which enrichment is achieved by the movement of a zone of partial melting through the mantle by a process of continual solution and crystallization of mantle material with increasing concentration of the incompatibles in the transported melt.

Considerable objections have been raised to these mechanisms by Gast (1968) and O'Hara (1968) both of whom essentially question their continued effectiveness over a prolonged period of magma genesis. As the processes are untestable, relatively poorly defined and cannot easily be quantified, they must remain as possible but speculative enrichment processes in a geological environment.

It must be concluded therefore that the major enrichment processes are, degree of partial melting and eclogite fractionation, with the latter probably solely responsible for enrichment factors > 40, if the limits to effective partial melting proposed by O'Hara (1968) are valid. A combination of both mechanisms can explain the observed enrichment factors in the Mauritian parental magmas with variable degrees of partial melting and further passive concentration through subsequent crystal fractionation producing the factors in the Older and Younger Series; while a combination of partial melting, variable degrees of eclogite fractionation and further passive concentration can satisfactorily account for the pronounced enrichment trends in the Intermediate Series lavas.

7.5. PETROGENETIC SCHEME

On the basis of the preceeding discussion, and the conclusions from earlier chapters, the following petrogenetic schemes are suggested to account for the formation and differentiation of the three series on Mauritius. It should be appreciated however that these schemes must be somewhat speculative, particularly in the light of the complexity of high pressure processes and the present limited knowledge of their extent.

A. Older Series

1. Partial melting of mantle material with the composition of garnet-lherzolite nodules in kimberlite, possibly in the order of 7%, to produce a hypersthene normative picrite basalt at circa 30 Kb., 100 Km.

2. Segregation and accumulation of magma in the region of generation. Slow ascent or cooling in the range 30-25 Kb., with minor fractionation of garnet-harzburgite or harzburgite and development of transitional character, followed by a faster ascent to high crustal levels within the expanding primary phase volume of olivine. Alternatively, ascent from 30 Kb. in the olivine field with limited interruption in the 25-15 Kb. range allowing lherzolite fractionation to take place.

3. Accumulation of parental magma at high crustal levels with crystallization and fractionation of olivine + clinopyroxene to form a suite of picrite-basalts, olivine-basalts and basalts. Formation of dunite and wehrlite cumulates, elutriated as inclusions in the picrite-basalts.

4. Onset of more complex crystallization as olivine + clinopyroxene are joined by plagioclase + titanomagnetite. Differentiation of the magmas to hawaiites and mugearites with the appearance of anorthoclase and apatite as fractionating phases in the mugearites.

5. Probable limited development of hydrous conditions in the sub-volcanic zone, possibly resulting from extensive polyphase fractionation of anhydrous minerals. Evidence for hydrous conditions lies in the appearance of kaersutite in hawaiites and mugearites and perhaps in the extremely calcic plagioclase phenocrysts found in the feldsparphyric basalts. Conditions apparently sufficiently stable for the formation of bytownitic anorthosite cumulates, elutriated as small inclusions in the feldsparphyric basalts.

6. Extreme fractionation of olivine + clinopyroxene + plagioclase + titanomagnetite + anorthoclase ± kaersutite leads to the development of trachytic and phonolitic-trachyte residua. Several lines of evidence point to each of these bodies developing independently but along similar fractionation paths, with an overall trend towards the phonolitic minimum in the system Qz - Ne - Ks.

B. INTERMEDIATE SERIES

1. Partial melting of mantle garnet-lherzolite, probably around 16% at 30 Kb., forming a hypersthene-normative picrite basalt.

2. Segregation and accumulation of magma. Liquid either remains at the site of generation or rises slowly through the

pressure range 30-25 Kb. with the loss of olivine and orthopyroxene as crystallizing phases and the onset of eclogite fractionation possibly to a maximum of 71%, producing a suite of undersaturated lavas with variable enrichment factors. Slow ascent of magmas within the range 25-15 Kb., fractionating lherzolite and enhancing their undersaturated character.

3. Relatively rapid ascent to surface within the olivine primary phase volume from the intermediate pressure range 25-15 Kb. Eruption of lavas which show skeletal or quench olivine textures and some indication of non-equilibration with one atmosphere cotectics.

C. YOUNGER SERIES

1. Partial melting of mantle garnet-lherzolite, probably around 11% at 30 Kb., forming a hypersthene normative picrite basalt. Either small variations in the degree of partial melting or limited eclogite fractionation takes place to produce the cross trends apparent in some incompatible element variation diagrams.

2. Segregation and accumulation of magma, possibly with minor eclogite fractionation above 25 Kb., as described above.

3. Limited fractionation of garnet-harzburgite with falling pressure in the range 30-25 Kb. or harzburgite or lherzolite fractionation in the range 25-15 Kb., with the development of mildly undersaturated chemistry, followed by a more rapid ascent within the olivine primary phase volume. Eruption onto surface with some indications of olivine accumulation in lavas.

ACKNOWLEDGEMENTS

I am indebted to my supervisor Dr. B.G.J. Upton both for the opportunity of undertaking research on Mauritius, and for his continuous support and advice throughout my period of study at the Grant Institute of Geology.

I would also like to extend my appreciation to Dr. K.G. Cox, formerly of the Grant Institute, and now at the Department of Geology and Mineralogy, Oxford University, for devoting many hours of his time to extending my knowledge of igneous petrology.

Field work on Mauritius was only possible through a N.E.R.C. travel and maintenance grant, and financial assistance from the Grant Institute, to whom I extend my gratitude.

The following people all provided invaluable technical support and advice and to whom I am extremely grateful:

Mr. G.R. Angell and Mr. M.J. Saunders for instruction in the analytical techniques of X-ray fluorescence and classical chemistry, respectively.

Mr. C. Chaplin, Chief Technician, and the technical staff at the Grant Institute of Geology for the preparation of thin sections, polished thin sections and photographs.

Time on the Manchester University electron microprobe was arranged by Dr. A.C. Dunham, to whom I extend my appreciation.

Field work on Mauritius was greatly facilitated by the support of Dr. O.E. Vaughan of the Mauritius Sugar Institute, the staff of the Mauritius Museum, Port Louis, and the officers and guides of the Mauritian Forestry Commission, and to these

people I extend my sincere gratitude and appreciation.

This work was carried out during the tenure of a N.E.R.C. research studentship.

REFERENCES

ABBOTT, M.J., 1969. Petrology of the Nandewar Volcano, N.S.W., Australia. Contr. Mineral. Petrol. 20, 115-134.

ANDERMAN, G. & KEMP, J.W., 1958. Scattered X-rays as internal standards in X-ray emission spectroscopy. Analyt. Chem., 30, 1306-1309.

AOKI, K., 1963. The Kaersutites and Oxykaersutites from Alkali Rocks of Japan and Surrounding Areas. J. Petrology 4, 198-210.

AOKI, K., 1970. Petrology of Kaersutite-Bearing Ultramafic and Mafic Inclusions in Iki Island, Japan. Contr. Mineral. Petrol. 25, 270-283.

ATKINS, F.B., BAKER, P.E., BELL, J.D., SMITH, D.G.W., 1964. Oxford Expedition to Ascension Island, 1964. Nature, 204, 722-724.

BAILEY, D.K. & SCHAIRER, J.F. 1966. The system Na_2O-Al_2O_3-Fe_2O_3-SiO_2 at 1 atmosphere, and the petrogenesis of alkaline rocks. J. Petrology 7, 114-170.

BAKER, I., 1969. Petrology of the volcanic rocks of St. Helena, S. Atlantic. Bull. geol. Soc. Am. 80, 1283-1310.

BANDY, M.C., 1937. Geology and petrology of Easter Island. Bull. geol. Soc. Am. 48, 1589-1610.

BEST, M.G., 1970. Kaersutite-Peridotite Inclusions and Kindred Megacrysts in Basanitic Lavas, Grand Canyon, Arizona. Contr. Mineral. Petrol. 27, 25-44.

BOWEN, N.L., 1945. Phase equilibria bearing on the origin and differentiation of alkaline rocks. Am. J. Sci., Daly Vol. 243A, 75-89.

BROWN, G.M., 1957. Pyroxenes from the early and middle stages of fractionation of the Skaergaard magma. Miner. Mag. 31, 511-543.

BROWN, G.M., 1967. Mineralogy of basaltic rocks. in: The Poldervaart treatise on rocks of basaltic composition. Vol. 1. Eds. Hess, H.H. & Poldervaart, A. Interscience.

BUNCE, E.T., BOWIN, C.O. & CHASE, R.L., 1966. Preliminary results of the 1964 cruise of R.V. Chain to the Indian Ocean. Phil. Trans. R. Soc. Lond. A. 259, 218-226.

CARSWELL, D.A. & DAWSON, J.B., 1970. Garnet peridotite xenoliths in South African kimberlite pipes and their petrogenesis. Contr. Mineral. Petrol. 25, 163-184.

CHAMALAUN, F.H., & McDOUGALL, I., 1966. Dating geomagnetic polarity epochs in Reunion. Nature, 210, 1212-1214

CHAYES, F., 1963. Relative abundance of intermediate members of the oceanic basalt-trachyte association. J. Geophys. Res. 68, 1519-34.

CLARKE, D.B., 1970. Tertiary basalts of Baffin Bay: Possible primary magma from the mantle. Contr. Mineral. Petrol. 25, 203-224.

CLARK, S.P., SCHAIRER, J.F., De NEUFVILLE, J., 1962. Phase relations in the system $CaMgSi_2O_6 - CaAl_2SiO_6 - SiO_2$ at low and high pressure. Carnegie Inst. Wash. Yearbook, 61, 59-68.

COOMBS, D.S., 1963. Trends and affinities of basaltic magmas and pyroxenes as illustrated on the diopside-olivine-silica diagram. Spec. Pap. miner. Soc. Am. 1, 227-250.

COX, K.G., GASS, I.G., MALLICK, D.I.J., 1968. The evolution of the volcanoes of Aden and Little Aden, South Arabia. Q. Jl. geol. Soc. Lond. 124, 283-308.

DARWIN, C., 1844. Coral reefs, volcanic islands and South American geology. London.

DAVIES, D., & FRANCIS, T.J.G., 1964. The crustal structure of the Seychelles Bank. Deep-Sea Research, 11, 921-927.

DAWSON, J.B., 1972. Kimberlites and their relation to the mantle. Phil. Trans. R. Soc. Lond. A. 271, 297-311.

DeCHAZAL, M., & BAISSAC, J. De B., 1949. Étude sur la géologie de l'Île Maurice. Proc. Soc. Arts. Sci. Mauritius, 1, 53-72.

DEER, W.A., HOWIE, R.A., & ZUSSMAN, J., 1963. Rock forming minerals: 5 volumes. London: Longmans.

De HAGA HAIG, H., 1895. The physical features and geology of Mauritius. Q. Jl. geol. Soc. Lond. 51, 463-471.

ERLANK, A.J., 1968. The terrestial abundance relationship between potassium and rubidium. From: Origin and Distribution of the Elements, ed. Ahrens, L.H. Pergamon Press.

FISHER, R.L., JOHNSON, G.L., HEEZEN, B.C., 1967. Mascarene Plateau, Western Indian Ocean. Bull. geol. Soc. Am. 78, 1247-1266.

FISHER, R.L., SCLATER, J.G., & McKENZIE, D.P., 1971. Evolution of the Central Indian Ridge, Western Indian Ocean. Bull. geol. Soc. Am. 82, 553-562.

FLOWER, M.F.J., 1970. The Petrology and Geochemistry of Volcanic Rocks from Anjouan, Comores Archipelago. Univ. Manchester Ph.D. Thesis (Unpubl.)

GAST, P.W., 1965. Terrestial ratio of potassium to rubidium and the composition of the Earth's mantle. Science. 147, 858-860.

GAST, P.W., 1968. Trace element fractionation and the origin of tholeiitic and alkaline magma types. Geochim. Cosmochim. Acta. 32, 1057-1086.

GIROD, M., CAMUS, G., VIALETTE, Y., 1971. Tholéiites à l'Île Saint-Paul (Océan Indien). Contr. Mineral. Petrol. 33, 108-117.

GREEN, D.H., & RINGWOOD, A.E., 1967. The genesis of basaltic magmas. Contr. Mineral. Petrol. 15, 103-190.

GRIFFIN, W.L., & MURTHY, V.R., 1969. Distribution of K, Rb, Sr and Ba in some minerals relevant to basalt genesis. Geochim. Cosmochim. Acta. 33, 1389-1414.

GURNEY, J.J. & BERG, G.W., 1969. Potassium, Rubidium and Caesium in South African Kimberlites and their Peridotite Xenoliths. Trans. Geol. Soc. S. Afr., Spec. Pub. No. 2. "Upper Mantle Project".

HAMILTON, D.L., & MACKENZIE, W.S., 1965. Phase equilibrium studies in the system $NaAlSiO_4$(nepheline) - $KAlSiO_4$(kalsilite) - SiO_2 - H_2O. Miner. Mag. 34, 214-231, Tilley Vol.

HARRIS, P.G., 1957. Zone-refining and the origin of potassic basalts. Geochim. Cosmochim. Acta. 12, 195-208.

HARRIS, P.G., 1963. Comments on a paper by F. Chayes, 'Relative abundance of intermediate members of the oceanic basalt-trachyte association'. J. Geophys. Res. 68, 5103-5107.

HARRIS, P.G., REAY, A., & WHITE, I.G., 1967. Chemical composition of the Upper Mantle. J. Geophys. Res. 72, 6359-6369.

HARRIS, P.G., & MIDDLEMOST, E.A.K., 1970. The evolution of Kimberlites. Lithos. 3, 77-88.

HART, S.R., & ALDRICH, L.T., 1967. Fractionation of K/Rb by amphiboles, implications regarding composition. Science. 155, 325-327.

HEEZEN, B.C., & THARP, M., 1965(a). Physiographic diagram of the Indian Ocean. Spec. Pub. Geol. Soc. Am.

HEEZEN, B.C., & THARP, M., 1965(b). Tectonic fabric of the Atlantic and Indian Oceans and continental drift. from: A symposium on continental drift. Phil. Trans. R. Soc. Lond. A. 258, 90-106.

HEEZEN, B.C., & THARP, M., 1966. Physiography of the Indian Ocean. Phil. Trans. R. Soc. Lond. A. 259, 137-149.

HEIER, K.S., 1964. Geochemistry of the nepheline-syenite in Sternoy, North Norway. Norsk. Geol. Tiddskr. 44, 205-215.

HOLLOWAY, J.R., & BURNHAM, C. WAYNE, 1972. Melting Relations Of Basalt With Equilibrium Water Pressure Less Than Total Pressure. J. Petrology 13, 1-29.

HYTÖNEN, K., & SCHAIRER, J.F., 1961. The plane enstatite-anorthite-diopside and its relation to basalts. Carnegie Inst. Wash. Yearbook, 60, 125-141.

ITO, K., & KENNEDY, G.C., 1967. Melting and phase relations in a natural peridotite to 40 Kilobars. Am. J. Sci. 265, 519-538.

ITO, K., & KENNEDY, G.C., 1968. Melting and phase relations in the plane tholeiite-lherzolite-nepheline basanite to 40 kilobars with geological implications. Contr. Mineral. Petrol. 19, 177-211.

JACKSON, E.D., & WRIGHT, T.L., 1970. Xenoliths in the Honolulu Volcanic Series, Hawaii. J. Petrology 11, 405-430.

JAEGER, J.C., 1961. The cooling of irregularly shaped igneous bodies. Am. J. Sci., 259, 721-734.

JAMIESON, B.G., 1966. Evidence on the evolution of basaltic magma at elevated pressures. Nature, 212, 243-246.

JAMIESON, B.G., 1969. Natural rock projection into a pseudo-quaternary system. Progress in Experimental Petrology, N.E.R.C. 1st. Report, Manchester: Edinburgh.

JAMIESON, B.G., 1970. Phase relations in some tholeiitic lavas illustrated by the system $R_2O_3 - XO - YO - ZO_2$. Miner. Mag. 37, 537-554.

JAMIESON, B.G., & CLARKE, D.B., 1970. Potassium and Associated Elements in Tholeiitic Basalts. J. Petrology 11, 183-204.

JENKINS, R., & De VRIES, J.L., 1967. Practical X-ray Spectrometry. Philips Technical Library, Eindhoven.

KESSON, S., & PRICE, R.C., 1972. The Major and Trace Element Chemistry of Kaersutite and Its Bearing on the Petrogenesis of Alkaline Rocks. Contr. Mineral. Petrol. 35, 119-124.

KUNO, H., YAMASAKI, K., IIDA, C., & NAGASHIMA, K., 1957. Differentiation of Hawaiian magmas. Jap. Jour. Geol. Geog., 28, 179-218.

KUSHIRO, I., 1960. Si-Al relation in clinopyroxenes from Igneous rocks. Am. J. Sci. 258, 548-554.

LE MAITRE, R.W., 1962. Petrology of Volcanic Rocks, Gough Island, South Atlantic. Bull. geol. Soc. Am. 73, 1309-1340.

LE MAITRE, R.W., 1968. Chemical variation within and between Volcanic Rock Series - A statistical approach. J. Petrology 9, 220-252.

MACDONALD, G.A., 1963. Relative abundance of intermediate members of the oceanic basalt-trachyte association. J. Geophys. Res. 68, 5100-5102.

MACDONALD, G.A., 1967. Forms and Structures of Extrusive Basaltic Rocks: in; The Poldervaart treatise on rocks of basaltic composition. Vol. 1. Eds. Hess, H.H., & Poldervaart, A. Interscience.

MACDONALD, G.A., 1968. Composition and origin of Hawaiian Lavas. From: Studies in Volcanology, eds., Coats, R.R., Hay, R.L., & Anderson, C.A. Mem. geol. Soc. Am. 116, 477-522. Howell Williams Volum

MACDONALD, G.A., & KATSURA, T., 1964. Chemical composition of Hawaiian lavas. J. Petrology 5, 82-133.

MATTHEWS, D.H., & DAVIES, D., 1966. Geophysical studies of the Seychelles Bank. Phil. Trans. R. Soc. Lond. A. 259, 227-239.

McBIRNEY, A.R., & AOKI, K., 1966. Petrology of the Galápagos Islands. Inst. Sci. Proj. Symposia of the Galapagos Proc.

McBIRNEY, A.R., & AOKI, K., 1968. Petrology of the Island of Tahiti. From. Studies in Volcanology, eds. Coats, R.R., Hay, R.L., & Anderson, C.A. Mem. geol. Soc. Am. 116, 523-556. Howell Williams Volume.

McDOUGALL, I., & COMPSTON, W., 1965. Strontium isotope composition and potassium-rubidium ratios in some rocks from Reunion and Rodriguez, Indian Ocean. Nature, 207, 252-253.

McDOUGALL, I., UPTON, B.G.J., WADSWORTH, W.J., 1965. A geological reconnaisance of Rodriguez Island, Indian Ocean. Nature, 206, 26-27.

McDOUGALL, I., & CHAMALAUN, F.H., 1969. Isotopic dating and geomagnetic polarity studies on Volcanic rocks from Mauritius, Indian Ocean. Bull. geol. Soc. Am. 80, 1419-1442.

McKENZIE, D.P. & SCLATER, J.G., 1971. The Evolution of the Indian Ocean since the Late Cretaceous. Geophys. J.R. Astr. Soc. 25, 437-528.

MENARD, H.W., 1964. Marine Geology of the Pacific. International Series in the Earth Sciences, ed. Shrock, R.R. McGraw-Hill.

MUIR, I.D., & TILLEY, C.E., 1961. Mugearites and their place in alkali igneous rock series. J. Geol. 69, 186-203.

NASH, W.P., CARMICHAEL, I.S.E., & JOHNSON, R.W., 1969. The Mineralogy and Petrology of Mount Suswa, Kenya. J. Petrology 10, 409-501.

NICHOLLS, J. & CARMICHAEL, I.S.E., 1969. Peralkaline Acid Liquids: A Petrological Study. Contr. Mineral. Petrol. 20, 268-294.

NOE-NYGAARD, A., 1968. On extrusion forms in plateau basalts. Scientia Islandica, Aniversary Volume 1968, 10-13; ed. Fridriksson, S., Visindafélag Íslandinga, Reykjavík.

O'HARA, M.J., 1963(a). Melting of garnet peridotite at 30 kilobars. Carnegie Inst. Wash. Yearbook, 62, 71-76.

O'HARA, M.J., 1963(b). Melting of biminerallic eclogite at 30 kilobars. Carnegie Inst. Wash. Yearbook, 62, 76-77.

O'HARA, M.J., 1965. Primary magmas and the origins of basalts. Scott. J. Geol. 1, 19-40.

O'HARA, M.J., 1968. The bearing of phase equilibria studies in synthetic and natural systems on the origin and evolution of basic and ultrabasic rocks. Earth-Sci. Rev. 4, 69-133.

O'HARA, M.J., 1969. The origin of eclogite and ariegite nodules in basalt. Geol. Mag. 106, 322-330.

O'HARA, M.J., 1970. Upper mantle composition inferred from laboratory experiments and observation of volcanic products. Phys. Earth. Planet. Interiors 3, 236-245.

O'HARA, M.J., & YODER, H.S., 1963. Origin of igneous rocks. Carnegie Inst. Wash. Yearbook, 62, 66-71.

O'HARA, M.J., & YODER, H.S., 1967. Formation and fractionation of basaltic magma at high pressures. Scott. J. Geol. 3, 67-117.

POLDERVAART, A., & HESS, H.H., 1951. Pyroxenes in the crystallization of basaltic magmas. J. Geol. 59, 472-489.

POWERS, H.A., 1955. Composition and origin of basaltic magma of the Hawaiian Islands. Geochim. Cosmochim. Acta, 7, 77-107.

PRINZ, M., 1967. Geochemistry of basalts: Trace elements. in: The Poldervaart treatise on rocks of basaltic composition. Vol. 1. Eds. Hess, H.H., & Poldervaart, A. Interscience.

RICHEY, J.E., 1961. Scotland: The Tertiary volcanic districts: 3rd ed., British Region, Geol. H.M. Stat. Office, Edinburgh.

RIDLEY, W.I., 1970. The Petrology of the Las Canadas Volcanoes, Tenerife, Canary Islands. Contr. Mineral. Petrol. 26, 124-160.

RINGWOOD, A.E., 1962. A model for the Upper Mantle. J. Geophys. Res. 67, 4473-4477.

RINGWOOD, A.E., 1966(a). Chemical evolution of the terrestial planets. Geochim. Cosmochim. Acta. 30, 41-104.

RINGWOOD, A.E., 1966(b). The chemical composition and origin of the earth; in: Advances in Earth Science, ed. Hurley, P.M. M.I.T. Press, Cambridge, Mass.

RINGWOOD, A.E., 1969. Composition and Evolution of the Upper Mantle. In: The Earth's Crust and Upper Mantle. Am. Geophys. Union. Geophys. Mon. 13, 1-17.

RINGWOOD, A.E., MACGREGOR, I.D., & BOYD, F.R., 1964. Petrological constitution of the Upper Mantle. Carnegie Inst. Wash. Yearbook, 63, 147-152.

ROSE, H.J., ADLER, I., & FLANAGAN, F.J., 1963. X-ray fluorescence analysis of the light elements in rocks and minerals. Appl. Spectrosc., 17, 81-85.

SHAND, S.J., 1933. The Lavas of Mauritius. Q. Jl. geol. Soc. Lond. 89, 1-13.

SHAPIRO, L., & BRANNOCK, W.W., 1962. Rapid analysis of silicate, carbonate and phosphate rocks. U.S. Geol. Surv. Bull. 1144-A.

BHOR, G.G., & POLLARD, D.D., 1963. Seismic investigations of Seychelles and Saya de Malha Banks, northwest Indian Ocean. Science 142, 48-49.

SIMPSON, E.S.W., 1950. The Geology and Mineral Resources of Mauritius. Col. Geol. Miner. Res., 1, 217-238.

SPRY, A.H., 1962. The origin of columnar jointing, particularly in basalt flows. Geol. Soc. Australia Jour., 191-216.

STEARNS, H.T., 1966. Geology of the State of Hawaii. Pacific Books, California.

STRONG, D.F., 1972. Petrology of the lavas of Grande Comore. J. Petrology 13, 181-217.

TAKIN, M., 1966. Rapid computation of the gravitational attraction of topography on a spherical earth. Geophys. Prospect. 14, 119-142.

THOMPSON, R.N., ESSON, J., & DUNHAM, A.C., 1972. Major element Chemical variation in the Eocene lavas of the Isle of Skye, Scotland. J. Petrology. 13, 219-253.

THORNTON, C.P., & TUTTLE, O.F., 1960. Chemistry of igneous rocks. 1. Differentiation index. Am. J. Sci. 258, 664-684.

TILLEY, C.E., 1950. Some aspects of magmatic evolution. Q. Jl. geol. Soc. Lond. 106, 37-61.

TILLEY, C.E., & MUIR, I.D., 1964. Intermediate members of the oceanic basalt-trachyte association. Geol. För. Stockh. Forh. 85, 436-444.

TURNER, F.J., & VERHOOGEN, J., 1960. Igneous and Metamorphic petrology. New York: McGraw Hill.

TUTTLE, O.F., & BOWEN, N.L., 1958. Origin of granite in the light of experimental studies in the system $NaAlSi_3O_8$-$KAlSi_3O_8$-SiO_2-H_2O. Mem. geol. Soc. Am. 74.

UPTON, B.G.J., 1973 (in Press). The Alkaline Province of S.W. Greenland. In: Alkaline Rocks, ed. Sørensen, H. Interscience.

UPTON, B.G.J., & WADSWORTH, W.J., 1966. The basalts of Reunion Island, Indian Ocean. Bull. Volc. 29, 7-24.

UPTON, B.G.J., & WADSWORTH, W.J., 1972. Aspects of magmatic evolution on Reunion Island. Phil. Trans. R. Soc. Lond. A. 271, 105-130.

VINCENT, E.A., 1960. Analysis of gravimetric and volumetric methods, flame photometry, colorimetry and related techniques. In: Methods in Geochemistry, eds. Smales, A.A., & Wager, L.R. New York and London. Interscience.

VINOGRADOV, A.P., 1962. Average contents of chemical elements in the principal types of igneous rocks of the Earth's crust. Geochemistry, 1962, 641-664.

WAGER, L.R., 1968. Rhythmic and Cryptic Layering in Mafic and Ultramafic Plutons: in; The Poldervaart treatise on rocks of basaltic composition. Vol. 2. Eds. Hess, H.H., & Poldervaart, A. Interscience.

WALKER, F., & NICOLAYSEN, L.O., 1954. The Petrology of Mauritius. Col. Geol. Miner. Res. 4, 3-43.

WEGENER, A., 1924. The origin of Continents and Oceans. London.

WILKINSON, J.F.G., 1956. Clinopyroxenes of alkali olivine-basalt magma. Am. Miner. 41, 724-743.

WILKINSON, J.F.G., 1961. Some aspects of the calciferous amphiboles, oxyhornblende, Kaersutite and barkevikite. Am. Miner. 46, 340-354.

WILSON, A.D., 1958. A new method for the determination of ferrous iron in rocks and minerals. Bull. geol. Surv. Gt. Br., 9, 56-58.

WILSON, J.T., 1963. Evidence from islands on the spreading of ocean floors. Nature, 197, 536-538.

YAGI, K., & ONUMA, K., 1967. The join $CaMgSi_2O_6$-$CaTiAl_2O_6$ and its bearing on the titanaugites. Hokkaido Univ. Jour. Fac. Sci., Ser IV, 14, 463-483.

YODER, H.S., 1969(a). Experimental Studies bearing on the origin of anorthosite; in. Y. Isachsen, ed., Origin of Anorthosite and Related Rocks. New York State Museum and Science Service Mem. 18.

YODER, H.S., 1969(b). Calcalkalic Andesites: Experimental Data Bearing On The Origin Of Their Assumed Characteristics. in; Proceedings of the Andesite Conference, ed. McBirney, A.R. International Upper Mantle Project, Scientific Report 16, 77-90.

YODER, H.S., & SAHAMA, T.G., 1957. Olivine X-ray determinative curve. Am. Miner., 42, 475-491.

YODER, H.S., & TILLEY, C.E., 1962. Origin of basaltic magmas: an experimental study of natural and synthetic rock systems. J. Petrology 3, 342-532.

APPENDIX 1: SAMPLE PREPARATION

A. BULK ROCK POWDERS

1. Wash and scrub hand specimen samples (generally 500-1000 g. initial weight) with a hard bristle brush under running water to remove any loose weathered material or acquired dust. Rinse in deionised water and dry.

2. Reduce hand specimens to approx. 3 cm. chips, using a CUTROCK hydraulic splitter. Discard any weathered surfaces.

3. Crush chips to approx. 50 mesh B.S. MANCHESTER ROLLERS used initially at this stage were superseded later by a STURTEVANT jaw crusher. As samples were prepared by both methods, comparative tests were made for any systematic elemental contamination induced by changing to the jaw crusher and the results are presented in Table A-1. No significant chemical difference between samples prepared by these two methods was detected.

4. Cone and quarter samples until a 150 g. representative portion is obtained.

5. Reduce portion to 100 mesh B.S. (check by sieving) on an agate TEMA. Generally around 10 minutes grinding on the 750 r.p.m. motor was required to achieve this grain size.

6. Transfer samples to bottles and dry for 24 hrs. at 105°C.

7. Seal bottles and store until required.

TABLE A-1

COMPARATIVE CONTAMINATION TESTS ON MANCHESTER ROLLERS AND STURTEVANT JAW CRUSHER

	A90		A103		A160	
	1	2	1	2	1	2
Wt.%						
SiO_2	46.68	46.72	47.28	47.40	45.50	45.58
TiO_2	3.07	3.07	2.89	2.95	3.41	3.43
Al_2O_3	14.75	14.85	14.14	14.00	15.86	15.90
FeO Tot.	11.10	11.18	11.40	11.32	12.69	12.67
MnO	0.19	0.15	0.17	0.17	0.18	0.16
MgO	6.38	6.50	7.00	7.10	6.34	6.24
CaO	10.84	10.92	11.16	11.12	9.77	9.83
Na_2O	2.92	2.92	2.67	2.69	2.97	3.07
K_2O	1.33	1.37	1.13	1.13	1.14	1.16
P_2O_5	0.58	0.54	0.43	0.49	0.51	0.53
P.P.M.						
Ni	180	148	152	140	54	72
Cr	120	142	112	100	14	26
V	400	420	362	348	378	340
Zr	252	272	191	195	210	186
Y	40	44	40	36	40	40
Ba	360	354	308	318	358	340
Sr	515	537	420	452	500	516
Rb	40	44	38	40	37	39

1 : HYDRAULIC SPLITTER → MANCHESTER ROLLERS → AGATE TEMA

2 : HYDRAULIC SPLITTER → STURTEVANT JAW CRUSHER → AGATE TEMA

B. MINERAL SEPARATES

General procedure for separation of phenocryst silicates:

1. Inspect thin section of sample to determine general size of phenocrysts to be separated; check for presence of inclusions in phenocrysts.

2. Crush fresh rock chips to approx. ½ phenocryst dimensions, to obtain a good yield of phenocryst-only fragments.

3. Wash sample to remove fine dust sample produced on crushing. Dry sample at 105°C.

4. Extract ore rich groundmass and composite groundmass/phenocryst fragments by repeatedly passing sample through FRANTZ isodynamic separator, vertically aligned, and at full field strength with vibrating table removed. Up to 80% phenocryst yield is obtained by this technique.

Specific mineral separations

Plagioclase

1. Refine crude portion obtained at stage 4 above, by repeatedly passing sample along vibrating table in a moderately inclined FRANTZ isodynamic separator at high field strength. This effectively separates any remaining groundmass and also the magnetic ferromagnesian phenocrysts from the non-magnetic plagioclase.

2. Final purification by floating off plagioclase (s.g. 2.63-2.76) from impure fragments, in ANALAR tetrabromoethane (s.g. 2.95 at 20°C), which is diluted with ANALAR acetone to a specific gravity of approx. 2.63.

3. If inclusions are present in the phenocrysts then

grind sample to 100 mesh B.S. and repeat specific stages 1 and 2 above.

4. Wash separate thoroughly and dry at 105°C for 24 hrs.

Olivine and Clinopyroxene

Olivine is virtually the only phenocryst phase in the Intermediate and Younger Series, allowing relatively rapid separation; however in the Older Series lavas olivine and clinopyroxene almost always coexist, and as their physical properties partially overlap, considerable difficulty is met with in producing pure separates of each. The following rather lengthy process, however, has been found effective in most cases.

1. Pass crude separate repeatedly along vibrating table in moderately inclined FRANTZ separator at low field strength. This effectively removes any remaining ore rich groundmass or composite fragments.

2. Remove any plagioclase phenocrysts present by flotation in pure ANALAR tetrabromoethane (s.g. 2.95), which does not displace the much denser olivine (s.g. 3.22-3.49) or clinopyroxene (s.g. 2.96-3.55).

3. Thoroughly wash sample and dry at 105°C.

4. Tests showed that generally, coexisting olivine and clinopyroxene in the lavas had marginally different specific gravities, sufficient to allow a gradual separation. The optimum specific gravity for effective separation however, was found to vary slightly from sample to sample, due to minor compositional changes in the olivines and clinopyroxenes, and could only be found by a process of trial and error.

Samples were placed in warm Clerici's solution (s.g. 4.0 at 10°C) which was diluted with warm deionised water until visible separation of olivine (green) and clinopyroxene (black) began; the samples were then centrifuged and the fractions separated. The process was then repeated until pure separates of each were obtained.

5. Thoroughly wash sample to remove all traces of Clerici's solution and dry at 105°C for 24 hrs.

6. If inclusions are present in the phenocrysts, grind pure separates to 100 mesh B.S. and repeat specific stages 1-5 above.

APPENDIX 2: ANALYTICAL TECHNIQUES

A. X-RAY SPECTROGRAPHIC ANALYSIS

The theoretical basis and general principles of X-ray spectrographic analysis are discussed in detail by Jenkins and De Vries (1967). All trace and major elements with the exception of FeO, Na_2O and H_2O were determined by this method using a PHILIPS PW 1212 automatic spectrometer under the standard operating conditions in use at Edinburgh University, shown in Table A-2. A computer program available in this department calculates the analyses, involving initial correction of raw counts for instrument drift and calculation of a least squares regression line from the standards, against which the unknown samples are measured.

Major elements were calculated using the method described by Rose et al. (1963). Essentially this involves eliminating matrix and mass absorption interference in the bulk sample due to its crystalline structure and high major element concentrations by a process of dilution with lithium tetraborate and a heavy absorber - lanthanum oxide, and fusing the mixture to a glass. The sample is then crushed, pressed into a disc and analysed. The preparation technique is described below.

1. Dry 100 mesh B.S. bulk rock powder at 105°C for 24 hours.
2. Dry SPECPURE lithium tetraborate and SPECPURE lanthanum oxide, separately, at 400°C for 24 hours.
3. Weigh out sample, lanthanum oxide and lithium tetraborate in the ratio 1:1:8. Generally the proportions 0.75 g:0.75 g:6.0 g are used.

TABLE A-2

XRF OPERATING CONDITIONS FOR MAJOR AND TRACE ELEMENTS

TUBE

Chromium for major elements, tungsten for trace elements.

DISCRIMINATION

Automatic except for Mg.

METHOD

P = Peak

B = Background.

COUNTER

F = Flow counter

S = Scintillation counter.

COLLIMATOR

F = FINE

C = COARSE

TIME

Counting time in seconds.

TABLE A-2

ELEMENT & LINE		KV	mA	Crystal	Method	Counter	Time	Collimator	Vacuum	Notes
Al	Kα	60	24	PE	P	F	20	C	YES	
Ba	Kα	80	24	LiF	P/BK	S	40	F	NO	
Ca	Kα	40	24	PE	P	F	10	F	YES	
Cr	Kα	80	24	LiF	P-BK	F	40	F	YES	CORRECTION FOR V Kα
Fe	Kα	60	24	LiF	P	S	20	C	NO	
K	Kα	60	24	PE	P	F	10	F	YES	
Mg	Kα	40	32	KAP	P-BK	F	100	C	YES	DISCRIMINATE AGAINST KAP PEAK
Mn	Kα	60	24	LiF	P	F	20	F	YES	
Ni	Kα	80	24	LiF	P/BK	F	40	F	YES	
P	Kα	60	24	PE	P-BK	F	40	F	YES	
Rb	Kα	80	24	LiF	P/BK	S	40	F	NO	
Si	Kα	60	24	PE	P	F	20	C	YES	
Sr	Kα	80	24	LiF	P/BK	S	40	F	NO	
Ti	Kα	60	24	LiF	P	F	10	C	YES	
V	Kα	80	24	LiF	P-BK	F	40	F	YES	CORRECTION FOR Ti Kα
Y	Kα	80	24	LiF	P/BK	S	40	F	NO	CORRECTION FOR Rb Kβ
Zr	Kα	80	24	LiF	P/BK	S	40	F	NO	CORRECTION FOR Sr Kβ

4. Mix thoroughly and transfer to a carbon crucible.

5. Fuse mixture in furnace at 1050°C for 30 minutes.

6. Remove samples from furnace, allow to cool till solid, then place in desiccator to cool completely.

7. Make sample up to 1:1:8 ratio with dry SPECPURE lithium tetraborate. This corrects for any weight losses by volatilization during fusion.

8. Crush to 200 mesh B.S. in tungsten carbide TEMA. Generally 2 minutes on the 1000 r.p.m. motor were required to achieve this grain size. Check by sieving.

9. Transfer samples to bottles. Dry for 24 hours at 105°C.

10. Press powders to discs with a boric acid jacket in a hydraulic press at 15 tons pressure for 45 seconds. Inspect powder surface of disc and reject if not perfect as the characteristic radiation of the lighter elements (Si, Mg, Al) has a very limited surface penetration.

Trace elements have high dilution factors in the samples, and if the peak/background method of Anderman and Kemp (1958) is used, interference effects are minimised and determinations can be made directly on bulk rock powders. Samples were exposed to radiation as loose 100 mesh B.S. powders, in special containers with a replaceable MYLAR film base.

The precision of the major and trace element analytical methods used here are summarised in Table A-3 for one sample A.56, and are comparable with results obtained by other research workers at Edinburgh. The accuracy of the method was calculated from the three standards AGV1, E1 and N-117 and the results are presented in Table A-4.

TABLE A-3

X-RAY FLUORESCENCE: ANALYTICAL PRECISION

Wt.%	$\bar{x}$	n	r	s	c%
SiO_2	50.09	6	0.30	0.280	0.55
TiO_2	2.54	6	0.10	0.050	1.94
Al_2O_3	15.35	6	0.32	0.170	1.02
FeO Tot.	10.41	6	0.21	0.170	1.76
MnO	0.16	6	0.01	0.006	3.80
MgO	5.09	6	0.23	0.100	1.96
CaO	8.44	6	0.10	0.045	0.54
K_2O	1.86	6	0.02	0.008	0.43
P_2O_5	0.43	6	0.05	0.017	3.80
P.P.M.					
Ni	68	6	6	3	4
Cr	47	6	13	5	12
V	325	6	35	15	5
Zr	310	6	17	7	2
Y	42	6	6	2	6
Ba	364	6	52	22	6
Sr	495	6	31	13	3
Rb	55	6	9	16	7

$\bar{x}$ = Mean concentration

n = No. of samples

r = Range of concentrations

s = Standard Deviation

c = Relative deviation in %. $100\, s/\bar{x}$

TABLE A-4

X-RAY FLUORESCENCE: ANALYTICAL ACCURACY

	AGV-1		N-117		E-1	
	1	2	1	2	1	2
Wt.%						
SiO_2	59.00	59.07	49.50	49.28	36.80	36.58
TiO_2	1.07	1.06	2.31	2.29	4.60	4.56
Al_2O_3	17.08	17.30	9.08	9.18	10.38	10.30
FeO Tot.	6.18	6.27	10.35	10.30	25.27	25.44
MgO	1.50	1.45	14.90	14.77	6.55	6.20
CaO	4.98	4.99	7.27	7.22	8.35	8.24
K_2O	2.89	2.88	1.53	1.55	0.24	0.23
P_2O_5	0.49	0.45	0.35	0.32	1.91	1.92

1 Given standard concentration.

2 Mean concentration obtained over period of analysis.

B. WET CHEMISTRY

FeO

Ferrous iron was determined using the method described by Wilson (1955). The technique involves cold solution of the bulk powder sample with hydrofluoric acid and in the presence of excess ammonium vanadate, in PTFE crucibles and titration of the excess vanadate against ammonium ferrous sulphate dissolved in a mixture of boric and sulphuric acid, using sodium diphenylamine as an indicator. The precision of the method is summarised in Table A-5 for the sample A.56. ANALAR or SPECPURE reagents were used throughout.

Na_2O

Sodium was determined using an EEL flame photometer, Vincent (1960). The particular method in use at Edinburgh was developed by the departmental analyst M.J. Saunders, and is summarised below. ANALAR or SPECPURE reagents were used throughout.

1. Dissolve bulk powder sample with conc. nitric and hydrofluoric acid, in platinum crucibles.
2. Remove excess hydrofluoric acid by addition and evaporation of 1 + 1 sulphuric acid.
3. Add dilute sulphuric acid to maintain solution and then dilute with deionised water to ensure all sodium enters the solution.
4. Allow any insoluble calcium sulphate residue to settle.
5. Analyse solution in flame photometer with a double Na filter to minimise interference from any remaining calcium in solution.

TABLE A-5

FERROUS IRON DETERMINATIONS: PRECISION

$\bar{x}$	3.29
n	6
r	0.25
s	0.039
c %	1.19

$\bar{x}$ = Mean FeO concentration, Wt. %.

n = No. of samples.

r = Range of concentrations

s = Standard deviation

c % = Relative deviation in %. $100\, s/\bar{x}$

Estimates of the precision of this method for one sample A.56, are presented in Table A-6.

$\underline{H_2O}$

Water was determined gravimetrically by a modification of the method described by Shapiro and Brannock (1962). 1 g of bulk powder sample was fused with 3 g of flux (lead oxide: lead chromate = 2:1) in a test tube, and the water evolved absorbed on a preweighed filter paper. The filter paper was reweighed and the amount of evolved water calculated by difference. Table A-7 summarises the precision of this technique.

TABLE A-6

SODIUM DETERMINATIONS: PRECISION

$\bar{x}$	3.45
n	6
r	0.09
s	0.031
c %	0.90

$\bar{x}$ = Mean Na_2O concentration, Wt. %.

n = No. of samples.

r = Range of concentrations.

s = Standard deviation.

c % = Relative deviation in %. $100\, s/\bar{x}$

TABLE A-7

WATER DETERMINATIONS: PRECISION

$\bar{x}$	1.77
n	6
r	0.17
s	0.10
c %	5.65

$\bar{x}$ = Mean H_2O concentration, Wt. %

n = No. of samples

r = Range of concentrations

s = Standard deviation

c % = Relative deviation in %. $100\ s/\bar{x}$

C. X-RAY DIFFRACTION

Where only partial olivine analyses were required i.e. forsterite content, compositions were determined on separates using the X-ray diffraction technique described by Yoder and Sahama (1957), which involved measuring the olivine (130) reflection using sodium chloride as an internal standard. The accuracy of the method was assessed by these authors as ± 4%.

D. ELECTRON MICROPROBE ANALYSES

Partial analyses of olivines, clinopyroxenes, kaersutites and feldspars were determined using the CAMBRIDGE INSTRUMENTS microscan electron microprobe at Manchester University. A standard program in use at Edinburgh University was used to correct raw data for absorption, fluorescence and dead time factors.

E. OPTICAL DETERMINATIONS

Unless otherwise stated plagioclase compositions were determined on a flat stage microscope, by the Michel-Levy method.

Modal data was determined on a SHADOWMASTER projection microscope with a 600 point grid.

APPENDIX 3: ANALYTICAL DATA

A. OLDER SERIES

B. INTERMEDIATE SERIES

C. YOUNGER SERIES

Major elements in wt. %

Trace elements in p.p.m.

Norm in wt. %.

D.I. = Differentiation index.

O.R. = Oxidation ratio ($Fe_2O_3/FeO + Fe_2O_3$)

A. OLDER SERIES

N.B.

Norms are calculated on a standardised

O.R. = 0.26 ($Fe_2O_3/FeO + Fe_2O_3 = 1:3.80$)

for analyses with O.R. > 0.26.

	A2	A3	A4	A7	A9	A10	A11	A13
SiO_2	46.45	46.55	46.06	46.56	48.25	46.06	46.53	44.53
TiO_2	3.02	3.13	2.88	3.42	3.42	2.60	3.09	2.24
Al_2O_3	14.52	14.81	13.99	15.13	15.17	12.30	14.66	9.96
Fe_2O_3	6.77	7.86	3.82	[illegible].90	4.33	5.43	5.25	3.65
FeO	5.64	4.62	7.71	5.90	7.89	7.77	7.05	9.48
MnO	0.16	0.15	0.15	0.15	0.15	0.17	0.15	0.17
MgO	5.79	5.51	7.29	4.53	5.31	11.51	5.53	15.41
CaO	11.26	10.31	10.98	10.45	10.24	10.00	10.68	10.92
Na_2O	2.89	2.79	2.66	3.08	3.37	2.67	3.16	1.89
K_2O	1.23	1.27	1.30	1.41	1.55	0.95	1.32	0.72
H_2O	1.89	2.58	1.78	1.76	0.86	1.19	0.99	0.70
P_2O_5	0.43	0.44	0.49	0.45	0.48	0.34	0.45	0.32
Total	100.05	100.12	99.11	99.74	101.42	100.99	98.86	99.99
Ni	82	103	187	78	52	479	136	562
Cr	46	98	188	66	30	487	91	687
V	344	319	284	384	346	278	336	263
Zr	222	261	255	287	326	200	278	157
Y	39	55	45	46	50	36	48	33
Ba	354	350	373	404	465	287	398	263
Sr	502	486	505	536	556	393	516	350
Rb	33	35	38	43	44	31	34	19
K/Rb	310	302	284	272	292	254	322	314
D.I.	31.28	32.06	30.21	34.71	36.71	26.78	33.68	18.39
O.R.	0.55	0.63	0.33	0.54	0.35	0.41	0.43	0.28
Qz	-	-	-	-	-	-	-	-
Ne	1.34	-	0.97	0.59	1.11	1.81	1.98	2.36
Hy	-	4.20	-	-	-	-	-	-
Di	25.02	20.29	24.00	21.52	21.16	23.08	23.49	28.60
Ol	8.57	6.64	11.47	7.31	8.22	20.54	8.57	26.24
Or	7.43	7.73	7.90	8.53	9.15	5.63	7.98	4.29
Ab	22.52	24.33	21.35	25.59	26.45	19.34	23.72	11.74
An	23.52	24.87	23.02	23.85	21.67	18.84	22.43	16.68
Mt	4.71	4.74	4.49	4.87	4.62	4.99	4.73	5.04
Ilm	5.86	6.13	5.62	6.65	6.49	4.96	6.01	4.28
Ap	1.04	1.07	1.19	1.09	1.14	0.81	1.09	0.76
H_2O	1.89	2.58	1.78	1.76	0.86	1.19	0.99	0.70
Rest	-	-	-	-	-	-	-	-

	A17	A18	A20	A22	A24	A28	A35	A37
SiO_2	48.70	46.34	47.71	46.35	44.12	44.16	45.70	46.81
TiO_2	3.50	2.93	3.12	2.84	2.17	2.70	2.66	3.02
Al_2O_3	14.41	14.41	14.67	13.98	9.62	11.49	12.11	14.75
Fe_2O_3	5.61	4.26	3.14	3.25	2.71	2.18	1.62	5.19
FeO	6.68	7.87	8.69	8.83	9.80	10.97	10.50	6.61
MnO	0.17	0.15	0.20	0.16	0.17	0.17	0.17	0.16
MgO	3.43	6.60	4.98	6.96	16.50	13.58	11.14	5.81
CaO	8.36	11.07	8.93	11.30	10.39	10.87	9.60	11.33
Na_2O	3.91	2.79	3.12	2.71	1.98	2.18	2.70	2.70
K_2O	1.86	1.15	1.88	1.18	0.82	0.90	1.01	1.18
H_2O	1.98	1.76	3.12	1.69	1.45	1.08	1.36	2.48
P_2O_5	0.66	0.41	0.46	0.35	0.28	0.39	0.45	0.46
Total	99.27	99.74	100.02	99.60	100.01	100.67	99.02	100.50
Ni	0	132	46	151	620	420	338	100
Cr	9	89	49	150	835	435	381	95
V	261	317	223	295	252	296	281	360
Zr	403	227	312	215	160	197	229	238
Y	68	42	54	41	33	34	41	41
Ba	461	330	383	304	267	288	281	379
Sr	527	445	557	475	355	434	429	486
Rb	54	32	58	37	32	24	32	33
K/Rb	286	298	268	264	212	312	262	298
D.I.	45.39	30.31	38.70	29.43	18.47	19.84	27.71	30.47
O.R.	0.46	0.35	0.27	0.27	0.22	0.17	0.13	0.44
Qz	-	-	-	-	-	-	-	-
Ne	-	0.88	-	1.31	4.07	4.75	2.11	-
Hy	2.38	-	4.18	-	-	-	-	1.61
Di	17.78	23.92	17.57	25.91	28.21	26.27	22.17	23.74
Ol	4.49	10.52	6.54	10.62	29.33	25.67	23.09	7.48
Or	11.32	6.94	11.46	7.12	4.92	5.34	6.11	7.13
Ab	34.07	22.49	27.24	21.00	9.48	9.74	19.49	23.35
An	16.76	23.90	21.12	22.97	15.15	18.98	18.37	25.18
Mt	4.75	4.69	4.65	4.71	3.99	3.17	2.40	2.53
Ilm	6.85	5.68	6.11	5.51	4.18	5.15	5.17	5.86
Ap	1.61	0.99	1.12	0.85	0.67	0.93	1.09	1.11
H_2O	1.98	1.76	3.12	1.69	1.45	1.08	1.36	2.48
Rest	-	-	-	-	-	-	-	-

	A39	A41	A45	A46	A48	A49	A56	A57
SiO_2	46.81	45.63	46.00	45.55	44.05	43.88	50.09	50.27
TiO_2	2.82	2.99	3.19	3.21	3.11	2.81	2.54	2.53
Al_2O_3	13.81	16.29	14.67	14.70	13.33	11.37	15.35	15.55
Fe_2O_3	5.38	3.75	4.30	4.06	3.97	3.50	7.83	5.49
FeO	6.79	7.66	7.70	8.16	8.73	10.19	3.29	4.92
MnO	0.15	0.14	0.15	0.15	0.16	0.17	0.16	0.19
MgO	7.32	5.27	6.59	7.13	8.24	12.35	5.09	4.87
CaO	10.53	10.94	10.34	10,53	10.53	10.49	8.44	8.95
Na_2O	2.78	3.35	2.99	2.59	2.71	2.10	3.45	3.58
K_2O	1.17	0.66	1.34	1.24	1.28	0.88	1.86	1.87
H_2O	1.87	1.94	1.50	2.13	2.11	1.98	1.77	1.56
P_2O_5	0.45	0.49	0.52	0.45	0.41	0.35	0.43	0.41
Total	99.88	99.11	99.29	99.90	98.63	100.07	100.30	100.19
Ni	237	115	135	172	203	376	68	74
Cr	241	79	123	143	212	361	47	46
V	316	311	310	304	311	304	325	318
Zr	238	247	287	272	246	211	310	292
Y	44	42	46	49	44	37	42	40
Ba	360	353	410	373	364	295	364	328
Sr	423	593	604	575	524	478	495	443
Rb	32	30	46	42	47	40	55	59
K/Rb	304	182	242	244	226	182	280	264
D.I.	31.11	31.47	32.63	29.70	28.31	21.68	40.96	42.02
O.R.	0.44	0.33	0.36	0.33	0.31	0.26	0.70	0.53
Qz	-	-	-	-	-	-	-	-
Ne	-	2.05	1.61	0.27	3.90	2.04	-	-
Hy	1.07	-	-	-	-	-	8.75	4.26
Di	22.81	19.81	20.95	20.28	24.40	25.19	15.10	17.31
Ol	11.55	8.94	11.13	12.54	13.99	22.31	3.77	5.43
Or	7.07	4.02	8.10	7.50	7.84	5.30	11.20	11.23
Ab	24.04	25.40	22.92	21.94	16.58	14.34	29.76	30.79
An	22.23	28.27	23.18	25.40	21.17	19.36	21.31	21.18
Mt	4.67	4.46	4.64	4.75	5.00	5.17	4.15	3.93
Ilm	5.47	5.85	6.20	6.24	6.12	5.44	4.92	4.88
Ap	1.09	1.19	1.26	1.09	1.01	0.84	1.04	0.99
H_2O	1.87	1.94	1.50	2.13	2.11	1.98	1.77	1.56
Rest	-	-	-	-	-	-	-	-

	A58	A60	A63	A64	A66	A67	A68	A69
SiO_2	48.45	48.70	51.01	50.55	51.18	50.44	49.30	44.18
TiO_2	2.91	2.92	2.88	2.87	2.87	3.04	3.28	3.20
Al_2O_3	15.85	15.90	16.17	15.65	15.59	15.40	15.32	16.85
Fe_2O_3	3.85	4.68	4.98	4.68	4.29	4.67	5.13	4.35
FeO	6.73	6.07	4.26	6.58	6.72	6.51	6.68	8.55
MnO	0.17	0.17	0.17	0.19	0.22	0.22	0.20	0.17
MgO	4.70	4.68	2.76	3.74	3.58	3.71	4.21	5.66
CaO	9.58	9.68	8.60	7.83	7.77	7.89	8.02	11.15
Na_2O	3.40	3.43	4.78	4.57	4.78	4.27	3.82	2.32
K_2O	1.67	1.63	1.71	1.69	1.70	1.60	1.48	0.66
H_2O	1.41	1.23	0.97	0.92	0.44	1.21	1.41	1.72
P_2O_5	0.55	0.51	0.76	0.63	0.82	0.81	0.71	0.28
Total	99.27	99.60	99.05	99.90	99.96	99.77	99.56	99.09
Ni	88	94	0	0	0	0	0	54
Cr	60	69	6	11	11	7	10	29
V	315	379	245	204	251	264	294	451
Zr	274	279	354	371	336	336	308	193
Y	40	37	60	66	58	61	59	32
Ba	336	356	444	394	403	375	322	207
Sr	511	517	610	583	576	559	550	595
Rb	51	55	59	54	61	54	54	22
K/Rb	272	246	240	260	232	246	228	250
D.I.	39.51	39.35	50.80	48.95	50.66	46.31	41.91	24.19
O.R.	0.36	0.44	0.54	0.42	0.39	0.41	0.43	0.34
Qz	-	-	-	-	-	-	-	-
Ne	-	-	1.00	0.32	0.14	-	-	-
Hy	1.39	1.26	-	-	-	7.59	10.84	3.05
Di	17.41	17.87	16.88	14.62	14.21	13.15	12.45	16.69
Ol	7.04	6.93	3.38	7.72	7.37	2.45	1.51	9.58
Or	10.09	9.81	10.32	10.10	10.10	9.60	8.92	4.01
Ab	29.42	29.55	39.48	38.53	40.42	36.70	32.98	20.18
An	23.57	23.59	18.00	17.40	16.15	18.41	20.70	34.55
Mt	4.09	4.12	3.51	4.28	4.17	4.27	4.53	5.02
Ilm	5.65	5.65	5.59	5.51	5.48	5.86	6.36	6.25
Ap	1.33	1.23	1.84	1.51	1.95	1.95	1.72	0.68
H_2O	1.41	1.23	0.97	0.92	0.44	1.21	1.41	1.72
Rest	-	-	-	-	-	-	-	-

	A70	A71	A72	A73	A75	A76	A78	A80
SiO_2	48.80	47.85	47.33	51.41	50.70	51.22	54.84	50.01
TiO_2	3.02	3.38	3.14	2.26	2.15	2.18	1.57	2.38
Al_2O_3	16.54	15.75	16.03	17.71	17.40	17.95	18.01	17.31
Fe_2O_3	4.73	4.74	3.89	7.50	7.96	8.39	2.47	3.68
FeO	5.75	7.39	7.24	2.38	2.43	1.67	5.65	6.43
MnO	0.18	0.18	0.17	0.18	0.20	0.21	0.26	0.23
MgO	4.37	4.68	5.14	2.41	3.04	2.17	2.20	3.29
CaO	8.65	10.13	10.08	6.89	6.93	6.44	5.01	7.24
Na_2O	3.98	3.29	3.28	4.40	4.56	4.48	4.97	4.42
K_2O	1.35	1.13	1.27	2.28	2.24	2.42	3.31	2.16
H_2O	1.90	1.01	1.35	1.60	1.45	1.10	1.66	1.23
P_2O_5	0.52	0.51	0.68	0.93	0.90	0.85	0.50	0.91
Total	99.79	100.04	99.60	99.95	99.96	99.08	100.45	99.29
Ni	30	87	102	17	18	17	0	0
Cr	16	65	70	29	23	26	12	11
V	332	427	349	179	169	151	94	168
Zr	249	210	252	298	325	347	544	263
Y	49	43	45	54	52	56	62	44
Ba	318	260	351	620	621	636	837	617
Sr	554	474	553	902	819	792	738	967
Rb	40	44	42	81	77	93	132	71
K/Rb	280	214	250	234	242	216	208	252
D.I.	42.06	34.90	35.90	51.77	52.84	53.55	62.37	50.98
O.R.	0.45	0.39	0.35	0.77	0.77	0.79	0.30	0.36
Qz	-	-	-	-	-	-	-	-
Ne	-	-	-	-	-	-	-	0.23
Hy	2.48	4.16	1.21	8.52	0.25	6.58	4.60	-
Di	13.32	18.25	16.83	5.33	6.86	4.02	3.83	7.56
Ol	6.84	5.22	8.33	1.78	9.07	3.53	4.59	9.31
Or	7.57	6.75	7.64	13.76	13.50	14.67	19.80	13.02
Ab	34.49	28.15	28.26	38.01	39.34	38.88	42.57	37.73
An	24.14	25.14	25.73	22.30	20.79	22.28	17.27	21.44
Mt	4.02	4.62	4.30	3.67	3.86	3.73	3.13	3.91
Ilm	5.87	6.49	6.07	4.38	4.16	4.25	3.02	4.61
Ap	1.26	1.22	1.64	2.25	2.17	2.06	1.20	2.20
H_2O	1.90	1.01	1.35	1.60	1.45	1.10	1.66	1.23
Rest	-	-	-	-	-	-	-	-

	A82	A83	A86	A88	A90	A91	A93	A94
SiO_2	47.06	47.40	47.31	48.75	46.70	47.58	46.80	48.00
TiO_2	3.08	2.83	2.98	2.89	3.07	3.00	3.18	3.03
Al_2O_3	15.28	14.35	14.27	14.70	14.80	14.81	14.97	15.12
Fe_2O_3	4.65	5.99	6.83	5.14	3.85	5.30	3.41	7.94
FeO	7.04	5.60	4.99	6.47	7.64	6.09	8.67	3.91
MnO	0.18	0.17	0.18	0.18	0.17	0.16	0.16	0.15
MgO	5.52	5.97	5.92	5.13	6.44	6.23	5.45	4.98
CaO	10.55	10.59	10.61	10.18	10.88	10.81	10.81	10.37
Na_2O	2.96	2.71	2.73	3.25	2.92	2.81	2.87	3.32
K_2O	1.40	1.22	1.16	1.18	1.35	1.37	1.35	1.23
H_2O	1.47	1.86	1.80	0,97	0.92	1.24	1.87	0.62
P_2O_5	0.48	0.43	0.49	0.44	0.56	0.47	0.39	0.51
Total	99.67	99.12	99.27	99.28	99.30	99.87	99.93	99.18
Ni	112	142	112	57	164	147	51	77
Cr	60	93	52	25	131	129	44	32
V	381	375	338	396	410	346	307	352
Zr	246	249	218	222	262	261	245	219
Y	40	41	38	49	42	41	44	44
Ba	362	338	282	250	357	363	341	327
Sr	491	507	432	415	526	533	501	465
Rb	43	37	35	39	42	46	45	37
K/Rb	270	274	274	252	266	248	250	276
D.I.	33.87	31.07	30.83	35.13	32.29	32.38	32.64	36.03
O.R.	0.40	0.52	0.58	0.44	0.34	0.47	0.28	0.67
Qz	-	-	-	-	-	-	-	-
Ne	0.11	-	-	-	1.13	-	0.30	-
Hy	-	7.35	8.03	6.61	-	2.13	-	1.34
Di	20.70	22.07	21.90	21.30	22.27	22.07	22.55	21.13
Ol	9.07	4.36	3.76	3.42	10.06	8.04	8.57	6.82
Or	8.43	7.43	7.06	7.11	8.11	8.22	8.14	7.41
Ab	25.32	23.64	23.78	28.02	23.05	24.15	24.20	28.63
An	24.74	24.11	23.94	22.46	23.68	24.13	24.45	23.15
Mt	4.49	4.45	4.51	4.43	4.42	4.33	4.69	4.43
Ilm	5.96	5.54	5.83	5.59	5.93	5.79	6.16	5.86
Ap	1.16	1.05	1.19	1.06	1.35	1.13	0.94	1.23
H_2O	1.47	1.86	1.80	0.97	0.92	1.24	1.87	0.62
Rest	-	-	-	-	-	-	-	-

	A96	A97	A98	A99	A100	A101	A102	A103
SiO_2	47.55	48.14	47.44	47.14	48.11	47.38	47.43	47.34
TiO_2	3.13	2.99	2.83	3.09	2.91	3.09	2.94	2.92
Al_2O_3	16.17	14.94	13.96	15.23	14.48	14.75	14.11	14.07
Fe_2O_3	3.03	6.11	3.89	4.67	4.67	6.01	7.16	3.77
FeO	8.10	5.66	7.76	7.18	7.36	5.13	5.01	7.93
MnO	0.16	0.17	0.16	0.18	0.17	0.21	0.16	0.17
MgO	3.92	5.53	7.15	5.68	6.16	5.94	6.35	7.05
CaO	9.50	10.27	11.84	10.36	11.08	10.89	11.28	11.14
Na_2O	3.78	3.05	2.49	3.00	2.71	2.67	2.69	2.68
K_2O	1.86	1.22	1.12	1.30	1.10	1.28	1.16	1.13
H_2O	2.54	1.27	1.14	1.51	1.07	1.71	0.90	1.58
P_2O_5	0.61	0.46	0.57	0.55	0.47	0.50	0.49	0.46
Total	100.35	99.81	100.35	99.89	100.27	99.56	99.68	100.24
Ni	27	108	181	76	141	136	145	146
Cr	27	74	117	20	104	73	137	106
V	244	389	371	377	382	411	378	355
Zr	386	219	185	242	206	222	199	193
Y	58	47	37	41	36	36	36	38
Ba	454	324	310	326	291	340	283	313
Sr	664	448	430	489	432	481	442	436
Rb	57	44	38	49	39	46	46	39
K/Rb	270	230	244	220	234	230	210	240
D.I.	41.31	33.59	27.92	33.65	29.70	30.90	30.08	29.77
O.R.	0.25	0.52	0.33	0.40	0.39	0.54	0.59	0.32
Qz	-	-	-	-	-	-	-	-
Ne	3.09	-	-	-	-	-	-	-
Hy	-	6.06	3.56	1.62	7.81	6.34	3.79	2.85
Di	18.03	20.28	25.63	19.51	22.74	21.82	24.56	24.00
Ol	6.62	4.84	7.85	8.70	4.14	4.38	6.78	8.81
Or	11.23	7.33	6.67	7.82	6.56	7.75	6.96	6.77
Ab	26.99	26.26	21.25	25.83	23.14	23.15	23.12	23.00
An	22.14	23.88	23.80	24.68	24.32	25.08	23.36	23.35
Mt	4.34	4.46	4.46	4.54	4.58	4.25	4.58	4.50
Ilm	6.08	5.78	5.42	5.97	5.58	6.01	5.67	5.62
Ap	1.48	1.11	1.36	1.33	1.12	1.21	1.18	1.10
H_2O	2.54	1.27	1.14	1.51	1.07	1.71	0.90	1.58
Rest	-	-	-	-	-	-	-	-

	A104	A105	A108	A109	A110	A111	A112	A113
SiO_2	49.07	47.06	47.24	47.41	47.67	47.25	47.08	47.90
TiO_2	2.89	2.91	2.96	2.84	3.15	3.22	3.08	3.06
Al_2O_3	15.14	14.56	14.46	14.22	14.80	14.40	15.00	14.92
Fe_2O_3	5.63	5.47	7.22	5.60	4.82	4.38	3.40	3.91
FeO	6.11	6.90	4.30	6.05	7.11	7.84	8.45	8.18
MnO	0.17	0.15	0.16	0.15	0.17	0.15	0.17	0.17
MgO	4.70	5.64	5.63	6.88	4.64	6.05	5.66	6.37
CaO	10.16	10.03	10.97	10.34	10.43	10.51	10.84	10.48
Na_2O	3.18	3.18	2.98	2.76	3.18	2.77	3.03	3.15
K_2O	1.17	1.22	1.27	1.08	1.39	1.38	1.18	1.22
H_2O	1.39	1.32	1.94	2.17	1.25	1.07	0.86	0.51
P_2O_5	0.44	0.52	0.45	0.41	0.46	0.45	0.50	0.54
Total	100.05	98.96	99.58	99.91	99.07	99.47	99.25	100.41
Ni	69	149	127	201	71	142	76	139
Cr	19	83	90	133	11	122	58	108
V	397	397	396	374	433	378	395	394
Zr	208	216	215	210	251	270	217	225
Y	46	43	38	37	43	49	49	38
Ba	289	299	369	288	337	409	296	341
Sr	415	420	459	392	490	513	502	471
Rb	40	44	43	38	49	40	48	38
K/Rb	244	230	244	236	236	286	204	266
D.I.	34.35	35.01	33.56	30.49	35.95	32.13	32.95	33.86
O.R.	0.48	0.44	0.63	0.48	0.40	0.36	0.28	0.32
Qz	-	-	-	-	-	-	-	-
Ne	-	-	0.09	-	-	-	0.23	0.06
Hy	10.15	0.75	-	7.03	1.13	3.60	-	-
Di	19.93	20.53	24.36	21.09	22.42	21.85	22.08	20.74
Ol	0.53	9.60	7.88	6.59	6.15	7.24	9.00	10.71
Or	7.02	7.40	7.71	6.54	8.41	8.29	7.09	7.22
Ab	27.33	27.61	25.76	23.95	27.54	23.84	25.64	26.58
An	23.95	22.42	22.95	23.81	22.52	23.17	24.23	23.00
Mt	4.46	4.76	4.37	4.46	4.60	4.70	4.58	4.59
Ilm	5.57	5.67	5.78	5.53	6.12	6.22	5.95	5.82
Ap	1.06	1.26	1.10	1.00	1.12	1.08	1.20	1.28
H_2O	1.39	1.32	1.94	2.17	1.25	1.07	0.86	0.51
Rest	-	-	-	-	-	-	-	-

	A116	A117	A118	A119	A121	A122	A123	A124
SiO_2	47.61	46.41	45.24	46.48	47.92	47.10	47.63	47.10
TiO_2	3.22	3.29	2.39	3.09	2.96	3.17	3.08	3.14
Al_2O_3	14.85	15.25	9.83	14.31	14.51	14.15	14.78	14.27
Fe_2O_3	4.42	4.49	4.04	5.12	4.22	6.67	3.33	4.24
FeO	7.57	7.72	8.64	6.75	6.99	5.69	7.73	7.52
MnO	0.17	0.18	0.18	0.16	0.17	0.16	0.17	0.16
MgO	5.36	5.27	16.09	7.65	6.41	6.81	6.24	6.69
CaO	9.66	10.80	10.16	10.02	10.10	10.30	10.02	10.61
Na_2O	3.36	2.94	1.46	2.40	3.43	2.79	3.22	2.95
K_2O	1.43	1.37	0.81	1.36	1.42	1.33	1.46	1.34
H_2O	1.73	0.92	1.33	2.64	0.64	1.58	0.81	0.84
P_2O_5	0.57	0.54	0.31	0.67	0.69	0.59	0.58	0.58
Total	99.95	99.18	100.48	100.65	99.46	100.34	99.05	99.44
Ni	102	74	692	187	190	216	185	213
Cr	62	36	705	159	180	155	164	154
V	401	435	310	332	368	394	358	386
Zr	252	237	129	228	250	227	257	228
Y	42	45	26	38	36	47	44	42
Ba	386	443	273	392	399	392	395	401
Sr	504	567	384	494	509	505	546	499
Rb	49	52	37	47	50	43	51	44
K/Rb	242	218	182	240	236	256	238	254
D.I.	37.58	32.90	17.30	28.97	36.88	31.96	36.21	33.12
O.R.	0.37	0.37	0.32	0.43	0.38	0.54	0.30	0.36
Qz	-	-	-	-	-	-	-	-
Ne	-	0.81	-	-	1.20	-	0.37	0.30
Hy	0.21	-	5.74	8.77	-	3.77	-	-
Di	19.10	21.36	24.55	17.38	21.00	20.65	20.08	22.28
Ol	9.27	8.56	24.20	7.92	10.23	8.93	10.13	10.58
Or	8.61	8.25	4.83	8.21	8.50	7.98	8.78	8.04
Ab	28.97	23.84	12.47	20.75	27.18	23.97	27.06	24.79
An	21.62	24.82	18.04	24.79	20.26	22.50	21.95	22.06
Mt	4.61	4.70	4.86	4.55	4.29	4.67	4.28	4.52
Ilm	6.23	6.36	4.58	6.00	5.69	6.11	5.95	6.05
Ap	1.38	1.30	0.74	1.62	1.66	1.42	1.40	1.39
H_2O	1.73	0.92	1.33	2.64	0.64	1.58	0.81	0.84
Rest	-	-	-	-	-	-	-	-

	A127	A128	A129	A132	A138	A144	A146	A152
SiO_2	44.46	47.12	47.22	45.94	44.52	45.50	49.93	49.22
TiO_2	4.03	2.93	2.96	2.46	2.93	2.86	2.71	2.49
Al_2O_3	14.97	16.41	16.13	12.97	17.79	14.12	16.49	14.68
Fe_2O_3	5.38	3.17	2.66	9.80	5.27	6.33	8.00	6.19
FeO	8.79	8.18	8.80	2.85	6.79	5.15	2.41	4.60
MnO	0.18	0.19	0.16	0.21	0.15	0.19	0.18	0.16
MgO	5.88	5.55	5.48	7.82	5.70	4.95	3.68	5.75
CaO	10.49	8.50	9.01	9.12	11.48	11.80	7.62	8.55
Na_2O	2.67	3.53	3.37	2.21	2.30	2.52	4.10	3.65
K_2O	0.83	1.43	1.41	1.31	0.63	1.20	2.00	1.53
H_2O	1.52	1.76	1.85	4.98	2.20	2.49	1.54	1.84
P_2O_5	0.39	0.61	0.46	0.64	0.32	0.62	0.88	0.53
Total	99.79	99.38	99.51	100.31	100.08	97.73	99.54	99.19
Ni	21	48	43	283	53	142	0	204
Cr	6	66	71	227	29	68	10	176
V	509	293	218	258	424	359	197	271
Zr	134	221	262	273	92	204	323	290
Y	30	45	49	41	26	36	51	50
Ba	224	353	340	408	159	268	487	365
Sr	515	645	627	658	544	417	614	414
Rb	27	58	46	40	21	35	70	53
K/Rb	254	206	254	272	250	284	238	240
D.I.	28.07	39.25	37.71	27.90	23.73	29.92	47.68	41.13
O.R.	0.39	0.28	0.24	0.77	0.44	0.55	0.77	0.57
Qz	-	-	-	-	-	-	-	-
Ne	-	-	-	-	-	-	-	-
Hy	1.13	0.11	0.12	16.61	2.84	1.78	5.52	4.97
Di	19.24	11.24	14.15	16.64	15.44	26.51	9.57	16.58
Ol	10.38	12.49	11.37	4.68	9.67	5.10	4.74	7.30
Or	5.01	8.65	8.53	8.17	3.81	7.47	12.11	9.31
Ab	23.07	30.59	29.18	19.73	19.92	22.45	35.56	31.82
An	26.96	25.31	25.30	22.79	37.21	24.93	21.20	19.73
Mt	5.46	4.43	4.48	4.85	4.63	4.49	3.88	4.12
Ilm	7.81	5.70	5.75	4.93	5.70	5.72	5.28	4.87
Ap	0.94	1.48	1.12	1.60	0.78	1.55	2.14	1.29
H_2O	1.52	1.76	1.85	4.98	2.20	2.49	1.54	1.84
Rest	-	-	-	-	-	-	-	-

	A153	A154	A155	A156	A157	A158	A159	A160
SiO_2	50.60	49.97	49.41	45.89	45.32	46.15	46.06	45.54
TiO_2	2.49	2.54	2.88	3.45	3.44	3.32	3.31	3.42
Al_2O_3	15.00	14.94	17.51	16.01	15.76	15.62	15.93	15.88
Fe_2O_3	4.36	5.19	7.20	7.82	4.91	6.85	8.56	2.54
FeO	5.80	5.14	4.23	5.95	8.77	6.33	4.73	10.37
MnO	0.17	0.15	0.14	0.17	0.15	0.17	0.16	0.15
MgO	5.82	5.64	2.89	4.98	6.11	5.02	5.46	6.29
CaO	8.67	8.93	8.24	9.33	9.83	9.65	9.91	9.80
Na_2O	3.73	3.59	3.91	3.03	2.97	3.03	2.94	3.02
K_2O	1.53	1.58	1.67	1.08	1.02	1.16	1.08	1.13
H_2O	1.49	2.22	2.52	1.51	1.01	1.30	0.92	0.51
P_2O_5	0.61	0.42	0.63	0.47	0.36	0.51	0.52	0.52
Total	100.27	100.31	101.23	99.69	99.65	99.11	99.58	99.17

Ni	186	183	0	78	65	81	73	63
Cr	158	161	8	20	17	27	34	20
V	287	258	210	447	380	420	369	359
Zr	290	319	351	211	235	208	204	198
Y	46	52	55	44	54	42	42	40
Ba	406	394	486	312	327	317	366	349
Sr	423	418	749	474	486	484	499	508
Rb	60	50	51	31	31	39	38	38
K/Rb	212	262	272	288	274	246	236	246
D.I.	41.23	40.57	43.67	32.74	31.01	33.32	31.83	31.46
O.R.	0.43	0.50	0.63	0.57	0.36	0.52	0.64	0.20
Qz	-	-	-	-	-	-	-	-
Ne	-	-	-	-	0.72	-	-	1.41
Hy	8.45	5.58	6.40	4.89	-	3.82	3.26	-
Di	15.92	17.88	9.69	13.70	16.37	15.93	15.56	15.59
Ol	4.29	5.66	3.17	8.12	12.83	7.95	9.16	14.59
Or	9.18	9.54	10.03	6.52	6.12	7.03	6.50	6.77
Ab	32.05	31.03	33.64	26.21	24.17	26.29	25.33	23.29
An	19.97	20.42	25.72	27.49	27.05	26.24	27.57	26.79
Mt	3.87	3.94	4.28	5.22	5.25	5.04	4.97	3.73
Ilm	4.80	4.93	5.56	6.70	6.63	6.46	6.40	6.58
Ap	1.47	1.02	1.52	1.14	0.87	1.24	1.25	1.25
H_2O	1.49	2.22	2.52	1.51	1.01	1.30	0.92	0.51
Rest	-	-	-	-	-	-	-	-

	A162	A163	A167	A168	A169	A170	A171	A172
SiO_2	46.76	44.92	46.93	47.31	47.31	46.85	46.85	46.88
TiO_2	2.37	2.13	2.57	2.66	2.66	2.19	2.54	2.59
Al_2O_3	12.34	10.43	12.99	13.55	13.03	12.03	12.75	13.73
Fe_2O_3	10.24	2.62	4.97	1.55	4.25	4.55	2.18	8.50
FeO	3.31	9.67	7.42	10.45	7.83	7.82	9.54	3.73
MnO	0.20	0.17	0.14	0.15	0.16	0.17	0.16	0.16
MgO	8.99	14.99	9.24	9.73	9.60	12.45	10.47	7.70
CaO	10.48	9.41	9.60	9.87	9.61	9.85	10.01	9.72
Na_2O	2.30	2.21	2.70	2.92	2.82	2.31	2.59	2.77
K_2O	0.82	0.76	0.96	1.02	1.01	0.78	0.95	1.15
H_2O	2.15	0.55	1.43	0.33	0.88	0.66	1.47	1.80
P_2O_5	0.51	0.36	0.43	0.42	0.46	0.39	0.40	0.42
Total	100.47	98.22	99.38	99.96	99.62	100.05	99.91	99.15
Ni	557	726	389	352	390	594	415	328
Cr	749	923	438	349	408	742	426	305
V	269	246	285	263	284	265	261	310
Zr	169	151	178	179	184	154	172	199
Y	43	27	39	32	30	31	36	35
Ba	307	256	277	268	301	255	278	299
Sr	378	366	406	418	397	365	394	421
Rb	23	29	30	31	34	24	30	32
K/Rb	296	218	266	274	246	270	264	298
D.I.	24.87	22.76	29.16	29.64	30.23	24.33	27.96	31.27
O.R.	0.76	0.21	0.40	0.13	0.35	0.37	0.19	0.69
Qz	-	-	-	-	-	-	-	-
Ne	-	1.16	-	1.42	-	-	-	-
Hy	11.07	-	6.18	-	3.99	5.55	0.79	4.61
Di	22.98	23.00	20.06	20.69	20.20	21.13	21.89	19.96
Ol	8.78	28.66	12.86	20.42	14.55	18.87	19.62	11.04
Or	4.96	4.60	5.80	6.05	6.05	4.64	5.70	7.03
Ab	19.91	17.00	23.36	22.17	24.18	19.69	22.26	24.24
An	21.41	16.68	20.95	20.92	20.18	20.30	20.68	22.37
Mt	5.04	3.89	4.77	2.26	4.63	4.70	3.21	4.63
Ilm	4.61	4.14	4.99	5.07	5.12	4.19	4.90	5.09
Ap	1.24	0.87	1.04	1.00	1.10	0.93	0.96	1.03
H_2O	2.15	0.55	1.43	0.33	0.88	0.66	1.47	1.80
Rest	-	-	-	-	-	-	-	-

	A173	A175	A179	A181	A182	A183	A185	A187
SiO_2	45.87	48.43	45.97	46.07	46.82	46.13	61.92	45.50
TiO_2	2.78	2.66	2.54	2.78	2.52	2.61	0.15	3.10
Al_2O_3	13.36	14.59	12.63	13.73	12.27	12.09	19.14	14.24
Fe_2O_3	7.44	4.14	3.54	3.44	3.95	4.14	2.72	4.09
FeO	4.48	7.18	8.39	8.36	8.01	7.84	1.74	8.12
MnO	0.15	0.15	0.16	0.17	0.17	0.16	0.22	0.16
MgO	8.47	6.20	10.77	9.03	11.06	11.68	0	8.28
CaO	10.64	11.82	10.49	9.56	10.13	10.49	0.68	9.19
Na_2O	2.52	2.99	2.41	3.14	2.41	2.61	7.91	2.72
K_2O	1.12	0.85	1.02	0.93	0.95	0.95	5.53	1.39
H_2O	2.22	1.39	1.41	1.28	1.06	0.86	0.92	1.76
P_2O_5	0.51	0.30	0.40	0.50	0.52	0.51	0.01	0.58
Total	99.56	100.70	99.73	98.99	99.87	100.07	100.94	99.13
Ni	362	94	372	303	508	481	0	235
Cr	351	120	520	325	627	604	18	194
V	310	304	316	233	293	305	4	309
Zr	197	177	167	210	164	164	1798	241
Y	30	41	33	39	31	32	108	45
Ba	334	241	281	313	267	288	30	366
Sr	520	397	440	517	397	396	2	579
Rb	29	21	35	47	31	25	214	54
K/Rb	320	336	242	164	254	316	214	214
D.I.	28.82	30.39	26.46	31.71	26.33	26.60	92.20	32.09
O.R.	0.62	0.37	0.30	0.29	0.33	0.35	0.61	0.33
Qz	-	-	-	-	-	-	-	-
Ne	-	-	0.49	1.31	-	1.58	8.90	-
Hy	0.87	0.44	-	-	5.05	-	-	0.63
Di	22.95	26.76	23.51	19.40	21.93	24.43	2.61	15.97
Ol	13.62	8.20	18.55	16.58	15.89	19.55	2.84	15.94
Or	6.83	5.03	6.13	5.62	5.68	5.66	32.72	8.44
Ab	21.99	25.36	19.84	24.77	20.65	19.35	50.59	23.65
An	22.52	23.93	20.99	21.11	20.10	18.63	0.39	23.16
Mt	4.53	4.50	4.62	4.60	4.59	4.58	1.65	4.75
Ilm	5.44	5.06	4.91	5.40	4.85	5.00	0.29	6.05
Ap	1.25	0.71	0.96	1.21	1.25	1.22	0.02	1.41
H_2O	2.22	1.39	1.41	1.28	1.06	0.86	0.92	1.76
Rest	-	-	-	-	-	-	-	-

	A190	A193	A194	A195	A196	A197	A198	A200
SiO_2	46.59	45.84	49.20	49.67	50.35	46.33	53.24	50.56
TiO_2	3.97	3.66	2.97	2.99	2.87	3.86	1.85	3.06
Al_2O_3	16.32	17.16	16.15	16.25	16.55	15.56	17.36	15.10
Fe_2O_3	7.29	5.30	3.89	3.50	6.57	8.92	7.78	6.09
FeO	5.03	7.39	7.56	7.95	4.75	4.09	1.71	5.29
MnO	0.14	0.14	0.18	0.18	0.18	0.12	0.18	0.16
MgO	4.80	4.66	4.26	4.77	3.61	3.75	1.92	4.42
CaO	10.94	11.80	8.24	8.11	8.34	10.73	6.12	7.79
Na_2O	2.94	2.60	4.12	4.12	4.10	3.03	5.63	4.42
K_2O	0.96	0.92	1.43	1.44	1.47	1.25	2.12	0.97
H_2O	1.58	0.88	0.99	0.70	0.57	1.51	0.62	1.93
P_2O_5	0.38	0.40	0.57	0.57	0.76	0.43	0.85	0.42
Total	100.94	100.75	99.56	100.25	100.12	99.58	99.38	100.21
Ni	0	20	0	0	0	1	0	79
Cr	0	5	23	13	13	3	18	34
V	373	441	179	193	187	338	81	371
Zr	153	140	232	230	231	173	319	221
Y	40	42	48	46	43	49	63	51
Ba	206	184	328	352	348	300	542	440
Sr	460	437	599	616	625	490	908	383
Rb	29	42	49	46	46	32	60	25
K/Rb	274	182	242	260	266	324	292	322
D.I.	30.86	27.52	43.96	43.58	43.71	33.84	60.68	44.01
O.R.	0.59	0.42	0.34	0.31	0.58	0.69	0.82	0.54
Qz	-	-	-	-	-	-	-	-
Ne	-	-	-	-	-	-	0.61	-
Hy	2.70	0.68	1.30	2.16	8.10	0.93	-	9.20
Di	19.16	19.29	13.17	12.26	11.63	21.31	7.67	14.53
Ol	5.38	7.28	8.40	8.88	2.46	4.68	6.43	2.12
Or	5.73	5.45	8.58	8.55	8.75	7.57	12.74	5.85
Ab	25.13	22.06	35.39	35.03	34.95	26.27	47.33	38.16
An	28.79	32.53	21.67	21.69	22.58	25.79	16.11	18.87
Mt	4.60	4.78	4.40	4.37	4.22	4.89	3.50	4.32
Ilm	7.62	6.97	5.73	5.71	5.49	7.51	3.57	5.93
Ap	0.91	0.95	1.37	1.36	1.81	1.04	2.05	1.01
H_2O	1.58	0.88	0.99	0.70	0.57	1.51	0.62	1.93
Rest	-	-	-	-	-	-	-	-

	A201	A203	A205	A211	A212	A214	A215	A218
SiO_2	47.23	46.97	49.22	46.49	47.62	47.21	45.86	46.43
TiO_2	3.05	3.05	2.46	2.74	3.53	2.71	2.93	2.73
Al_2O_3	14.94	15.42	18.28	13.85	15.72	13.62	13.76	13.66
Fe_2O_3	5.73	5.66	4.50	3.45	3.63	3.40	3.90	2.17
FeO	5.84	5.28	5.23	8.65	8.36	8.33	8.32	9.68
MnO	0.15	0.17	0.17	0.15	0.15	0.15	0.15	0.15
MgO	4.56	5.15	2.78	8.69	5.56	8.78	9.13	8.87
CaO	9.42	10.59	7.00	9.56	9.42	10.14	10.12	10.41
Na_2O	3.67	3.58	2.00	2.91	3.26	2.65	2.65	2.72
K_2O	1.51	0.62	5.15	1.03	1.27	1.07	0.94	0.96
H_2O	2.14	3.06	3.14	0.84	1.28	1.50	1.38	0.66
P_2O_5	0.50	0.46	0.65	0.38	0.43	0.36	0.34	0.39
Total	98.74	100.01	100.58	98.74	100.23	99.92	99.48	99.83
Ni	69	107	4	224	63	243	253	268
Cr	35	127	9	257	46	315	317	365
V	327	365	226	279	330	276	338	275
Zr	239	202	364	213	213	169	172	190
Y	43	39	53	53	53	36	38	47
Ba	383	165	626	284	284	223	238	240
Sr	437	535	575	436	436	404	380	391
Rb	42	22	165	35	35	32	24	26
K/Rb	298	234	258	244	302	278	324	306
D.I.	40.07	34.69	48.67	31.37	35.47	29.21	28.45	28.55
O.R.	0.49	0.52	0.46	0.29	0.30	0.29	0.32	0.18
Qz	-	-	-	-	-	-	-	-
Ne	1.67	0.50	-	-	-	-	0.09	0.79
Hy	-	-	6.01	0.32	3.53	4.26	-	-
Di	20.07	21.32	4.08	19.17	15.96	21.16	20.62	22.20
Ol	7.57	7.67	4.71	16.05	7.86	12.27	16.37	17.20
Or	9.26	3.79	31.28	6.22	7.59	6.42	5.66	5.78
Ab	29.14	30.40	17.39	25.15	27.89	22.79	22.69	21.98
An	20.58	24.99	26.41	22.15	24.78	22.46	23.33	22.64
Mt	4.48	4.21	3.74	4.71	4.60	4.54	4.73	3.20
Ilm	6.01	5.99	4.80	5.32	6.78	5.23	5.67	5.28
Ap	1.23	1.13	1.58	0.92	1.03	0.87	0.82	0.94
H_2O	2.14	3.06	3.14	0.84	1.28	1.50	1.38	0.66
Rest	-	-	-	-	-	-	-	-

	A219	A220	A221	A222	A223	A224	A225	A226
SiO_2	47.12	46,85	47.26	45.97	45.64	46.83	45.96	46.54
TiO_2	2.51	2.81	3.10	2.93	3.65	2.83	2.81	3.08
Al_2O_3	12.53	14.05	15.81	12.81	16.05	12.83	12.55	15.21
Fe_2O_3	2.15	3.71	3.46	3.63	5.79	3.15	3.38	4.25
FeO	9.40	8.37	8.46	8.39	7.65	9.12	9.29	7.39
MnO	0.15	0.15	0.14	0.16	0.16	0.16	0.16	0.15
MgO	11.01	8.04	6.25	10.24	5.12	10.58	10.82	5.78
CaO	11.45	10.25	9.39	10.05	9.55	10.11	10.00	11.08
Na_2O	2.42	2.83	3.06	2.72	2.97	2.63	2.76	2.59
K_2O	0.84	1.04	1.43	0.93	1.26	0.89	0.93	1.31
H_2O	0.55	1.12	1.42	0.48	1.94	0.97	1.14	2.78
P_2O_5	0.35	0.38	0.53	0.36	0.50	0.34	0.36	0.47
Total	100.48	99.60	100.31	98.67	100.28	100.44	100.16	100.63
Ni	355	213	144	409	0	424	345	89
Cr	579	345	117	434	5	458	437	73
V	260	309	309	304	352	335	303	318
Zr	154	178	206	148	249	161	184	236
Y	33	45	55	34	41	36	41	45
Ba	213	260	501	216	346	204	243	378
Sr	356	440	585	336	548	325	415	547
Rb	20	25	35	25	38	19	26	40
K/Rb	348	346	340	308	276	388	298	272
D.I.	24.52	30.57	34.73	28.38	33.19	27.65	27.74	30.33
O.R.	0.19	0.31	0.29	0.30	0.43	0.26	0.27	0.36
Qz	-	-	-	-	-	-	-	-
Ne	1.11	-	-	0.79	-	-	1.65	-
Hy	-	0.72	2.49	-	1.63	0.95	-	2.41
Di	27.16	21.18	14.74	22.49	14.49	22.09	22.84	21.53
Ol	18.75	13.62	10.77	17.57	10.04	17.82	19.01	7.51
Or	4.97	6.24	8.55	5.60	7.59	5.29	5.55	7.92
Ab	18.45	24.32	26.18	21.99	25.60	22.37	20.54	22.42
An	20.86	22.92	25.46	20.37	27.24	20.68	19.29	26.60
Mt	3.12	4.67	4.59	4.65	5.14	4.59	4.87	4.49
Ilm	4.77	5.42	5.95	5.67	7.06	5.40	5.39	5.98
Ap	0.83	0.91	1.27	0.87	1.21	0.81	0.86	1.14
H_2O	0.55	1.12	1.42	0.48	1.94	0.97	1.14	2.78
Rest	-	-	-	-	-	-	-	-

	A228	A231	A232	A235	A238	A240	A242	A243
SiO_2	45.85	47.03	46.98	48.28	47.14	44.35	47.02	47.63
TiO_2	2.04	3.45	2.93	3.49	3.46	3.71	3.01	3.08
Al_2O_3	10.06	13.95	14.42	15.25	15.50	16.37	14.81	14.51
Fe_2O_3	2.83	8.03	3.93	5.10	4.40	4.96	4.71	4.69
FeO	8.85	5.07	7.77	6.32	7.61	8.84	7.01	7.26
MnO	0.15	0.19	0.16	0.18	0.16	0.14	0.15	0.15
MgO	15.63	4.34	6.75	3.81	5.13	5.51	6.24	5.90
CaO	11.12	8.38	10.54	8.02	9.84	10.42	11.20	10.64
Na_2O	1.68	3.97	2.40	3.89	3.09	2.79	2.72	3.07
K_2O	0.76	2.00	1.89	2.22	1.65	1.04	1.22	1.14
H_2O	1.03	2.23	2.93	2.61	2.09	1.12	1.99	1.34
P_2O_5	0.28	0.64	0.42	0.58	0.60	0.39	0.48	0.45
Total	100.28	99.28	101.12	99.75	100.67	99.64	100.56	99.86
Ni	698	49	140	3	24	28	106	85
Cr	764	12	113	13	23	22	54	51
V	231	365	325	340	305	354	337	331
Zr	120	200	190	290	341	192	195	199
Y	22	54	47	42	50	45	39	44
Ba	223	346	384	456	481	295	326	294
Sr	296	643	408	437	628	614	472	407
Rb	16	51	55	75	59	29	32	33
K/Rb	394	326	286	246	232	298	316	286
D.I.	18.71	44.21	32.07	46.53	36.45	28.99	30.70	33.24
O.R.	0.24	0.61	0.34	0.45	0.37	0.36	0.40	0.39
Qz	-	-	-	-	-	-	-	-
Ne	0.16	3.27	-	1.11	-	1.47	-	-
Hy	-	-	0.94	-	0.37	-	1.17	1.80
Di	28.69	19.62	21.93	15.57	17.67	16.69	22.95	22.65
Ol	26.10	7.98	10.43	7.09	8.88	11.38	8.75	7.89
Or	4.52	12.23	11.38	13.53	9.90	6.24	7.32	6.85
Ab	14.03	28.72	20.69	31.89	26.55	21.28	23.38	26.40
An	17.79	14.83	23.43	18.14	23.91	29.54	24.99	22.81
Mt	4.13	5.01	4.52	4.41	4.61	5.30	4.48	4.58
Ilm	3.90	6.78	5.67	6.83	6.67	7.16	5.81	5.94
Ap	0.67	1.57	1.01	1.42	1.44	0.94	1.15	1.08
H_2O	1.03	2.23	2.93	2.61	2.09	1.12	1.99	1.34
Rest	-	-	-	-	-	-	-	-

	A244	A246	A247	A249	A252	A253	A254	A255
SiO_2	46.94	47.04	46.65	62.15	46.72	46.13	46.31	46.91
TiO_2	2.65	2.41	3.17	0.13	2.64	2.67	2.44	2.76
Al_2O_3	12.93	11.76	14.91	18.17	13.86	13.92	12.46	14.63
Fe_2O_3	4.51	3.23	4.81	3.50	4.56	5.13	5.18	3.75
FeO	7.44	8.29	7.14	0.95	7.53	7.52	6.28	8.18
MnO	0.17	0.16	0.15	0.16	0.15	0.17	0.15	0.15
MgO	9.83	11.99	5.96	0.00	9.67	9.88	10.72	6.31
CaO	9.89	10.81	11.01	0.19	9.28	9.15	9.72	11.41
Na_2O	2.55	2.30	2.53	6.99	2.73	2.77	2.40	2.48
K_2O	1.19	1.04	1.36	5.09	1.05	1.05	1.01	0.97
H_2O	1.76	1.21	1.96	1.36	0.73	1.23	2.20	2.16
P_2O_5	0.49	0.39	0.54	0.00	0.37	0.37	0.36	0.36
Total	100.35	100.63	100.19	98.69	99.29	99.99	99.23	100.07
Ni	377	483	131	0	298	291	356	75
Cr	354	524	69	19	274	305	437	46
V	292	280	330	0	242	274	250	302
Zr	221	157	234	1582	153	216	174	204
Y	34	20	32	67	29	66	34	43
Ba	345	281	401	18	275	308	280	265
Sr	453	490	519	0	521	431	377	373
Rb	27	39	40	295	27	42	30	30
K/Rb	366	222	282	144	322	208	280	268
D.I.	29.05	25.76	30.01	91.88	29.77	30.05	27.13	27.30
O.R.	0.38	0.28	0.40	0.79	0.38	0.41	0.45	0.31
Qz	-	-	-	-	-	-	-	-
Ne	-	-	-	-	-	0.01	-	-
Hy	3.79	0.16	4.03	2.22	3.26	-	5.10	5.99
Di	20.85	26.07	21.36	-	17.29	16.77	21.21	23.54
Ol	14.81	19.26	6.78	2.18	16.24	19.56	15.56	5.83
Or	7.14	6.18	8.19	30.97	6.30	6.29	6.16	5.86
Ab	21.91	19.57	21.82	60.91	23.46	23.75	20.97	21.44
An	20.63	18.80	25.80	0.97	22.82	22.76	20.90	26.48
Mt	4.58	4.42	4.58	1.66	4.64	4.82	4.43	4.64
Ilm	5.11	4.60	6.14	0.25	5.09	5.14	4.78	5.36
Ap	1.18	0.93	1.30	-	0.89	0.89	0.88	0.87
H_2O	1.76	1.21	1.96	1.36	0.73	1.23	2.20	2.16
Rest	-	-	-	0.84	-	-	-	-

	A256	A257	A260	A261	A264	A267	A268	A269
SiO_2	46.56	48.22	61.67	61.09	60.87	50.49	49.49	48.98
TiO_2	2.48	2.66	0.20	0.36	0.30	2.41	2.97	3.11
Al_2O_3	11.67	13.73	17.96	18.45	18.46	17.08	17.19	17.33
Fe_2O_3	6.24	2.82	3.59	3.88	2.26	2.80	2.97	2.98
FeO	5.83	9.01	1.23	1.28	1.93	7.85	8.33	8.34
MnO	0.15	0.15	0.20	0.14	0.18	0.18	0.18	0.18
MgO	11.17	8.09	0.18	0.01	0.06	2.63	4.03	4.04
CaO	10.27	10.19	0.77	0.73	1.36	7.99	8.06	7.72
Na_2O	2.10	2.72	7.52	6.72	7.94	4.97	4.01	3.76
K_2O	0.98	1.14	5.26	4.60	5.12	1.85	2.10	2.15
H_2O	2.15	0.79	1.00	1.19	1.01	0.66	0.54	1.26
P_2O_5	0.34	0.39	0.00	0.05	0.06	1.04	0.71	0.66
Total	99.94	99.91	99.58	98.45	99.55	99.67	100.31	100.18
Ni	439	219	0	0	0	20	25	23
Cr	623	307	20	24	22	0	0	0
V	301	260	2	11	4	105	245	250
Zr	131	196	1476	908	1175	285	325	327
Y	184	58	290	112	29	78	51	59
Ba	446	302	15	1095	582	640	535	595
Sr	572	378	7	181	127	995	640	585
Rb	30	36	231	142	286	53	73	68
K/Rb	272	262	190	148	149	284	238	261
D.I.	24.16	30.01	90.99	87.15	89.99	51.27	45.65	44.85
O.R.	0.52	0.24	0.74	0.75	0.54	0.26	0.26	0.26
Qz	-	-	-	0.58	-	-	-	-
Ne	-	-	5.62	-	9.81	2.45	0.78	-
Hy	8.02	6.56	-	5.44	-	-	-	1.63
Di	24.02	21.33	3.42	-	5.74	11.78	10.39	8.22
Ol	13.52	9.87	3.18	-	2.31	6.82	9.65	9.20
Or	5.94	6.79	31.60	28.00	30.75	11.01	12.40	12.80
Ab	18.22	23.21	53.76	58.57	49.43	37.82	32.47	32.05
An	20.02	22.08	-	3.39	-	18.96	22.69	24.23
Mt	4.61	4.12	1.54	1.94	0.58	4.09	4.30	4.35
Ilm	4.83	5.10	0.39	0.70	0.58	4.61	5.64	5.95
Ap	0.83	0.93	-	0.12	0.14	2.48	1.68	1.57
H_2O	2.15	0.79	1.00	1.19	1.01	0.66	0.54	1.26
Rest	-	-	0.48	1.24	0.66	-	-	-

B. INTERMEDIATE SERIES

N.B.

Norms are calculated on a standardised

O.R. = 0.15 (Fe_2O_3/FeO + Fe_2O_3 = 1:6.48)

for analyses with O.R. > 0.15.

	B1	B2	B3	B4	B5	B6	B7	B9
SiO_2	45.80	45.00	45.42	45.07	44.13	44.93	44.12	45.60
TiO_2	1.65	1.65	1.73	1.58	2.34	2.11	2.12	1.89
Al_2O_3	14.21	13.95	13.80	13.80	13.02	12.31	12.39	15.39
Fe_2O_3	2.77	3.02	2.24	4.34	2.24	1.91	2.88	1.70
FeO	10.71	10.58	10.45	9.52	8.97	9.29	8.78	10.14
MnO	0.21	0.23	0.18	0.16	0.16	0.16	0.17	0.18
MgO	10.41	10.82	10.65	10.79	10.64	13.14	12.81	8.89
CaO	9.99	9.58	9.99	9.45	12.08	11.43	11.49	11.32
Na_2O	2.85	2.49	2.76	2.47	3.09	2.67	2.17	2.68
K_2O	0.34	0.31	0.35	0.30	1.15	0.78	0.90	0.28
H_2O	1.58	2.22	1.06	1.72	0.64	1.12	1.58	0.90
P_2O_5	0.24	0.23	0.21	0.18	0.43	0.41	0.39	0.20
Total	100.76	100.08	98.84	99.38	99.89	100.26	99.80	99.17
Ni	425	440	379	473	335	474	459	250
Cr	361	342	347	355	360	469	466	304
V	229	207	237	196	253	242	237	244
Zr	104	100	108	94	152	138	126	92
Y	31	34	31	87	39	38	37	36
Ba	171	170	190	206	491	431	432	144
Sr	281	285	305	305	545	454	479	307
Rb	9	11	10	9	42	21	30	6
K/Rb	314	234	290	276	228	308	250	388
D.I.	24.43	23.10	24.29	23.26	23.91	21.52	19.61	22.91
O.R.	0.21	0.22	0.18	0.31	0.20	0.17	0.25	0.14
Qz	-	-	-	-	-	-	-	-
Ne	2.27	0.38	2.03	-	11.38	6.99	5.36	2.18
Hy	-	-	-	0.10	-	-	-	-
Di	18.94	16.71	19.93	16.75	31.97	28.17	27.15	21.33
Ol	24.67	26.77	24.23	26.88	17.43	23.29	23.75	19.28
Or	2.03	1.87	2.12	1.82	6.92	4.65	5.42	1.68
Ab	20.13	20.85	20.15	21.44	5.61	9.88	8.83	19.05
An	25.19	26.56	24.79	26.35	18.59	19.47	21.83	29.64
Mt	3.03	3.10	2.89	3.14	2.54	2.53	2.62	2.70
Ilm	3.16	3.20	3.36	3.08	4.52	4.04	4.11	3.65
Ap	0.57	0.56	0.51	0.44	1.04	0.98	0.94	0.48
H_2O	1.58	2.22	1.06	1.72	0.64	1.12	1.58	0.90
Rest	-	-	-	-	-	-	-	-

	B10	B14	B15	B18	B19	B20	B21	B22
SiO_2	46.24	45.35	45.67	46.28	45.58	44.74	45.32	44.06
TiO_2	1.77	1.85	2.12	1.77	1.91	1.85	1.86	1.86
Al_2O_3	14.31	13.92	13.91	14.10	13.74	13.27	13.48	13.26
Fe_2O_3	8.52	2.95	2.46	1.74	1.86	3.68	2.62	2.17
FeO	4.84	8.76	9.69	10.35	10.88	10.53	10.58	10.74
MnO	0.15	0.16	0.16	0.16	0.19	0.22	0.19	0.27
MgO	9.58	10.59	9.76	10.39	10.69	10.10	10.90	10.61
CaO	10.04	10.36	10.68	10.58	10.42	10.15	10.40	10.21
Na_2O	2.85	2.29	2.49	2.58	2.96	2.18	2.40	2.41
K_2O	0.36	0.58	0.50	0.40	0.63	0.51	0.54	0.53
H_2O	1.25	3.28	1.52	0.57	0.62	2.18	1.43	1.50
P_2O_5	0.20	0.20	0.24	0.24	0.28	0.28	0.25	0.24
Total	100.10	100.29	99.20	99.16	99.76	99.69	99.97	97.86
Ni	483	330	296	277	361	330	416	333
Cr	385	364	313	402	378	384	395	362
V	264	200	253	200	241	232	235	231
Zr	94	89	116	79	115	99	105	101
Y	32	29	38	30	39	32	33	38
Ba	160	199	211	207	238	249	235	236
Sr	253	502	320	276	346	311	318	332
Rb	11	38	19	11	22	10	12	13
K/Rb	272	126	218	302	238	424	374	338
D.I.	25.85	23.26	24.00	23.92	24.89	22.04	22.53	22.38
O.R.	0.64	0.25	0.20	0.14	0.15	0.26	0.20	0.17
Qz	-	-	-	-	-	-	-	-
Ne	1.00	0.31	0.71	0.73	4.87	-	1.56	2.41
Hy	-	-	-	-	-	0.78	-	-
Di	19.35	20.16	21.74	20.77	22.56	19.82	21.10	21.36
Ol	22.36	22.97	20.86	22.51	22.80	24.26	24.41	24.32
Or	2.16	3.54	3.03	2.40	3.75	3.09	3.24	3.25
Ab	22.68	19.41	20.27	20.80	16.28	18.94	17.73	16.72
An	25.63	26.81	25.91	26.07	22.53	25.58	24.78	24.70
Mt	2.91	2.68	2.78	2.75	2.88	3.23	2.99	2.99
Ilm	3.42	3.62	4.12	3.41	3.66	3.61	3.59	3.67
Ap	0.48	0.49	0.58	0.58	0.67	0.68	0.60	0.59
H_2O	1.25	3.28	1.52	0.57	0.62	2.18	1.43	1.50
Rest	-	-	-	-	-	-	-	-

	B23	B24	B25	B26	B27	B28	B29	B31
SiO_2	45.49	45.81	46.49	45.46	45.27	46.60	43.56	47.17
TiO_2	2.15	2.10	2.08	1.81	1.71	2.01	2.37	2.15
Al_2O_3	12.87	12.79	12.23	13.24	13.47	12.59	12.22	12.76
Fe_2O_3	2.94	1.83	2.76	2.24	2.81	8.29	6.60	3.34
FeO	8.38	8.13	8.97	10.34	9.56	3.59	5.64	8.31
MnO	0.16	0.16	0.16	0.17	0.17	0.18	0.19	0.16
MgO	11.60	12.09	11.65	11.61	11.99	10.87	12.46	11.57
CaO	10.99	10.99	10.37	10.22	10.26	10.60	11.49	10.68
Na_2O	2.69	2.35	2.59	2.97	2.26	2.58	3.18	2.72
K_2O	0.84	0.84	0.64	0.56	0.42	0.67	0.90	0.72
H_2O	0.68	1.69	0.44	0.68	2.02	1.39	1.28	0.37
P_2O_5	0.33	0.31	0.29	0.23	0.26	0.34	0.46	0.31
Total	99.12	99.09	98.67	99.53	100.20	99.71	100.35	100.26
Ni	407	390	497	414	427	495	448	471
Cr	444	442	456	363	385	449	425	478
V	236	250	240	239	237	197	280	233
Zr	123	119	123	103	95	119	164	126
Y	36	36	51	32	31	38	42	34
Ba	369	360	306	218	196	329	517	302
Sr	404	443	391	324	380	413	545	396
Rb	26	27	16	18	10	22	32	19
K/Rb	268	258	232	258	348	252	234	314
D.I.	24.02	23.39	25.19	24.43	21.50	25.75	22.58	25.59
O.R.	0.26	0.18	0.24	0.18	0.23	0.70	0.54	0.28
Qz	-	-	-	-	-	-	-	-
Ne	4.93	2.45	1.17	5.14	0.62	0.75	11.93	2.06
Hy	-	-	-	-	-	-	-	-
Di	26.09	25.22	24.44	23.02	19.67	24.47	30.72	24.67
Ol	21.48	21.82	22.76	24.29	26.23	21.20	21.73	21.80
Or	5.05	5.09	3.85	3.35	2.53	4.05	5.39	4.26
Ab	14.05	15.86	20.17	15.94	18.35	20.95	5.26	19.26
An	20.91	22.41	20.22	21.39	25.86	21.27	16.63	20.53
Mt	2.55	2.32	2.66	2.85	2.81	2.58	2.67	2.59
Ilm	4.15	4.09	4.02	3.48	3.31	3.91	4.57	4.09
Ap	0.79	0.75	0.70	0.55	0.63	0.82	1.10	0.74
H_2O	0.68	1.69	0.44	0.68	2.02	1.39	1.28	0.37
Rest	-	-	-	-	-	-	-	-

	B33	B34	B37	B38	B39	B40	B41	B42
SiO_2	43.54	42.80	47.01	44.91	46.43	44.10	45.84	44.30
TiO_2	2.36	2.71	1.96	1.61	1.76	2.15	2.43	2.57
Al_2O_3	12.29	12.12	12.52	13.95	14.10	13.97	12.17	11.92
Fe_2O_3	6.54	3.80	7.22	3.80	10.50	3.74	1.42	3.37
FeO	5.74	8.82	4.71	8.27	2.87	9.04	10.38	8.71
MnO	0.18	0.18	0.16	0.18	0.18	0.17	0.17	0.17
MgO	13.12	12.58	10.41	11.25	9.92	10.79	12.90	12.95
CaO	11.30	11.09	10.05	11.13	10.35	10.75	10.19	10.54
Na_2O	3.26	2.60	2.58	2.20	2.57	2.67	2.54	2.52
K_2O	0.76	1.33	0.62	0.33	0.45	0.60	1.01	0.64
H_2O	0.88	1.61	2.20	2.16	1.39	1.43	0.59	1.75
P_2O_5	0.43	0.51	0.32	0.21	0.19	0.32	0.41	0.43
Total	100.41	100.15	99.76	100.00	100.71	99.73	100.05	99.87
Ni	448	427	490	441	455	329	542	506
Cr	431	367	436	386	425	307	440	438
V	283	296	216	225	217	261	287	330
Zr	171	198	116	92	97	130	86	101
Y	36	35	35	35	47	38	26	22
Ba	524	571	298	186	221	239	465	485
Sr	520	595	368	335	271	464	394	462
Rb	13	46	17	4	11	14	40	32
K/Rb	486	240	302	686	340	356	210	166
D.I.	22.08	21.69	26.26	19.78	24.63	22.20	24.62	21.99
O.R.	0.53	0.30	0.60	0.31	0.79	0.29	0.12	0.28
Qz	-	-	-	-	-	-	-	-
Ne	12.16	10.23	-	1.51	0.16	5.24	3.51	4.29
Hy	-	-	4.17	-	-	-	-	-
Di	29.73	28.05	22.55	22.10	20.26	22.23	23.51	24.78
Ol	23.16	23.22	18.40	23.90	22.43	22.94	24.68	24.78
Or	4.53	7.99	3.77	2.00	2.70	3.61	6.00	3.86
Ab	5.39	3.47	22.49	16.27	21.77	13.34	15.12	13.84
An	16.80	17.76	21.37	27.86	25.98	24.82	18.91	19.72
Mt	2.68	2.83	2.63	2.72	2.85	2.88	2.67	2.72
Ilm	4.52	5.23	3.83	3.13	3.39	4.16	4.64	4.98
Ap	1.03	1.23	0.78	0.51	0.46	0.77	0.98	1.04
H_2O	0.88	1.61	2.20	2.16	1.39	1.43	0.59	1.75
Rest	-	-	-	-	-	-	-	-

	B43
SiO_2	45.21
TiO_2	2.48
Al_2O_3	11.85
Fe_2O_3	3.58
FeO	8,24
MnO	0.17
MgO	12.85
CaO	10.33
Na_2O	1.99
K_2O	0.91
H_2O	1.74
P_2O_5	0.39
Total	99.74

Ni	519
Cr	419
V	288
Zr	86
Y	31
Ba	512
Sr	435
Rb	29
K/Rb	260
D.I.	22.34
O.R.	0.30

Qz	-
Ne	0.43
Hy	-
Di	23.02
Ol	25.05
Or	5.50
Ab	16.41
An	21.17
Mt	2.67
Ilm	4.81
Ap	0.94
H_2O	1.74
Rest	-

C. YOUNGER SERIES

N.B.

Norms are calculated on a standardised

O.R. = 0.15 ($Fe_2O_3/FeO + Fe_2O_3$ = 1:6.48)

for analyses with O.R. > 0.15.

	C2	C4	C11	C18	C20	C23	C25	C29
SiO_2	46.27	45.93	46.16	46.23	46.19	46.56	46.58	46.48
TiO_2	2.33	2.06	1.99	1.69	1.73	1.54	1.57	1.83
Al_2O_3	15.99	15.64	15.38	13.76	15.02	15.16	15.12	15.70
Fe_2O_3	2.43	2.52	2.32	1.51	1.42	4.18	3.07	1.39
FeO	10.44	9.73	10.11	11.09	10.49	7.45	8.61	10.13
MnO	0.16	0.15	0.17	0.18	0.17	0.18	0.17	0.16
MgO	6.31	8.24	8.44	11.34	9.62	8.91	9.92	8.35
CaO	10.75	10.44	11.20	9.96	11.31	10.84	10.79	11.62
Na_2O	3.12	3.38	2.59	2.87	2.88	2.78	2.88	2.87
K_2O	0.46	0.58	0.30	0.35	0.29	0.51	0.50	0.33
H_2O	0.81	0.26	1.32	0.53	0.26	0.81	0.46	0.46
P_2O_5	0.21	0.27	0.19	0.21	0.16	0.24	0.27	0.21
Total	99.28	99.20	100.17	99.72	99.54	99.16	99.94	99.53
Ni	108	163	201	383	258	333	310	149
Cr	102	109	268	328	329	366	359	237
V	266	190	268	226	256	196	213	261
Zr	125	124	92	100	75	121	123	86
Y	44	41	39	36	34	34	33	34
Ba	163	195	114	176	106	300	312	137
Sr	341	391	284	301	326	396	401	326
Rb	13	17	5	10	12	15	12	4
K/Rb	294	284	498	290	200	282	346	686
D.I.	27.97	28.01	23.50	24.63	23.32	25.74	25.10	24.26
O.R.	0.19	0.21	0.19	0.12	0.12	0.36	0.26	0.12
Qz	-	-	-	-	-	-	-	-
Ne	1.90	5.18	0.56	2.28	3.47	1.53	2.84	2.61
Hy	-	-	-	-	-	-	-	-
Di	19.87	20.04	20.58	19.97	22.84	20.63	20.38	22.48
Ol	15.53	18.52	19.04	25.01	20.08	19.58	21.26	17.41
Or	2.76	3.47	1.79	2.08	1.73	3.07	2.97	1.97
Ab	23.31	19.37	21.14	20.26	18.12	21.14	19.29	19.68
An	28.71	26.08	29.80	23.81	27.38	27.90	27.02	29.24
Mt	2.92	2.76	2.80	2.85	2.69	2.60	2.60	2.60
Ilm	4.49	3.96	3.82	3.23	3.31	2.98	3.00	3.51
Ap	0.51	0.65	0.46	0.50	0.38	0.58	0.64	0.50
H_2O	0.81	0.26	1.32	0.53	0.26	0.81	0.46	0.46
Rest	-	-	-	-	-	-	-	-

	C32	C33	C38	C40	C41	C46	C47	C50
SiO_2	46.03	44.76	45.11	44.76	45.95	44.77	46.26	45.23
TiO_2	1.96	1.62	1.87	1.94	1.47	2.15	2.09	1.93
Al_2O_3	15.36	14.82	14.00	14.23	15.12	15.05	15.55	14.53
Fe_2O_3	2.17	4.50	2.15	1.55	3.56	2.47	1.50	2.42
FeO	9.95	8.60	10.42	10.85	9.12	9.28	10.37	9.98
MnO	0.17	0.21	0.18	0.16	0.18	0.16	0.16	0.17
MgO	7.75	10.22	10.73	10.60	10.04	9.15	7.87	10.18
CaO	11.61	9.65	10.45	10.67	9.89	12.25	11.12	10.86
Na_2O	2.98	2.33	3.11	3.10	2.58	2.97	3.28	2.69
K_2O	0.38	0.21	0.52	0.59	0.18	0.59	0.44	0.43
H_2O	0.77	3.20	0.51	0.55	1.19	0.68	0.68	0.55
P_2O_5	0.27	0.16	0.26	0.28	0.15	0.30	0.24	0.22
Total	99.40	100.28	99.31	99.28	99.43	99.82	99.56	99.19
Ni	142	283	375	326	369	202	137	320
Cr	193	354	319	264	332	257	163	345
V	281	231	250	259	236	294	232	250
Zr	100	64	108	112	65	110	107	99
Y	39	27	27	36	37	30	43	39
Ba	156	135	205	257	83	288	165	200
Sr	299	236	364	387	193	457	381	333
Rb	7	11	21	21	4	17	12	10
K/Rb	450	158	206	234	374	288	304	358
D.I.	24.96	21.64	24.58	24.15	23.34	22.32	26.92	22.78
O.R.	0.18	0.34	0.17	0.12	0.28	0.21	0.13	0.20
Qz	-	-	-	-	-	-	-	-
Ne	3.41	-	6.11	7.02	-	7.75	4.45	3.40
Hy	-	3.01	-	-	1.71	-	-	-
Di	23.61	14.70	22.57	22.97	15.74	26.94	22.48	21.55
Ol	16.46	23.80	22.81	22.21	23.45	17.04	16.62	21.94
Or	2.28	1.28	3.11	3.53	1.08	3.52	2.63	2.58
Ab	19.28	20.35	15.36	13.60	22.25	11.05	19.84	16.81
An	27.79	30.31	22.98	23.45	29.71	26.23	26.69	26.67
Mt	2.75	2.98	2.85	2.82	2.85	2.63	2.70	2.81
Ilm	3.77	3.18	3.59	3.73	2.85	4.12	4.01	3.72
Ap	0.65	0.39	0.62	0.67	0.36	0.72	0.57	0.53
H_2O	0.77	3.20	0.51	0.55	1.19	0.68	0.68	0.55
Rest	-	-	-	-	-	-	-	-

	C52	C54	C55	C56	C58	C59	C60	C62
SiO_2	45.18	45.84	45.95	44.80	45.39	45.98	46.26	44.80
TiO_2	1.94	1.79	1.65	1.87	1.90	1.91	1.99	1.66
Al_2O_3	14.55	14.27	14.67	13.54	14.81	14.04	16.08	15.25
Fe_2O_3	3.03	5.88	3.76	4.60	5.79	1.52	1.81	3.17
FeO	9.36	7.03	8.66	8.47	7.18	10.77	10.65	9.07
MnO	0.17	0.17	0.17	0.18	0.15	0.17	0.17	0.16
MgO	10.44	9.39	10.02	11.52	9.65	10.59	7.90	8.92
CaO	11.07	10.79	10.61	10.27	10.46	10.90	10.48	11.51
Na_2O	2.30	2.87	2.59	2.35	2.34	2.96	3.10	2.68
K_2O	0.16	0.26	0.25	0.33	0.43	0.38	0.40	0.35
H_2O	1.43	0.70	0.75	1.45	2.36	0.22	0.81	0.77
P_2O_5	0.16	0.18	0.17	0.21	0.26	0.21	0.20	0.17
Total	99.79	99.17	99.25	99.59	100.72	99.65	99.85	98.51
Ni	355	325	361	462	341	343	175	211
Cr	346	318	349	438	326	210	50	159
V	242	240	238	256	221	263	261	205
Zr	95	77	72	88	91	87	97	74
Y	32	37	37	29	35	32	40	34
Ba	189	130	185	190	192	161	150	164
Sr	362	256	261	356	377	344	327	391
Rb	5	6	3	7	12	12	7	8
K/Rb	266	360	691	392	298	262	474	364
D.I.	20.26	24.27	23.13	21.22	22.79	23.82	26.75	21.89
O.R.	0.24	0.45	0.30	0.35	0.44	0.12	0.15	0.26
Qz	-	-	-	-	-	-	-	-
Ne	0.60	2.42	0.78	1.28	-	4.27	2.50	4.09
Hy	-	-	-	-	0.54	-	-	-
Di	20.64	22.51	19.75	20.02	17.93	23.52	18.13	22.95
Ol	22.75	20.69	22.60	25.73	22.33	21.73	18.97	19.50
Or	0.96	1.57	1.50	1.99	2.59	2.26	2.39	2.12
Ab	18.71	20.28	20.85	17.94	20.20	17.29	21.87	15.68
An	29.41	25.77	28.13	25.96	29.21	24.02	29.05	29.24
Mt	2.80	2.87	2.79	2.93	2.88	2.77	2.81	2.78
Ilm	3.75	3.46	3.19	3.63	3.68	3.65	3.82	3.23
Ap	0.39	0.43	0.41	0.51	0.63	0.50	0.48	0.41
H_2O	1.43	0.70	0.75	1.45	2.36	0.22	0.81	0.77
Rest	-	-	-	-	-	-	-	-

	C66	C68	C69	C71	C74	C76	C77	C78
SiO_2	46.02	46.51	45.67	47.03	46.36	45.47	46.01	45.89
TiO_2	1.50	1.86	1.94	1.67	1.56	1.73	1.54	2.00
Al_2O_3	14.29	15.67	15.35	15.43	14.58	15.24	14.90	16.01
Fe_2O_3	1.93	2.41	1.82	0.72	2.14	2.06	3.26	2.88
FeO	10.54	9.18	10.41	10.43	9.81	9.71	9.03	9.16
MnO	0.19	0.15	0.17	0.16	0.18	0.17	0.17	0.15
MgO	11.49	8.04	8.61	8.80	9.75	9.72	9.88	7.23
CaO	10.43	11.28	11.35	11.36	10.86	11.43	10.84	11.62
Na_2O	2.57	3.09	2.48	2.87	2.67	2.70	2.59	3.10
K_2O	0.23	0.39	0.35	0.29	0.28	0.34	0.22	0.44
H_2O	0.57	0.29	1.17	0.24	0.52	0.46	0.73	1.03
P_2O_5	0.20	0.26	0.26	0.21	0.21	0.22	0.17	0.25
Total	99.96	99.13	99.58	99.21	98.92	99.35	99.34	99.76
Ni	412	182	181	210	346	284	362	156
Cr	373	232	230	103	125	85	369	153
V	222	229	239	218	239	231	238	254
Zr	64	93	95	68	72	70	67	93
Y	43	42	35	31	28	29	32	33
Ba	108	146	196	116	123	144	108	183
Sr	311	351	321	289	246	326	257	373
Rb	9	12	13	12	3	13	7	13
K/Rb	212	270	224	200	674	218	260	280
D.I.	22.07	26.14	22.68	24.93	23.84	22.13	22.73	25.55
O.R.	0.15	0.21	0.15	0.06	0.18	0.18	0.27	0.24
Qz	-	-	-	-	-	-	-	-
Ne	1.39	3.14	0.87	1.55	0.95	3.58	0.99	4.35
Hy	-	-	-	-	-	-	-	-
Di	19.32	21.94	20.66	21.89	21.13	22.07	20.08	22.91
Ol	25.53	17.04	19.32	18.31	21.38	20.48	22.22	15,53
Or	1.37	2.33	2.10	1.73	1.68	2.03	1.32	2.64
Ab	19.31	20.66	19.71	21.65	21.21	16.51	20.42	18.57
An	26.94	28.07	30.19	28.63	27.41	28.81	28.81	28.86
Mt	2.80	2.61	2.78	2.53	2.71	2.66	2.77	2.70
Ilm	2.87	3.58	3.74	3.20	3.01	3.33	2.97	3.85
Ap	0.48	0.62	0.63	0.50	0.51	0.53	0.41	0.60
H_2O	0.57	0.29	1.17	0.24	0.52	0.46	0.73	1.03
Rest	-	-	-	-	-	-	-	-

	C79	C82	C83	C86	C91	C92
SiO_2	45.62	45.60	46.97	45.88	46.47	46.09
TiO_2	1.44	1.77	1.87	1.59	2.10	1.71
Al_2O_3	14.33	14.20	15.85	14.80	15.84	14.21
Fe_2O_3	2.42	2.93	2.12	1.40	1.62	2.42
FeO	9.30	9.75	9.65	10.35	10.24	9.89
MnO	0.17	0.17	0.16	0.17	0.22	0.18
MgO	11.29	11.17	6.90	10.61	7.82	10.71
CaO	10.61	10.62	11.65	10.59	11.46	10.71
Na_2O	2.37	2.96	2.97	2.58	3.10	2.93
K_2O	0.34	0.44	0.36	0.22	0.44	0.45
H_2O	0.62	0.48	0.55	1.10	0.44	0.22
P_2O_5	0.19	0.30	0.22	0.16	0.22	0.30
Total	98.70	100.39	99.27	99.45	99.97	99.82
Ni	504	383	142	320	134	401
Cr	470	330	228	419	194	332
V	212	251	240	232	266	251
Zr	77	105	89	79	98	81
Y	29	33	39	33	33	37
Ba	176	192	185	136	165	162
Sr	314	338	355	254	323	319
Rb	9	16	8	6	12	16
K/Rb	314	228	374	304	304	234
D.I.	21.68	23.52	26.22	22.60	25.73	24.26
O.R.	0.21	0.23	0.18	0.12	0.14	0.20
Qz	-	-	-	-	-	-
Ne	0.98	4.93	1.65	1.07	3.81	3.90
Hy	-	-	-	-	-	-
Di	19.79	21.61	22.90	19.26	22.53	21.93
Ol	24.61	23.78	14.86	23.39	16.42	22.69
Or	2.05	2.60	2.16	1.32	2.61	2.67
Ab	18.65	15.99	22.42	20.21	19.31	17.70
An	28.01	24.20	29.23	28.61	28.13	24.39
Mt	2.66	2.82	2.66	2.68	2.66	2.75
Ilm	2.79	3.37	3.60	3.07	4.01	3.26
Ap	0.46	0.71	0.53	0.39	0.52	0.71
H_2O	0.62	0.48	0.55	1.10	0.44	0.22
Rest	-	-	-	-	-	-

APPENDIX 4: MODAL AND PETROGRAPHIC DATA

A. Older Series

B. Intermediate Series

C. Younger Series

O = Oceanite
A = Ankaramite
TOB = Transitional olivine basalt
TB = Transitional basalt
FB = Feldsparphyric basalt
H = Hawaiite
M = Mugearite
T = Trachyte
PT = Phonolitic trachyte
AB = Alkali basalt
ABtd = Alkali basanitoid
AOB = Alkali olivine basalt
AOBtd = Alkali olivine basanitoid

\- = Absent

\+ = Present

A. OLDER SERIES

Rock No.	Rock Name	Vol. % Phenocrysts								G/mass mineralogy					Occ.	Notes
		ol	cpx	plag	tm	af	ks	ap	ne	ol	cpx	plag	tm	af		
A2	TB	-	-	-	-	-	-	-	-	+	+	+	+	-	FLOW.	Rather altered.
A3	TB	3.3	0.2	1.2	-	-	-	-	-	+	+	+	+	-	FLOW.	Ol iddingsitised
A4	TB	3.0	1.7	0.5	-	-	-	-	-	+	+	+	+	-	FLOW.	Sub-fluidal g/mass, tm rich.
A7	TOB	4.8	2.8	-	-	-	-	-	-	+	+	+	+	-	FLOW.	
A9	H	0.8	0.5	1.3	-	-	-	-	-	+	+	+	+	-	FLOW.	Pheno plag An_{52}.
A10	O	14.3	6.0	3.5	-	-	-	-	-	+	+	+	+	-	FLOW.	Pheno plag An_{68}.
A11	TOB	6.2	4.2	2.3	-	-	-	-	-	+	+	+	+	-	FLOW.	Pheno plag An_{52}. Glomeroporphyritic ol + cpx.
A13	O	28.5	11.3	-	-	-	-	-	-	+	+	+	+	-	FLOW.	Dunite inclusions.
A17	H	0.2	0.1	1.2	-	-	-	-	-	+	+	+	+	-	DYKE.	Plag rich g/mass
A18	TOB	4.5	2.3	0.8	-	-	-	-	-	+	+	+	+	-	FLOW.	Plag phenos An_{50}
A20	H	2.2	5.0	1.5	-	-	-	-	-	+	+	+	+	-	FLOW.	Pheno plag An_{56}, g/mass An_{32+}
A22	TOB	2.0	4.7	0.5	-	-	-	-	-	+	+	+	+	-	FLOW.	Rare wehrlite inclusions
A24	O	25.3	10.3	-	-	-	-	-	-	+	+	+	+	-	FLOW.	Wehrlite inclusions. Two generations of olivine (i) Strained (ii) Undeformed
A28	O	19.8	13.5	-	-	-	-	-	-	+	+	+	+	-	FLOW.	Wehrlite inclusions.
A35	O	17.5	7.5	-	-	-	-	-	-	+	+	+	+	-	FLOW.	Occ. Wehrlite incl. Large ol phenos show strain lamellae.
A37	TB	0.7	1.2	2.2	-	-	-	-	-	+	+	+	+	-	FLOW.	Ol phenos serpentinised.
A39	TB	1.8	1.7	-	-	-	-	-	-	+	+	+	+	-	FLOW.	g/mass f/g.
A41	TB	1.0	3.0	2.4	-	-	-	-	-	+	+	+	+	-	FLOW.	
A45	TOB	6.0	6.0	6.1	-	-	-	-	-	+	+	+	+	-	FLOW.	f/g g/mass.

Rock No.	Rock Name	Vol. % Phenocrysts ol	cpx	plag	tm	af	ks	ap	ne	G/mass mineralogy ol	cpx	plag	tm	af	Occ.	Notes
A46	TOB	2.7	3.0	5.7	-	-	-	-	-	+	+	+	+	-	FLOW.	
A48	TOB	4.7	7.7	2.7	-	-	-	-	-	+	+	+	+	-	FLOW.	
A49	A	11.7	14.0	-	-	-	-	-	-	+	+	+	+	-	FLOW.	Zoned cpx phenos
A56	H	-	-	-	-	-	-	-	-	+	+	+	+	-	FLOW.	Fluidal plag rich g/mass
A57	H	3.5	0.5	-	-	-	-	-	-	+	+	+	+	-	FLOW.	
A58	H	2.4	3.8	9.9	-	-	-	-	-	+	+	+	+	-	FLOW.	Zeolitised, chabazite & analcime.
A60	H	1.9	3.1	5.3	-	-	-	-	-	+	+	+	+	-	FLOW.	Plag pheno An_{55}.
A63	M	-	-	-	-	-	-	-	-	+	+	+	+	-	FLOW.	Aphyric fluidal.
A64	H	-	-	-	-	-	-	-	-	+	+	+	+	-	DYKE.	Rare interstitial biotite.
A66	M	-	-	-	-	-	-	-	-	+	+	+	+	-	FLOW.	Aphyric.
A67	H	-	-	-	-	-	-	-	-	+	+	+	+	-	FLOW.	Aphyric. High propn. of interstitial af.
A68	H	-	-	-	-	-	-	-	-	+	+	+	+	-	FLOW.	Aphyric. fluidal plag rich g/mass.
A69	FB	2.1	-	18.9	-	-	-	-	-	+	+	+	+	-	FLOW.	Anorthosite inclusions An_{80}.
A70	H	1.3	4.4	20.1	2.0	-	-	-	-	+	+	+	+	-	FLOW.	Plag pheno An_{50-48}.
A71	H	3.1	3.8	11.0	0.1	-	-	-	-	+	+	+	+	-	FLOW.	Plag pheno An_{54}.
A72	H	4.1	7.3	15.5	0.8	-	-	-	-	+	+	+	+	-	FLOW.	Strongly zoned plag. phenos.
A73	M	-	0.6	1.3	1.3	-	-	-	-	+	+	+	+	-	FLOW.	Apatite m/ph. Plag phenos An_{45} core An_{14} rims.
A75	M	-	0.9	6.1	1.2	-	0.5	0.5	-	+	+	+	+	-	FLOW.	G/mass apatite. Opacite rims to Ks.
A76	M	-	-	3.8	-	-	-	<.1	-	+	+	+	+	-	FLOW.	Apatite m/ph. Feldspar rich g/mass.

Rock No.	Rock Name	Vol. % Phenocrysts ol	cpx	plag	tm	af	ks	ap	ne	G/mass mineralogy ol	cpx	plag	tm	af	Occ.	Notes
A78	M	<.1	-	2.8	0.1	<.1	-	-	-	+	+	+	+	-	FLOW.	Trace anorthoclase phenos. Plag. phenos ~ An_{15}.
A80	M	1.8	-	13.8	0.8	-	-	<.1	-	+	+	+	+	-	FLOW.	Pheno plag cores An_{45} Rims An_{14}. Apatite m/ph.
A82	TOB	1.3	6.3	4.6	-	-	-	-	-	+	+	+	+	-	FLOW.	
A83	TB	0.4	0.5	-	-	-	-	-	-	+	+	+	+	-	FLOW.	
A86	TB	2.9	1.1	-	-	-	-	-	-	+	+	+	+	-	FLOW.	ol serpentinised.
A88	H	-	1.6	0.6	-	-	-	-	-	+	+	+	+	-	FLOW.	Sub fluidal g/mass plag rich.
A90	TOB	4.3	3.2	1.0	-	-	-	-	-	+	+	+	+	-	FLOW.	Pheno plag An_{54}.
A91	TOB	3.6	3.5	0.5	-	-	-	-	-	+	+	+	+	-	FLOW.	
A93	TB	0.7	1.3	-	-	-	-	-	-	+	+	+	+	-	DYKE.	Pheno cpx pink-brown. G/mass ilmenite.
A94	H	-	-	-	-	-	-	-	-	+	+	+	+	-	FLOW.	Plag rich fluidal g/mass.
A96	H	0.3	0.6	3.8	-	-	-	-	-	+	+	+	+	-	DYKE.	Pheno plag An_{60}.
A97	TOB	2.6	5.9	0.5	-	-	-	-	-	+	+	+	+	-	FLOW.	cpx phenos brown-mauve titanaugite.
A98	TB	3.0	0.8	-	-	-	-	-	-	+	+	+	+	-	FLOW.	Fluidal g/mass.
A99	TB	-	-	-	-	-	-	-	-	+	+	+	+	-	FLOW.	
A100	TB	2.5	1.0	-	-	-	-	-	-	+	+	+	+	-	FLOW.	cpx phenos zoned to sharp brown rims.
A101	TB	-	-	-	-	-	-	-	-	+	+	+	+	-	FLOW.	
A102	TB	1.8	1.5	-	-	-	-	-	-	+	+	+	+	-	FLOW.	Plag An_{54}.
A103	TOB	3.5	1.5	-	-	-	-	-	-	+	+	+	+	-	FLOW.	
A104	TOB	0.3	1.8	3.8	-	-	-	-	-	+	+	+	+	-	FLOW.	ols serpentinised.
A105	TOB	3.5	1.0	1.0	-	-	-	-	-	+	+	+	+	-	FLOW.	Rather altered g/mass.

Rock No.	Rock Name	Vol. % Phenocrysts								G/mass mineralogy					Occ.	Notes
		ol	cpx	plag	tm	af	ks	ap	ne	ol	cpx	plag	tm	af		
A108	TOB	0.5	5.6	-	-	-	-	-	-	+	+	+	+	-	FLOW.	Slightly vesicular, infilled by calcite.
A109	TB	2.2	2.2	-	-	-	-	-	-	+	+	+	+	-	FLOW.	Ol completely iddingsitised.
A110	H	-	-	-	-	-	-	-	-	+	+	+	+	-	FLOW.	Fluidal g/mass.
A111	TB	2.3	2.2	-	-	-	-	-	-	+	+	+	+	-	DYKE.	cpx zoned from colourless cores to brown rims.
A112	TB	0.9	0.5	-	-	-	-	-	-	+	+	+	+	-	FLOW.	
A113	TOB	7.8	2.4	0.8	-	-	-	-	-	+	+	+	+	-	FLOW.	cpx greenish diopsidic augite cores zoned to brown rims.
A116	H	1.9	1.6	-	-	-	-	-	-	+	+	+	+	-	FLOW.	
A117	TB	-	-	-	-	-	-	-	-	+	+	+	+	-	FLOW.	Aphyric.
A118	O	31.6	4.9	-	-	-	-	-	-	+	+	+	+	-	FLOW.	Euhedral-subhedral marginally iddingsitised ol.
A119	TOB	3.5	4.8	1.9	-	-	-	-	-	+	+	+	+	-	FLOW.	Pheno plag An_{52}. slightly vesicular.
A121	H	7.4	1.0	-	-	-	-	-	-	+	+	+	+	-	FLOW.	Very f/g g/mass.
A122	TOB	3.1	2.9	1.3	-	-	-	-	-	+	+	+	+	-	FLOW.	Rather altered. Occ. glomeroporphyritic ol + cpx.
A123	TOB	5.1	0.3	-	-	-	-	-	-	+	+	+	+	-	FLOW.	Sub fluidal plag rich g/mass.
A124	TOB	5.0	3.3	0.5	-	-	-	-	-	+	+	+	+	-	FLOW.	
A127	FB	2.5	-	19.3	3.1	-	-	-	-	+	+	+	+	-	FLOW.	Occ. anorthosite inclusions.
A128	H	2.1	-	8.5	1.1	-	-	-	-	+	+	+	+	-	FLOW.	Fluidal plag rich g/mass. Plag phenos An_{62} cores.
A129	H	-	-	4.2	-	-	-	-	-	+	+	+	+	-	DYKE.	sub ophitic g/mass texture pink cpx.

Rock No.	Rock Name	Vol. % Phenocrysts								G/mass mineralogy					Occ.	Notes
		ol	cpx	plag	tm	af	ks	ap	ne	ol	cpx	plag	tm	af		
A132	TOB	8.9	-	-	-	-	-	-	-	+	+	+	+	-	FLOW.	Ol phenos embayed.
A138	FB	3.5	-	33.8	-	-	-	-	-	+	+	+	+	-	FLOW.	Pheno plag An_{81}
A144	TOB	7.0	4.6	-	-	-	-	-	-	+	+	+	+	-	FLOW.	G/mass altered.
A146	H	-	-	6.6	-	-	-	-	-	+	+	+	+	-	FLOW.	Sub-fluidal plag rich g/mass.
A152	H	2.9	5.7	5.8	-	-	-	-	-	+	+	+	+	-	FLOW.	Pheno plag An_{58}. High propn. interstitial af.
A153	H	3.8	8.5	8.5	-	-	-	-	-	+	+	+	+	-	FLOW.	Pheno plag An_{58} cores strongly zoned.
A154	TOB	7.8	3.2	10.7	-	-	-	-	-	+	+	+	+	-	DYKE.	
A155	H	-	-	-	-	-	-	-	-	+	+	+	+	-	DYKE.	Plag An_{52}. Mauve-brown cpx.
A156	H	-	-	-	-	-	-	-	-	+	+	+	+	-	FLOW.	Fluidal plag rich g/mass
A157	TB	-	-	-	-	-	-	-	-	+	+	+	+	-	DYKE.	Very f/g g/mass.
A158	TB	-	-	-	-	-	-	-	-	+	+	+	+	-	FLOW.	Occ. m/ph ol. Plag An_{46}.
A159	TB	-	-	-	-	-	-	-	-	+	+	+	+	-	FLOW.	
A160	TB	-	-	-	-	-	-	-	-	+	+	+	+	-	FLOW.	Aphyric – microphyric. Plag An_{48}.
A162	TOB	10.7	-	-	-	-	-	-	-	+	+	+	+	-	FLOW.	Two generations ol. (1) Strained, associated with dunite inclusions. (2) Undeformed.
A163	O	16.2	-	-	-	-	-	-	-	+	+	+	+	-	FLOW.	2 generations ol as above. Approx. 11.5% ol is derived, anhedral.
A167	TB	-	-	-	-	-	-	-	-	+	+	+	+	-	FLOW.	
A168	TB	1.1	-	-	-	-	-	-	-	+	+	+	+	-	FLOW.	Rare marg. idd ols. g/mass ilmenite.
A169	TB	3.3	-	-	-	-	-	-	-	+	+	+	+	-	FLOW.	Occ. dunite inclusions.

Rock No.	Rock Name	Vol. % Phenocrysts								G/mass mineralogy					Occ.	Notes
		ol	cpx	plag	tm	af	ks	ap	ne	ol	cpx	plag	tm	af		
A170	O	18.3	-	-	-	-	-	-	-	+	+	+	+	-	FLOW.	Flow associated with dunite inclusions.
A171	TB	3.8	-	-	-	-	-	-	-	+	+	+	+	-	FLOW.	"Parental Magma"
A172	TB	-	-	-	-	-	-	-	-	+	+	+	+	-	FLOW.	Ol heavily iddingsitised.
A173	TB	2.0	-	-	-	-	-	-	-	+	+	+	+	-	FLOW.	skeletal m/ph ol.
A175	TB	2.0	0.3	-	-	-	-	-	-	+	+	+	+	-	DYKE.	Ilmenite in g/mass.
A179	TOB	9.0	-	-	-	-	-	-	-	+	+	+	+	-	FLOW.	
A181	TB	3.3	-	-	-	-	-	-	-	+	+	+	+	-	FLOW.	Occ. dunite inclusions.
A182	TOB	14.3	-	-	-	-	-	-	-	+	+	+	+	-	FLOW.	Rare dunite inclusions, very f/g g/mass
A183	TOB	10.0	-	-	-	-	-	-	-	+	+	+	+	-	FLOW.	Two generations of ol phenos.
A185	PT	-	-	-	-	14.2	-	-	-	-	+	-	+	+	DOME.	M/pheno euhedral nepheline prominent. Phenocryst anorthoclase.
A187	TB	2.0	-	-	-	-	-	-	-	+	+	+	+	-	FLOW.	f/g g/mass
A190	FB	0.5	-	15.0	0.2	-	-	-	-	+	+	+	+	-	FLOW.	Bytownitic anorthosite inclusions An_{76}.
A193	FB	0.7	-	29.3	-	-	-	-	-	+	+	+	+	-	FLOW.	Bytownitic anorthosite inclusions An_{83}, same as pheno plag.
A194	H	0.3	-	0.3	-	-	-	-	-	+	+	+	+	-	FLOW.	g/mass plag rich. Phenos An_{42}
A195	H	-	-	-	-	-	-	-	-	+	+	+	+	-	FLOW.	Fluidal f/g plag rich g/mass.
A196	H	-	-	0.5	-	-	-	-	-	+	+	+	+	-	FLOW.	
A197	TOB	0.5	3.8	9.7	-	-	-	-	-	+	+	+	+	-	FLOW.	Plag phenos An_{54}.
A198	M	-	-	-	-	-	-	-	-	+	+	+	+	-	FLOW.	Plag An_{30}. m/pheno apatite.
A200	H	-	-	-	-	-	-	-	-	-	+	+	+	-	FLOW.	Highly altered. Chlorite + epidote + secondary amphibole.

Rock No.	Rock Name	Vol. % Phenocrysts ol	cpx	plag	tm	af	ks	ap	ne	G/mass mineralogy ol	cpx	plag	tm	af	Occ.	Notes
A201	H	-	-	-	-	-	-	-	-	-	+	+	+	-	FLOW.	As above.
A203	H	-	-	-	-	-	-	-	-	-	+	+	+	-	FLOW.	As above.
A205	H	-	-	-	-	-	-	-	-	-	+	+	+	-	FLOW.	As above.
A211	TOB	10.0	2.0	3.8	-	-	-	-	-	+	+	+	+	-	FLOW.	Pheno plag An_{68}
A212	H	3.0	-	6.2	0.8	-	-	-	-	+	+	+	+	-	FLOW.	Pheno plag An_{54}
A214	TOB	5.8	4.2	1.0	-	-	-	-	-	+	+	+	+	-	FLOW.	Brown glass in g/mass. Ilmenite in g/mass.
A215	TB	2.5	-	0.7	-	-	-	-	-	+	+	+	+	-	FLOW.	Ol iddingsitised.
A218	TOB	9.2	-	-	-	-	-	-	-	+	+	+	+	-	FLOW.	Ol shows strain lemellae
A219	TOB	10.7	-	-	-	-	-	-	-	+	+	+	+	-	FLOW.	
A220	TOB	5.2	-	-	-	-	-	-	-	+	+	+	+	-	FLOW.	Embayed ol. phenos.
A221	TOB	2.7	2.0	3.0	-	-	-	-	-	+	+	+	+	-	FLOW.	Ol embayed/skeletal. Plag phenos An_{66} Dunite incl. associated with flow.
A222	TOB	7.0	-	-	-	-	-	-	-	+	+	+	+	-	FLOW.	f/g g/mass. Assoc. dunite incl.
A223	TB	-	-	-	-	-	-	-	-	+	+	+	+	-	DYKE.	Ilmenite in coarse grained g/mass.
A224	TOB	9.3	-	-	-	-	-	-	-	+	+	+	+	-	FLOW.	Strain lamellae in some ols. Flow associated with dunite inclusions.
A225	TOB	8.8	-	-	-	-	-	-	-	+	+	+	+	-	DYKE.	Occ. interstitial brown glass. Flow assoc. with dunite/wehrlite inclusions.
A226	TB	-	3.0	3.0	-	-	-	-	-	+	+	+	+	-	DYKE.	Coarse doleritic texture. Ilmenite in g/mass.
A228	A	18.7	23.8	-	-	-	-	-	-	+	+	+	+	-	FLOW.	Occ. strain lamellae in ol phenos. Pale brown cpx strongly zoned to mauve rims.

Rock No.	Rock Name	Vol. % Phenocrysts ol	cpx	plag	tm	af	ks	ap	ne	G/mass mineralogy ol	cpx	plag	tm	af	Occ.	Notes
A231	H	-	-	-	-	-	-	-	-	+	+	+	+	-	DYKE.	
A232	TB	-	-	-	-	-	-	-	-	+	+	+	+	-	FLOW.	Altered.
A235	H	-	-	-	-	-	-	-	-	+	+	+	+	-	FLOW.	Secondary epidote, amphibole.
A238	H	1.0	0.5	1.0	-	-	-	-	-	+	+	+	+	-	DYKE.	Ilmenite in g/mass.
A240	TB	3.8	-	3.0	1.3	-	-	-	-	+	+	+	+	-	DYKE.	
A242	TB	1.5	-	-	-	-	-	-	-	+	+	+	+	-	FLOW.	
A243	TOB	2.0	3.2	-	-	-	-	-	-	+	+	+	+	-	FLOW.	Ol phenos serpentinised.
A244	TB	-	-	-	-	-	-	-	-	+	+	+	+	-	FLOW.	
A246	A	15.8	20.3	0.5	-	-	-	-	-	+	+	+	+	-	FLOW.	cpx phenos green diopsidic cores zoned to mauve rims.
A247	TB	2.0	1.7	-	-	-	-	-	-	+	+	+	+	-	FLOW.	
A249	T	-	-	-	-	0.5	-	-	4.5	-	+	-	+	+	DOME.	tm rare. Highly fluidal g/mass
A252	TOB	13.7	-	3.3	-	-	-	-	-	+	+	+	+	-	FLOW.	Occ. dunite inclusions.
A253	TOB	13.7	0.5	1.2	-	-	-	-	-	+	+	+	+	-	DYKE.	Ol phenos skeletal.
A254	O	17.7	2.3	-	-	-	-	-	-	+	+	+	+	-	FLOW.	Ol marginally iddingsitised.
A255	TB	0.2	1.2	3.8	-	-	-	-	-	+	+	+	+	-	DYKE.	Plag phenos An_{68}.
A256	O	16.0	-	-	-	-	-	-	-	+	+	+	+	-	FLOW.	Ol phenos skeletal
A257	TB	2.0	-	-	-	-	-	-	-	+	+	+	+	-	FLOW.	Very f/g g/mass
A260	PT	-	-	-	-	3.0	-	-	10.0	-	+	-	+	+	DOME.	Nepheline largely pseudomorphed by clay minerals.
A261	T	-	-	-	-	1.7	-	-	-	+	+	-	+	+	DOME.	Ore jacketed g/mass ol.

Rock No.	Rock Name	Vol. % Phenocrysts ol	cpx	plag	tm	af	ks	ap	ne	G/mass mineralogy ol	cpx	plag	tm	af	Occ.	Notes
A264	PT	-	2.0	-	-	25.0	-	-	-	-	+	-	+	+	DOME.	Aegerine-augite phenocrysts. Anorthoclase phenocrysts.
A267	M	0.2	1.3	16.0	1.0	-	-	0.8	-	+	+	+	+	-	FLOW.	Pheno plag An_{29}. M/ph apatite.
A268	H	2.2	0.6	12.3	1.3	-	5.3	-	-	+	+	+	+	-	FLOW.	Apatite m/ph. Plag phenos An_{53} core, An_{62} rim.
A269	H	1.7	1.3	11.7	1.3	-	4.5	-	-	+	+	+	+	-	FLOW.	Apatite m/phenos. Plag phenos An_{61} cores, An_{48} rims.

B. INTERMEDIATE SERIES

Rock No.	Rock Name	Vol % Phenocrysts			G/mass mineralogy				Vol % Vesicles	Occ.	Notes
		ol	cpx	plag	ol	cpx	plag	tm			
B1	AB	3.3	-	-	+	+	+	+	10.0	FLOW.	Some aragonite filling vesicles
B2	AOB	5.6	-	-	+	+	+	+	20.3	FLOW.	" " " "
B3	AOB	7.1	-	-	+	+	+	+	20.0	FLOW.	G/Mass plag An_{56}
B4	AOB	6.6	-	-	+	+	+	+	6.7	FLOW.	G/Mass plag An_{56}
B5	AOBtd	4.5	1.0	-	+	+	+	+	-	FLOW.	Skeletal ol.
B6	AOBtd	6.2	2.2	-	+	+	+	+	-	FLOW.	
B7	AOBtd	12.7	-	-	+	+	+	+	-	FLOW.	? m/pheno CPX
B9	AOB	10.4	-	-	+	+	+	+	20.0	FLOW.	Coarse Intersertal G/Mass. Plag An_{60-58} cores, An_{44} margins.
B10	AOB	9.4	-	-	+	+	+	+	20.0	FLOW.	Skeletal ol. G/Mass very f/g.
B14	AB	4.0	-	-	+	+	+	+	-	FLOW.	Some ol phenos showing strain lamellae. Coarse slightly fluidal g/mass. Plag. An_{54-50}.
B15	AOB	7.2	-	-	+	+	+	+	-	FLOW.	Pheno ol occasionally strained.
B18	AOB	6.6	-	-	+	+	+	+	16.0	FLOW.	Very coarse g/mass. Plag An_{62}. High propn. of interstit. A.feldspar
B19	AOB	8.3	-	-	+	+	+	+	-	FLOW.	Plag An_{64}
B20	AB	4.4	-	-	+	+	+	+	5.3	FLOW.	Calcite infilling some vesicles
B21	AOB	6.6	-	-	+	+	+	+	3.3	FLOW.	
B22	AOB	6.8	-	-	+	+	+	+	5.0	FLOW.	Granular, altered g/mass
B23	AOB	11.9	-	-	+	+	+	+	3.3	FLOW.	Skeletal ol. Very f/g g/mass.

Rock No.	Rock Name	Vol % Phenocrysts			G/mass mineralogy				Vol % Vesicles	Occ.	Notes
		ol	cpx	plag	ol	cpx	plag	tm			
B24	AOB	11.7	-	-	+	+	+	+	-	FLOW.	Occasional m/pheno cpx. Very f/g g/mass.
B25	AOB	10.7	-	-	+	+	+	+	3.3	FLOW.	Ilmenite in g/mass. Plag An_{48} minimum.
B26	AOBtd	10.5	-	-	+	+	+	+	-	FLOW.	
B27	AOB	9.2	-	-	+	+	+	+	-	FLOW.	Fluidal g/mass
B28	AOB	9.5	-	-	+	+	+	+	-	FLOW.	" "
B29	O	15.0	-	-	+	+	+	+	-	FLOW.	Very f/g g/mass, cpx rich.
B31	O	15.0	-	-	+	+	+	+	-	FLOW.	
B33	O	15.5	-	-	+	+	+	+	-	FLOW.	Skeletal ol. Occasional m/pheno cpx. f/g g/mass.
B34	AOBtd	9.0	-	-	+	+	+	+	-	FLOW.	Skeletal ol, showing c-axis elongation. Very f/g g/mass
B37	AOB	9.3	-	-	+	+	+	+	-	FLOW.	Granular g/mass. Ilmenite.
B38	AOB	10.5	-	-	+	+	+	+	-	FLOW.	Ophitic g/mass texture. High propn. interstitial A.feld.
B39	AOB	11.7	-	-	+	+	+	+	20.0	FLOW.	
B40	AOBtd	13.3	-	-	+	+	+	+	-	FLOW.	Plag An_{58}
B41	AOB	14.7	-	-	+	+	+	+	-	FLOW.	Dunite fragments. Fragmental ol prob derived from these, ~ 8.3% phenos.
B42	O	19.5	-	-	+	+	+	+	-	FLOW.	Very f/g g/mass
B43	O	17.2	-	-	+	+	+	+	-	FLOW.	Skeletal ol. Some dunite fragments.

C. YOUNGER SERIES

Rock No.	Rock Name	Vol. % Phenocrysts ol	cpx	plag	G/mass mineralogy ol	cpx	plag	tm	Vol. % Vesicles	Occ.	Notes
C2	AOB	6.8	-	-	+	+	+	+	-	FLOW.	Coarse sub-ophitic textured g/mass
C4	ABtd	4.7	-	8.5	+	+	+	+	-	FLOW.	As above. Ols marginally iddingsitised.
C11	AOB	6.7	-	-	+	+	+	+	25.2	FLOW.	Vent type
C18	AOB	9.8	-	-	+	+	+	+	-	FLOW.	Vent type
C20	AOB	8.3	-	-	+	+	+	+	-	FLOW.	
C23	AB	-	-	-	+	+	+	+	-	FLOW.	Coarse ophitic g/mass
C25	AB	4.0	-	12.3	+	+	+	+	-	FLOW.	
C29	AOB	10.0	-	-	+	+	+	+	18.3	FLOW.	Vent type
C32	AOB	8.0	-	10.0	+	+	+	+	-	FLOW.	
C33	AOB	6.3	-	-	+	+	+	+	9.0	FLOW.	Coarse g/mass
C38	AOBtd	8.0	-	-	+	+	+	+	10.0	FLOW.	Coarse sub-ophitic texture
C40	AOBtd	6.2	-	-	+	+	+	+	-	FLOW.	
C41	AOB	6.2	-	-	+	+	+	+	-	FLOW.	Vent type. Ols iddingsitised
C46	AOBtd	9.1	-	-	+	+	+	+	9.8	FLOW.	Coarse g/mass with titanaugite
C47	AB	1.5	-	-	+	+	+	+	20.2	FLOW.	Ophitic texture. Titanaugite
C50	AOB	5.0	-	-	+	+	+	+	6.7	FLOW.	Prominent spinels in ols.
C52	AOB	6.2	-	15.0	+	+	+	+	16.0	FLOW.	Coarse doleritic texture
C54	AOB	5.0	-	-	+	+	+	+	10.0	FLOW.	Vent type
C55	AOB	5.5	-	-	+	+	+	+	13.3	FLOW.	Vent type
C56	AOB	8.4	-	-	+	+	+	+	36.7	FLOW.	Vent type

Rock No.	Rock Name	Vol. % Phenocrysts ol	cpx	plag	G/mass mineralogy ol	cpx	plag	tm	Vol. % Vesicles	Occ.	Notes
C58	AOB	5.8	-	-	+	+	+	+	20.0	FLOW.	cpx highly zoned to titanaugite
C59	AOB	8.4	-	-	+	+	+	+	12.5	FLOW.	Euhedral ol phenos. Sub ophitic g/mass
C60	AB	4.8	-	22.9	+	+	+	+	30.0	FLOW.	ols iddingsitised
C62	AB	-	-	-	+	+	+	+	-	FLOW.	Spinels prominent in larger ols
C66	AOB	7.4	-	-	+	+	+	+	16.0	FLOW.	
C68	AOB	6.4	-	16.4	+	+	+	+	16.0	FLOW.	
C69	AOB	6.4	-	1.4	+	+	+	+	16.0	FLOW.	ols marginally iddingsitised
C71	AB	-	-	-	+	+	+	+	-	FLOW.	Coarse sub ophitic texture
C74	AB	3.8	-	-	+	+	+	+	20.0	FLOW.	ols marginally iddingsitised
C76	AOB	9.2	-	-	+	+	+	+	16.0	FLOW.	
C77	AB	4.0	-	-	+	+	+	+	16.0		Vent type. Magnetite rich g/mass
C78	AOB	7.6	-	8.4	+	+	+	+	16.0	FLOW.	Coarse g/mass. Zoned titanaugite
C79	AOB	10.6	-	-	+	+	+	+	16.0	FLOW.	
C82	AB	3.3	-	-	+	+	+	+	23.5	FLOW.	Coarse sub ophitic g/mass. Zoned titanaugite.
C83	AB	1.3	-	5.6	+	+	+	+	20.0	FLOW.	As above
C86	AB	-	-	-	+	+	+	+	30.0	FLOW.	Vent type
C91	AB	3.3	-	-	+	+	+	+	-	FLOW.	Coarse g/mass with sub-fluidal texture
C92	AOB	10.0	-	-	+	+	+	+	-	FLOW.	ol glomeroporphyritic. Coarse g/mass.

MAURITIUS

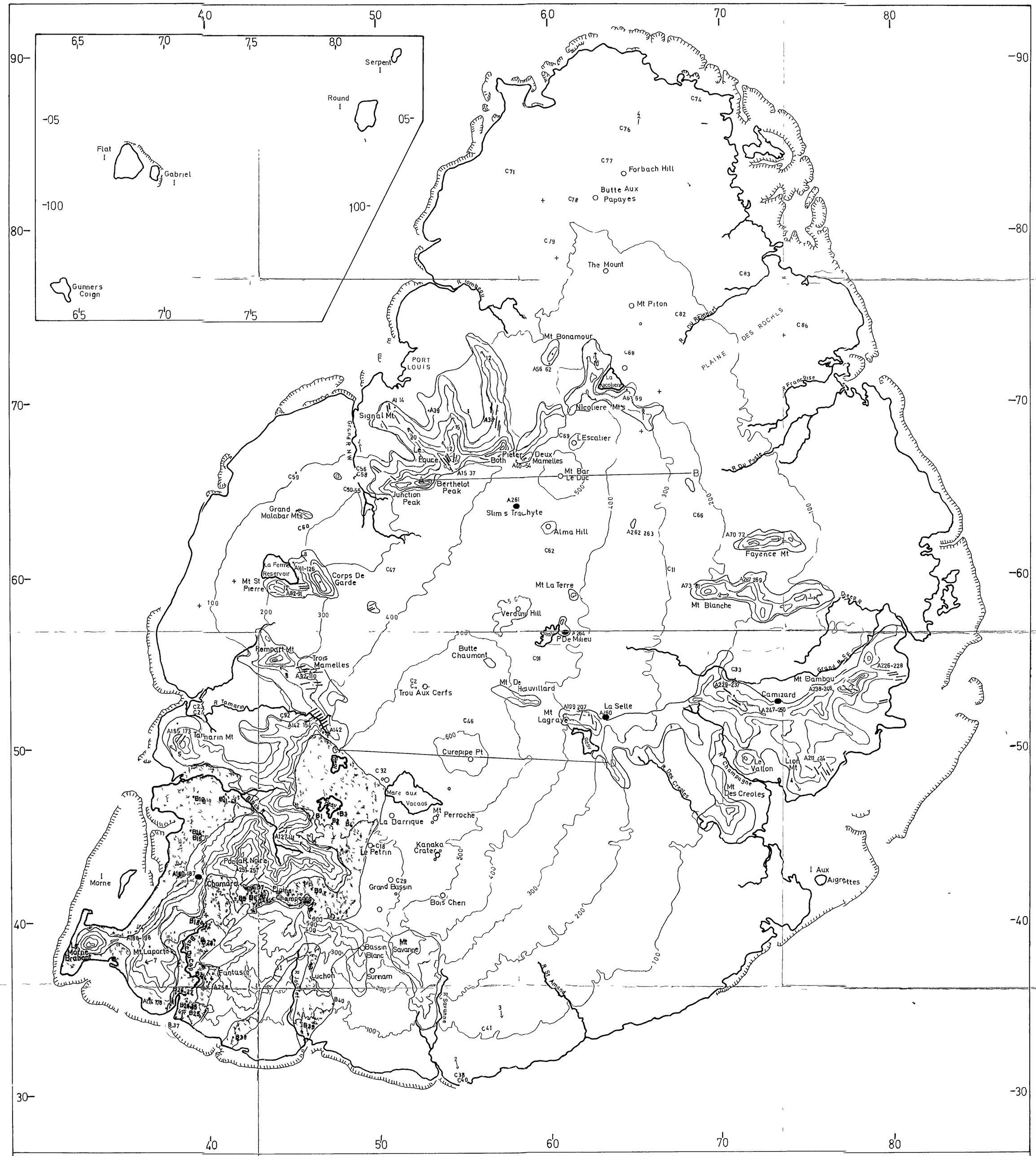

ADAPTED FROM D SURVEY WAR OFFICE AND AIR MINISTRY
SERIES Y662
MAURITIUS
EDITION I GSGS

GEOLOGY MODIFIED AFTER

SIMPSON (1949)

SCALE 1/ 100 000

CONTOUR INTERVAL 100 METRES

0 1 2 3 4 5 6 7 8 9 10 KILOMETRES

KEY

SAMPLE LOCALITIES

A 56 OLDER SERIES
B 33 INTERMEDIATE SERIES
C 91 YOUNGER SERIES
RIVER
LAKE OR RESERVOIR

GEOLOGY.

OLDER SERIES
INTERMEDIATE SERIES
YOUNGER SERIES
DYKE
TRACHYTE BODIES
DIP OF LAVA FLOW OR UNIT
HORIZONTAL DIP
VENT
PARISITIC CONE } YOUNGER SERIES
CORAL REEF

N TRUE
N GRID
0 12